IN THE NAME OF ALLAH, THE BENEFICIENT, THE MERCIFUL

SOLID ELECTROLYTE OXYGEN SENSORS

A Thesis submitted for the degree of

DOCTOR OF PHILOSOPHY

by

RIAD MOUHAMED ADEL KOCACHE

to

THE UNIVERSITY OF ASTON IN BIRMINGHAM

SEPTEMBER 1980

SUMMARY

The relevant developments in: science,engineering,and technology; and their confluence at different times resulting in the concept,feasibility, and the emergence of the solid electrolyte oxygen sensor ,are traced from the last century to the present time -when a number of commercial devices are marketed.General rules are set out for the choice of an electrolytic system for a solid electrolyte oxygen sensor.

The major markets and applications for which the sensor is suitable for are described and in particular the combustion efficiency market.The available commercial instruments are reviewed,and a number of desirable sensor features are identified.

The theory of the oxygen solid electrolyte concentration cell is outlined ,and the major error contributing parameters reviewed.

The design,development,optimisation,and fabrication of a miniature, rugged,accurate,versatile,and easy to manufacture sensor are detailed.The electrical conductivity of samples of solid electrolytes is examined by an especially developed A.C.measurement technique,and the influence of structural defects on the electrical conductivity is assessed as a potential means of solid electrolyte material quality control.

The sensor's characteristics are evaluated in detail and errors due to sample gas composition are measured for a number of commonly encountered gases.The degrading effect of certain gases and reducing atmospheres on the sensor's electrodes is also investigated.

The versatility of the design is demonstrated by using the sensor in different configurations: with a sealed in reference, as an oxygen pump , and in a feedback mode.

Examples of industrial commercial use of the sensor as: a flue gas oxygen analyser, and a wide-range instrument are described,showing its suitability for such applications.

This is a summary of a thesis submitted by
RIAD MOUHAMED ADEL KOCACHE
For the degree of DOCTOR OF PHILOSOPHY
September,1980.

KEYWORDS : solid electrolyte,oxygen sensor,oxygen analyser.

ACKNOWLEDGEMENTS

I would like to thank Dr. P.F.Pagey President - Sybron Corporation for encouraging me to do an industrial based Ph.D. I am also grateful for the Sybron Corporation for allowing and supporting the work.

My thanks are due to Professor F.M. Page for his encouragement and guidance and for Mr. R. Mudie for his support and supervision.

My special thanks are due to Mr. D. Holman who transformed my concepts and ideas through his skill and dexterity into practical realities.

I would also like to thank the following for their help:
Dr. J. Swan, Dr. D. Nuttal, Mr. M. Chewter, Mr. T. Jenkinson, Mr. D. Barnbrook, Mr. R. Windemer and Mr. R.H. Sunderland.

The help of Mr. J.C. McKenzie of the Sybron Patent Department is also greatly appreciated.

My sincere thanks are due to Mrs. S. Wickens for securing the reference papers, and for typing the manuscript.

STATEMENT

This thesis, submitted to the University of Aston in Birmingham in partial fulfilment of the requirements for the degree of Doctor of Philosophy, describes work done under the supervision of: Prof. F.M. Page, B.A., Ph.D., Sc.D. of the Department of Chemistry, The University of Aston in Birmingham, and Mr. R. Mudie, C.ENG.,M.I.E.E. Technical Manager, Taylor Instrument Ltd.,(Analytics); from April 1975 to September 1980. Other than where references have been given in the text, the work described herein is original and has not been submitted for any other award.

R. Kocache.

During the reign of Caliph Haroon Al-Rashid, it was customary for talented people - poets, singers, artisans, scholars, etc. - from all corners of the empire to attend his court in Baghdad, in the hope of gaining an audience during which their talents could be shown to the cultured and wise Caliph and, hopefully, generously rewarded.

It is told that one day a man appeared at the court and requested an audience. He was told to wait for his turn and was led eventually to the audience hall where the Caliph sat surrounded by state dignitaries, advisors, and court favourites. The man saluted and was granted permission to proceed. He produced a number of sewing needles and a small cushion which he placed on the floor and then, from a distance of a few yards, started to throw the needles in the direction of the cushion. The first needle went into the cushion, the second went into the eye of the first, the third into the eye of the second, and so on. When he had used all the needles he turned and bowed to the Caliph and stood awaiting his pleasure. The court was definitely impressed with such a skilful performance and anticipated a generous reward for such a unique skill.

The Caliph paused for a while, then called for both his treasurer and his executioner. The court went silent, awaiting the unexpected outcome of the Caliph's deliberation. The Caliph ordered his treasurer to award the man a hundred golden dinars and addressed the man saying:- "This is for your unusal skill". The man was overjoyed and started to praise and thank the Caliph for his generosity. "Wait a minute!" said the Caliph and he turned round and ordered his executioner to give the man a hundred lashes. The order was executed and the man took his punishment in silence. He and the court were puzzled by the sentence. When the last blow was struck, the man stood unsteadily facing the Caliph, who addressed him saying, "These are for spending your time and talent on a skill which is of no benefit to anyone".

To Noëlle

CONTENTS

LIST OF FIGURES

PAGE

LIST OF TABLES

LIST OF SYMBOLS

D.C.	Direct current
A.C.	Alternating current
^{o}C	Degrees centigrade
^{o}K	Degrees kelvin
E:e.m.f.	Electro motive force
U	Migration velocity +VE ions
V	Migration velocity -VE ions
Ci	Concentration of the ith species
R	Universal gas constant
T	Absolute temperature in degrees kelvin
F	Faraday constant
ln	Natural logarithm
t_{ion}	Sum of ionic transference numbers of electrolyte
μ_{O2}	Chemical potential of oxygen at a reversible electrode
AB, $\hat{A}$ B	
$\hat{A}\hat{B}$, $A\hat{B}$	Solid electrolyte systems
Δ G	Reaction free energy
n	Number of equivalents passed across cell
Δ S	Change in entropy
$\frac{\partial E}{\partial T}$	Temperature coefficient of cell
Δ H	Heat of reaction
K	Equilibrium constant for reaction at specified temperature
E^{o}, ΔG^{o},	Standard value of property at
ΔS^{o}, ΔH^{o}	Specified temperature and pressure
ml/M	Millil^{i}ter per minute
atm	Atmosphere
MHD	Magneto-hydro-dynamic
BOD	Biochemical oxygen demand
TOD	Total oxygen demand

$\mu^{\circ}_{O_2}$	Standard oxygen potential at $T^{\circ}K$
$H^{\circ}_{O_2}$	Standard oxygen molar enthalpy
σ	Total conductivity
σ_i	Partial conductivity of i th species
n_i	Number of carriers of species
q_i	Charge on specei in coulombs
U_i	Mobility in cm^2 per volt second
V_M	Unionized - cationic vacancy
V_X	Unionized - anionic vacancy
V_M'	Singly ionized - cationic vacancy
$V_X^{\cdot}$	Singly ionized - anionic vacancy
e	Electron - electronic defect
e'	Excess electron
h	Electron - hole
M_i	Unionized cation in interstitial position
X_i	Unionized anion in interstitial position
Ai	Foreign cationic impurity in interstitial position
A_M	Cationic impurity ion on a cationic site
B_X	Anionic impurity ion on an anionic site
t_e	Electronic transference number
E_a	Activation energy
O_o	Oxygen ion in normal lattice site
O_i''	Interstitial oxygen ion
α	Coefficient of thermo electric motive force
E	Modulus of elasticity
Ω	Ohms
$\sim$	Mhos
t_i	Transference number of one type of species
K	Boltzman constant
P'_{O_2}, P''_{O_2}	Oxygen partial pressure

P_{e^-}	Oxygen partial pressure at which ionic conductivity is equal to excess electron conductivity
P_{e_h}	Oxygen partial pressure at which ionic conductivity is equal to electron-hole conductivity
$\%O_2$ S	Percentage oxygen in sample gas
L	Flow rate of gas ml/M
I	Electric current
PPM	Parts per million
M	Minutes, money
ΔT	Time interval
W	Watts
Hz	Hertz
RH	Relative Humidity
Lit.	Litre
DPM	Digital Panel Meter

1. PREFACE

The success of an industrial product can be assessed by many criteria; each criterion however is formulated from a specific area of interest and reflects strongly its own point of view. One can enumerate many possible criteria reflecting different areas of interest:

PRODUCTION - The manufacturing of the product should utilize the most efficient methods and techniques resulting in the lowest possible cost consistent with the required quality.

CUSTOMER - The product should have a long reliable life, requiring a minimum of maintenance and having a 'low cost of ownership'; and meet its stated specification.

SALES - The product should have a 'performance/price relationship enabling it to secure a large share of the market.

DESIGN - The product should have the ability to be adapted easily for use in new markets and in new environments.

ECOLOGY - The product should consume a minimum of energy during manufacturing and during use, it should make efficient use of raw materials and use components that can be re-cycled.

INVESTOR - The product should return a good profit on investment.

It is clear from the above, that a successful product needs to satisfy a variety of criteria emanating from different areas of interest. This usually leads to some conflicting requirements and a compromise may be necessary. The choice of the criteria and the importance associated with each of them, is a matter of company policy. To be able to design, develop and produce a product that goes a long way to satisfying a number of criteria; the project must move, from the outset, within a reference framework outlined by these desired features.

The formulation and outlining of this framework and the detailing of the product specification is one of the most important tasks in ensuring the emergence of a successful new product and, in many instances, the main cause of product failure. Some of the major causes of bad formulation of such a framework are: inadequate market research, use of opinion rather than factual data, not enough careful consideration, very little updating of data and fragmentation of project control leading to the distortion of the framework.

In many modern industrial organisations the specifications for a new product and the general framework are usually determined by the marketing department. The project usually proceeds serially, from one department to another; viz. - research and development, engineering, production, sales etc.....-. At any given instant during the product's progress the overall project control is effectively in the hands of the department which happens to be working on the project at that time. As there is a natural tendency within each department to view the project from their own specialized points of view- this results in warping the framework and slowing down the project, then a correction is needed later on to counter-act that effect. In order to minimize this, the organisation can be set up so that a unit (product management) takes over the overall control and co-ordination of a given product. This ensures that all the aspects of the product development are kept in perspective. This unit ensures that the framework and specification are up-to-date, it monitors the project's progress through the different departments and requests corrections when necessary.

Having outlined the framework and stated the specification of a new product, and set up an administrative mechanism for its monitoring and control, it is necessary that the individual departments are capable of appreciating the framework, able to work within its boundaries and are willing to respond to requests for corrective actions.

The shaping of an R & D department so that it does not become an isolated ivory tower, and can work as part of an organisation similar to the one just described is not an easy task. The need for specialisation leads many workers to limit their outlook to confined and very narrow boundaries, and they are quite happy to be blissfully unaware of anything outside their limited areas of interest. To be able to contribute effectively and efficiently, an industrial R & D unit cannot afford to isolate itself. In addition to its specific functions and areas of specialisation, requiring experts and a specialists approach, it should also have a comprehensive outlook capable to appreciating fully the frameworks within which the various products are specified and enabling it to work within them without distorting them. Its interest in the product should extend from its original inception to its performance in both the field and market-place. This need is even more so in the domain of industrial measurements where, due to the size and variety of modern industry, the measurement of the same parameter is required under widely varying conditions and under an even tougher competition. Many products start life with certain applications and have to evolve later to cope with an ever widening range of applications in conjunction with the need to be re-designed to include technological production improvements enabling it to stay competitive. The serious worker in this field has to extend the boundaries of his awareness to cover every area relevant to the product, and should develop the skill to be able to move from the analytical specific mode required to solve a given problem to the holistic overall view required to keep things in perspective.

Given the task of designing a product to a given specification and within a certain framework, there exist many possibilities. Only a few however will contain a balanced mixture that produces a design which is simple, functional, aesthetically pleasing, easy to

manufacture, cheap to produce, and of excellent quality. To steer a design to such regions one has to act as a point of confluence whereby the science, the technology and engineering, the art and craft, and the economy blend together and form a harmonious entity. Such products are very rare and far between, but not yet extinct. It is the drive for excellence that fuels such enterprises. Whenever we are lucky to use a device that one might call excellent, we realize that the effort expended in the quest for excellence is always worthwhile.

This thesis is submitted as an example of industrial applied research in the field of instrument science where, as far as possible, the points discussed above were prominent in the motivation and direction of the work.

CHAPTER TWO

THE EVOLUTION OF SOLID ELECTROLYTE OXYGEN SENSORS

2.1 THE MEASUREMENT OF OXYGEN[1]

Oxygen is the most abundant element on earth, it accounts for about 23% of the weight of the air and almost half of the weight of the earth's crust. Its strong chemical activity and its role in supporting human life makes its monitoring and measurement highly desirable. As world industry and technology develop and grow, the need to monitor oxygen to a higher degree of accuracy and to lower levels, and in environments which are increasingly hostile poses extremely difficult problems for the measurement scientist. Advances in science and technology have helped him towards solving some of these problems and workers in this field were quick to develop a wide range of instruments based on the physical and the chemical properties of oxygen. Applications requiring the measurement of oxygen cover:-

Medical[2] - pulmonary, anaesthesia, deep sea diving...

Research and Laboratory[3] - combustion, metabolism, gas purity, physiology...

Industrial[4] - process monitoring, flue gas, alarms.....

Early methods and techniques were mostly chemical (volumetric analysis)[5] - Orsat, Haldane, Lloyd Haldane, Bone and Wheeler, and Scholander. Inferential thermal conductivity and catalytic combustion methods were also used. The ability of oxygen to absorp low-energy beta radiation forms the basis of the electron capture type of detector. A number of developments utilized the strong, paramagnetic susceptibility of oxygen, relative to other gases, and several types of instruments ensued: Thermo-Magnetic, Quincke and Magneto-Dynamic. Electrochemical methods: polarography, coulometry and galvanic; form the basis of a variety of instruments. One of the latest additions to this class of instruments is the solid electrolyte type.

The choice of the type of instrument for a given application depends on factors such as: sample composition, sample condition, environmental conditions, degree of accuracy required, and economy. A thorough understanding of the basic principles upon which the measurement is based and the ability to estimate the errors of the measurement, help in selecting the most suitable type of instrument for a specific application. It should be noted that no one method or technique is suitable for all the measurement conditions one encounters in practice.

2.2 EARLY WORK DEMONSTRATING THE FEASIBILITY OF USING SOLID ELECTROLYTE CONCENTRATION CELLS AS OXYGEN SENSORS

At the turn of the century Nernst was working on alternative and more efficient means of producing visible light than the carbon filament lamp[6]. He chose ionic conductors as means of getting both selective radiation and electric conduction. In 1899[7] he reported the electrolytic conduction of solid solutions at very high temperatures. He investigated oxides such as: SiO_2, ZrO_2, MgO and others; by pressing them into rods, using platinum end connections and observing their conductivity at different temperatures by heating them in an air furnace. He observed: the conductivity of pure oxides increases slowly with temperature and remains relatively low; mixed oxides (e.g. Y_2O_3-ZrO_2) show, at high temperatures, a conductivity much greater than the best wet electrolytes; O_2 evolution at the anode when rods were heated with D.C. These observations, although not conclusive, led Nernst to suggest that a nearly pure electrolytic (oxygen ion) conduction was taking place in the solid electrolyte rods.

Electrolytic conduction of molten salts was first reported by Faraday. A number of workers investigated the conductivity of mixed salts. Van't Hoff[8] collected their results and put a case for the phenomena of solid solutions - isomorphic, mixed crystals, and solid amorphous. He discussed diffusion and ionic flow in solid solutions

and their inter-relationship, and osmotic pressure which gives rise to diffusion. Fritsch[9] measured for a large number of salts, at temperatures between 10 and 180°C, the difference in the electrolytic conductivity between pure and mixed salts. He found that in most cases a small amount of impurity led to a large increase in conductivity. Nernst[10] was the first to give a theory for electrolytic thermo-cells; using the theories of osmotic pressure and ionic migration, he developed an equation for the e.m.f. between the boundary of two solutions of the same substance; but of different concentration:

$$E = \frac{U - V}{U + V} \quad RT \ln \frac{C_1}{C_2} \quad . \quad . \quad . \quad . \qquad (1)$$

where: U is the migration velocity of the +ve ions; V is the migration velocity of the -ve ions; C_1 and C_2 are the concentrations at either side of the boundary; T is the absolute temperature of the system in degrees K; R is the gas constant.

Duane[11] in a number of experiments verified the validity of the Nernst equation for wet electrolytes. Reynolds[12] extended the study of the conductivity of mixed oxides. Haber and St Tolloczko[13] reported the first quantitative study of the electrolysis of solid electrolytes such as $BaCl_2$ and confirmed the validity of Faraday's law. They constructed also Daniell cells using solid electrolytes - $PbCl_2/AgCl$ - that worked in the range 145-250°C, and measured e.m.f. values in agreement with theory.

Many workers attempted; but failed to generate an e.m.f. from the reaction of C/CO with O_2. Haber and Moser[14] achieved this by constructing a cell Fig.1 that used a solid electrolyte (heated Thüringen glass) and porous platinum electrodes on either side of the electrolyte disc. The e.m.fs measured - for concentration changes of gases such as CO, O_2 and H_2/H_2O on one electrode whilst the other was kept on either air or O_2 - were in good agreement with their

calculations. This work demonstrated for the first time the feasibility of using a concentration cell with a solid electrolyte as means of oxygen measurement. The authors state in the introduction: "The idea of constructing a gas fuel cell which would operate at about 500°C or lower using platinum electrodes, in which bringing together CO and O_2 results in their combining under the catalytic action of the platinum was considered and its extensive use for gas analysis purposes was envisaged". Haber designed, with Fleischman[15,16] another cell Fig.2 with which they measured e.m.fs for oxygen and hydrogen concentration cells; and oxy-hydrogen cells with platinum or gold electrodes. The electrolyte was disc shaped made of glass (for 460-580C°) or glazed porcelain (for 800-1100°C). Their results were in good agreement with their theoretical calculations. Further work[17] on H_2 and O_2 concentration cells and on oxy-hydrogen cells showed the e.m.f to be independent of the electrode material. Haber[18] used also iron as electrode material and caustic potash and molten soda as electrolyte. He concluded that platinum on glass or porcelain makes a good oxygen electrode at high temperatures. Katayama[19] constructed solid electrolyte: amalgam concentration cells; metal-halogen cells; and Daniell cells.

So by 1910 solid electrolytes were shown to obey Farady's law and Nernst's equation. Concentration cells - gas, amalgam - and fuel cells were also constructed using solid electrolytes. The use of concentration cells for gas analysis was proposed. The transport of oxygen (pumping) from one electrode to another through the mixed oxide (Y_2O_3-ZrO_2) was observed and Nernst suggested that the conduction was purely ionic (oxygen ion). Though the principle of the measurement, the basic cell design, and some suitable solid electrolytes were known; it took a further half a century to establish the solid electrolyte oxygen sensor as a practical oxygen measurement method. It is also

worth noting that nearly all of todays solid electrolyte oxygen sensors are merely well engineered modifications of the basic design features set out in these early cells.

2.3 PRE-WAR WORK ON REFRACTORIES WITH SOLID ELECTROLYTE PROPERTIES

Zirconium oxide[20], other than its use in the Nernst "glow bar" was of great interest as a potential refractory material. It has a high melting point (2950 ± 20K) a high softening temperature, low porosity and an excellent chemical resistance. Ruff with a number of associates studied this material for over thirty years. They studied the effect the methods and techniques of manufacture[21,22] (powder preparation, impurities, binding agents, firing temperature) have on the: rigidity, shrinkage rate, and porosity; of the product. They observed a large shrinkage (18-20%) around 900°C. They measured also the melting point of pure zirconia and the effect of additions such as: SiO_2, BeO, MgO, Al_2O_3, ThO_2, and Y_2O_3; have on it. They determined the conditions and processes needed to transfer ZrO_2 into a plastic state[23] and developed various ways of "slip" preparation, which included acid or alkaline 'activation'. Of particular interest was their discovery that wares made out of pure ZrO_2 tended to crack, whilst those made with certain additives such as: MgO, Y_2O_3, ThO_2; were more stable. They suspected the existence of a second ZrO_2 form and proposed that the transfer from one form to another caused the cracking. Other workers[24,25,26] had also observed the existence of several forms of ZrO_2 at different temperatures, by using X-ray crystallography. They reported a monoclinic form at medium and low temperatures which transforms into a fluorite type above, 1000°C, a metastable form was also observed. Crystal forms and the effect of additives were investigated - using x-rays - by Ruff and Ebert[27] and they established the presence of a reversible transformation (about 1000°C) from monoclinic to tetragonal, and determined the lattice parameters.

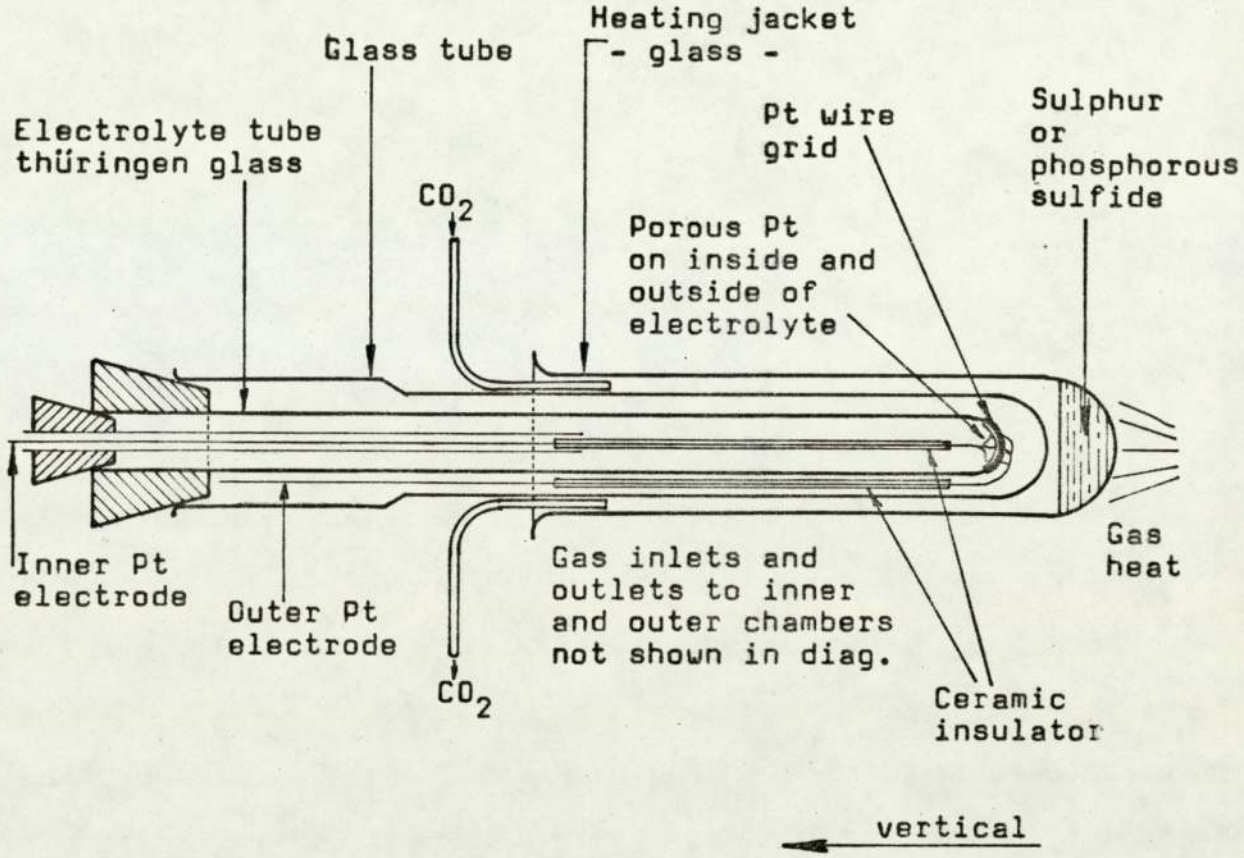

FIG. 1 Fuel/concentration gas cell
- Haber and Moser -

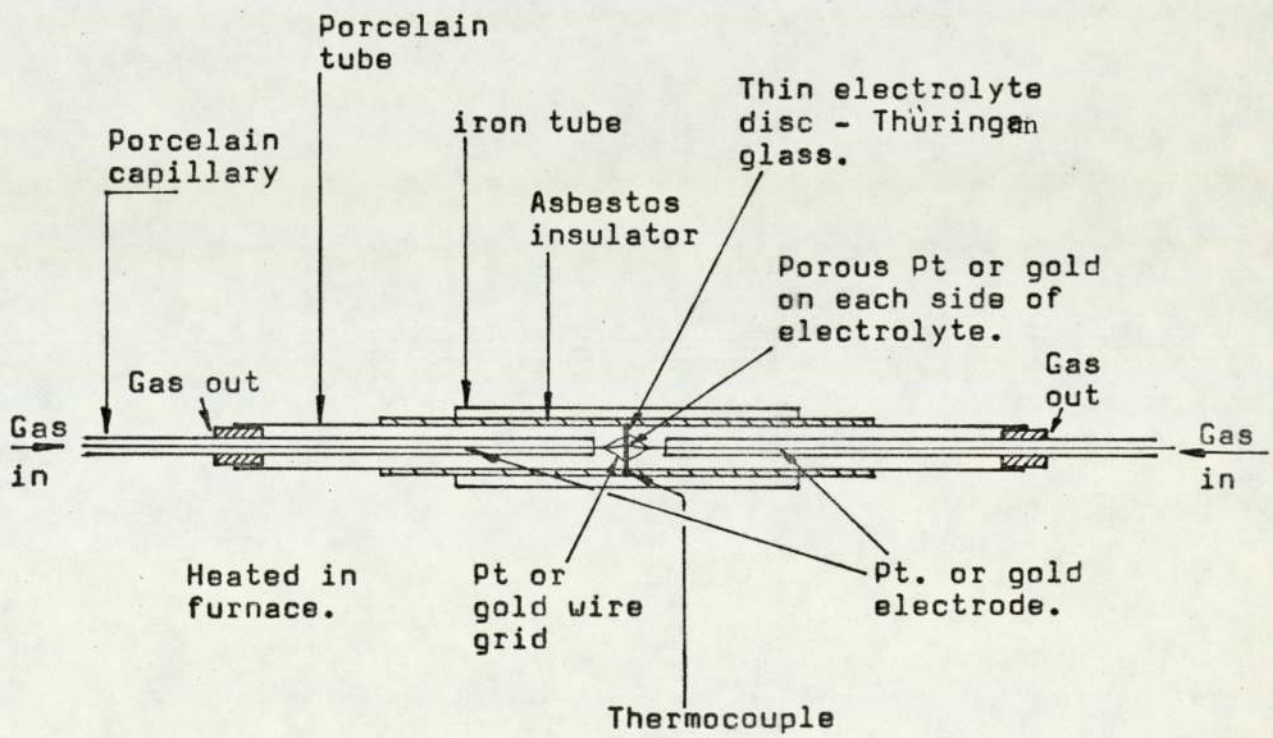

FIG. 2 Oxyhydrogen/concentration gas cell
- Haber and Fleischman -

They also discovered that by limited additions of foreign oxides, such as: MgO, CaO, Sc_2O_3, Y_2O_3 and CeO_2; a cubic lattice of the fluorite type exists, which can stay in the solid phase up to around 1700°C, remaining thus volumetrically stable as it does not suffer any transformation. The systems studied were: (ZrO_2-MgO), (ZrO_2-CaO)[28], (ZrO_2-ThO_2)[29], (ZrO_2-BeO)[30,31], and other combinations [32,33]. Cohn and Tollksdorf[34], using x-rays, measured the parameters of the ZrO_2 monoclinic form (up to 1000°C) and observed the tetragonal form at low and high temperatures. The phase diagram of the system (ZrO_2-MgO) was constructed by Ebert and Cohn[35]. Clarck and Reynolds[36] studied the thermal behaviour of Zirconylchloride and Zirconylhydroxide and found a tetragonal form below 600°C.

The Nernst filament (85% ZrO_2 - 15% Y_2O_3) was well established, by then, as a spectral source; but it was difficult to manufacture. Tingwaldt[37,38] discusses solutions to some of these problems and describes the use of an element in a 2000°C furnace. Ketelaar and Willems[39] investigated the system (SrF_2-LaF_3) and found, using x-rays, solid solutions with a fluorite structure. They demonstrated that this takes place by filling lattice vacancies. X-ray investigations into the systems: (TiO_2-MgO), (ZrO_2-MgO) and (ZrO-TiO_2); were conducted by Bussem et al[40]. Ryschkewitsch[41] reviewed the pure oxide ceramic products and described present-day applications. The phase diagrams of an oxide series with CeO_2 were investigated by Von Wartenberg and Eckhardt[42].

The most relevant parts of all this work were: the discovery of the different crystal forms of pure Zirconia and its transformation from a monoclinic to a tetragonal form around 1050°C; The possibility of stabilizing the crystal lattice into a cubic form by suitable additions forming a solid solution; and the large number of possible - mixed oxides - solid solutions that could be formed.

2.4 PRE-WAR DEVELOPMENTS IN THE THEORY OF CONDUCTION IN SOLID ELECTROLYTES.

It is appropriate at this point to trace the developments of the theory of conduction in solid electrolytes. Thiele[43] investigated thermo-electric currents in electrolytes and measured them in solid electrolytes, for reversible and for non-reversible cells. Joeffe[44], for many years, investigated the phenomena of conductivity in crystals and the factors affecting it: method of preparation, purity, temperature and radiation. He experimented also on the electrolysis of crystals. He proposed the concept that only dissociative ions contribute to the conduction of the crystals. Frenkel[45] formalised this concept quantitatively using temperature dependent probabilities which refer to the dissociation of atoms; their displacement into the inter-lattice space and their recombination with vacancies. He calculated from this the electrical conductivity of binary salts as a function of temperature. Reinhold[46] interpreted the thermo-electric force as a complex quantity - a homogenous and a hetrogenous thermo-electric effect - he calculated these for a solid electrolyte with metallic and gas electrodes and confirmed their existence experimentally. Wagner[47] derived a formula, for a solid solution electrolyte, that relates the diffusion coefficient to conductivity and transport numbers. Wagner and Schottky[48] formulated a theory (ordered mixed phases) for binary systems and proposed the following possible lattice defects: occupation of interstities, vacancies in the sub-lattice of one component, and substitution. Using statistical thermo dynamics they calculated the number of imperfections as well as the chemical potential and activities, as a function of composition. In 1933 Wagner[49] calculated the e.m.f. of a galvanic cell with a mixed conduction solid electrolyte and gave the following expression for the e.m.f. of an oxygen concentration cell:

$$E = -\frac{1}{4F}\int_{\mu'_{O_2}}^{\mu''_{O_2}} t_{ion}\, d\mu_{O_2} \quad \ldots\ldots (2)$$

Where: t_{ion} is the sum of the ionic transference numberes of the electrolyte; μ_{O_2} is the chemical potential of oxygen at the reversible electrodes; and F is the Faraday constant.

Schottky[50] discussed the conversion of chemical to electrical energy with the aid of heated solid electrolytes (proposed initially by Haber) in light of the Wagner theory[49,51]. Reinhold[52] related measurements of the e.m.f. of a solid electrolyte cell to the formation constant of the solid. Wagner[53] developed the theoretical requirements from which the formation constant for silver sulphide can be deduced from the e.m.f. of a cell. Jost[54,55,56] discussed the mechanism of diffusion and electrolytic conduction in solids (based on Frenkel's treatment) and attempted to identify the constants appearing in the empirical formulae. He considered the influence of polarisation and by accounting for it, obtained better agreement with reported experimental results. Schottky[57] refined these calculations by dropping the assumption of equal number of holes, of each kind of ion, to the number of inter-lattice ions of the same kind, and considered also non-stoichiometric conditions. Jost[58] refined his earlier calculations and allowed for the displacement of ions surrounding an imperfect ion site. Koch and Wagner[59] conducted systematic measurements on the ionic conduction of solid salts ($AgCl+CdCl_2$) and discovered that the conductivity of solid silver chloride is raised considerably by adding cadmium chloride. Now Zintl and co-workers[60,61,62] have shown, using x-rays, for a number of solid solutions that the introduction of some salt into a lattice results in oxygen-ion vacancies in the sub-lattice ($CeO_2+La_2O_3$). Oxide phases with a defect oxygen lattice have also been reported by

Sillen et al[63,64]. Rogner[65] who used D.C. to measure the resistance of ceramic substances (Al_2O_3, BeO, ZrO_2, ThO_2) between 400-1100°C, was aware of the effects of small amounts of impurity on the conductivity. All these developments allowed Wagner[66] in 1943 to explain the electrical conductivity of the Nernst "glow bar" as a predominant oxygen ion conduction resulting from a large concentration of mobile oxygen vacancies in the lattice.

2.5 SUMMARY OF THE RELEVANT DEVELOPMENTS UP TO THE EARLY FORTIES.

Over thirty years had passed since the feasibility of the solid electrolyte: fuel cell, concentration cell and pump were demonstrated; but the tremendous amount of work done in the field of material science and the theory of ionic conduction in solid electrolytes was necessary before the situation was ripe for further progress. These developments can be briefly summarised as:

a) The validity of the Faraday and the Nernst laws were demonstrated for a large number of solid electrolytes.

b) The feasibility of using solid electrolytes for: fuel and concentration cells; and as ionic pumps was demonstrated.

c) Phase studies of solid electrolytes (ZrO_2 in particular) in binary and higher order mixtures were conducted and their crystal structures studied.

d) The influence of selected impurities on the crystal structure stability and on the conductivity of solid electrolytes was under intensive study. (In particular zirconia based solid solutions having a predominent oxygen ion conduction).

e) A theory of conduction for solid solutions was being established and its validity was beginning to be well supported by measurements.

The work of Bauer on fuel cells and in particular on carbon fuel cells working at high temperature (1000°C) using solid electrolytes

such as (85% ZrO_2 + 15% Y_2O_3), should be mentioned here [67,68] as an example of a practical application.

2.6. POST-WAR DEVELOPMENTS LEADING TO THE EMERGENCE OF THE MODERN SOLID ELECTROLYTE OXYGEN SENSOR

Geller et al[69] studied the effect of some oxide additions on the thermal length changes of zirconia. They showed that irregular thermal length changes accompanying phase transformations in Zirconia may be prevented by changing the crystal to the stable cubic form; and they determined the ranges of the additives required to achieve this. They pointed out the low thermal conductivity of the material relative to other ceramics and concluded that high resistance to thermal shock cannot be expected of the stabilized product. Curtis [70] worked on determining the required limits to stabilize zirconia. He identified some mixes which had good resistance to thermal shock; but in all these a small amount of inversion was present resulting in a small and gradual thermal expansion coefficient. Croatto and Bruno [71] constructed galvanic cells using solid electrolytes and used them to measure the affinity, the heat of formation and the entropy of formation at various temperatures. They discuss in other works [72, 73] the electro motive forces of cells with solid electrolytes and consider the general case of electrolytes with mixed conduction, and the possible mechanisms of electrical conduction in solids in relation to lattice disorders in the solid.

They classified cells containing solid electrolytes into:

GALVANIC CELLS	- A/AB/B	(formation type reaction)
CONCENTRATION CELLS	- A_{con}/AB/A_{dil}	(dilution type reaction)
DANIELL CELLS	- A/AB/A'B/A'	(substitution type reaction)
HABER CELLS	- A/AB/A'B/A'B'/AB'/A	(double exchange)

They also listed the fields of interest that result from studying the e.m.f.'s of cells containing solid electrolytes:

a) The determination of the affinity of formation of compounds used as electrolytes.

b) The study of thermo-electric forces connected with solid electrolytes.

c) The study of lattice disorders of solid electrolytes.

d) Chemical manometry.

e) The study of chemical reactions in the solid state.

f) The study of corrosive phenomema.

g) Fuel cells.

Hund and co-workers[74] worked on solid solutions and lattice disturbance using x-rays and density measurements. They investigated the systems: (ThO_2-La_2O_3)[75], (ZrO_2-Y_2O_3)[76], (YOF)[77], (ThO_2-Y_2O_3)[78] and (ZrO_2-CaO)[79]. Hund was also interested in the relation between lattice disorders and electrical conductivity[80] and concluded that the cation lattice was completely occupied and that empty places occur in the anion section and that the oxygen ions' movement though the lattice vacancies are the major source of conductivity. It is worth noting that about this time work on oxide mixtures which have electronic conductivity (semi-conductors) was going on[81,82]. Augustinik and Antselevish[83] investigated the electrical properties of solid solutions in (ZrO_2-MgO and CaO) systems. Charlesby[84] studied the electrical properties of thin oxide films of zirconium. Trombe and Foex[85] studied the electrical conductivity of the system (ZrO_2-CaO) at high temperature. Weininger and Zeimany[86] demonstrated that $O^{=}$ was the means of conduction in the Nernst "glow bar". Duwez and co-workers studied the phase relationships in the systems (ZrO_2-Ce_2O_3)[87], (ZrO_2-Y_2O_3)[88] and (ZrO_2-CaO and MgO)[89]. Trombe et al[90] investigated the properties of Zirconia melted in a solar furnace and observed a substantial change in the electrical conductivity near the zone of transformation.

An interesting work by St Pierre[91] on the PH - viscosity

relationships in the system zirconia-water-polyvinyl alcohol-hydrochloric acid is useful for making zirconia slips.

The (UO_2-ZrO_2) system was investigated by Lamberston and Mueller[92]. Dietzel and Tober[93] conducted a thorough investigation on ZrO_2 binary systems (29 oxides). An example of an investigation into a ternary mixture (In_2O_3-Y_2O_3 and ZrO_2) is the work by Schusterius and Padurow[94]. The (ZrO_2-TiO_2) system was investigated by Brown and Duwez[95] and by Coughanour et al [96] - who also investigated the system (ZrO_2-Nb_2O_5)[97] - and at high temperature by Wallaeys et al[98]. Keler and Godina[99] studied the reactions occuring in mixtures of ZrO_2 and CaO and carbon during heating. Rabenau[100] found perovskite and fluorite phases in ternary mixtures of (ZrO_2-LaO-MgO-CaO). Wittels and Sherril[101] showed, as a result of fast neutron bombardment that monoclinic ZrO_2 is transformed into the cubic phase. They explain this by two mechanisms: stress acting about trapped interstitial atoms and thermal spike effects. A brief review of the zirconia reactions in binary oxide systems is given by Roth[102].

Early work on the stabilization of zirconia resulted in many discrepancies due mainly to: errors in x-ray analysis, impurities, methods of preparation and thermal history; this lead to later workers repeating most of the previous work.

Weber et al[103] determined the characteristics of: CaO, MgO, and CeO_2 stabalized zirconia using high temperature and room temperature x-ray analysis; they investigated also the stability of the solid solutions after heat treatment and confirmed the instability of zirconia stabalized with MgO and CeO_2 whilst showing that CaO remained stable to room temperature. Phase relationships for (ZrO_2-ThO_2) were investigated by Duwez and Loh[104]. A dilatometric study of the behaviour of ZrO_2 and its solid solutions with MgO and CaO was made by Keler and Andreev[105]. They reported dissociation of zirconia

solid solutions (10% MgO, 10% CaO) by cyclic heating to 1200°C and cooling to room temperature. The iron II oxide-ZrO_2 system was investigated above 1300°C by Fischer & Hoffmann [106]. Stocker and co-workers studied: the (ZrO_2- SnO_2) system[107]; the preparation of powders by anamorphous precipitation[108]; the preparation of cubic solid solutions of ZrO_2[109]; the preparation and configuration of some compounds formed by ZrO_2 with tetravalent or trivalent metal oxides[110]; the structure of ZrO_2 based solid solutions [111], the stabilization of cubic zirconia [112]; the evolution of the structure of quadratic zirconia caused by dissolving small quantities of foreign oxides [113], the stability and manner of decomposition of cubic solid solutions of zirconia[114]. Further work on the destabilization of the cubic form of ZrO_2 was carried out by Margulis and Gul'ko[115].

Concentration cells for the study of the activities of co-existing elements in molten iron III, were used by Sanbongi and Ohtani[116]. Aronson and Belle[117] used a cell of the form

$$Fe, FeO/(ZrO_2 + CaO)/UO_{2+x}, \text{ pt } (x: 0.01 \text{ to } 0.2)$$

to investigate the uranium-oxygen system. Kiukkola and Wagner[118] used cells of the form

A, A(O)/solid electrolyte/B,B(O)

to obtain the standard molar free energy of formation of a number of oxides and sulphides. Peters and co-workers used solid electrolyte cells to investigate the equilibria:[119]

$$CO + \tfrac{1}{2} O_2 \rightleftharpoons CO_2$$

and $$C + CO_2 \rightleftharpoons 2CO.,$$

The dissociation equilibrium[120] of CO_2, and the

$$Fe + CO_2 \rightleftharpoons FeO + CO$$

equilibrium[121]. Detailed work on fuel cells using solid electrolyte was conducted by Mobius[122,123]. In a number of patents (one with Peters)[124], he described stable electrodes for fuel cells, and detailed several designs, based essentially on the Haber cells, for

oxygen sensors using solid electrolytes. He also proposed the use of metal/metal oxide as an alternative reference to air. This work heralded the re-emergence of the oxygen sensor utilizing a number of, by now, well researched solid electrolytes. Work continued on the properties of solid electrolyte materials. Cocco[125] re-examined the limits of composition of the cubic phase in the binary system (ZrO_2 - CaO) at high temperatures. An application of using solid electrolytes for high temperature heaters is described by Keler and Nikitin[126]. An interesting study was conducted by Kingery et al[127] on the oxygen mobility in cubic $Zr_{0.85}\ Ca_{0.15}\ O_{1.85}$, which was determined by exchange measurements using the stable isotope O^{18} and a mass spectrometer. They report a nearly wholly ionic conductivity. Conductivity measurements at various temperatures on mixed oxides was made by Noddack et al[128]. Stocker[129] reviewed (in 1960) zirconia and the problems of stabilizing it and reported his contributions to the subject; he mentions that the mechanism of the stabilization and the nature of the product are still not well known. The electrical conductivity of the system (CeO_2 - ZrO_2) was studied by Pal'Guef and Volchenkova[130], they reported a very small ionic conductivity in this system. They also studied thoroughly the (ZrO_2 - CaO) system[131]. Pal'guev and Neuimin[132] studied the conductivity of solid oxides by the measurement of the e.m.f. Equilibrium diagrams for the systems zirconia - rare earths were presented by Collongues et al[133], they used the co-precipitation method whose formation mechanism is described by Lefevre et al[134] and Stocker[135].

Though industrial interest in solid electrolytes was in their potential use in fuel cells, some corporations began to sense their importance as oxygen sensors. Weissbart and Ruka who reported an "oxygen gauge"[136] in 1961, which was basically an engineered Haber

cell using a ($ZrO_{2\ 0.85}$ - $CaO_{0.15}$) solid electrolyte system; reported also a solid electrolyte fuel cell[137] of a very similar design. They were also the first in the west to file a patent application relating to the use of solid electrolyte systems as oxygen sensors, and describe their construction, usage, and suitable electrolytes, (application U.S. No. 126098, July 1961; U.S. patent 3,400,054). The validity of the claims in the patent are a matter of controversy; nevertheless this was the commercial beginning of the solid electrolyte oxygen sensor which, in the years to come, was to carve for itself a major position in the field of oxygen measurement .

2.7 GENERAL RULES FOR THE CHOICE OF AN ELECTROLYTE SYSTEM FOR A SOLID ELECTROLYTE OXYGEN SENSOR

Some general rules could be laid down for such a choice. The electrolyte system should have the following features:

a) it should not form deposits on the electrodes;

b) it should have the same basic reaction at either electrode;

c) it should have nearly pure oxygen-ion conductivity;

d) it should present a high enough conductivity at the working temperature range so as to make the e.m.f. measurement feasible;

e) the solid electrolyte should be stable with temperature and with time;

f) the solid electrolyte should present a reasonable - working - resistance to thermal shocks;

g) the cost of the raw materials and the manufacturing processes should not be prohibitive.

2.8 FURTHER DEVELOPMENTS

2.8.1 MATERIALS

Weber[138] draws attention to the inconsistencies in zirconia literature due to the early papers by the pioneers who drew erroneous conclusions from their observations due to the use of impure materials. Smith and Cline[139] reported the existence of cubic zirconia at high

temperature, a claim which is challenged by Weber. A detailed study of the system (ZrO_2 and rare earths) was undertaken by Perez Y Jorba[140]. An important note by Buckley[141] discusses the deterioration of calcia partially stabilized zirconia subjected to severe thermal cycling, the loss of stabilization is brought about by the Ca diffusing out of the solid solution. Schmalzried[142] discusses the ($CaO-ZrO_2$) system as electrolyte for electro-chemical experiments at high temperatures. Aleshin and Roy[143] determined limits on the possibilities of ionic substitution in pyrochlore and prepared a large number of compounds with both cationic and anionic substitutions. LeFevre[144] studied in detail the systems ZrO_2 and HfO_2. Buckley and Wilson[145] reported again on the de-stabilization of zirconia by cyclic heating. This was investigated further by Smoot and King[146]; They related it to impurity levels in the solid solution, and recommended a total impurity level below 0.5% for CaO stabilized ZrO_2. The use of solid solutions, possessing the fluorite lattice, of some Group IIa or IIIa oxides in thoria and zirconia, as solid electrolytes, is discussed by Alcock and Steele[147]. Smoot and Whittemore[148] confirmed earlier results on improved stability of stabilized zirconia by minimising impurities. Delamarre and Perez Y Jorba[149] studied the hafnia system. Barbariol[150] determined the field of existence of the cubic phase for the system (ZrO_2-CaO). Deportes et al[151] reported a self crucible method for the preparation of homogenous and dense samples of stabilized zirconia. Mazdiyasni et al[152] developed a method for preparing ultra-high-purity submicron refractory powders. They also described a method for cubic phase stabilization of transluscent Yttria-zirconia at very low temperatures[153]. Bartuska[154] discusses problems encountered with the stabilization and sintering of zirconia. Baker and West[155] examined a number of solid electrolytes for their suitability for use at steel making temperatures. Noguchi et al[156]

measured the freezing points of compositions in the (ZrO_2-CaO) system using a solar furnace. Bessonov and Taksis[157] developed a method of heating and simultaneous x-ray and thermographic analysis, and monitoring of electrical resistance. They used this to study the reported instabilities in the zirconia calcia system, and reported the formation of calcium zirconate which passes into the solid solution. Demonis and Popil'skii[158] reported that (ZrO_2-8-12 mole % Y_2O_3) was stable under prolonged heating. The system (ZrO_2-CeO_2-Y_2O_3) was studied by Forestier et al[159]. The phase diagrams of the system (HfO_2-Y_2O_3) was obtained by Duclot et al[160]. Michel et al[161] reported the production of calcia stabilized zirconia mono-crystals. Gravie[162] determined the range of existence of the cubic phase in the system (CaO-ZrO_2). Baukal and Scheidegger[163] determined the lattice constants for the cubic solid solutions (ZrO_2-CaO and ZrO_2-Y_2O_3). Kohler and Glushkova[164] discuss the influence of additions of rare-earth oxides on the polymorphism of zirconia and hafnia. Spitsbergen and Houpt[165] used an arc melting procedure for rapid heating of mixtures of zirconia and rare-earth oxides which they examined by x-rays. White[166] reported on the progress in high temperature, zirconia electrolyte technology at General Electric. He announced also that GE are developing an oxygen sensor to the stage of a commercial product, for laboratory and for industrial applications.

2.8.2 MEASUREMENTS OF ELECTRICAL PROPERTIES

Work on the polarization in electrolytic solutions was still being conducted in the early fifties[167]. MacDonald[168] developed a linear theory to account for the behaviour of solid or liquid materials which have charge carriers capable of free movement within the material only. Friauf[169] measured the polarization effects in the ionic conductivity of silver bromide. Danforth studied polarization in thorium oxide crystals[170].

Hoffmann and Fischer[171] measured the conductivity of calcia stabilized zirconia at different temperatures and with the inclusion of some iron oxides. Tien and Subbarao[172] studied the system (ZrO_2 - CaO) using x-rays and conductivity measurements. The same system was studied by Cocco and Barbariol[173]. This was also investigated by Vest[174]. The electrical resistivity of stabilized zirconia at elevated temperatures was measured by a four-probe technique by Dixon et al[175]. Schmalzried[176] used a gas galvanic cell to investigate the ionic and electronic conduction in binary oxide electrolytes. The high temperature electrical conductivity in the systems (CaO - ZrO_2) and (CaO - HfO_2) were measured by Johansen and Cleary[177]. The electrical conductivity of the system (ZrO_2 - $CaZrO_3$) was measured by Tien[178] who also measured the grain boundary conductivity of the ($Zr_{0.84}$ $Ca_{0.16}$ $O_{1.84}$) ceramic. Strickler and Carlson[180] examined the ionic conductivity of cubic solid solutions in the system (CaO - Y_2O_3 - ZrO_2). Vest et al[181] investigated the defect structure of monoclinic zirconia by measuring the oxygen partial pressure dependence of the electrical conductivity and sample weight. Bray andMerten[182] give a simple theoretical treatment of conduction in solids and apply it to stabilized zirconia. Oxygen exchange and diffusion in calcia-stabilized zirconia was measured by Simpson and Carter[183]. Rhodes and Carter[184] measured the Cationic diffusion in Calcia-stabilized zirconia. Takahashi and Iwaharah[185] measured the oxygen ion conduction in the system (CeO_3 - La_2O_3). Lasker and Rapp[185] developed a model for the prediction of mixed conduction in ThO_2 and (ThO_2 - Y_2O_3) solutions. Hartung and Moebius[187] discuss the AC polarization on platinum electrodes in oxygen ion conducting solid electrolytes. The oxygen pressure dependence and electro-chemical polarization of oxygen-ion conducting mixed oxides are discussed by Peters and Radeke[188]. Mixed conduction in

$(Zr_{0.85}\ Ca_{0.15}\ O_{1.85})$ and $(Th_{0.85}\ Y_{0.15}\ O_{1.925})$ solid electrolytes were measured using a d-c polarization technique by Patterson et al[189]. Steele et al[190] measured the electrical conductivity of selected oxide solid solutions possessing the fluorite, pyrochlore and perovskite structures. The electrical conductivity and structural defects of monoclinic HfO_2 at high temperature were investigated by Robert et al[191]. Carter and Roth [192] discussed the conductivity and structure in Calcia-stabilized zirconia. Alcock[193] discussed the transport of ions and electrons in ceramic oxides. Duclot and Deportes[194] described apparatus that produces the change of both thermal expansion and electrical conductivity as a function of temperature. Solov'eva et al[195] examined concentration polarization in solid electrolytes. An excellent review paper that covers the subject of the electrical properties of solid oxide electrolytes comprehensively was given by Etsell and Flengas[196]. Hammou et al[197] studied the conductivity of the solution $(ThO_2)_{0.75}$ - $(CeO_2)_{0.25}$ with temperature. Iqbal and Baker[198] measured the total A.C conductivity of Thoria-Yttria solid solutions at high oxygen pressures. The oxygen self-diffusion and electrical transport properties of non-stoichiometric ceria and ceria solid solutions were measured by Steele and Floyd[199]. Heyne and Beekmans[200] discussed the electronic transport in calcia-stabilized zirconia. Bauerle[201] studied solid electrolyte polarization by a complex admittance method. Etsell and Flengas[202] studied N-type conductivity in stabilized zirconia. Schouler et al[203,204] applied the complex admittance method to the study of some electrode reactions of stabilized zirconia. Schouler and Kleitz[205] studied the capacitive effects at an oxygen-silver-stabilized zirconia interface. Schouler et al[206] plotted the complex impedance of electro-chemical cells based on yttria doped thoria. Beekmans and Heyne[207] established a

correlation between impedance, micro structure and composition of calcia - stabilized zirconia. Foultier and Kleitz[208] directly determined the electrical conductivity - nonstoichiometry relationship in ionically conducting metallic oxides.

2.8.3 APPLICATIONS OF OXYGEN-ION CONDUCTING SOLID ELECTROLYTES

In a number of papers Mobius[209,210,211] examines the possible applications of oxygen-ion conducting solid electrolytes, and thoroughly reviews the available electrolytes. The following main applications emerge: fuel cells (these will not be discussed), galvanic cells, potentio-metric analysis of hot gases, and the measurement of absolute temperature.

GALVANIC CELLS FOR THERMODYNAMIC STUDIES - The thermodynamic characteristics, for a chemical reaction or other reversible process which tends to occur spontaneously at any specified constant temperature and pressure and which can be harnessed into a galvanic cell, are the following as given by Rose et al[212].

$$-\Delta G = nFE \quad \ldots\ldots\ldots\ldots (3)$$

$$\Delta S = nF \frac{\partial E}{\partial T} \quad \ldots\ldots\ldots\ldots (4)$$

$$-\Delta H = -\Delta G - T\Delta S = nFE - nFT \frac{\partial E}{\partial T} \quad \ldots\ldots (5)$$

Where: ΔG is the free energy of the reaction; n the number of equivalents passed across the cell; ΔS the change in entropy; $\frac{\partial E}{\partial T}$ the temperature coefficient of the cell; ΔH the heat of reaction; and K the equilibrium constant for the reaction at the specified temperature. Moreover if all the substances participating in the reaction are at unit activity, (at a partial pressure of 1 atmosphere) the quantities E, $-\Delta G$, ΔS and $-\Delta H$ will have their "standard" values E°, $-\Delta G^\circ$, ΔS° and $-\Delta H^\circ$ for the specified temperature and,

$$nFE^\circ = -\Delta G^\circ = RT\ln k \quad \ldots\ldots\ldots\ldots (6)$$

Early work in this field used cells with molten or solid salts, and the use of solid electrolytes for such applications has been mentioned earlier[116,117,118,119,120,121]. Carter[213] determined the dissociation pressures of solid solutions from Fe_3O_4 to $0.4(Fe_3O_4)$. ($Co\ Fe_2O_4$) as a function of temperature. Schmalzried[214] measured the free reaction enthalpy with the formation of spinel phases from single oxides; and with Benz[215] measured the free formation enthalpies of solid phases in the ($PbO - SiO_2$) system. Horsley[216] observed the variation of the e.m.f. with temperature for cells having a variety of metal oxides. The thermodynamic characteristics of niobium oxides were investigated by Gerasimov et al[217]. Rapp and Maak[218] measured the properties of solid copper-nickel alloys. The uranium oxides were studied by Kiukkola[219]. Hoch et al[220] used cells with NbO, FeO and TiO. Rapp[221] determined the free energy of formation of MoO_2. Blumenthal and Whitmore[222] studied phase equilibria in the Titanium-oxygen system. Data on spinel phases (chromite, ferrite, aluminate) were measured by Tretjakow and Schmalzried[223]. Zador[224] conducted non-stoichiometric measurements in dioxides of the rutile structure. Kubik and Alcock[225] surveyed experiments on activities in solid binary systems. Rickert and Steiner[226] measured the oxygen diffusion in metals at elevated temperatures.

Partial free energies of solution of oxygen in liquid lead and values for the solubility of oxygen in liquid lead were measured by Alcock and Belford[227]. Pluschkell and Engell[228] determined the oxygen content of molten copper; whilst Fischer and Ackermann[229] determined the oxygen content of molten iron. Osterwald[230] measured e.m.f's in liquid copper in equilibrium with solid or liquid copper(I) oxide. The activities in PbO containing melts were discussed by Jeffes and Sirdhar[231]. Diaz and Richardson[232] described the

design and operation of a cell for the continuous measurement of oxygen in liquid silver and copper.

From these fundamental studies interest in industrial applications developed. Kolodney et al[233] describe a sensor for the continuous measurement of oxygen in liquid sodium; Pluschkell and Engell[234] describe a sensor for the determination of oxygen content of copper melts. Wilder[235] discusses the direct measurement of the oxygen content in liquid copper; and the activity of oxygen in dilute liquid Cu-O alloys. We can have an idea of the commercial interest in this method for measuring oxygen in molten metals by looking at the U.S. patents granted for such devices (Appendix I).

Steele[236] gives a comprehensive survey of the subject of high temperature thermodynamic measurements involving solid electrolyte systems.

POTENTIOMETRIC ANALYSIS OF HOT GASES - This application - first suggested by Haber - developed into the major industrial application of these devices, a glimpse at the U.S. patents granted for such devices (Appendix II) gives an idea of the extent of commercial interest. Littlewood[237] describes a sensor developed by BISRA for oxygen measurements in hot gases. Spacil[238] describes the principles and applications of the solid electrolyte oxygen sensor. Ullmann et al[239] discuss the continuous measurement of oxygen in gases. Lawrence et al[240] describe the theory and applications of the solid electrolyte oxygen sensor. Industrial uses of the sensors are described by Record[241] by Cooke et al[242] and by Fairbank[244]. Brown et al[243] describe the use of oxygen sensors in glass furnaces.

Pollution control regulation opened up a new market for car exhaust gas control, resulting in a tremendous commercial interest as indicated by the number of U.S. patents granted (Appendix III). Zechnall and Baumann[245] describe how a cleaner car exhaust gas can be obtained

by using a feedback control system based on an oxygen measurement.

MISCELLANEOUS APPLICATIONS - The use of a high temperature solid electrolyte oxygen sensor as means for the determination of high-fixed point temperatures on the thermo-dynamic scale is proposed by Lindsay and Ruka[246]. Rickert[247] discusses kinetic measurements with solid electrolytes - reaction rates and chemical potential of activities. The possible use of solid electrolytes as high-temperature electrode material for M.H.D. is discussed by Roberts[248] and by Casselton and Watson[249]. A method to measure BOD is described by Butzelaar and Hoogeveen[250]; whilst Voorn and Marlow[251] describe a meter for measuring TOD. A method of measuring oxygen fugacity is described by Williams[252]. Gauthier and others[253] describe the possible use of a modified sensor for the determination of gaseous oxides. A technique for generating partial oxygen pressure between 1 and 10^{-12} atm. is described by LeBrusq et al[254]. An oxygen leak source is described by Mogab[255]. Agrawal et al[256] gives a technique for controlling oxygen activities in Argon-Oxygen mixtures by coulometric titration. Foultier and Kleitz[257] describe an electrically renewable and controllable oxygen getter.

CHAPTER THREE

MARKETS FOR THE SOLID ELECTROLYTE OXYGEN SENSOR AND A REVIEW OF THE AVAILABLE COMMERCIAL INSTRUMENTS

3.1 THE MAIN FEATURES OF THE SOLID ELECTROLYTE OXYGEN SENSOR[259]

In considering the market potential of the solid electrolyte oxygen sensor, one must bear in mind its salient intrinsic features that distinguish it from other methods of oxygen measurements. These can be divided into:

DESIRABLE FEATURES:

Fast response	-	its intrinsic response is in milli-seconds;
Absolute measurement	-	its adherence to the Nernst equation offers the potential of an absolute measurement obviating the need for calibration gases and relying solely on accurate e.m.f. and absolute temperature measurements;
Logarithmic output	-	it has the same output per decade for any range, giving it an advantage at low O_2 levels;
Versatile shape	-	it can be made in a variety of shapes (discs, tubes, crucibles etc.)
In situ measurement	-	as a probe it gives the ability to do in situ measurements (wet analysis, no sampling system);
No moving parts	-	it is less fragile in that sense only;
Independent of pressure variations	-	if reference and sample are both at the same pressure.

UNDESIRABLE FEATURES:

Fragile	-	material cracks easily when exposed to thermal shocks and gradients;
High operating temperature	-	this poses safety problems, possible combusion at the electrode;

Logarithmic output	-	low sensitivity at high O_2 levels, need linearising for use as control parameter;
Need of a reference	-	Gas or sealed metal/ metal oxide .
Dependent on pressure	-	if reference and sample are at different pressures.

3.2 MEASUREMENT OF LOW O_2 CONCENTRATIONS

Low concentration O_2 in non combustible mixtures is an ideal application for the sensor, utilising its high sensitivity at low concentrations and fast response time. Applications such as: O_2 demand rate, O_2 efficiency, pulmonary functions in the medical field[259], OR, industrial and laboratory applications such as: oxygen impurities in high purity gases, inert gas blanketing, O_2 detection in inert atmospheres, dialysis and O_2 transmission through porous media, safety monitors etc.

Both industrial and laboratory instruments are available as shown in Table 1. The table compares some of the instruments' specifications. Most of these units use the basic "test tube" sensor as shown in Fig.3. A miniature "test tube" sensor with a sealed in Pd/PdO reference is shown in Fig. 4.

There is also a limited need for specialised instruments in this category such as a total oxygen demand meter (Philips marketed the PW 9625 for a while), and monitoring combustion in internal combustion engines (the equivalence ratio monitor is marketed by C.R. Lab.Services).

3.3 IN-SITU MONITORING OF INTERNAL COMBUSTION ENGINES EXHAUST[259,260]

The I.C. Engines' contribution to air pollution created a market for the monitoring of the air/fuel ratio in cars. This ratio significantly affects both the efficiency of the engine and the composition of the exhaust gas. Normal petrol engines are most efficient at a ratio of about 14.7 by weight (nearly the stoichiometric ratio). This also lowers the CO; the oxides of nitrogen; and hydrocarbon

SPECIFICATIONS OF SOME COMMERCIAL LOW CONCENTRATION SOLID ELECTROLYTE O_2 ANALYSERS

TABLE 1

MAKE	WESTINGHOUSE 209 (USA)	APPLIED ELECTRO CHEM. S-3A (USA)	ENGELHARD (UK)	SIMAC DS 2000 (UK)	McCANALSE TYPE S (F)	HERRMANN-MORITZ BB10 (F)
TYPE OF CELL	Test tube at $850^{o}C \pm 1.5^{o}C$	Test tube at $750^{o}C$	Test tube at $800^{o}C$	Test tube at $800^{o}C$	Test tube at $850^{o}C$	Miniature test tube Pd/PdO sealed in reference $700^{o}C$.
SPEED OF RESPONSE	1 m.s. (cell)	1 second (inst.)	20 seconds (inst.)	15 seconds (inst.)	excellent	———
RANGE	0.8-15 ppm 80-15,000 ppm 0.8%-100% O_2 Calib.in torr. possible.	0-100 ppm 0-10,000 ppm 0-100% O_2	0.01 vpm to 100%	0.01 vpm to 100% 8 ranges (auto)	21% to 0.3% 0.7% to 100vpm 210 to 3 vpm 7 to 0.1 vpm	1-100 ppm 100-10,000ppm 1-100%
ACCURACY: CELL INSTRUMENT	1% FSD $\pm$ 2% FSD	——— $\pm$ 0.1% FSD	——— $\pm$ 1mV	——— 1%	——— $\pm$ 2%	——— $\pm$ 2%
FLOW RATE ml/M	250	400	160	300	100	500

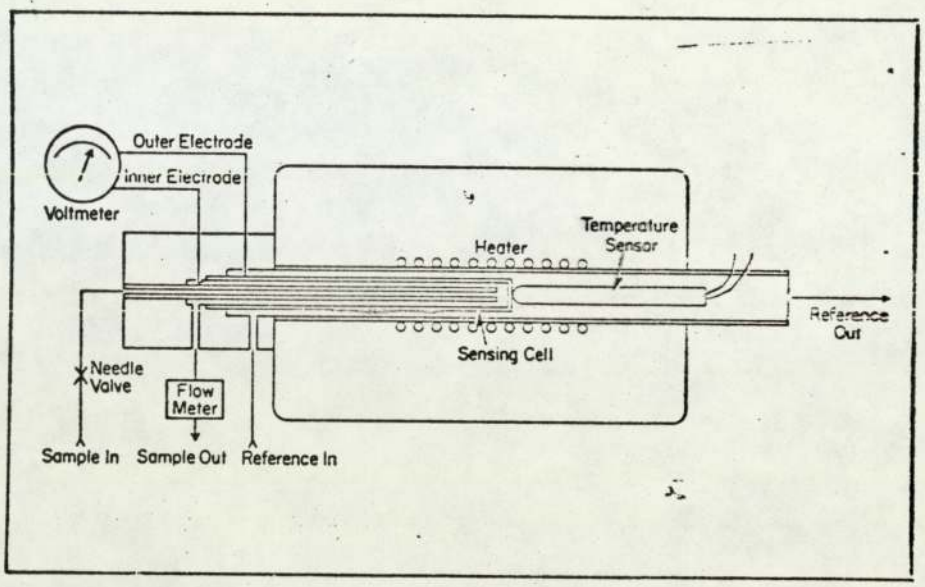

FIG 3 'TEST TUBE' TYPE SOLID ELECTROLYTE SENSOR.

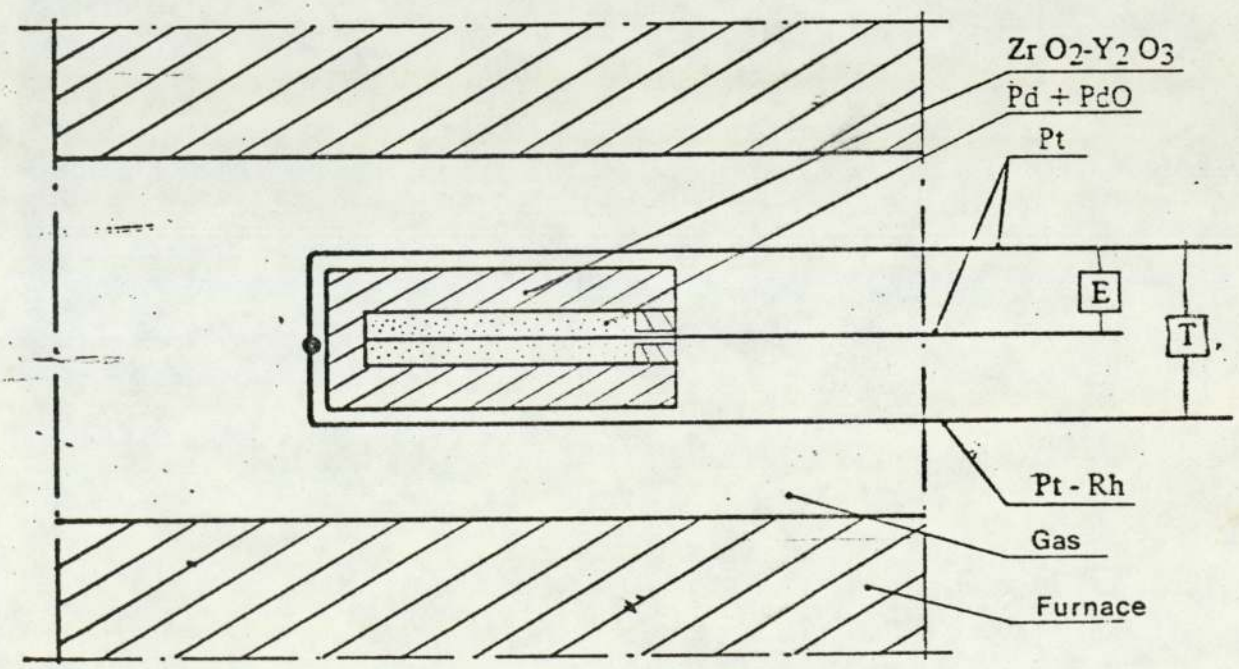

FIG. 4 MINIATURE 'TEST TUBE' SOLID ELECTROLYTE SENSOR WITH SEALED IN Pd/PdO REFERENCE

levels in the exhaust gas. Some modern engines are provided with a feedback control system using an O_2 sensor which monitors the O_2 concentration in the exhaust gas and that is taken as an indication of the actual ratio of the combustion mixture (e.g. U.S. Patents 4,094,186 and 4,655,792).

Numerous patents have been registered on such devices - the majority being either a variable resistance sensor or a solid electrolyte O_2 sensor. Fig. 5 a,b and c show typical commercial sensors of that type most of which are developed in association with car manufacturers. This is a high volume low cost market. The competition is fierce. The environment the sensor is required to function in is rough. It requires rugged, simple, cheap and reliable designs.

3.4 THE MONITORING OF O_2 ACTIVITY IN MOLTEN METALS[261,262]

The measurement of the oxygen activity of a molten metal is very desirable. It allows, for example, the production of steel with a desirable oxygen content; and the monitoring of oxygen content in liquid sodium (coolant in some nuclear reactors). The environmental conditions here are extreme and many designs attempting to solve problems such as life time, corrosion, thermal shock damage etc. have been proposed as indicated by the large number of patents taken in this field. Fig. 6 a and b show two examples. A commercial expendable probe manufactured by Leigh Instruments Ltd. was one of the first to appears in this market.

3.5 THE MONITORING OF ATMOSPHERES IN SPECIALISED FURNACES[263,264,265,266,267,268]

Although low concentration O_2 instruments can be used for this type of application, some instruments were developed specifically for this purpose. An example is the ARL EOM 600 probe shown in Fig.7 which can be inserted in heat treatment zones (600-1200^{o}C). It has been used in bright annealing furnaces where the sensor output can be related to

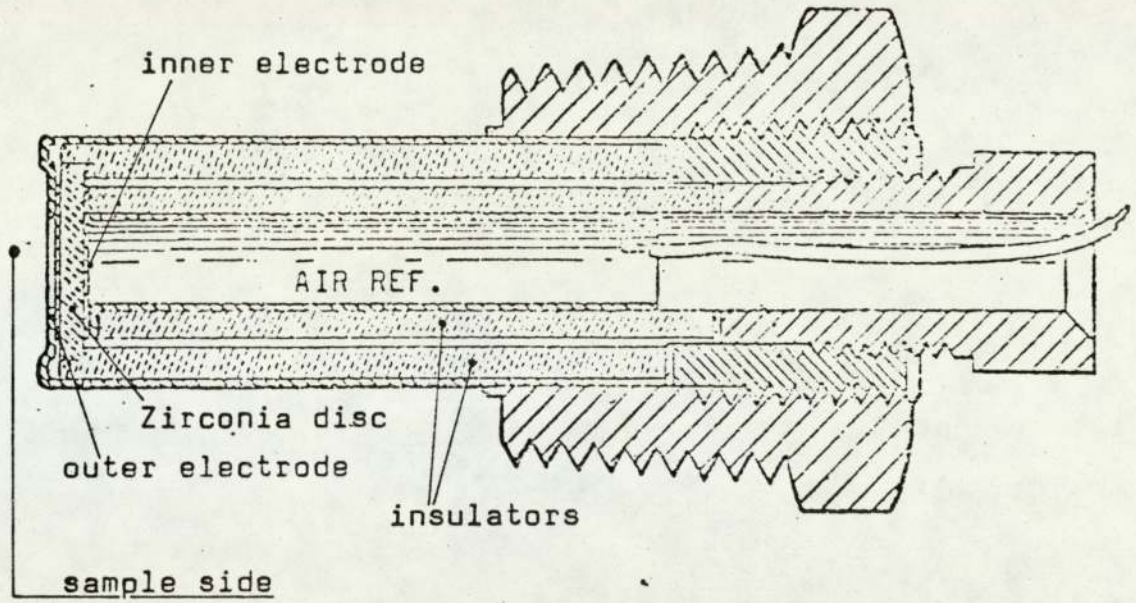

FIG. 5a

I.C. ENGINE S.E. O_2 SENSOR U.S. PATENT NO. 3,940,327 (Universal Oil Products Co.)

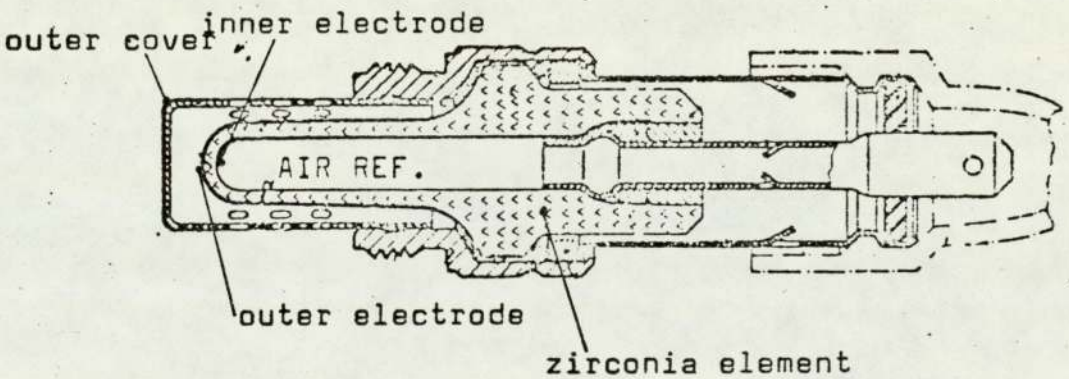

FIG. 5b

I.C. ENGINE S.E. O_2 SENSOR U.S. PATENT NO. 3,960,693 (R.Bosch G.m.b.H)

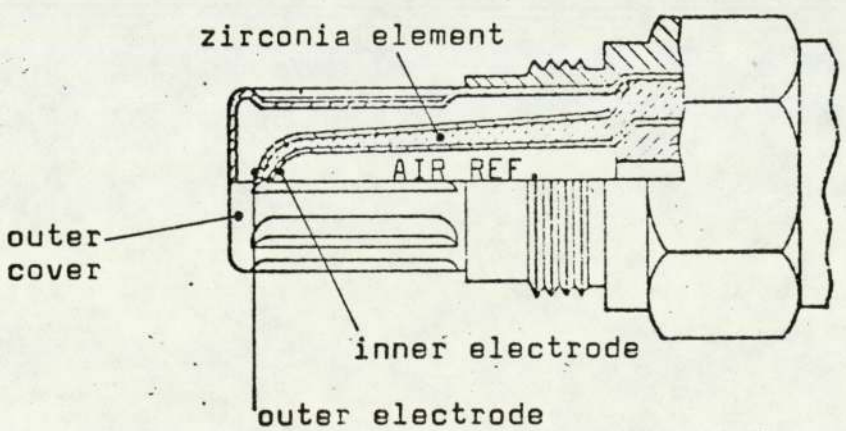

FIG. 5c

I.C. ENGINE S.E. O_2 SENSOR U.S. PATENT NO. 4,098,653 (Nissan Motor Co.)

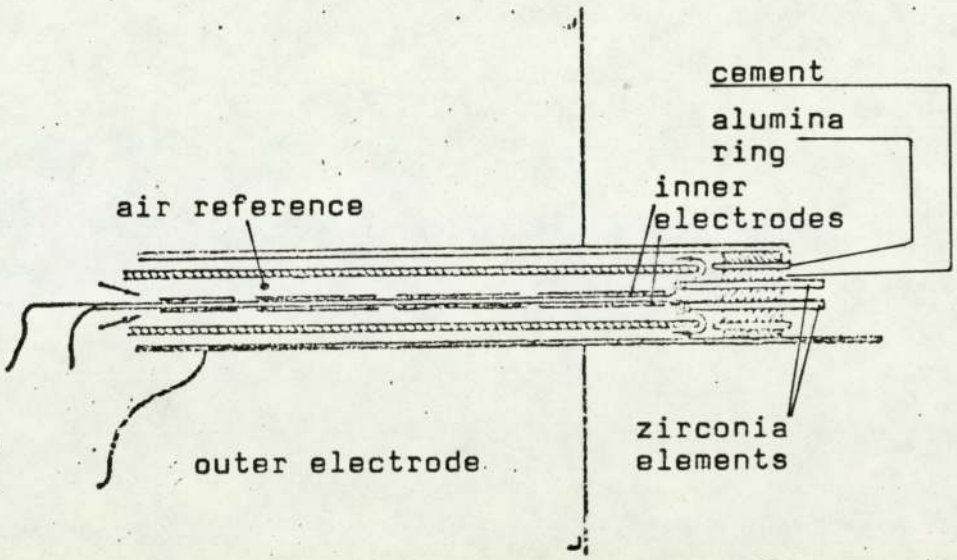

FIG.6a Solid electrolyte O_2 sensor for continuous measurements in Molten Metals U.S.P. No. 3,719,574 (U.K. origin)

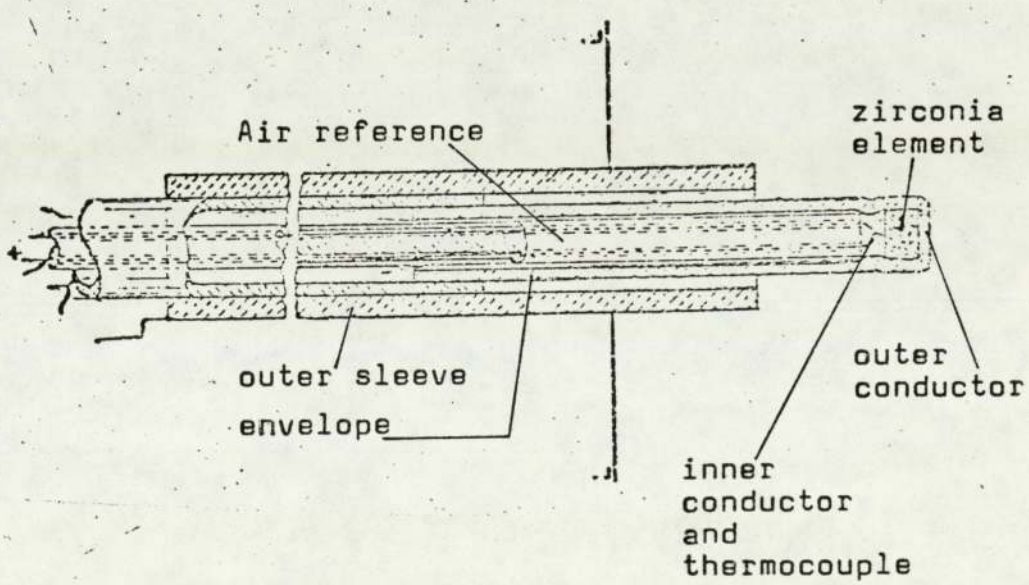

FIG. 6b Solid Electrolyte O_2 sensor for continuous measurements in Molten Metals U.S.P. No. 3,773,641 (U.S.A. origin)

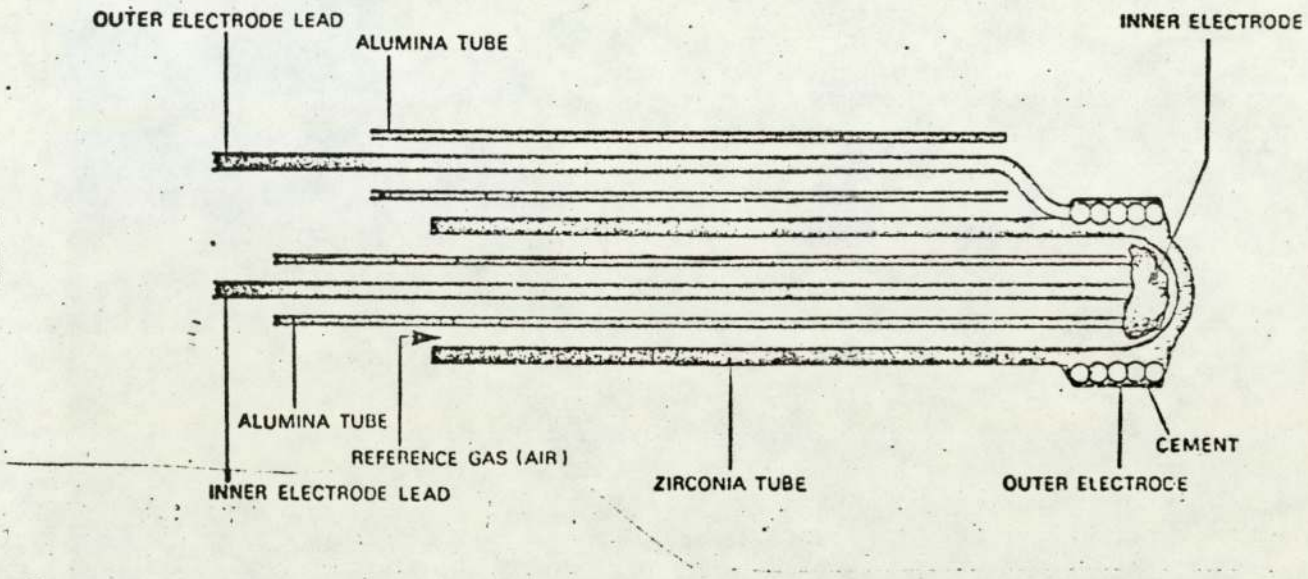

FIG. 7 ARL EOM 600 PROBE

Fig. 8a

The probe output corresponding to scaling and non-scaling conditions for the iron --wustite reaction at 700°C

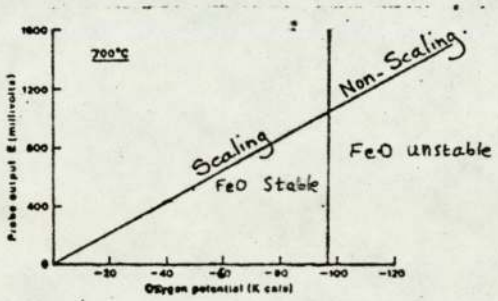

Fig. 8 b

The probe output corresponding to scaling and non-scaling conditions for the iron —wustite reaction at 1100°C

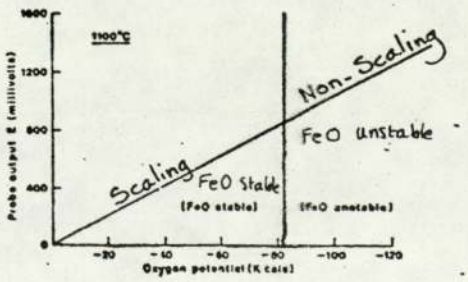

the oxygen potential and hence the scaling and the non-scaling conditions determined as shown in Fig.8 a and b. The instrument's sensitivity to carbon potential has found applications in carbonitriding and carburising atmospheres. Oxygen levels 10^{-2} to 10^{-20} atm. can be sensed with a stated accuracy of $\pm$ 5%.

3.6 OXYGEN MEASUREMENT IN HIGH TEMPERATURE[269]

Oxygen measurement in high temperature glass, ceramic and similar furnaces (1000-1600°C) have necessitated the development of sensors capable of operating at high temperatures. Corning offer the 00-3-HT sensor "test tube" partially stabilized zirconia. They quote a life time of about 6 months, a response time of about five seconds, a conformity to the Nernst equation to within $\pm$ 0.5% O_2 between 650-1600°C. The Westinghouse 310 Fig. 9 is interesting because it is operated in the current mode as an oxygen pump or in the check mode as normal. An applied e.m.f., between the electrodes, pumps the oxygen from the cavity to the air reference side, lowering thus the partial pressure of the O_2 within the cavity without changing the total pressure. O_2 diffusing from the process side to the cavity where it is pumped into the reference side results in a current which is directly proportional to it, hence a linear output. In reducing conditions, O_2 is pumped from the reference side to the cavity side protecting thus the electrodes from sulphurous reducing gases. Accuracy of $\pm$ 0.5% O_2 or 10% of reading, and response time of 1 second are quoted.

3.7 COMBUSTION CONTROL BY OXYGEN MONITORING[270,271,272,273]

This market which was a relatively modest one, expanded slightly in the early seventies due to the increased interest in pollution control; but developed into a huge market as a result of the so-called energy crisis. The increasing costs and diminishing sources of prime energy led to interest in means and ways of reducing fuel consumption. This resulted in the emergence of the air/fuel regulation method as a means

Fig. 9 — Probe end assembly of Model 310 (Westinghouse)

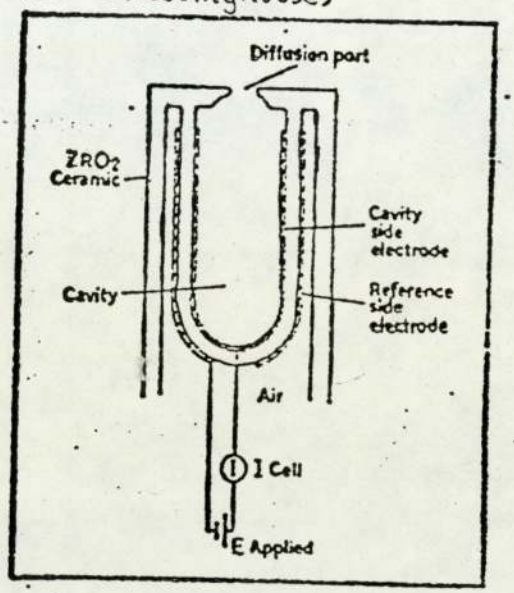

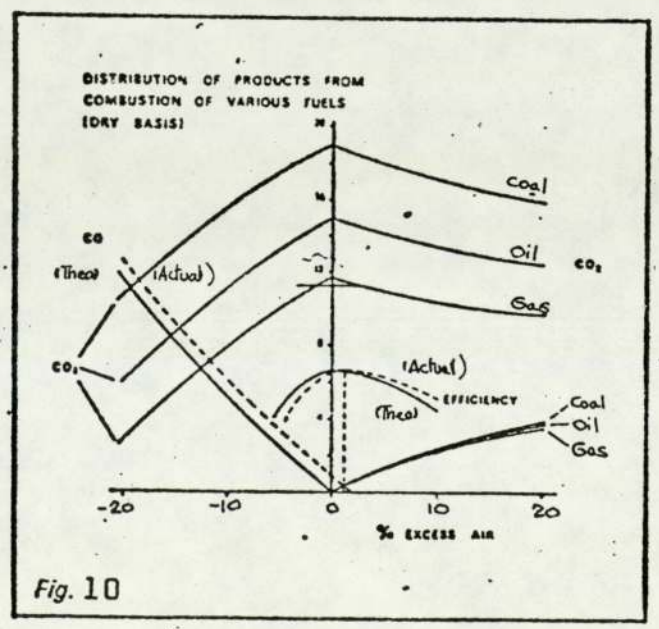

Fig. 10

of increasing combustion efficiency. Fig. 10 shows the products of combustion for various fuels and suggests that CO [274], CO_2 and O_2 can be used as control parameters. It is clear from the curve, however, that CO_2 concentration varies with combustion efficiency and the type of fuel used. It is also clear that for a given CO_2 value there exists two possible air values. CO is indefinite due to its very low concentration at the optimum level. On the other hand, O_2 has a more definite relationship, and it has been accepted as the most useful parameter. It suffers however from the effect of air leakage making the O_2 value, at a given sampling point, higher than that at the combustion level. The potential industrial market is huge: power boilers, recovery boilers, refinery process heaters, multiple fuel powered boilers, coke oven batteries, lime and cement kilns, blast furnaces, copper smelters, sulphur burners, large heating boilers etc. However, the market needs are not all the same resulting in a number of specific requirements.

3.7.1 The Combustion Process

This consists of mixing a combustible material with oxygen - usually air - in the correct ratio - stoichiometric - then if the temperature of the mixture is above that required for ignition, combustion occurs. The heat generated from the reaction depends on a number of parameters:

Fuel - This can be: solid (Coal, wood etc.); liquid (oils, process wastes etc.); gas (natural, process etc.). The U.K. energy consumption of pimary fuels for 1976 is shown in Table 2. Oil and coal being the main sources then.

Combustion equipment - For a given fuel, the combustion equipment plays a major role in determining plant efficiency. A main component there is the burner, and a good burner designed to suit the fuel used is essential. The burner should be capable of burning the fuel

TABLE 2

U.K. ENERGY CONSUMPTION OF PRIMARY FUELS 1976

Hydroelectric	0.5%
Nuclear	4.6%
Natural gas	18.0%
Oil	40.5%
Coal	37.0%

FIG. 11

THE RELATIONSHIP BETWEEN CO AND O_2 IN THE COMBUSTION GASES OF A MODERN OIL BURNER.

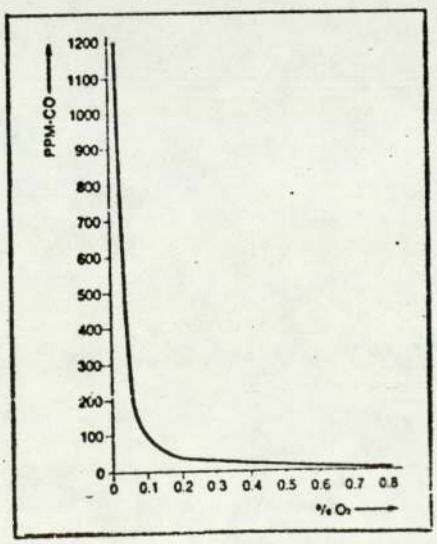

completely with a minimum of excess air and without soot formation. For oil it is essential to have a good atomising and mixing system which atomises the liquid to fine particles and then allows it to mix intensively with the combustion air. If the mixing is not good pyrolysis may occur at the centre of the flame and soot will form. Modern burners are extremely efficient. Fig. 11 shows the relationship between CO and O_2 for such a burner. A good guide for an efficient burner is the shape and colour of its flame. The boiler and heat exchanger design is fixed for a given installation and in most cases there is little one can do about it.

Air-volume - Ideally a stoichiometric mixture is required, in practice, however, due to imperfect fuel and air mixing and the dilution of the combustion products by inert gases (N_2); near complete combustion can only be achieved if a volume of air slightly greater than the ideal is supplied (excess air). Fig. 12 a & b shows heat losses against excess air curves[276,277]. If too much air is added, efficiency begins to decrease due to: loss of energy in heating excess inert gas and power required for fans; corrosion potential and air pollution also increase. If too little air is added incomplete combustion results in fuel and products of incomplete combustion being discharged. Another advantage of controlling excess air is the limiting of the production of the pollutants: SO_3, NO and NO_2. The sulphur bearing fuels produce SO_3 due to the presence of active oxygen. This combines later with water vapour and produces sulphuric acid. So whenever the fuel gas is cooled below its acid dew point (about 140°C) the resultant condensates present a serious potential corrosion and pollution problem. It must be emphasised that in practice, the most efficient combustion conditions are individual characteristics of a given boiler and the type of fuel used. Oxygen emerges as the most convenient parameter to use.

Fig. 12a

HEAT LOSSES AGAINST EXCESS AIR

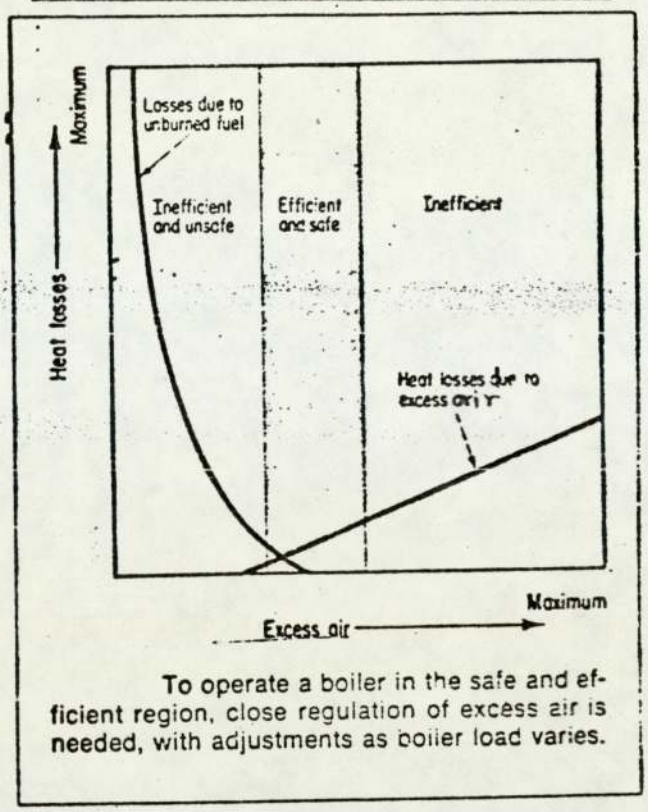

To operate a boiler in the safe and efficient region, close regulation of excess air is needed, with adjustments as boiler load varies.

Fig. 12b

HEAT LOSSES FOR A STEAM BOILER AGAINST EXCESS AIR

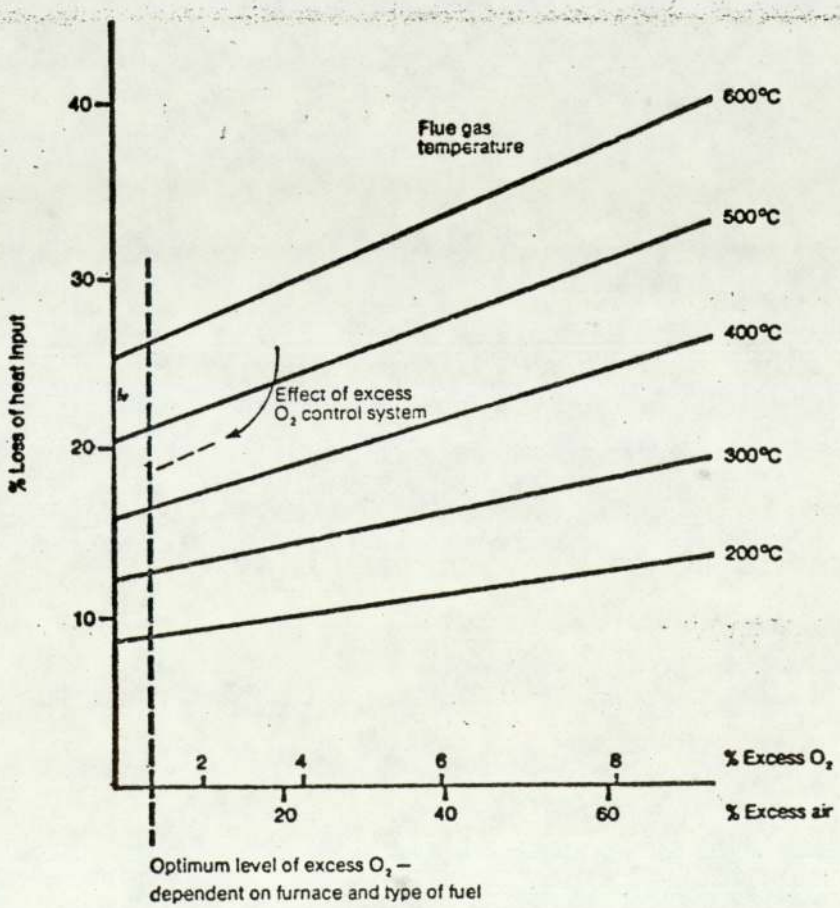

3.7.2 Combustion Control Systems[278,279,280,281,282]

There are several basic techniques:

Air/fuel ratio - This ratio can be fixed by design and a simple control system could be used as shown in Fig.13. The steam pressure is used as a measure of boiler load. The supply of fuel to the boiler is controlled to maintain constant steam pressure. This system, however, suffers from several disadvantages: the need for accurate fuel and air flow rates, the inability to compensate for variations in the energy content of the fuel; the air/fuel ratio for complete combustion varies with the load as shown in Fig.14, due to low velocities in the mixing zone.

Steam/Air - The fuel and air inputs to the boiler are related to steam flow rather than pressure - assuming constant boiler efficiency, this varies in practice with load and decreases with age. This type of system is not very satisfactory as under low excess air it can run out of control resulting in a boiler shut down and an explosive mixture within the boiler. It is useful on pulverised fuel fired boilers.

O_2 Content - The O_2 content in the exhausted gas is used to adjust the air/fuel ratio. This results in compensation for variations in fuel quality and errors in flow measurements. Manual systems such as the one shown in Fig.15, where the fuel flow to the boiler is controlled by the steam pressure, the operator adjusts either the air/fuel ratio controller or air dampers to maintain the desired O_2 level. This is most suitable for systems with a relatively steady load. Automatic control such as that shown in Fig.16, where the signal from the oxygen analyser is used to adjust the air/fuel ratio so as to maintain a pre-selected O_2 level in the exhaust gas of the boiler, is suitable for variable load conditions.

3.7.3 Commercial Instruments[283,284,285,286,287]

We can devide these into:

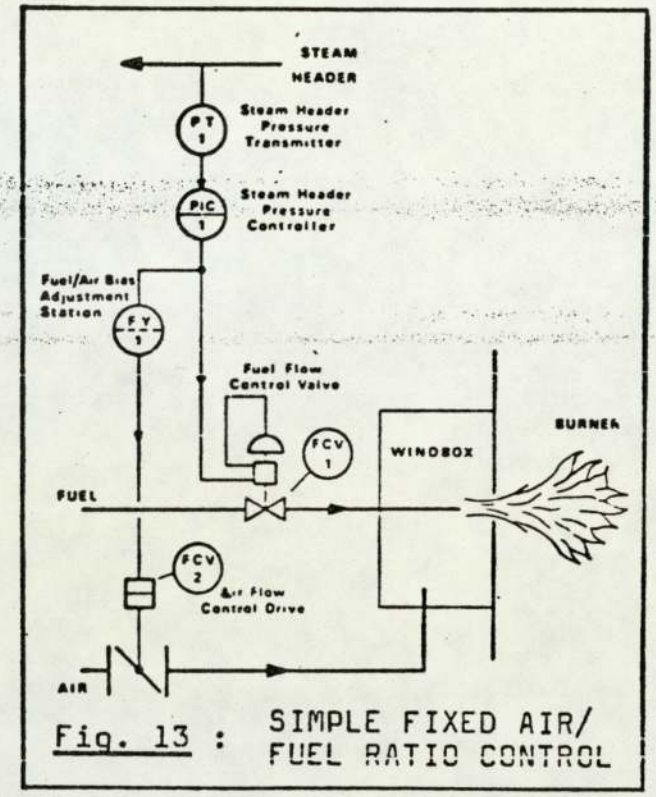

Fig. 13 : SIMPLE FIXED AIR/ FUEL RATIO CONTROL

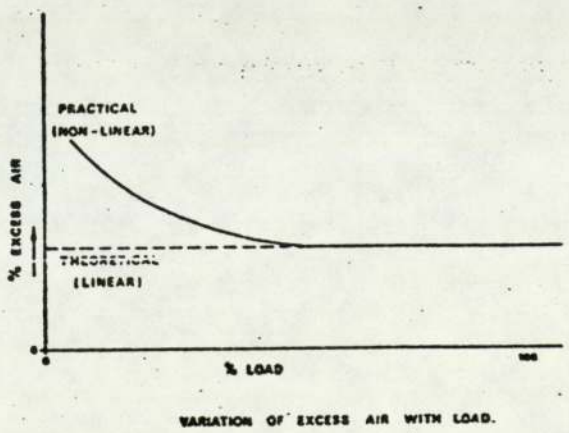

Fig. 14

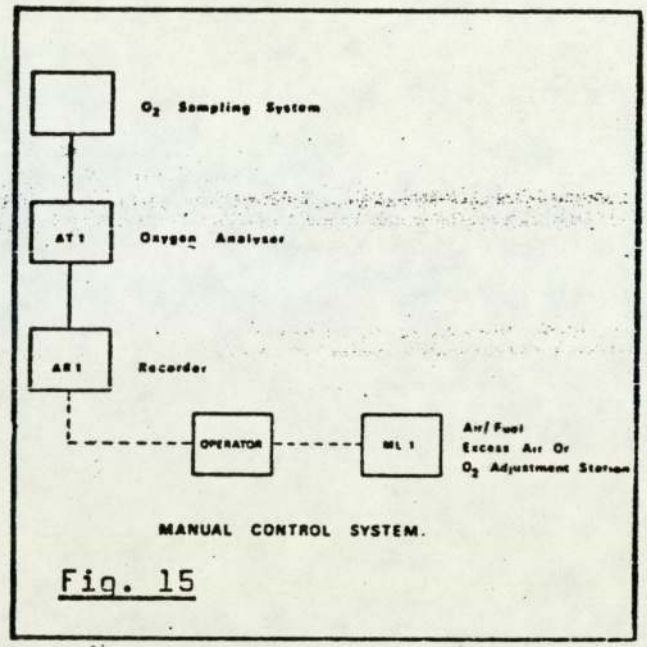

MANUAL CONTROL SYSTEM.

Fig. 15

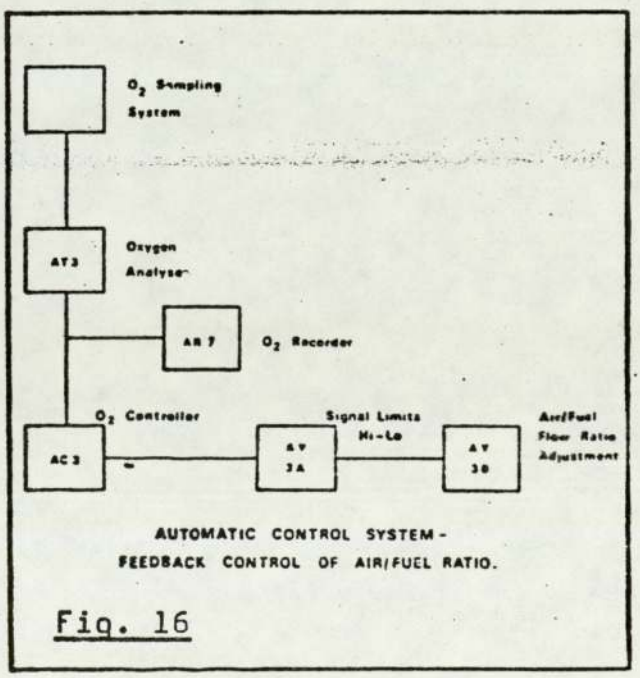

AUTOMATIC CONTROL SYSTEM -
FEEDBACK CONTROL OF AIR/FUEL RATIO.

Fig. 16

Analysers for Small Boilers - These are low cost small probes intended for small boilers such as, large flats, hospitals and small industrial boilers. A comparison of the specifications for some of these is given in Table 3. It is usual to offer with this a control package for controlling the air/fuel setting.

Flue Gas Analysers - These can be classified into:

Out of the Flue - These bring the flue gas by a pump or an aspirator. Examples of these are the Westinghouse 215 and the Thermox WDG-111. Table 4 lists the specifications for the WDG-111 and Fig.17 shows its sensor; the temperature gradients across the active part; its offset e.m.f.; and its response time.

In-situ - These are probes which are inserted directly in the flue obviating the need of a sampling system. Table 5 shows the specifications of a number of them. The most successful ones are the disc type. Fig. 18 shows some measured characteristics of the Westinghouse 218 probe.

3.7.4 Safety Considerations in the Flue

Under certain conditions such as start-up or flame-out, an explosive mixture of fuel and air is present in the flue. Any source of ignition is a safety hazard. Probes without heaters can be considered as the safest from that point of view. The use of flame arrestors in the gas path leading to the source of ignition have been used by manufacturers. This, however, does not allow for the condition, when due to an accident, or corrosion an intact pipe section is damaged, and an indirect path to the source of ignition is provided.

There is also the problem of area safety, and manufacturers have offered explosion proof cases and purging. The two are, however, connected and the safety consideration is one of the most difficult one to allow for in the design of the system, due to the high working temperature of the sensor.

SPECIFICATIONS FOR SMALL BOILER ANALYSERS

TABLE 3

	Westinghouse 132	Cleveland 8000	North American 8100	GSC 4000	C.S.I.R.O.	
Range	0.05-5% O_2 0.1 - 10% O_2 0.25-25% O_2	0.1 - 10% O_2 0.1 - 20% O_2 linear	0.2 - 98% O_2	0.1-10% O_2	-	
Accuracy	$\pm$ 5% of O_2 reading	$\pm$ 5% of O_2 reading	$\pm$ 0.1 % O_2	$\pm$ 4% of reading or $\pm$ 0.16% O_2	-	
Response time	Fast	Initial response 1 second (instrument)	1 m second (cell)	-	10 seconds	
Probe length Cable length	1 ft 20 ft	1.5, 4 or 6ft. 20 ft	- 100 ft	- -	- -	
Amb.temp. flue (electronic)	to 540°C	to 427°C 0 to + 55°C	to 1100°C or 1540°C 0 to + 55°C	to 1600°C -	to 1500°C -	

TABLE 4

THERMOX WDG - 111 SPECIFICATION

Range	possible 0.1 ppm to 10% O_2
Accuracy	$\pm$ 1% of actual measured value.
Repeatability	$\pm$ 0.2% of measured value.
Response	5 seconds for 90%
Drift	less than 0.1% of cell output per month
Ambient temp.	- 20 to 80°C sensor - 18 to 50°C electronics - 18 to 816°C sample
Sample flow rate	0.050 to 56 L/M @ 2 psig
Aspirator air	5 to 15 L/M, 15 to 100 psi
Hazardous areas	explosion-proof cabinet; + flame trap.
Length of cable	1000 ft max.

FIG (17) Test tube sensor with large electrode area.

(a) Schematic of sensor.

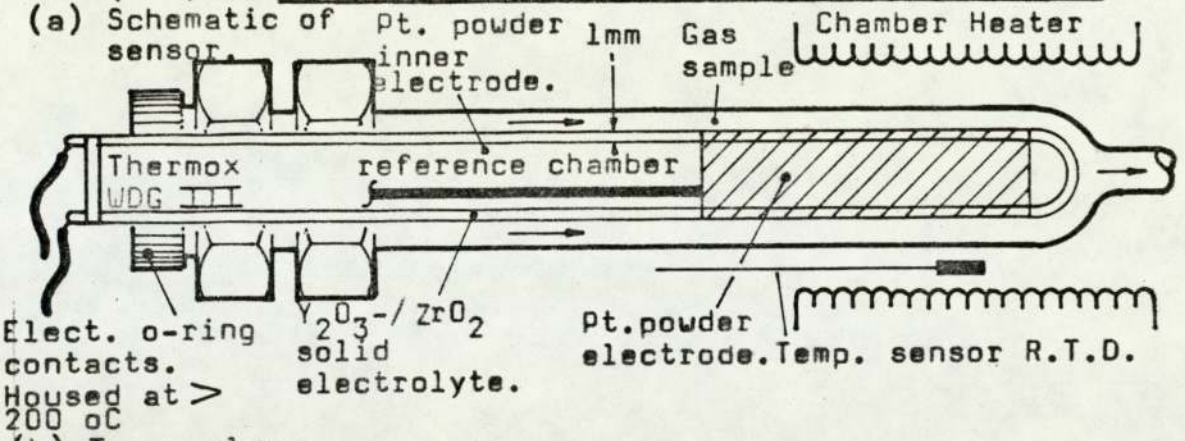

(b) Temp. along centre of furnace with probe withdrawn.

Temp. measured with Cr/AL T/C

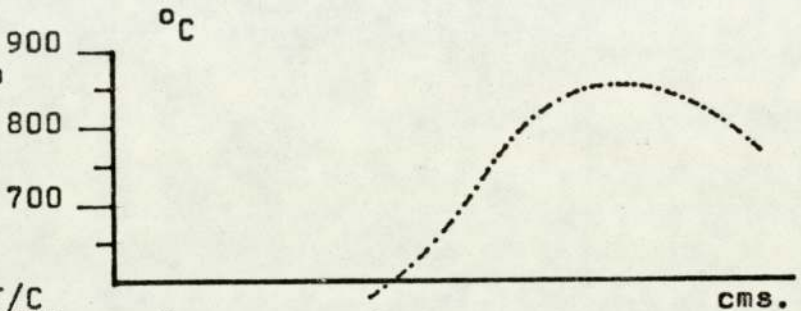

(c) Temp. along inner wall of sensor.

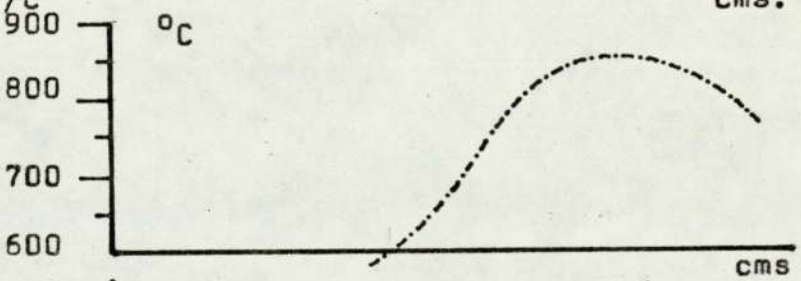

(d) Sensor offset, still air in both chambers, with temp. measured at tip of sensor from ref. chamber.

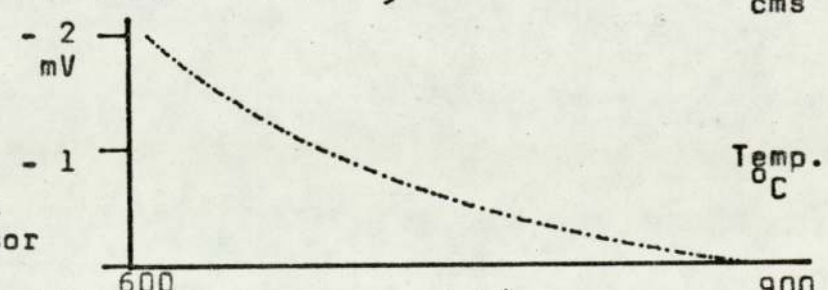

(e) Inst. response to change from 8.8 to 0.8% O_2.

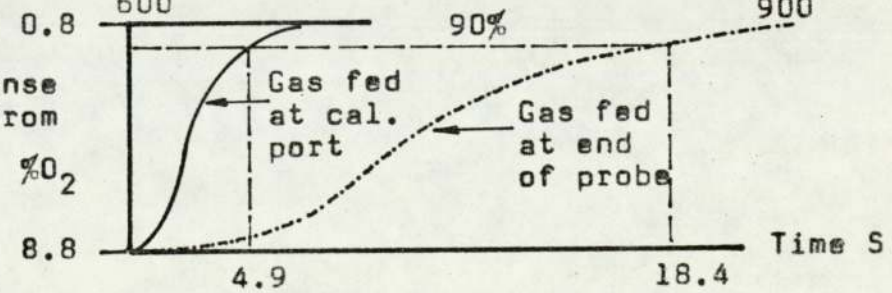

Instrument spec. of Thermox WDG-111

Stated accuracy ± 1% of measured value.
Stated repeatability ± 0.2% of measured value.
Drift < 0.1% of sensor cell O/P per month.
Calibration with analysed sample O_2 in N_2 and trim set temp.

THERMOX WDG-111

SPECIFICATIONS OF SOME IN-SITU PROBES

TABLE 5

	Westinghouse 218	Hays A - 10007	Mitaka 6721	Kent	MECl FD 1303	L & N 7875
Range	0.1 - 10% O_2 or 0.25 to 25% O_2	0-1/5/10/25 % O_2	0-1/5/10/25 % O_2	0.1-10% O_2	0.1/2/5/10 % O_2	0-2% O_2 0-5% O_2 0-10% O_2 0-25% O_2
Accuracy	Static ± 5% of reading dynamic ± 2%	± 2% (system)	± 1% of FSD 10-25% ± 2% of FSD 1-5%	± 5% of reading	± 7% of reading	± 5% of reading or ± 0.05% O_2
Response time	1 m.s. (cell) 3.s. system	1. s for 63%	3.s. 90% calib. gas inlet	-	-	3.s. 63% with filter 20 s.
Operating temperature	up to 760°C sample 4-49°C electronics	up to 760°C sample 0 to 50°C electronics	0 - 1400°C sample -	to 600°C sample -20 to 55°C electronics	700-1600°C sample -10 to + 55°C electronics	to 750°C sample 0 to 50°C electronics
Type of sensor	Disc	Disc	Disc	Test tube	Test tube	Two sensors with sealed in ref.
Op. temp.	844°C	-	850°C	700°C	-	700°C min.

Fig. 18

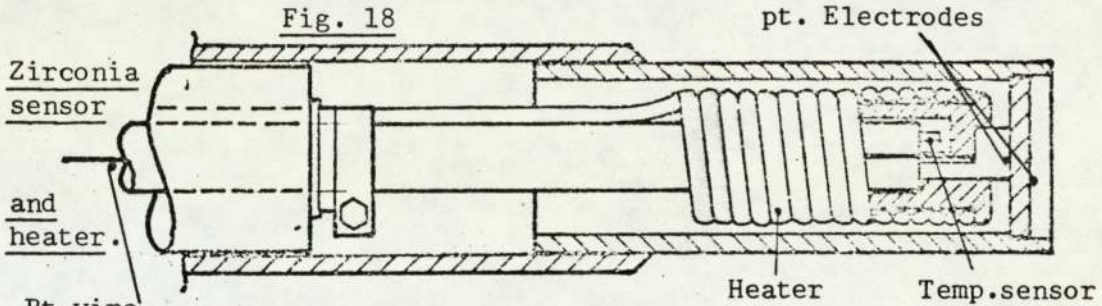

WESTINGHOUSE ZIRCONIA PROBE 218

a) Zirconia sensor and heater.

b) Temperature gradients

At a control thermocouple reading of 834°C, the average electrode temperature is 758°C.
The temperature gradient between the working electrodes is 6°C.

c) Sensor offset, with still air in both chambers, with temperature measured at electrodes. Offset measured directly between electrodes.

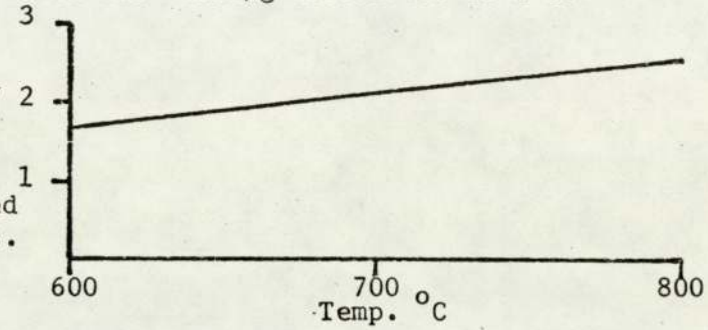

At 834°C control temperature the offset is approximately 17 mV when measured at the instrument sensor output. The outside electrode has a path through the instrument body where thermal emf's are generated.

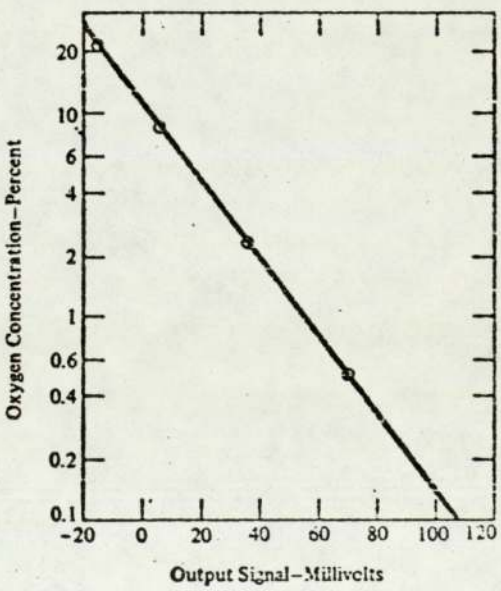

d) Instrument response to change from 9.0 to 0.19% O_2

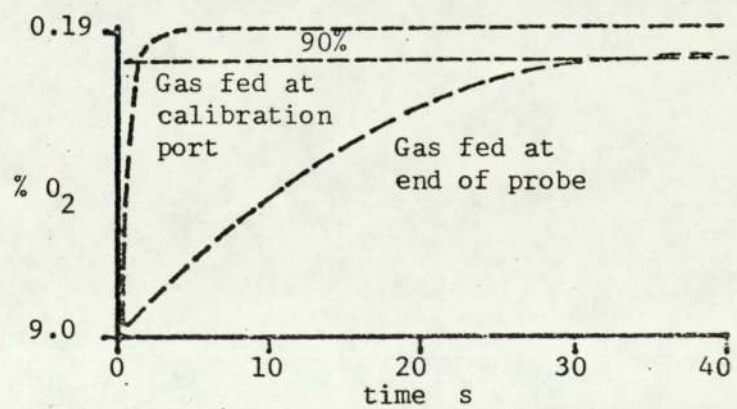

3.8 DESIRABLE SENSOR FEATURES

A number of desirable sensor features can now be listed:

a) Thermal shock resistance - This is the main weakness of this type of sensor, and reported cracking of the sensor is one of the most common reasons for customer complaint.

b) High accuracy. This is determined mainly by accurate e.m.f. and temperature measurements, avoidance of temperature gradients and thermal e.m.f.'s.

c) Short response time - Though the basic sensor has a very fast response time, it is always the associated system which dominates this parameter.

d) Long life time - The peeling and the clogging of the electrodes are the main causes of a short life time; that is assuming the sensor is shock resistant.

e) Simple design - versatile and simple design leads to reliability, low manufacturing cost and ease of maintenance.

CHAPTER FOUR

THEORY OF THE SOLID ELECTROLYTE OXYGEN SENSOR AND REVIEW OF THE MAJOR ERROR CONTRIBUTING PARAMETERS. (174, 186, 189, 288, 289, 290, 291, 292, 295, 296)

4.1. LATTICE DEFECTS AND IONIC CONDUCTION IN SOLIDS

Around 1930 the influence of lattice defects on the properties of real crystals was recognised. This was possible due to the development of the x-ray diffraction methods and high precision pyknometry which allowed the determination of the crystal structure and the defect density, and to the development of a theory dealing with forces within the atoms in the crystal (Frenkel, Schottky and Wagner).

Continuous ion migration in an ideal completely ordered crystal lattice (i.e. at absolute zero) is impossible for reasons of geometry or energy. The theory links the occurence of ionic conduction with the presence of defects in the lattice, and proposes that lattice defects arise as a result of thermal motion of the atoms in the lattice at temperatures higher than absolute zero and consist of: point defects (atoms pushed from their original position to interstitial positions - (interstitials), vacant lattice sites (vacancies), and of impurity atoms in lattice or interstitial positions; whilst electronic defects consist of electrons and electron holes. Table 6 gives a list of the defects and their symbols.

In simple substances lattice disorders are generally created by deviation from stoichiometric composition - this results in the creation of electrons or defect electrons hence electronic conductivity; or according to equilibria between ideal occupancy and defects which are temperature-dependent and follow thermodynamic laws, the disorder concentrations resulting from this are, however, relatively small and the conductivity is therefore low.

For defects in thermal equilibrium with the lattice a schottky

TABLE 6 PRINCIPAL EQUILIBRIUM DEFECTS IN SOLIDS

TYPE OF DEFECT		SYMBOL
VACANCY	:A lattice position left empty by an ion pushed in an interstitial position or to the surface.	V_M: Unionized-cationic vacancy V_X:Unionized-anionic vacancy $V_M^{'}$:Singly ionized-cationic vacancy $V_X^{\bullet}$:Singly ionized-anionic vacancy
ELECTRON :	:An electronic defect trapped at a lattice site(both an ion or a defect)or lying in the conduction band if sufficient thermal energy is available.	e
ELECTRON-HOLE	:Positively charged electronic defect sitting at lattice sites or in the valence band.	h
INTERSTITIAL	:Lattice or foreign impurity ion(or atom)sitting in an interstitial position.	M_i:Unionized cation in interstitial position X_i:Unionized anion in interstitial position A_i:Foreign cationic impurity in interstitial position
SUBSTITUTIONAL IMPURITY	:Aforeign impurity sitting in a regular lattice position.	A_M:A cationic type impurity ion on a cationic site B_X:An anionic type impurity ion on an anionic site
PHONON	:Quantised lattice vibration	

disorder can be formed (a vacant site from which the atom has migrated to the surface of the crystal) as shown in Fig. 19, or an anti-schottky disorder (+ve and -ve ion interstitials); and a frenkel disorder can be formed (an interstitial +ve ion and somewhere in the vicinity, the vacant site from which the +ve ion originated) as shown in Fig. 20, or an anti-frenkel disorder (equal concentration of interstitial -ve ions and -ve ion vacancies).

The presence of point defects in solids explains their electrical, optical and the anomalous temperature dependence of properties like density and heat capacity. They also explain the presence of drift processes of ions in solids either under a chemical (diffusion) or an electro-chemical (migration) potential gradient.

The nature of the disorder for a given compound depends on the relative magnitude of the energy of formation of the relative defects, which depends on the structure of the solid and on the electronic structure of the ions. Compounds having a fluorite structure present an anti-Frenkel (vacancies and interstitials in the anionic sublattice) disorder.

Ionic conduction in pure compounds with normal stacking of ions depends essentially on the degree of intrinsic disorder (thermal vibration), or extrinisic disorder (due to dissolved impurities) of the lattice, which in turn determines the number and the energy of vacancies, voids (positions intrinsically not occupied) and interstitials. These defects act as the intermediate (in a multi-step process) or the final position in an elementary motion step, which is just a jump of an ion from a lattice position to a neighbouring ion missing site. The relative contribution of the single (anionic + cationic) processes to the overall transport process depends primarily on the ratio of ion sizes, on the electronic structure of the ions and on the crystal structure.

If a close packed array of big anions and small cations is considered as shown in Fig. 21.a. The presence of a sufficient amount of anion

FIG. 19 A SCHOTTKY PAIR(a cationic and anionic vacancy) IN AN IONIC COMPOUND OF THE MX TYPE (alkalihalides)

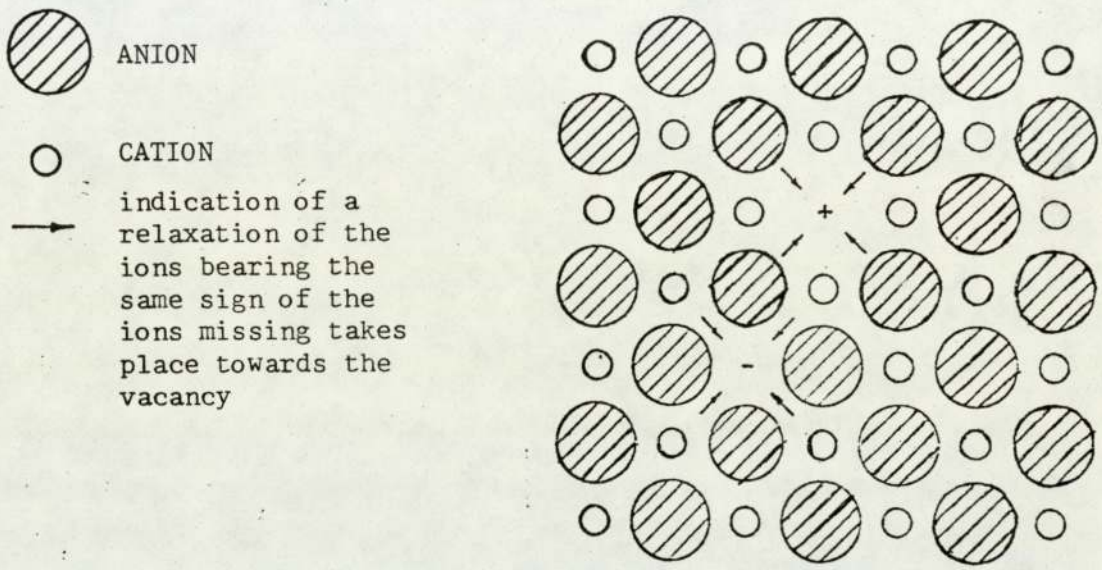

FIG. 20 A FRENKEL PAIR(a cation interstitial and a cation vacancy)IN A MX TYPE OF COMPOUND(silver halides)

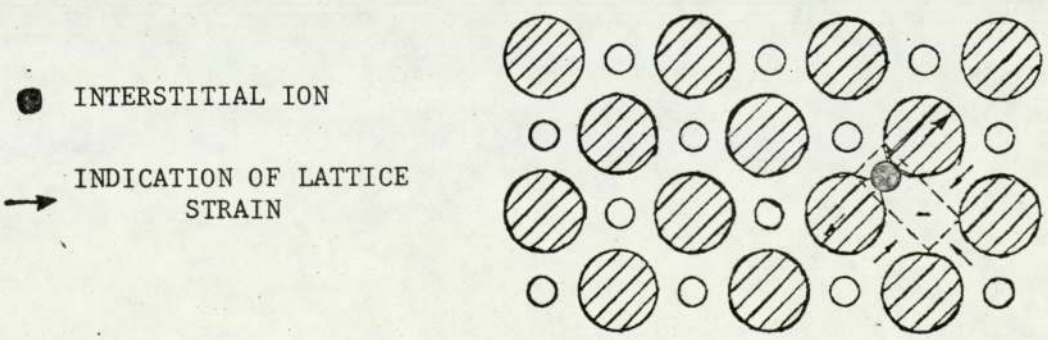

FIG. 21 MODEL FOR IONIC CONDUCTIVITY

A.INITIAL POSITION OF ANION

B.FINAL POSITION OF ANION

ANION

CATION

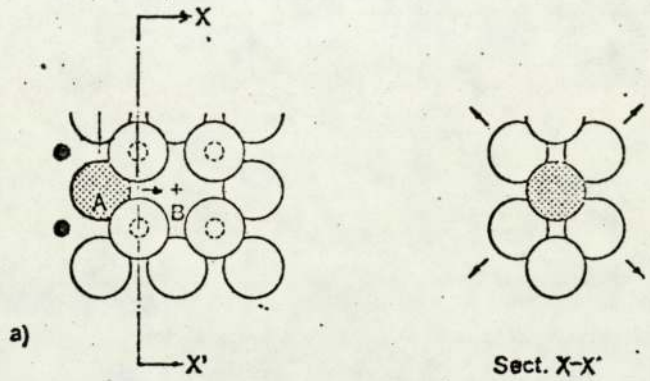

POTENTIAL WELLS BETWEEN

A & B THE CHANGE IN HEIGHT

IS A FUNCTION OF TEMPERATURE

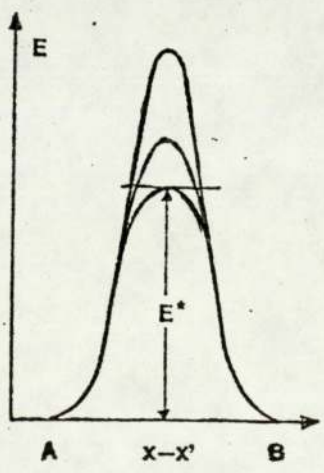

vacancies is imperative for the anions to move, so it could be assumed that the solid contains the equilibrium concentration of anion vacancies generated by thermal vibrations of the lattice. The elementary motion step from the initial position to the final position consists of the jump of an anion from a lattice position to a neighbouring vacancy across an interstitial position. This process is of the activated type and the magnitude of the energy barrier could be supposed to correspond to the amount of strain energy required for opening a port of sufficient width for the passage of the anion moving across the four anions. The energy of the particle and the height of the barrier depend on temperature - Fig. 21.b. The overall activation energy for the transport process should then be proportional to the sum of the energy of formation of a vacancy pair and the barrier energy.

For the motion of the small cations, direct vacancy and direct interstitial type mechanisms, or both are possible as shown in Fig. 22.

The number of ions sitting in equilibrium conditions can be calculated from Boltzmann statistics, and when an electric field is applied the conductivity can be calculated.

The presence of impurities, bearing the same charge as the host lattice ions strongly influences the electrical conductivity of a material if one of the following conditions is satisfied:

a) The impurity ions are more mobile than those of the host lattice.
b) The introduction of the impurity ions into the lattice induces structural changes in the lattice or influences the distribution of mobile ions in the lattice.
c) The induction of chemical reaction due to the additions, which modify the population of the free carriers.

4.2. CONDUCTION IN SOLID SOLUTIONS

The disorder concentrations resulting from thermodynamic equilibria

FIG. 22 POSSIBLE MOTIONS OF A SMALL CATION

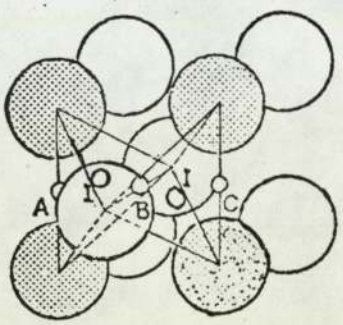

a)

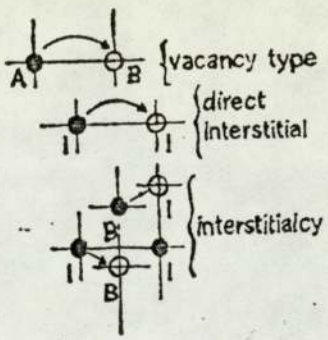

b)

Energy levels of different positions

c)

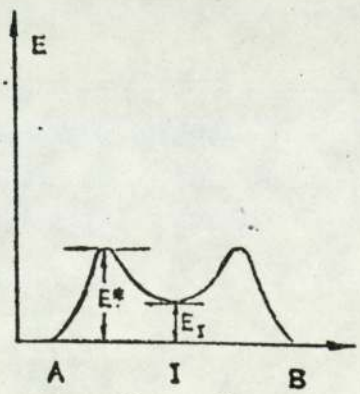

are relatively small leading to small conductivities. The investigation of mixed phases led to the discovery of substances which possess a larger temperature dependent number of oxygen ion defects whilst completely complying with stoichiometry. For example in a phase of variable composition one can find that the numbers of anions per basic cell was constant, but the number of cations varied. Deviations from normal occupancy are compensated for by cations in interstitial positions or by cation vacancies. Anion disorders can also be found (fluorides) where they are located in interstitial positions. Anion vacancies are more likely to be found in cases where the compound of a cation of lower valency is dissolved in that of a cation with higher valency ($A^n B^m$ dissolved in $C^{n+x} B^m$ where n and m are valencies). A whole series of such mixed oxide solid solutions has been discovered in which the mixed oxides crystallize in the fluorite type and are solid solutions of oxides of 2 - or 3 - valent metals (Mg, Ca, Y, La) in an oxide of a 4 - valent metal (Zr, Ce, Th). The 3 - or 2 - valent cations entering the lattice of the 4 - valent metal oxide carry with them one, or a half of one oxygen ion so that an oxygen ion vacancy is created by insertion of two each 3 - valent or one each 2 - valent cations. Depending on the radius of the inserted cation an expansion or narrowing of the lattice takes place at the same time as the vacancy concentration increases. These changes in lattice dimensions have a substantial effect on the magnitude of the electrical conductivities. Compared with the overall neutral crystal lattice, oxygen ion vacancies show a positive action due to the absence of two negative charges at these points. For the same reason 3 - valent, and, even more strongly, 2 - valent cations form negative centres in the fluorite lattice. It follows that an attraction must be expected between the various disorder positions which result in the movement of vacancies.

As an example, one of the most commonly used electrolytes in oxygen concentration cells can be considered: zirconia stabilized with

CaO, Y_2O_3, MgO, or [illegible] rare earth metal oxides. These solid solutions contain large concentrations of oxygen vacancies which are needed to accommodate the valence difference between the Zr^{4+} and the doped cations, hence conduction occurs at high temperature mainly due to the migration of doubly charged anion vacancies, and to a limited extent to holes (p-conduction) and excess electrons (n - conduction). This is enhanced by non stoichiometry and impurities. Conduction due to cation defects is negligible. (181, 183, 184, 192)

The total conductivity is the sum of the ionic conductivity (cations and anions) and the electronic conductivity (electrons and hole) this is given by:

$$\sigma = \sum n_i q_i u_i = \sum_i \sigma_i \quad \ldots\ldots\ldots \quad (7)$$

where n_i is the number of carriers of species, i per unit volume, q_i is the charge on the species in coulombs, u_i is the mobility in cm^2 per volt sec. and σ_i is the partial conductivity of the species.

The transference - number t_i is the quotient of the partial conductivity σ_i of the one type of species to the total conductivity.

$$t_i = \frac{\sigma_i}{\sum_i \sigma_i} = \frac{\sigma_i}{\sigma} \quad \ldots\ldots\ldots \quad (8)$$

Good solid electrolytes have a transference - number for the ions of nearly one and for electrons of nearly zero. It is often important that the transference - number of a special ion (e.g. oxygen) is one and those of the other ions are practically zero besides that of the electrons.

The electrical conductivity can be expressed by an Arrhenius equation:

$$\sigma = A \exp\left(-\frac{E_a}{KT}\right) \quad \ldots\ldots\ldots\ldots \quad (9)$$

where A is a pre exponential term, E_a the activation energy, k the Boltzmann constant and T the absolute temperature.

An example of the conductivity of a solid electrolyte system (Y_2O_3 - ZrO_2) is shown as a function of temperature and composition in Fig. 23. The conductivity isotherms and activation energy for the system are shown in Fig. 24. The high conductivity in this system is

FIG. 23 CONDUCTIVITY OF Y_2O_3-ZrO_2 AS A FUNCTION OF TEMPERATURE AND COMPOSITION

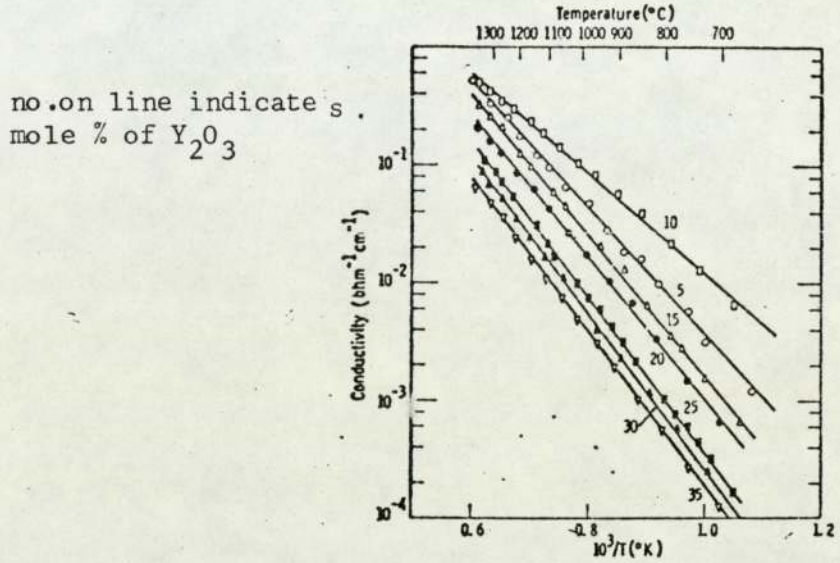

FIG.24 CONDUCTIVITY ISOTHERMS AND ACTIVATION ENERGY FOR THE SYSTEM Y_2O_3-ZrO_2

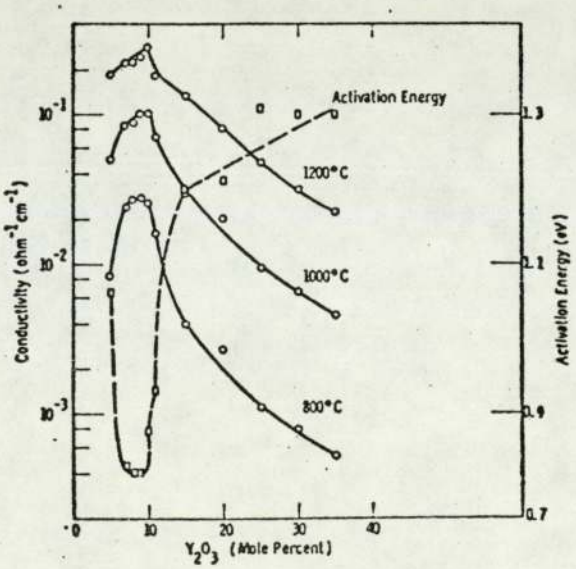

related to a lower activation energy rather than to the number of oxygen vacancies dictated by composition. (180) The transference number for the oxygen ion at 1000°c for the cubic solid solutions is greater than 0.99.

4.3. EMF ACROSS A SOLID ELECTROLYTE OXYGEN CONCENTRATION CELL WITH PURE IONIC CONDUCTION (301, 303)

Consider a solid electrolyte oxygen concentration cell Fig. 25 consisting of a solid electrolyte with a predominantly oxygen ion conductivity, and electronic conducting electrodes (e.g. Pt) on either side, and let the oxygen partial pressures be $P\grave{O}_2$ and $P\acute{O}_2$ on each side respectively. If we consider the cell as a thermodynamic system at constant pressure and temperature and undergoing a reversible process, we have seen from equation (3) that the change in the free energy ΔG is equal to the reversible electrical work.

$$-\Delta G = nFE$$

At the cathode gaseous oxygen of chemical potential μ''_{O_2} is ionized and incorporated into the lattice of the electrolyte. Fig. 26.(296, 299, 300)

$$O_2\,(P''O_2) + 4e \longrightarrow \overleftarrow{2O}^{2-}$$

At the anode the reverse reaction takes place and oxygen of chemical potential μ'_{O_2} is released so that

$$\overleftarrow{2O}^{2-} \longrightarrow O_2\,(P'O_2) + 4e$$

The overall cell reaction is given by

$$O_2\,(P''O_2) \longrightarrow O_2\,(P'O_2)$$

This is the transport of one mole of oxygen gas from potential μ''_{O_2} to a potential μ'_{O_2}. A potential difference E appears between the electrodes, the positive electrode being on the higher oxygen pressure side.

The free energy change under these conditions is equal to the difference in the chemical potential i.e.

FIG. 25 E M F ACROSS A SOLID ELECTROLYTE OXYGEN CONCENTRATION CELL

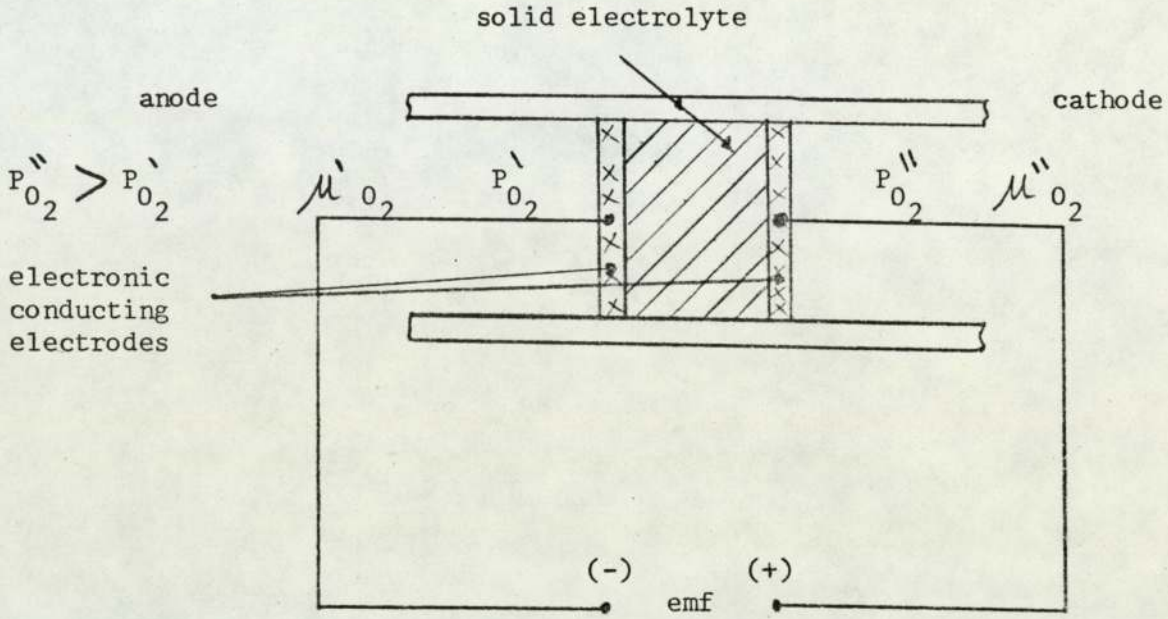

FIG.26 SCHEMATIC OF A SECTION SHOWING REACTION AT THE THREE PHASE BOUNDARY ZONE

$$O_2\ (P''_{O_2}) + 4\ e \longrightarrow 2\ O^{2-}$$

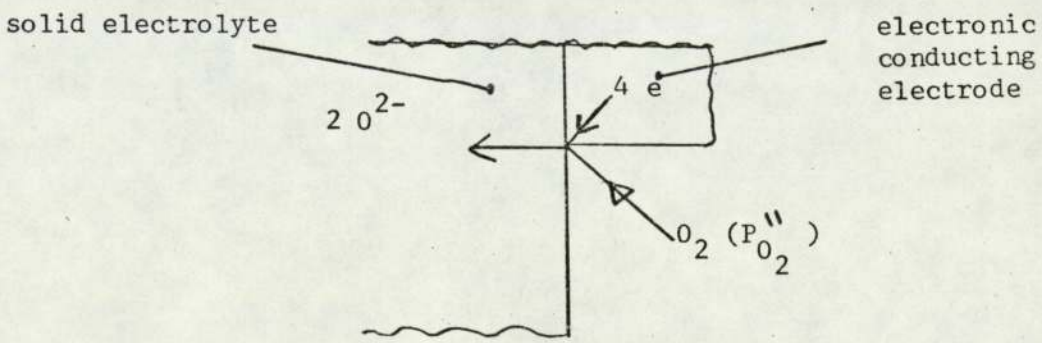

$$-\Delta G = \mu''_{O_2} - \mu'_{O_2} \quad \ldots\ldots\ldots\ldots\ldots (10)$$

where μ'_{O_2} is the oxygen chemical potential at the P'_{O_2} electrode and the μ''_{O_2} is the oxygen chemical potential at the P''_{O_2} electrode. The relationship between the chemical potential and the partial pressure of oxygen at a given electrode is given by:

$$\mu_{O_2} = \mu^{\circ}_{O_2} + RT \ln P_{O_2} \quad \ldots\ldots\ldots\ldots (11)$$

where $\mu^{\circ}_{O_2}$ is the standard chemical potential of oxygen. Combining these equations gives:

$$-\Delta G = nFE = RT \ln \frac{P''_{O_2}}{P'_{O_2}} \quad \ldots\ldots\ldots\ldots (12)$$

and using n = 4 for oxygen ions, this becomes:

$$E = \frac{RT}{4F} \ln \frac{P''_{O_2}}{P'_{O_2}} \quad \ldots\ldots\ldots\ldots\ldots\ldots (13)$$

This is known as the Nernst equation. If P_{O_2} is known and taken as a reference, the unknown value can be found. As this is a theoretical equation applicable to any cell geometry, a sensor based on this principle does not need any calibration. This equation is always valid regardless of whether the electrolyte consists of a solid oxide solution of two, three or more cationic constituents provided that only the transference number of oxygen ions is unity.

4.4. THE EFFECT OF ELECTRONIC CONDUCTIVITY ON THE EMF OF A SOLID ELECTROLYTE OXYGEN CONCENTRATION CELL. (142, 147, 155, 176, 188, 189, 193, 200, 202, 293, 302, 304)

In 4.3. a nearly pure ionic conduction was assumed, however under certain conditions of oxygen pressure and temperature a substantial electronic conductivity is exhibited.

Wagner's equation (2) for the e.m.f. of an oxygen concentration cell is valid for an idealized cell with established local equilibrium at the phase boundaries. If the ionic transfer number is less than unity, an internal short circuit is effectively present and cathodic

as well as anodic reactions have finite rates. Such deviations from local equilibrium may be minimised by using a thick electrolyte.

For the condition when P''_{O_2} does not differ very much from P'_{O_2} equation (2) gives:

$$E = t_{ion} \frac{RT}{4F} \ln \frac{P''_{O_2}}{P'_{O_2}} = \left(1 - t_e\right) \frac{RT}{4F} \ln \frac{P''_{O_2}}{P'_{O_2}} \quad \ldots\ldots\ldots (14)$$

where t_e is the electronic transference number.

The transference numbers for the ion and the electronic species are average values for the oxygen pressure range under consideration. A general solution requires the formulation of t_{ion} as a function of oxygen pressure.

The total conductivity of a mixed conductor is the sum of the partial conductivities of ions(σ_{ion}) excess electrons ($\sigma_{e'}$) and electron holes (σ_h) and hence:

$$\sigma = \sigma_{ion} + \sigma_{e'} + \sigma_h \quad \ldots\ldots\ldots\ldots\ldots (15)$$

From the definition of transference numbers it follows that:

$$t_{ion} = \frac{\sigma_{ion}}{\sigma} = \left[1 + \frac{\sigma_{e'}}{\sigma_{ion}} + \frac{\sigma_h}{\sigma_{ion}} \right]^{-1} \quad \ldots\ldots\ldots\ldots (16)$$

So as to combine the partial conductivities with oxygen partial pressure, the following models need to be discussed:

a) Low oxygen partial pressure: If the chemical potential of oxygen in the surrounding gas is decreased, oxygen is removed from the lattice of the oxide. This results in the formation of oxygen vacancies $V_x^{\bullet\bullet}$ and excess electrons e' :

$$\text{(lattice)} \quad O_o \rightleftarrows V_x^{\bullet\bullet} + 2\,e' + \tfrac{1}{2}\,O_2 \,(P\,O_2)$$

where O_o is an oxygen ion in a normal lattice site and $V_x^{\bullet\bullet}$ is a double ionized oxygen vacancy.

Under equilibrium conditions between the gas phase and the oxide provided there are no interactions between the charged defects, we can write the mass action law for the above reaction using concentrations

instead of activities:

$$(\grave{e}) = \text{const}_1 \; (V_x^{\cdot\cdot})^{-\frac{1}{2}} \; P_{O_2}^{-\frac{1}{4}} \quad \ldots\ldots\ldots \quad (17)$$

This leads to two different cases:

i) The concentration of the oxygen vacancies is half the concentration of the electrons: this is true if the concentrations of all other defects are sufficiently small.

Then:

$$(\grave{e}) = \text{const}_1' \; P_{O_2}^{-\frac{1}{6}} \quad \ldots\ldots\ldots\ldots \quad (18)$$

The mobility of electrons, in general, greatly exceeds that of the ionic species. Hence the transference number of electrons is near unity for an oxide with equivalent concentrations of oxygen vacancies and excess electrons (n type semi-conductor). Such electrolytes are not suitable for galvanic cells.

ii) The concentration of oxygen vacancies is high by appropriate oxide additions in some solid solutions (e.g. stabilized zirconia). The conductivity of the electrolyte is then mainly ionic, and only at very low oxygen pressures do the electrons contribute to the electrical conduction, this means

$$(\grave{e}) = \text{const}_1'' \; P_{O_2}^{-\frac{1}{4}} \quad \ldots\ldots\ldots\ldots \quad (19)$$

Hence the partial conductivity $\sigma_{\grave{e}}$ is proportional to the above, provided the excess electron mobility is not a function of oxygen pressure.

b) Large oxygen partial pressure: If a large oxygen potential in the gas phase exists, an excess of oxygen is accommodated in the lattice of the oxide. The defects formed are interstitial oxygen ions O_i'' or cation vacancies V_M''. To maintain neutrality electron holes are formed:

$$\tfrac{1}{2}\, O_2\,(P_{O_2}) \rightleftharpoons O_i'' + 2\, e_h$$

or

$$\tfrac{1}{2}\, O_2\,(P_{O_2}) \rightleftharpoons V_M'' + 2\, e_h + M\,O$$

When the interstitial oxygen ions equal to half the electron holes or the cation vacancies are equal to half the electron holes, the concentration of electron holes is proportional to $P_{O_2}^{1/6}$ in both cases. The electrolyte is then predominantly a p-type semiconductor and hence unsuitable for galvanic cells.

If the concentration of oxygen vacancies in the electrolyte is large the free lattice sites are occupied according to the reaction.

$$1/2\ O_2\ (P_{O_2}) + V_x^{\bullet\bullet} \rightleftharpoons O^{2-}(\text{lattice}) + 2e_h$$

since $V_x^{\bullet\bullet}$ is nearly constant we have:

$$(e_h) = \text{const}''_2 \left(P_{O_2}\right)^{1/4} \qquad \ldots\ldots\ldots\ldots\ldots\ldots (20)$$

which is also proportional to the partial electron hole conductivity σ_h.

Equation (16) can now be modified using the above mentioned relationships, if the special values of P_{O_2} at which the ionic conductivity of the oxide equals the conductivity by excess electrons or electron holes are used :

$$t_{ion} = \left[1 + \left(\frac{P_{O_2}}{P_{e_h}}\right)^{1/4} + \left(\frac{P_{O_2}}{P_{e'}}\right)^{-1/4}\right]^{-1} \qquad \ldots\ldots\ldots (21)$$

In certain electrolytes only electron or defect electron conductivity occurs at a given oxygen pressure.

Ionic transference number in a mixed conducting oxide is shown in Fig. 27 as a function of oxygen pressure. At $P_{e'}$ and P_{e_h} the ionic transference number is equal to $0.5.t_{ion}$ is unity over a wide range of oxygen partial pressures only if $P_{e'}$ is much smaller than P_{e_h}.

Equation (21) can now be modified and hence an expression for the emf of a cell with electronic conductivity can be obtained, assuming $P_{e'} \ll P_{e_h}$

$$E = \frac{RT}{F}\left[\ln \frac{P_{e_h}^{1/4} + P_{O_2}''^{1/4}}{P_{e_h}^{1/4} + P_{O_2}''^{1/4}} + \ln \frac{P_{e'}^{1/4} + P_{O_2}''^{1/4}}{P_{e'}^{1/4} + P_{O_2}''^{1/4}}\right] \qquad \ldots\ldots\ldots (22)$$

The following cases can be considered:

a) If $P''_{O_2} > P'_{O_2} \gg P_{e_h} \gg P_{e'}$ the electrolyte behaves as an electron hole.

or $P_{e_h} \gg P_{e'} \gg P''_{O_2} > P'_{O_2}$ the electrolyte behaves as an excess-electron semi-conductor. The e.m.f. is zero.

b) If $P_{e_h} \gg P''_{O_2} \gg P'_{O_2} \gg P_{e'}$

this leads to equation (13). This is the necessary condition for $t_{ion} \backsimeq$ unity.

c) If P'_{O_2} in (b) becomes smaller than $P_{e'}$, a constant e.m.f. is present which has a value dependent on the reference pressure and is given by:

$$E = \frac{RT}{4F} \ln \frac{P''_{O_2}}{P_{e'}} \qquad \text{.....(23)}$$

The linear dependence of the e.m.f. on $\ln P_{O_2}$ with decreasing P_{O_2} (case b) and its modification (case c) is shown in Fig. 28.

The e.m.f. cannot be zero since a thin layer of the electrolyte always remains as anionic conductor.

d) If $P''_{O_2} \gg P_{e_h} \gg P'_{O_2} \gg P_{e'}$

electron holes influence the e.m.f. value which is then given by:

$$E = \frac{RT}{4F} \ln \frac{P_{e_h}}{P'_{O_2}} \qquad \text{.....(24)}$$

This is shown as a function of $\lg P_{O_2}$ in Fig. 29. It is a straight line parallel to the curve which describes the ideal relation.

If P'_{O_2} and $P_{e'}$ are interchanged so that $P''_{O_2} \gg P_{e_h} \gg P_{e'} \gg P'_{O_2}$

it is shifted to a smaller value and the e.m.f. is a constant given by:

$$E = \frac{RT}{4F} \ln \frac{P_{e_h}}{P_{e'}} \qquad \text{.....(25)}$$

4.5. THE EFFECT OF TEMPERATURE ON THE EMF OF A SOLID ELECTROLYTE OXYGEN CONCENTRATION CELL.

4.5.1. Errors due to absolute temperature

Equation (13) shows the temperature dependence of the e.m.f. of a

FIG. 27

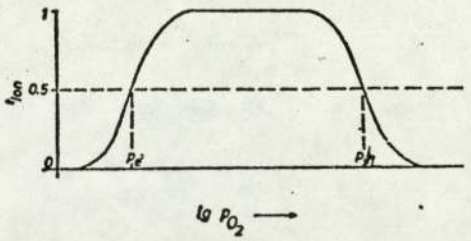

Ionic transference number in a mixed conducting oxide as a function of oxygen partial pressure.

FIG. 28

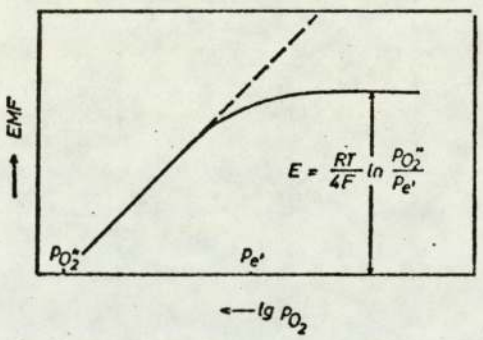

The e.m.f. of an oxygen concentration cell which has an electrolyte that exhibits *n*-type semiconduction at low oxygen pressure.

FIG. 29

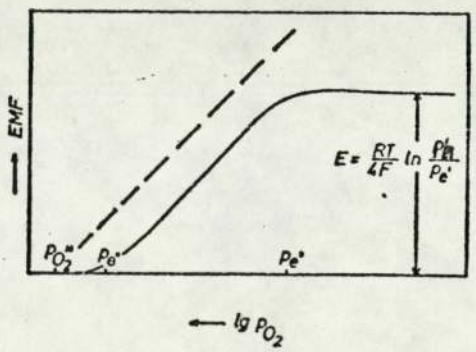

The e.m.f. of an oxygen concentration cell which has an electrolyte that exhibits *p*-type semiconduction at high and *n*-type semiconduction at low oxygen pressures.

concentration cell, this can be expressed in the form of the relative error in the e.m.f. as a function of an error in the absolute value of the temperature.

$$\frac{\Delta E}{E} = \frac{\Delta T}{T} \quad \ldots\ldots\ldots\ldots\ldots\ldots (26)$$

Showing that the relative error in the e.m.f. is equal to that in the temperature.

The relative error in the sample gas can be given in terms of the relative error in temperature:

$$\frac{\Delta P'_{O_2}}{P'_{O_2}} = -\left(\frac{\Delta T}{T}\right) \ln\left(\frac{P''_{O_2}}{P'_{O_2}}\right) \quad \ldots\ldots\ldots\ldots\ldots\ldots (27)$$

For an error in temperature of $\pm$ 1°K at 1000°K and using air as a reference, we get the errors shown in table (7) for different sample gas compositions.

4.5.2. Errors due to temperature gradients. (294, 297, 298, 306)

Two types of temperature gradients are relevant, the temperature difference between the electrodes at either side of the electrolyte, and the temperature gradients across an electrode face (especially if the electrode area is large). These are shown in Fig. (30).

Under steady state conditions these errors can be expressed for a concentration cell with oxygen partial pressures of P''_{O_2} and P'_{O_2} at the two electrodes at temperature of T_2 and T_1 as:

$$E = \frac{1}{nF} \int_{T_1}^{T_2} t_{ion} \cdot d\mu_{O_2} + \alpha (T_2 - T_1) \quad \ldots\ldots\ldots (28)$$

where t_{ion} is the transference number of oxygen ions in the electrolyte; μ_{O_2} is the chemical potential of oxygen, and α is the coefficient of the thermo electric motive force due to the temperature difference, it depends on the nature of the electrolyte and the metal electrodes. (About 0.1 mV/°C for CaO - ZrO_2 electrolyte and 0.05 mV/°C for Th_{O_2} - CaO electrolyte).

Assuming an oxygen ion transference number of unity this can be written as:

$$E = \frac{1}{4F}\left[\mu_{O_2}(T_2, P''_{O_2}) - \mu_{O_2}(T_1, P'_{O_2})\right] + \alpha[T_2 - T_1] \quad \ldots\ldots(29)$$

where:

$$\mu_{O_2} = \mu^{\circ}_{O_2} + RT \ln P_{O_2}$$

$\mu^{\circ}_{O_2}$ being the standard oxygen potential at T degrees K. and is given by (for the range 600-900°C)

$$\mu^{\circ}_{O_2} = -47.4T - 0.0053\,T^2 - H^{\circ}_{O_2} \quad \ldots\ldots\ldots\ldots (30)$$

$H^{\circ}_{O_2}$ being the standard molar enthalpy of oxygen.

The total error is of the order of 0.5mV for one degree gradient, most of this is due to the chemical potential difference at the two electrodes.

If the temperature gradient is across the face of the electrode itself, oxygen will be transferred from the lower temperature position to the higher, resulting in a mixed potential, the errors here will be of the same order of magnitude as those calculated above.

Another related error can be induced by the impingement of the sample or reference gas, especially if it is cold, on the face of the electrode, the effect is again equivalent to a temperature gradient error.

In the above calculations the oxygen partial pressure was assumed to be unaffected by the temperature difference between the electrodes. This, however, is not true if a sealed metal/metal oxide reference is used instead of air. The equilibrium pressure becomes then temperature dependent thus increasing the errors.

4.6. ERRORS DUE TO OXYGEN PRESSURE GRADIENT ALONG AN ELECTRODE.

If the electrode is very long and non equilibrium conditions occur along it inducing an oxygen pressure gradient, the e.m.f. will be affected.

TABLE 7 ERRORS DUE TO ABSOLUTE ERROR IN TEMPERATURE
air reference, 1 degree K error at 1000 degree K

% O_2 SAMPLE GAS	% ERROR IN O_2 READING
21.0	0
0.2	0.46
20.0 ppm	0.92
0.2 ppm	1.38

FIG. 30 TEMPERATURE GRADIENTS IN OXYGEN CONCENTRATION CELLS

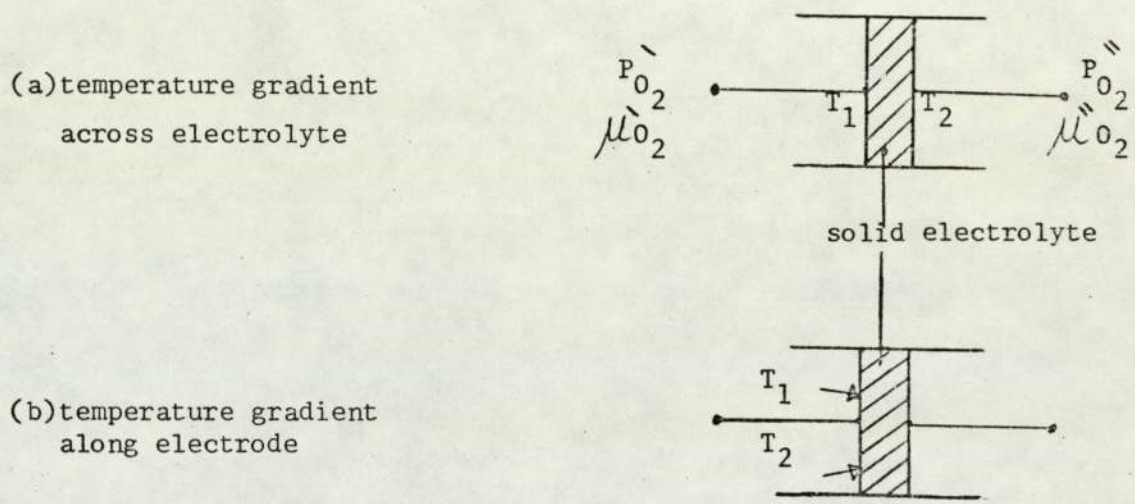

FIG . 31 ERRORS DUE TO OXYGEN PRESSURE GRADIENT ALONG AN ELECTRODE

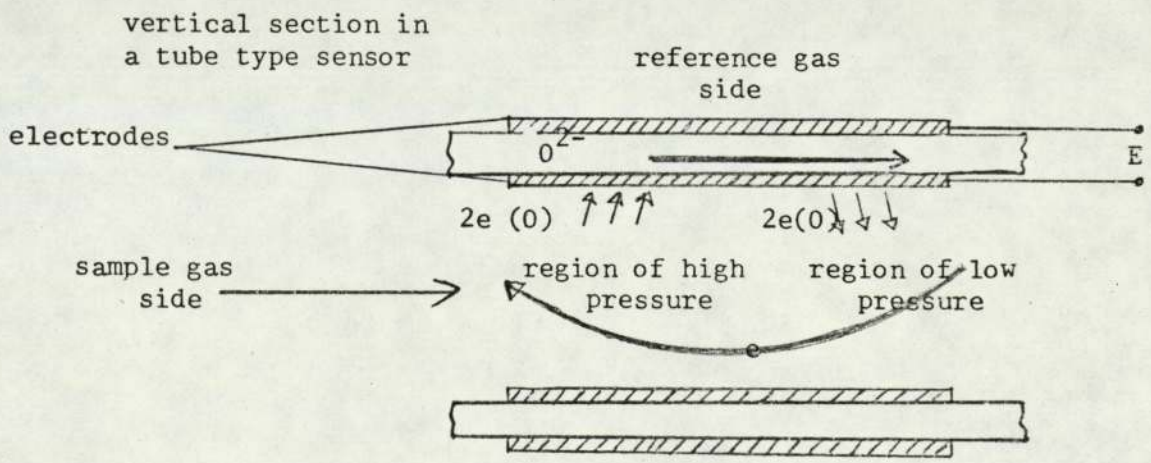

circulating current induces oxygen transfer when there is an oxygen pressure gradient along an electrode

Oxygen will be transferred as shown in Fig. 31 from the higher to the lower part by a circulating current, inducing thus errors.

4.7. ERRORS DUE TO ABSOLUTE PRESSURE GRADIENT BETWEEN THE ELECTRODES.

If the absolute pressure changes equally on the sample and on the reference side, there will be no errors induced in the e.m.f. value. However, if the absolute pressure on one side say the sample side increases from P to $P + \Delta P$.

The change in the e.m.f. due to that is given by:

$$\Delta E = \frac{RT}{4F} \ln\left(1 + \frac{\Delta P}{P}\right) \qquad \text{.....(31)}$$

A one percent change in the absolute value of the pressure at an operating cell temperature of 800°C results in about 0.23 mV error.

4.8. ERRORS DUE TO OXYGEN TRANSFER THROUGH THE SOLID ELECTROLYTE. (299, 300, 304, 305, 307)

As under practical conditions oxygen concentration cells are not under perfect thermodynamic equilibrium, the driving force for oxygen transfer through the solid electrolyte causes equalizing phenomena of oxygen pressure in the two electrode compartments.

Oxygen transfer through the electrolyte can take place by: internal electron current, Knudsen diffusion of gaseous oxygen through pores, chemical diffusion of oxygen through grain boundaries, and by molecular diffusion through micro cracks. These processes are shown schematically in Fig. 31b. (303)

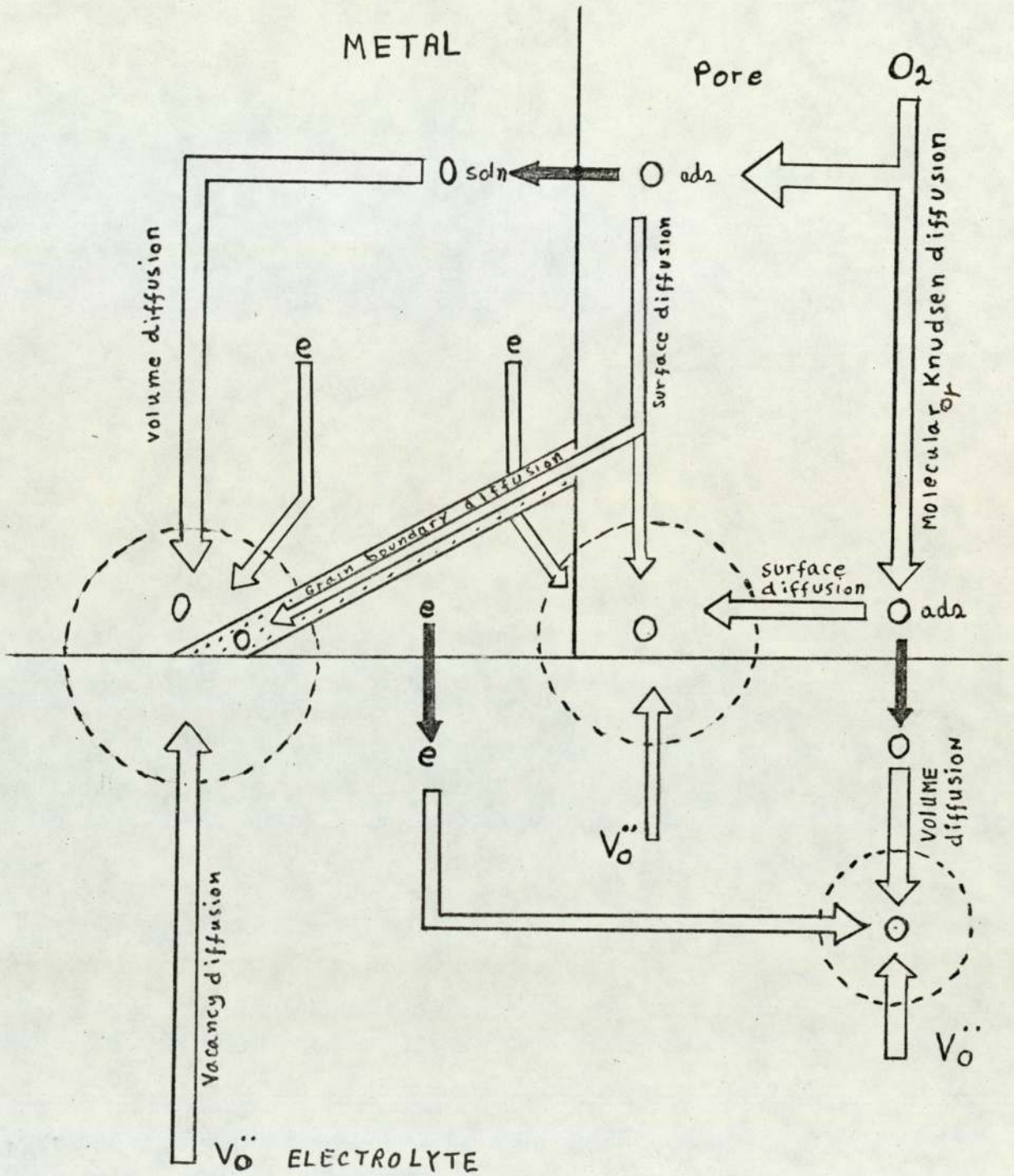

empty arrows indicate transport processes in the homogeneous phases

solid arrows indicate transport processes across a phase boundary

FIG. 31b.SCHEMATIC OF THE SINGLE POSSIBLE RATE-DETERMINING STEPS FOR THE OXYGEN REDUCTION AT A METAL-SUPPORTED GAS ELECTRODE AND ZIRCONIA BASED ELECTROLYTE.

CHAPTER FIVE

THE DESIGN, DEVELOPMENT AND FABRICATION OF A MINIATURE ACCURATE AND VERSATILE SOLID ELECTROLYTE OXYGEN SENSOR

5.1. SENSOR SPECIFICATION

A number of desirable sensor features were outlined in 3.8. These were based on field experience as reported by users and on examination and evaluation of marketed products. (Fig. 17 and 18). These plus an input from the marketing department at Taylor Instruments were used to list the following sensor desired specification:

a) Thermal shock resistance - users report fracture of large and small probes, and cracks in disc type probes.

b) Ruggedness - Ability to withstand normally encountered industrial shock and vibration and maintain good gas tight seals. Storage temperature of -40°C to + 60°C. Working environmental temperature 0°C to + 250°C and inlet gas temperature between 200°C to 800°C.

c) High accuracy - Present products in the market degrade their accuracy by: high thermal gradients between reference and sample electrodes, high thermal e.m.f.'s introduced through changing electric conductor material whilst going through large temperature differences, placing the electrode temperature sensor away from the electrode, and by use of heating systems which cannot cope with sample gas temperature variations.

d) Short response time - The 90% response time of the sensor to a change of gas at 200 ml/M from one end point to another to be less than 2.0 seconds.

e) Long life time - The sensor is to have a life time of at least one full year under continuous operation and under normal working conditions. Electrode peeling, fracture, and leaks seem to have been the main cause of short life of marketed products.

f) Easy to replace - The replacement of a faulty sensor in the field is to take no more than 15M. Some present designs necessitate the removal of the whole probe assembly.

g) Low sensitivity to flow rate variations - A change in the flow rate of the sample gas of ± 20 ml/M from the nominal 200 ml/M is to introduce less than 0.2% error in the reading.

h) Low sensitivity to sample gas temperature - A variation in the sample gas temperature from 200°C to 800°C should introduce less than 0.2% error in the reading.

i) Repeatable sensor characteristics - A change of sensor in the field should not normally necessitate a full re-calibration of the instrument, but a calibration check is recommended.

j) Calibration gas facility - The sensor is to be able to receive calibration gases to check its performance.

k) Simple design - The design should lead to a reliable product which is easy to manufacture. The total factory cost is not to exceed £M. Choice of manufacturing method or technology to be selected by achieving its objectives reliably at the lowest cost. The use of skilled manpower is to be minimised.

l) Versatile design - The first application envisaged for the sensor is "an out of the flue" flue gas analyser, but the sensor should be versatile enough to allow its use in the future for applications such as a ppm to % O_2 analyser (1 to 10^{-7} atm O_2) a sensor with a sealed-in reference, a limited range oxygen pump and to be able to be used in feedback configurations.

m) Low power consumption - To use the minimum power necessary to maintain the above requirements.

5.2. THE DEVELOPMENT OF A THERMAL DESIGN FOR THE SENSOR

The requirement of the sensor to withstand thermal shocks without failure was of such paramount importance that had it not been possible

to fulfil it the product would have been of a very limited commercial value. This problem was therefore tackled first.

Initial talks with ceramic manufacturers indicated their unwillingness to co-operate at this early stage and their preference to accepting a final design. Enquiries regarding tooling and sample-run costs indicated high expenditure levels. This and the absence of any ceramic laboratory facility and experience in-house, at the beginning of this project, led to the adoption of the strategy of model sensor building using a machinable ceramic in the green state (Pyrophyllite) which is reduced to a full ceramic by appropriate firing. Table 8 lists some of this materials' properties. The aim was to investigate a number of thermal designs and end up with one that can be given to a ceramic manufacturer with some degree of confidence to justify the associated expense.

5.2.1. The mechanisms of cracking due to thermal shock in ceramics

When a ceramic material is subjected to a rapid change in temperature (thermal shock) substantial stresses develop. The effect of this on the material depends on the stress level, stress distribution, and its duration. It also depends on the intrinsic properties of the material, such as its modulus of elasticity, its thermal conductivity and its coefficient of thermal expansion. Factors due to manufacturing such as homogeneity, porosity, and pre-existing flaws are also important.

The sensor, whilst in the field, could encounter thermal shocks of two main types: the insertion of a sensor which is at low temperature into a uniform high ambient temperature zone, and the sudden subjection of different parts of the sensor to a high temperature gradient. The stresses induced in the ceramic can be thus divided into two main related types:

a) Stress due to mechanical restraint- This is common when a ceramic is joined rigidly to another member which has a vastly differing thermal

TABLE 8 . CHARACTERISTICS OF PYROPHYLLITE

Naturally-occuring mineral having a variable chemical composition.

Typical Analysis: silica 56%, Alumina 33% , and smallamounts of Ferric oxide, Calcium oxide, Magnesium oxide and Titanium oxide.

DENSITY: 2.6 gm/ml

COMPRESSIVE STREANGTH: 22,000 lb/in^2

VOLUME RESISTIVITY: at 25 ^0C 10^{14} ohm-cm

at 900 ^0C 10^4 ohm-cm

THERMAL CONDUCTIVITY(1350 firing) : $30X10^{-4}$ cal/sec/cm $/^0C$

COEFFICIENT OF LINEAR THERMAL EXPANSION: 8.1×10^{-6} (20 -800 ^0C)

TABLE 9 .COMPARATIVE DATA FOR THERMAL STRESSES

MATERIAL	MODULUS OF ELAS. E. Psi @ R T	COEFF.OF LIN.THERM. EXPAN. $^0C^{-1}$	THERM. COND. @600 ^0C Cal/sec/Cm_2 $/^0C/$
Stab.ZrO_2	$20 X10^6$	$10 X10^{-6}$	$0.5 X 10^{-}$
Al_2O_3	55×10^6	9×10^{-6}	2×10^{-2}
SiO_2 (fused)	11×10^6	0.5×10^{-6}	0.5×10^{-2}
MULLITE	10×10^6	5×10^{-6}	2×10^{-2}
STEEL	30×10^6	16×10^{-6}	6×10^{-2}
P S Z (8 wt %) Y_2O_3	$20.6X10^6$	11.3×10^{-6}	0.6×10^{-2}

characteristics or is not being subjected to thermal shock. Tensile stresses are normally developed. The relevant parameters here are the modulus of elasticity and the coefficient of thermal expansion.

b) Stresses due to thermal gradients - A sudden temperature change can induce temperature gradients within the ceramic such that a free expansion of each volume-element cannot occur. Here also the factor that leads to stress is the restraint on free expansion. Another relevant parameter in this case is the thermal conductivity coefficient of the ceramic.

Comparative values for these parameters for stabilized zirconia, some ceramics and a metal are given in table 9. The values point out the weakness of the stabilized zirconia in its relatively high coefficient of thermal expansion, and its bad thermal conductivity.

5.2.2. Initial model designs

From the above, a number of points were included from the outset in the initial models: Small size, thin walls, uniform heating of ceramic. One of the early designs is shown in Fig. 32. This consisted basically of a small and thin disc to be eventually of the chosen solid electrolyte material. The disc separated two chambers, one being a reference chamber and the other a sample chamber. A specific area on each side of the disc was used as an electrode area in which a thermocouple of very fine wire was embedded into the centre of each face of the disc. The chambers were defined by a thin walled ceramic cylinder, this needs to be gas tight and could eventually be either of a different material than the disc (but of matched thermal characteristics) or of the same material. The chambers and the disc can be made in one part as shown in Fig. 32 (b) if they are the same material or in sections. When made in sections they have to be gas tight. Two pipes, an inlet and an outlet pipe provided means of admitting and removing the gas into the reference and the sample chambers. The electrical wires brought through

the cylinder through holes were sealed gas tight. An outer ceramic shield reduced the radiated heat emanating from a tight closely wound heater on the body section which provided the heat necessary to get the sensor to its operating temperature. An outer stainless steel cover provided overall coverage of the sensor whilst the electrical conductors were linked to thicker wires that went through one end sector as shown in Fig. 32 (c).

Models were constructed to that design in a variety of sizes (4mm to 20mm internal diameter, 20mm to 40mm overall length). Seals were made using copper foil heated to above 1000°C or appropriate sealing glasses. Pt wire was used for the heater. In accordance with the earlier mentioned points, the smaller sensors were preferred and a minimum size of about 4mm internal diameter was chosen as the smallest size which does not need extra skill in placing the electrodes whilst an overall length between 20-30mm was deemed suitable.

One pyrophyllite model constructed had a disc about 0.5mm thick and 4mm diameter and a cylindrical body 1mm thick and about 12mm overall length. The model was fitted with Pt/Pt 13% Rh 0.001" thermocouples on either side and active electrode areas using Pt paste of about 2mm diameter. Gas tight seals were made with thin copper foil heated at about 1000°C. A heater winding of 0.002" Pt wire tightly wound on grooves cut in the body and fixed with a ceramic adhesive. An applied power of about 25 watts was enough to take the model from room temperature to over 850°C in under two minutes as shown in Fig. 33. The switching of the power on and off did not seem to induce fracture in the ceramic despite the extremely high rates of heating and cooling. It induced however breaking of seals round the end body sections. Measurements of the temperature on either side of the disc showed an agreement within one degree centigrade. This becomes clear from the examination of Fig. 34 which shows a plot of the air temperature along

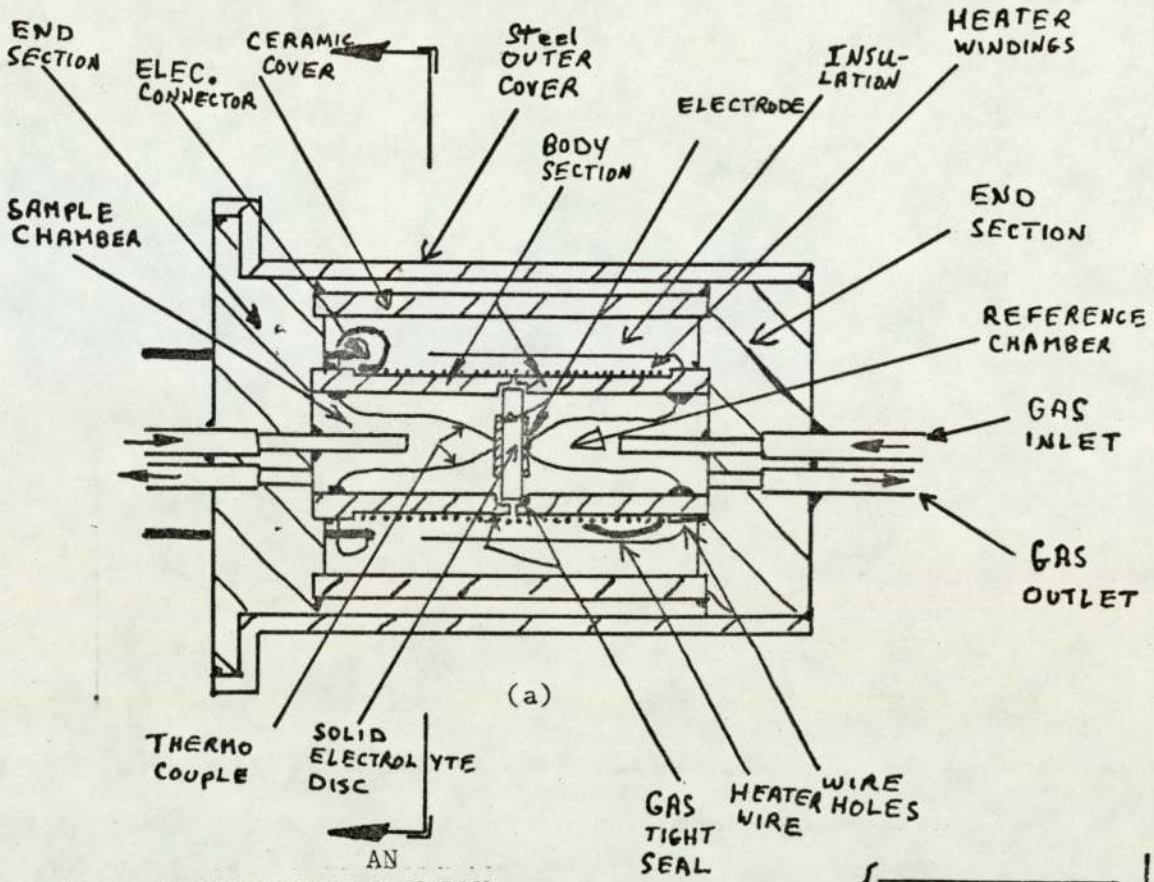

FIG.32 A SECTION THROUGH EARLY MODEL OF THE SENSOR

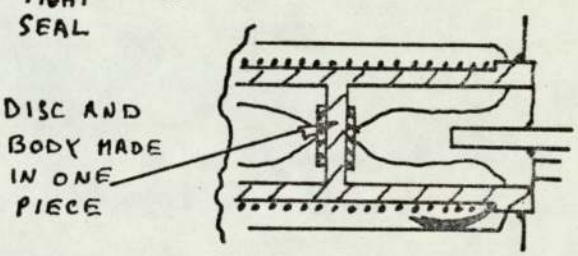

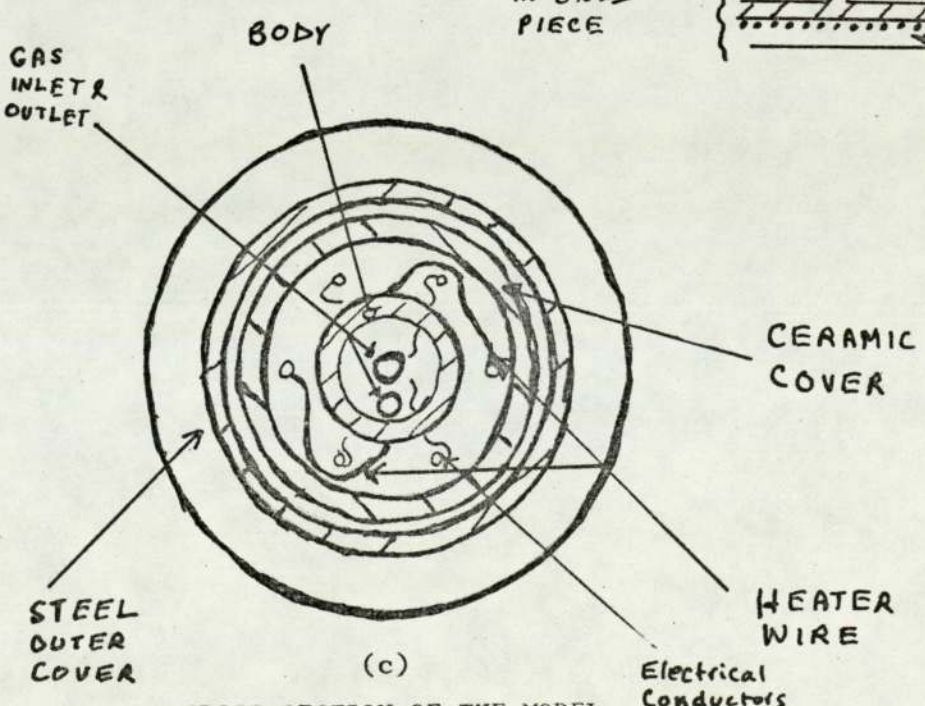

CROSS SECTION OF THE MODEL

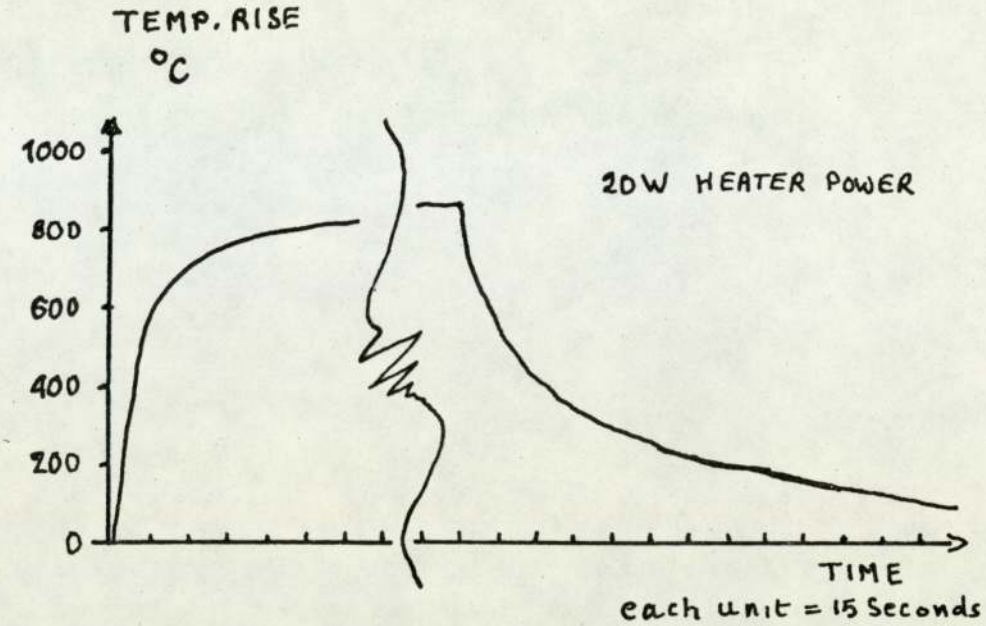

FIG. 33 TEMPERATURE RISE AND FALL OF MODEL AT CENTRE OF DISC

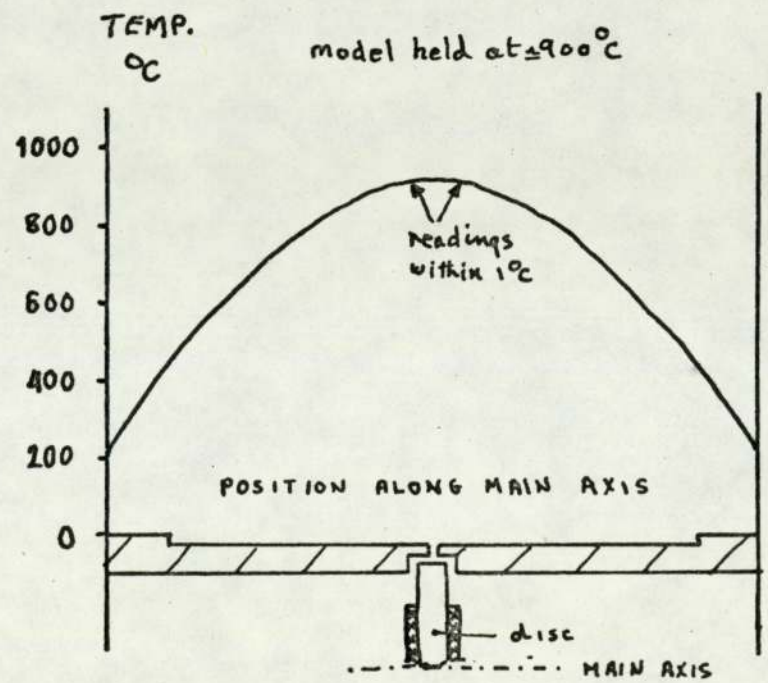

FIG. 34 AIR TEMPERATURE ALONG MAIN AXIS OF MODEL

the main axis of the model on either side of the disc showing the centre region where the disc is positioned to be a flat plateau. The cooling affect of the inlet gas (at room temperature) on the temperature of the disc was found to be negligible (less than 0.3°C) between 0-100 ml/M. The effect was appreciable at higher flow rates.

Tests on further models highlighted the need of a symmetrical shape. A slight asymmetry in the end parts of the ceramic cylinder or in what is joined to it resulted in a gross distortion of the air temperature along the main axis of the model as shown in Fig. 35. This can be compared with one which is symmetrical as shown in Fig. 36. The slight decrease in the electrical winding turn separation (from 0.5 to 0.33mm)seems to help also.

The position of the inlet gas pipe relative to the electrode was investigated further and it was found that the distance between the tip of the pipe and the electrode is an important parameter as shown in Fig. 37.

The above work led to the following conclusion; that a successful "shock immune" thermal design is feasible provided the following points were noted:

a) Size and mass to be kept small.

b) Body to be heated uniformly.

c) Disc and body to be thin.

d) Design to be symmetrical.

e) End section requires further work (leaks).

f) Gas inlet and outlet requires further work.

g) Pt heater fixed with ceramic cement is attacked after a while.

The next stage was to attempt to manufacture a model, based on the above considerations, in the appropriate solid electrolyte material. A body shape based on the above experiences was designed. The body could be made wholely in the solid electrolyte material as Fig. 38a,

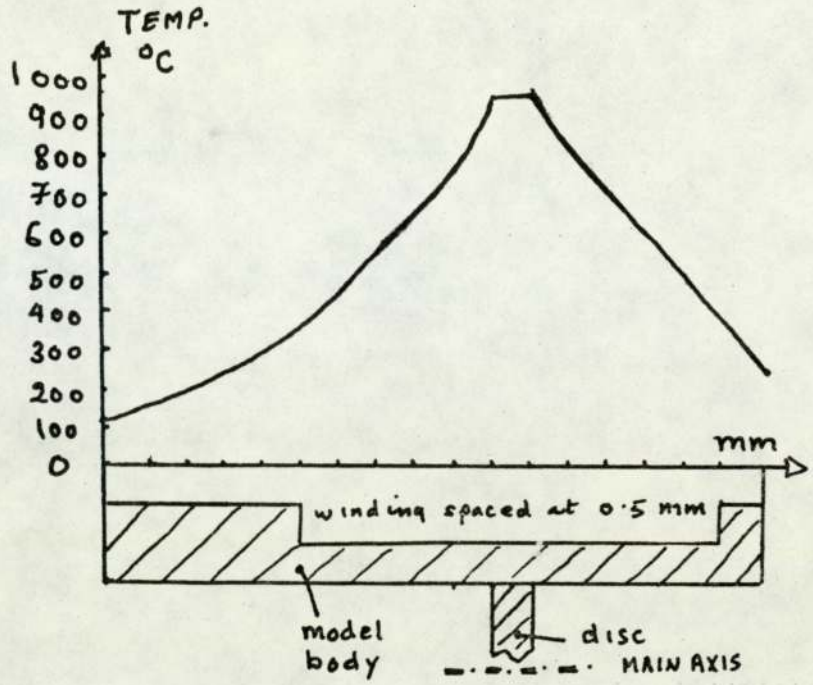

-- FIG.35 AIR TEMPERATURE ALONG MAIN AXIS OF MODEL WITH AN ASYMMETRICAL BODY

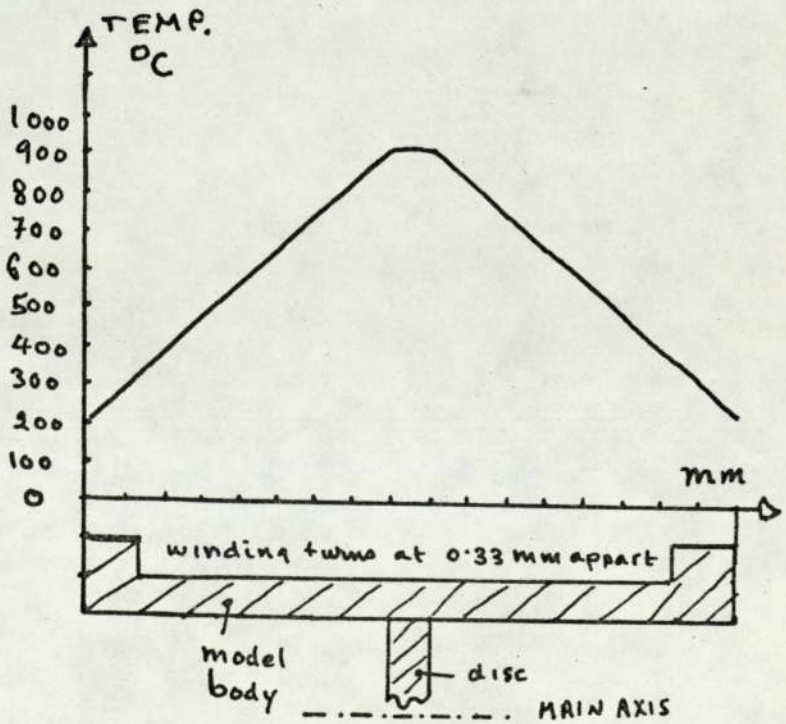

FIG. 36 AIR TEMPERATURE ALONG MAIN AXIS OF MODEL WITH A SYMMETRICAL BODY

in two pieces as in 38c, or in three as in 38b or 38d. This design was about 1 cm longer than the pyrophyllite models so as to lower the temperature at the ends and enhance the uniformity of the temperature at the centre.

5.3. CHOICE OF SOLID ELECTROLYTE MATERIAL [147, 155, 187, 190, 196, 236,322]

In selecting a solid electrolyte material for the oxygen sensor the following criteria were used for guidance:

a) It should have a nearly pure oxygen ion conduction at the temperature and measurement range of interest.

b) It should be gas tight at the operating temperature range.

c) It should be capable of forming reversible electrode reactions.

d) It should have a low enough conductivity at the operating temperature range so that normal instrumentation could be used.

e) It should be chemically stable and also stable with time.

f) It should offer a reasonable thermal shock resistance.

g) It should be commercially available at reasonable prices.

h) It should be capable of mass production.

The choice was made difficult by the huge number of the different materials available varying from glass and porcelain [15, 316] to multi-component solid solutions. Modern research work keeps producing more possibilities e.g. (Bi_2O_3 with SrO, CaO or La_2O_3) [308], (Bi_2O_3 - WO_3) [309] (Bi_2O_3 - Gd_2O_3) [310], (Bi_2O_3 - BaO) [311], (Bi_2O_3 - MoO_3) [312] (Bi_2O_3 - Y_2O_3) [313], (Bi_2O_3 - Er_2O_3) [314], (CeO_2 - Y_2O_3) [315] and (CO_{1-x} - Mg_xO) [317]. Some of these are prone to reduction and have electronic conduction under relatively low partial pressures of oxygen [308] but others have low electronic conductivity and have conductivities which are orders of magnitude higher than the other known materials. [310, 314] None of these however has been fully tested to justify their selection, though their progress should be followed. Some materials are suitable for high temperature use only e.g. calcium zirconate (40-55 mole % for

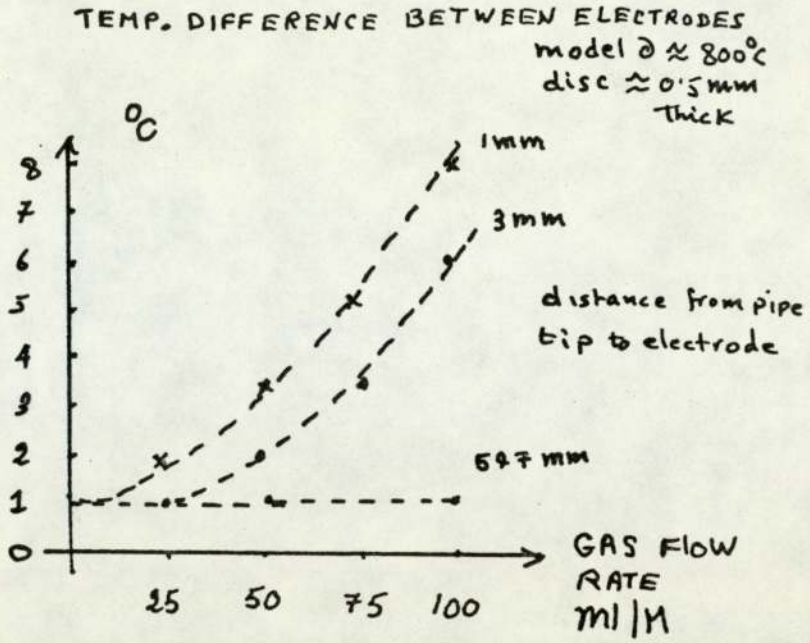

FIG. 37 EFFECT OF INLET GAS PIPE TIP TO ELECTRODE SEPARATION ON ELECTRODE TEMPERATURE

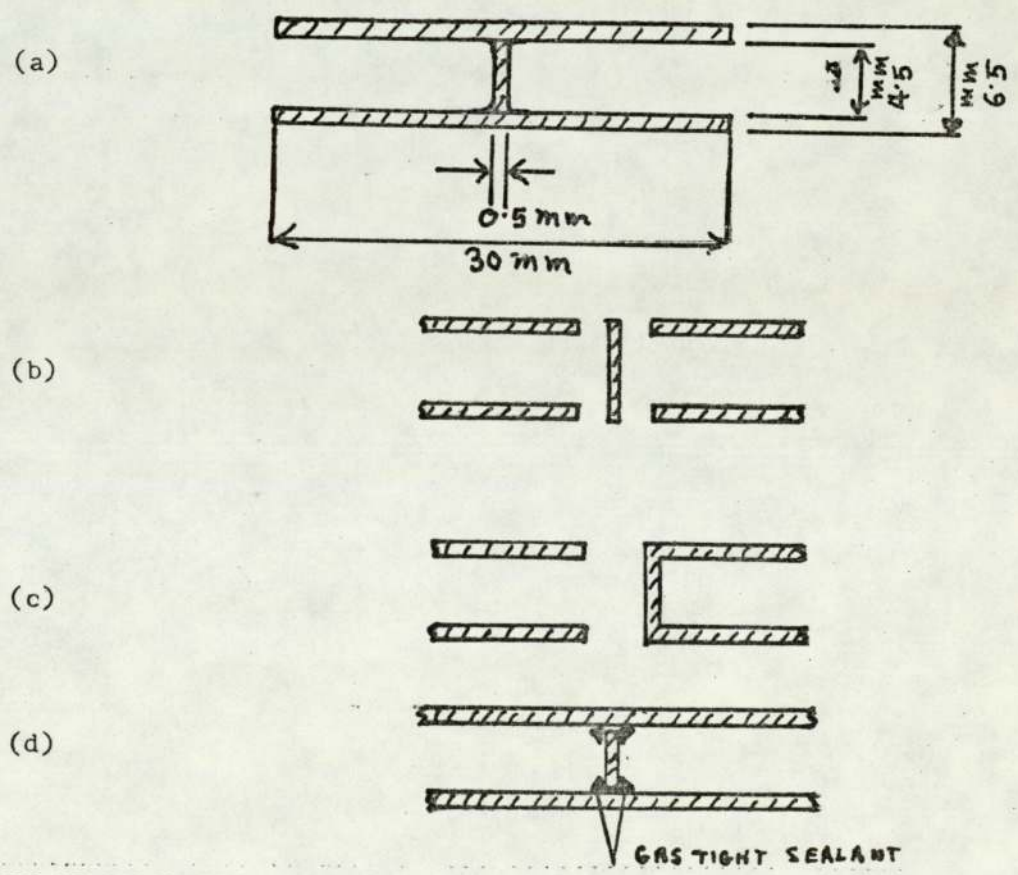

FIG.38 DESIGN OF SOLID ELECROLYTE BODY SUBMITTED TO CERAMIC MANUFACTURERS

1200 - 1600°C)[318]. Others are designed specifically to have mixed conduction for self compensation purposes. [319]. The attraction of a lower operating temperature have generated some work in that area e.g. β - Al_2O_3[320], and Calcia-Doped Ceria. [321]

The most successful and widely used solid electrolytes, however, have been those based on one of the group 1V B oxides - ZrO_2, HfO_2, CeO_2, or ThO_2 - forming a solid solution with either alkaline earth oxides - Sc_2O_3, Y_2O_3 or rare earth oxides. [195] An idea of two of the relevant parameters of some of these solid solutions [322] can be gained from Fig. 39 showing variations of ionic conductivity with temperature, and Fig. 40 showing the total conductivity as a function of oxygen partial pressure. Solid solutions of CaO, MgO and Y_2O_3 in ZrO_2 have been used extensively for many years. MgO which was popular for its shock resistance was later discovered to be unstable with time. [103, 105]. De-stabilization of the CaO - ZrO_2 was also reported[93,158] There were also reports on a slow increase of resistivity with time[192,196] Whilst Y_2O_3 stabilized ZrO_2 was reported to be stable with time [158], a change in its resistivity in air and in H_2 with time was also reported [192,330]. This ageing phenomena can be reduced to an acceptable rate if powder of a sufficiently fine grain is used. (U.S. patent 3,351,496). From Figs. 39 and 40 it seems that the yttria stablized zirconia fulfils both the conductivity and oxygen requirement range. Those solutions are, however, fully stabilized ones. Curtis [70] and later Etsell [323] reported an increased thermal shock resistance by partial stablized zirconia. Further work on PSZ of the system (CaO - ZrO_2) was conducted by Gravie & Nicholson [324] and by Green and others [325] who investigated its fracture behaviour and by El-Shiekh and Nicholson[326] who studied its thermal shock structure. It appears that grains of pure tetragonal ZrO_2 are distributed in a matrix of fully stabilized cubic material. This structure seems to provide an effective stress relieving mechanism during thermal shock. So PSZ bodies were found

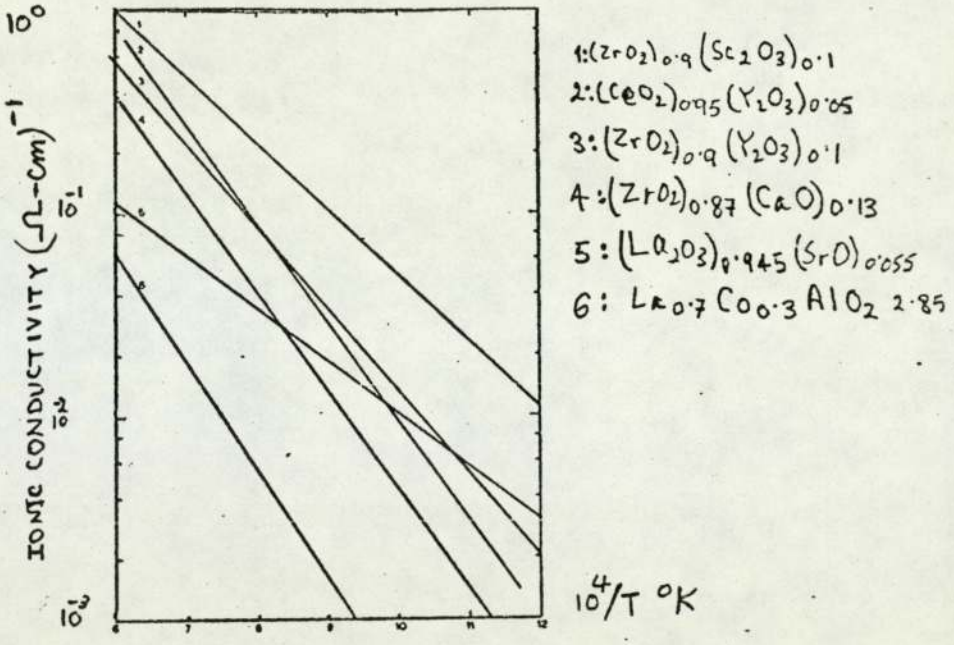

FIG. 39 Ionic conductivities of selected oxide electrolytes as a function of temperature.

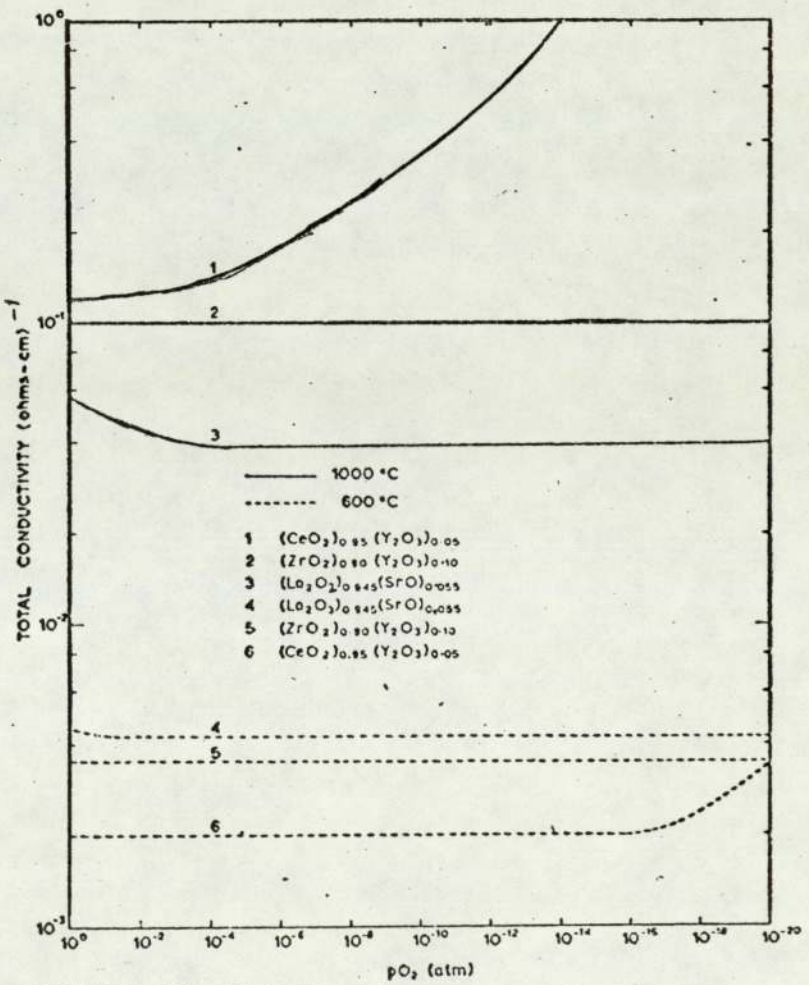

FIG. 40 TOTAL CONDUCTIVITIES OF SELECTED OXIDE ELECTROLYTES AS A FUNCTION OF OXYGEN PARTIAL PRESSURE

to be superior in thermal shock resistance not only to fully stabilized zirconia but also to most other polycrystalline refractory oxides. This prompted major manufacturers - Corning (USA)[244] and Desmarquest (France) - to offer a Y_2O_3 8 wt % PSZ. As this material seemed to satisfy the most critical requirements it was chosen.

Corning and Desmarquest were contacted and tubes of that material were obtained in the nearest diameter to the design of Fig. 38d. The disc was made by cutting, grinding and polishing a piece cut out of a larger diameter tube. A high temperature glass was used to seal the disc in the middle of the tube and the rest of the sensor was constructed as the early models. (Facilities for ceramic, grinding, cutting, drilling, polishing and pressing were by then established in-house). This sensor behaved very similarly to the models and being in the right material acted as an oxygen concentration cell. This prompted further enquiries to both manufacturers about the feasibility of manufacturing the design shown in Fig. 38. This resulted in:

i) Corning accepted an order to make 10 models as per Fig. 38 - the order took 15 months to be delivered and the samples had either holes or cracks in the disc area and were made by the joining of two sealed tubes together with matched ceramic adhesives. Further talks and an order of another 10 models resulted in a delivery after six months of, though better, unsatisfactory models made out of one sealed tube ground flat at the end and a tube sealed to it with matching ceramic adhesive. The units were crooked and one side (the tube side) had a domed end making the establishment of an electrode difficult there. Corning use the slip-casting method of manufacture - this made the cost per unit expensive and the finish not very good. However, further contact with Corning was abandoned due to their full commitment to car manufacturers, who planned to use oxygen sensors on the exhaust of motor cars. This has absorbed all their manufacturing capacity.

ii) Desmarquest which used moulding techniques accepted an order to make a tool as per Fig. 38 but asked the disc thickness to be relaxed to no greater than 0.8mm. The tool and the first samples took over a year to produce, but when they eventually arrived they were of very good quality and finish. A sample of 50 measured for dimensional variation showed the results given in table 10. All crucibles supplied by Desmarques included a mass spectrometer He leak test. These samples showed the feasbility of manufacturing such a design in mass production, at realistic costs and in acceptable dimensional tolerances and material quality.

5.4. IN-HOUSE PRODUCTION OF CRUCIBLES

The very long delays in supplying the samples brought out the aspect of the Company's vulnerability to supply delays, and when only one of the suppliers proved satisfactory this point was highlighted. The possibility of being able to produce the crucibles in-house under crisis conditions was then investigated.

5.4.1. Methods of crucible fabrication

There are basically four ways to manufacture the crucible:

a) Slip casting - This is an old established process of ceramic ware forming. It consists briefly of preparing a mixture of a powdered material and a liquid into a stable suspension (the slip). Pouring this slip into a porous mould (usually plaster of Paris) and allowing the liquid portion of slip to be partially absorbed by the mould. A layer of semi-hard material is formed against the mould surface as liquid is removed from the slip. The process is interrupted when a suitable wall thickness has been formed by pouring out the excess slip (drain casting), or when the entire mould cavity is filled with semi-hard material (solid casting). The material is dried in the mould (shrinkage usually occurs here) and the solid object removed from the mould. The article is usually hard enough to undergo trimming operations before firing. Although this method

TABLE 10 DIMENSIONAL SPREADS IN A SAMPLE OF 50 DESMARQUEST CRUCIBLES

	AVERAGE VALUE mm
DISC THICKNESS	: 0.69
LENGTH	: 30.5 ± 0.2
O/D	:6.5 ± 0.1
I/D	: 4.5 ± 0.1
SURFACE OF DISC AREA	:EXCELLENT
SURFACE FINISH	: VERY GOOD

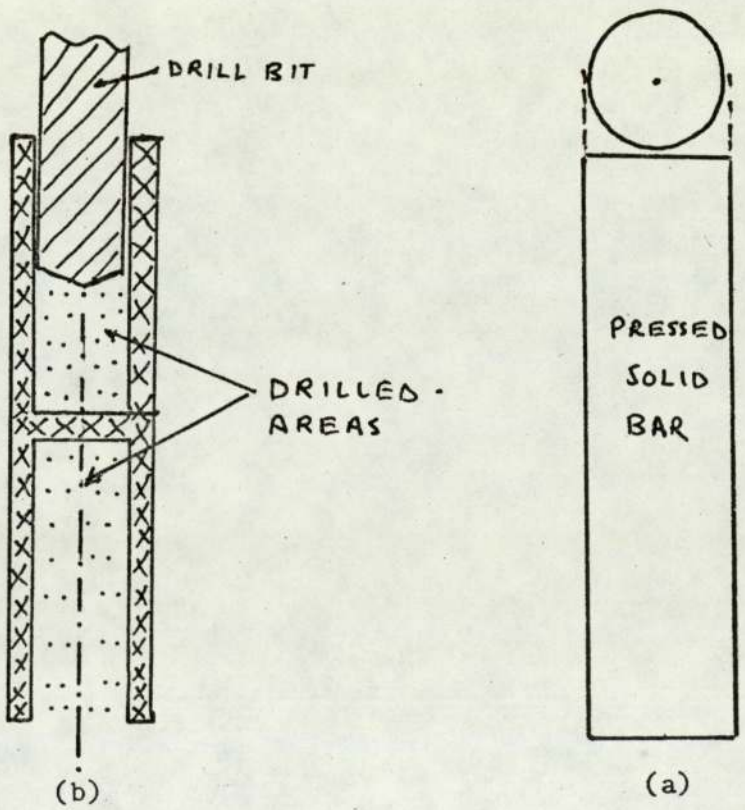

FIG. 41 CRUCIBLE MANUFACTURING BY MACHINING BAR IN THE GREEN STATE

is simple and ideal for producing thin-walled and complex shapes, and the moulds are inexpensive, it is advantageous for small production runs only. The failure of Corning to produce any satisfactory samples using this method led to the exclusion of this method.

b) Moulding - This process is used by Desmarquest and which is in a way similar to plastic moulding. A suitable steel tool to the required design is made and the material suitably prepared (this could take a very long time) is injected under pressure into the tool and hence takes its form. There is hardly any published data on this and the manufacturers are very reluctant to talk about it. Corning were working on a similar process, but have not been successful to date. This process was excluded due to lack of in-house experience and lack of facilities.

c) Plasma arc-spraying. This method developed by the G.E. Co.[166] consists of using a plasma-arc spray to deposit particles of the solid electrolyte onto a suitably shaped mandrel which is subsequently leached out. This is followed by sintering the free-standing body to render the electrolyte leak-tight. Feed material for the plasma-arc spray operation is prepared by spray-drying of commercial grade powders. G.E. were able to produce tubes to 0.005" thick and leak tight. This process though suitable for making tubes and test tube shapes, is not suitable for producing the required shape in one piece due to the position of the disc in the middle of the tube.

d) Machining - The machining of fired ceramics is hard and lengthy operation. However, if a pressed block of material is partially fired, at a lower temperature than the proper sintering temperature, it will have enough strength to undergo machining operations easily. The specimen once machined can now be fully fired. Though this method is not as cheap as (b) it is intended for use under emergency

conditions when normal supplies are cut. Its costs are estimated to be double that of process (b) but this is justified in periods of crisis. The equipment required is mainly normal ceramic machining equipment and suitable high temperature furnaces. This was the process chosen for the in-house fabrication of the crucibles.

5.4.2. Procedure for crucible manufacturing by machining.

a) The preparation of the solid solution: This is a very important part of the procedure, and the failure to achieve equilibrium during the preparation could lead to a considerable change in the electrical properties. Equilibrium in solid state reactions is often attained with great difficulty and requires very high temperatures. The most direct method of preparation is that of powder mixing. A procedure for powder mixing is given in Appendix (4). The final sintering temperature can be reduced if the oxide powders are very fine. One way of doing this is by hydroxide coprecipitation (76, 129, 134, 327) through which many ZrO_2 based solid solutions have been reported to have been formed at only 500-800°C. A procedure for coprecipitation mixing is given in Appendix (5). The precipitation atmosphere is an important factor in sintering solid solutions - this is discussed by Thompson and others (328). A technique for preparing ultra high-purity submicron powders is described by Mazdiyasni and others (152) who also used simultaneous decomposition of Y_2O_3 and ZrO_2 alkoxides to obtain an ideal mixture of powders having high surface activity, they achieved full stabilization by firing at 1000°C for 30M.

b) Pressing machining and firing the crucible: A tool-steel die having a cylindrical shape and having larger dimensions than the eventual crucible (about 15-20%) is needed. The powder mixture is then pressed in the die as described in Appendix (6). The machining procedure is shown in Fig. 41. The rate of shrinkage after firing

is a very important parameter, and when determined for a given solid solution and under given conditions, relatively accurate dimensions can be obtained. The requirement of the above procedure to fire at 2000°C necessitated the purchase of a furnace which can operate up to that temperature in air and in vacuum. This was a costly item which took well over a year to arrive and over six months to commission (due to the loss of a component at London Airport). When commissioned eventually it operated up to 1600°C before it tripped and it was discovered that the cooling water system was not adequate. A better system was designed, but not yet built due to the necessity of writing the thesis. Therefore the above procedures for machining crucibles were used on CaO stabilized zirconia which needed only 1600°C firing; a facility which was available at the laboratory. It is intended however that PSZ crucible in-house manufacturing be established within the next year.

5.5. Quality Control of Ceramic Crucible

In order to keep manufacturing costs down it is essential to do the inspection and quality assurance at the lowest possible level. One requirement for instance, that of gas tightness, was catered for by the crucible manufacturers themselves (using He-Mass Spec. leak detection). This could be duplicated in-house if the crucibles were manufactured there. The question of whether the solid electrolyte material has the required properties can only be established when a sensor has been made and tested and if then rejected, the cost would be great. A test at a lower level is clearly needed.

5.5.1. Common solid electrolyte material defects

Consideration of the Common Solid Electrolyte material defects is necessary at this point:

a) High porosity - this is detected by a gas-leak test.

b) Dimensional defects - early dimensional inspection can be introduced.

c) Surface quality - visual inspection for uneveness, cavities and impurities especially at the electrode areas, this could be done under magnification.

d) Correct solid solution - homogeniety, presence of impurities and material of deviating composition.

Testing for (a,b,c,) is easy enough - (d) however involves analysis of ceramics by chemical or x-ray methods and is expensive.[163] This may be feasible when a large batch of powder is being manufactured, but for individual crucibles a simpler method is needed.

5.5.2 Electrical conductivity measurements of solid electrolytes

The electrical conductivity of solid electrolytes has been measured by many workers as a function of temperature, composition, partial pressure of different gases and time.

Measurements on compressed cylinders, discs and single crystals have been done. The problems associated with such measurements are many and result in differences by a factor of ten between results obtained by different authors. Errors due to presence of porosities, electrode resistance, thermal pretreatments and measurement techniques, are the main causes of this. On the other hand if by careful consideration and design most of these errors are eliminated, the conductivity can be used as a simple convenient and economical parameter to check the electrical quality of the crucibles. Two basic measurement methods can be used.

a) D C - Direct DC measurement between inert electrodes with the sample mounted between them is not possible, due to polarisation of the electrodes. One way round this is by making a four electrode measurement as shown in Fig. 42. DC voltage is applied between the outer electrodes, another set of inner electrodes is used to measure the potential across a given length of the specimen. The conductivity can be found from this voltage and the current flowing in the outer circuit. As no current flows between the two inner electrodes no

polarization effects nor contact resistances errors are introduced. This technique gives very high accuracy but needs a cylindrical sample and is complicated. Another DC technique consists of switching a constant voltage or a constant current for a given time and monitoring the potential across the sample. An overvoltage builds up with time and the initial value of that voltage is the one corresponding to the drop across the sample due to the current flow, as shown in Fig. 43. The applied voltage should not exceed 2.5 volts so as to avoid a breakdown of the material.(360) This technique is also complicated; but can be simplified and its accuracy increased by the use of electronic switching.

b) AC - This method is simpler and commercial bridges and other instruments have been used in the range 1-3 K Hz. Polarization effects at the electrodes are negligible. However, polarization inside the ceramic material at the contacts between the crystalline grains of which the material is composed may occur. The crossing of oxygen ions between neighbouring crystallites may be inhibited to some extent by a so-called "second phase" (material of deviating composition) formed during the firing of the ceramic. Impurities, a by-product of secondary reactions at the firing temperature may also be found in between the grains. The electrical resistance to direct current of such material with a second phase may be much higher than that of a pure material without a second phase. Because the separating layers are thin, capacitive bridging of their resistance takes place at high frequencies, so measurements at high frequencies yield the same value as for pure materials.

5.5.3. Electrical conductivity as a quality control parameter

A correlation between the electrical impedance, micro-structure and composition of calcia stabilized zirconia has been established by Beckman's and Heyne.(207) They traced slow cell response, drift and high internal resistance to "second phase" phenomena in the ceramic

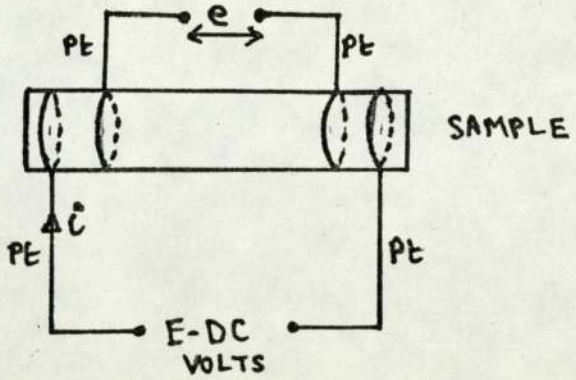

FIG. 42 . FOUR ELECTRODE DC TECHNIQUE FOR ELECTRICAL CONDUCTIVITY MEASUREMENT OF SOLID ELECTROLYTES

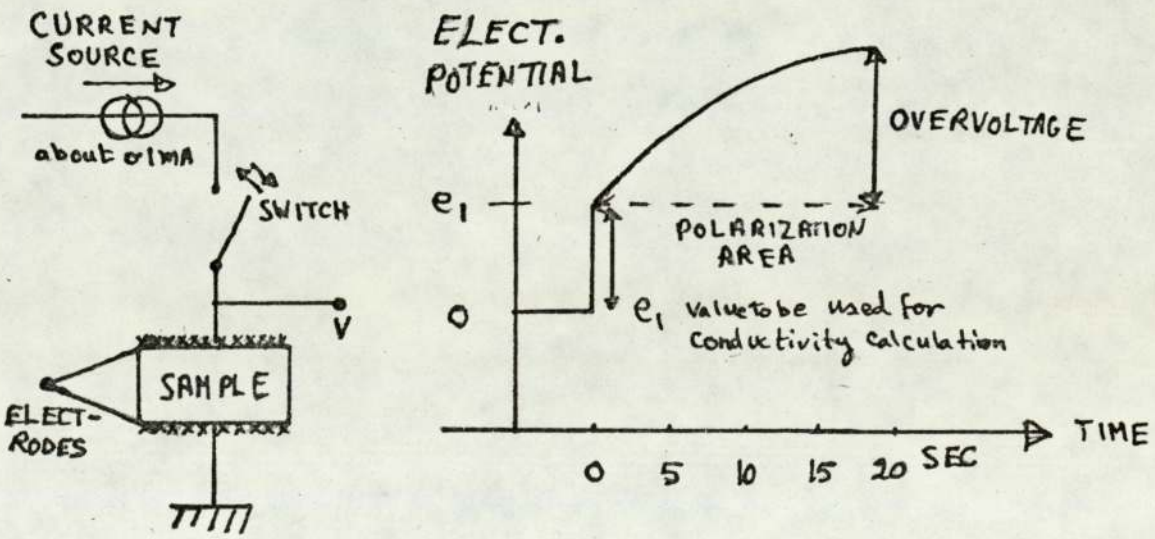

FIG. 43. ELECTRICAL CONDUCTIVITY MEASUREMENT BY SWITCHING-CURRENT TECHNIQUE

material. They measured the impedance of samples in the range 10^{-3} Hz to 10^{6} Hz. A general shape of the impedance - frequency curve of a non-ideal zirconia sample is shown in Fig. 44. At the low frequency range electrode polarization caused by non-reversible electrodes dominates giving a dispersion effect in that region. The choice of the appropriate electrodes (e.g. thin sputtered electrodes) can minimise this. In the intermediate range effects caused by the micro-structure dominate and lead to a dispertion region. At the high frequencies the impedance diminishes because of electrode capacitance. The choice of the measurement temperature is important so that the relevant information appears at convenient frequencies. The frequency dependance of impedance of various sintered zirconia samples at 550°C is shown in Fig. 45. (329)

The complex admittance technique has been used to study solid electrolyte polarization. Bauerle (201) who established the technique for solid electrolytes, studied the polarization behaviour of zirconia-yttria solid electrolyte specimens with platinum electrodes over a temperature range of 400° to 800°C and a wide range of oxygen partial pressure. He determined the complex admittance of specimen over a frequency range from D.C. to 100K Hz.

The analysis of his data indicated the presence of three polarizations:

(1) an electrode polarization characterized by a double layer capacity and an effective resistance for the total electrode reaction;

(2) a capacitive-resistive electrolyte polarization, due to a partial blocking of oxygen ions at the electrolyte grain boundaries by an impurity phase "second phase" and

(3) a pure ohmic electrolyte polarization. Many others used this technique to study different systems.(203, 204, 205, 206)

It is clear from the above that in the conductivity parameter either as an impedance - frequency scan or as a complex admittance frequency scan we have a convenient means of quality assurance that can ascertain the quality of both the electrode and the electrolyte.

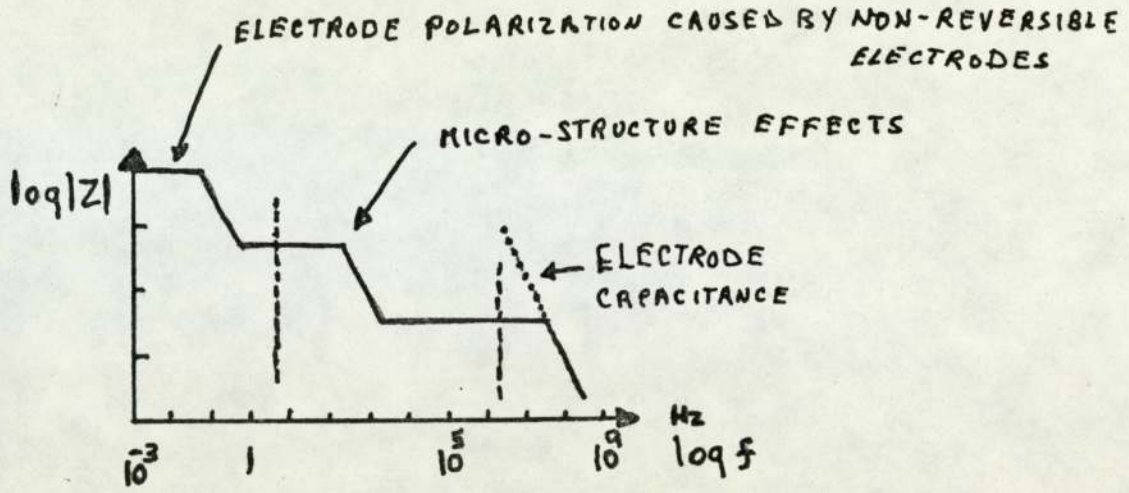

FIG. 44 . GENERAL SHAPE OF IMPEDANCE-FREQUENCY CURVE OF A NON IDEAL ZIRCONIA SAMPLE

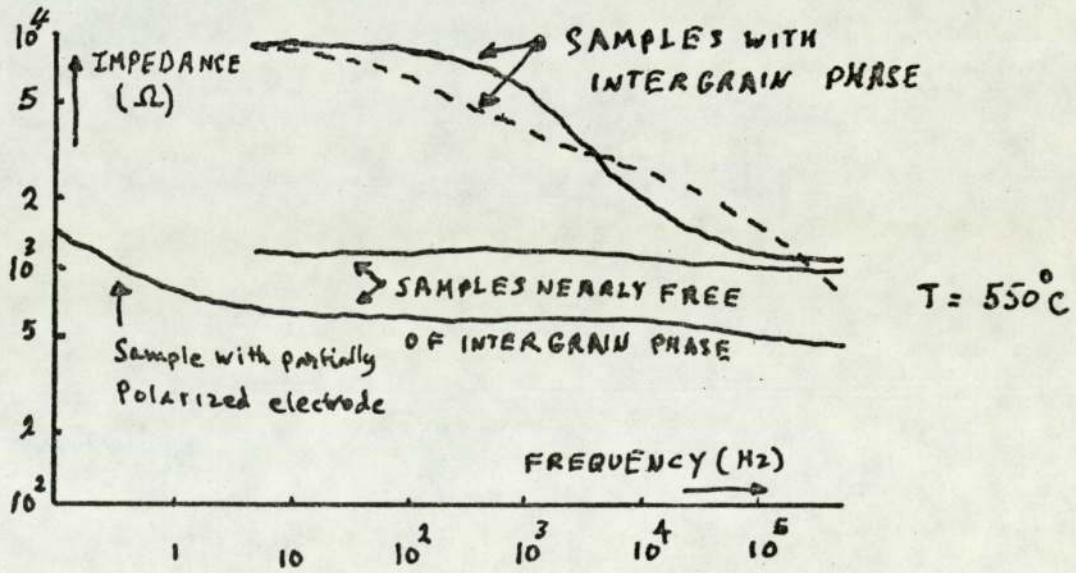

FIG.45. FREQUENCY DEPENDENCE OF IMPEDANCE OF VARIOUS ZIRCONIA SAMPLES

5.5.4. The design of an electrical conductivity measuring apparatus

The aim was to investigate the possibility of using the impedance/admittance-frequency techniques suitably simplified as a means of quality control in production.

The investigation was to proceed in two phases:

(1) the use of selected specimen with a variety of expected defects (e.g. non porous electrodes, wrong material, having "second phase") in the material chosen (Yttria PSZ) and obtain impedance-frequency scans for them, and compare them with a perfect specimen;

(2) select the minimum number of frequencies to identify each of these defects and design apparatus that can easily do these tests for production purposes.

It was necessary to proceed with phase (1) first, and for that the need to change the oxygen atmosphere was not deemed necessary so the requirement was for apparatus that can test especially manufactured specimen (discs) in the frequency range of $1\text{-}10^5$ Hz, lower frequencies being time consuming and in the temperature range of 700-850°C. The problems associated with such a measurement has been comprehensively discussed by Moulson & Popper (331) and they recommended the use of a circular disc having a guard electrode; this eliminates the extraneous leakage currents.

A novel measuring technique that meets the above requirements including the use of a third electrode and allows the data to be used for both impedance or complex admittance-frequency plots is shown in Fig. 46. The sample has to be disc shaped and is fully covered on one side by an electrode whilst the other face has a central active electrode and surrounding it a guard ring electrode. A stable oscillator having no DC component and a frequency range from $1\text{-}10^5$ Hz provides the variable frequency voltage this is monitored by a true RMS DVM and a frequency counter. The Hi electrode supplies the single electrode with voltage through a coaxial cable which has its sheath earthed at the sides of

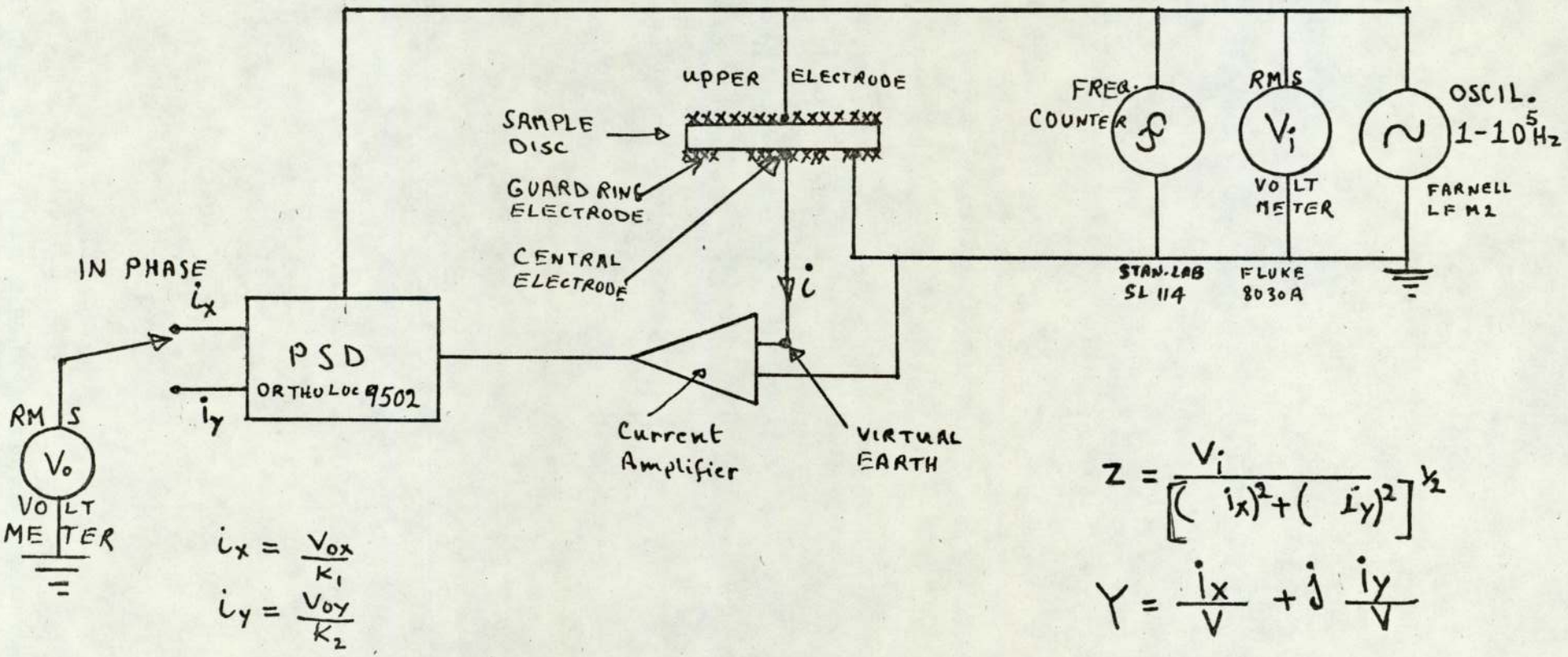

FIG.46. A METHOD FOR THE MEASUREMENT OF THE CONDUCTIVITY OF SOLID ELECTROLYTE SAMPLES

the instruments and connected to the guard ring area at the disc. This eliminates the extraneous leakage currents. The central active electrode is connected through a coaxial to a current amplifier whose other input is earthed. As the input of the current amplifier is a virtual earth, the potential between the central and the guard electrodes is nearly null and thus no errors are introduced that way. The current amplifier should have a passband greater than 2×10^5 Hz and be of a high quality (noise, drift, temperature coefficient and current offset). The output of this amplifier is fed to a phase sensitive detector which is driven from the oscillator. The output of the PSD is the in-phase and the quadrature components of the current through the disc. From the value of the applied voltage, its frequency, the gains in the system and the current in-phase and quadrature values, either an impedance value or the admittance components can be calculated. This system was built using the components listed on the diagram.

The sample holder-furnace part of the design was more involved and several schemes were partially built and abandoned before the design described was evolved. A horizontal furnace Fig. 47, was adopted due to the great temperature differentials encountered in vertical designs.(333) All the insulating material was high purity alumina. The furnace had an easy to change heater element placed on the inside of an alumina cylinder, the heater wire itself was run inside alumina insulators. The electrical conductors, three electrodes and a Pt/Pt 10% Rh T/C are brought out through ceramic insulators to an outside ceramic terminal strip. The general details of the sample holder which includes the Pt. electrodes is shown in Fig. 48. This shows the spring loaded and self centring feature of the design. The electrodes used on the present unit are Pt. paste fired electrodes, the use of an alternative in the future is contemplated. The discs have to be prepared so that they have the correct dimensions and polished to a mirror finish.

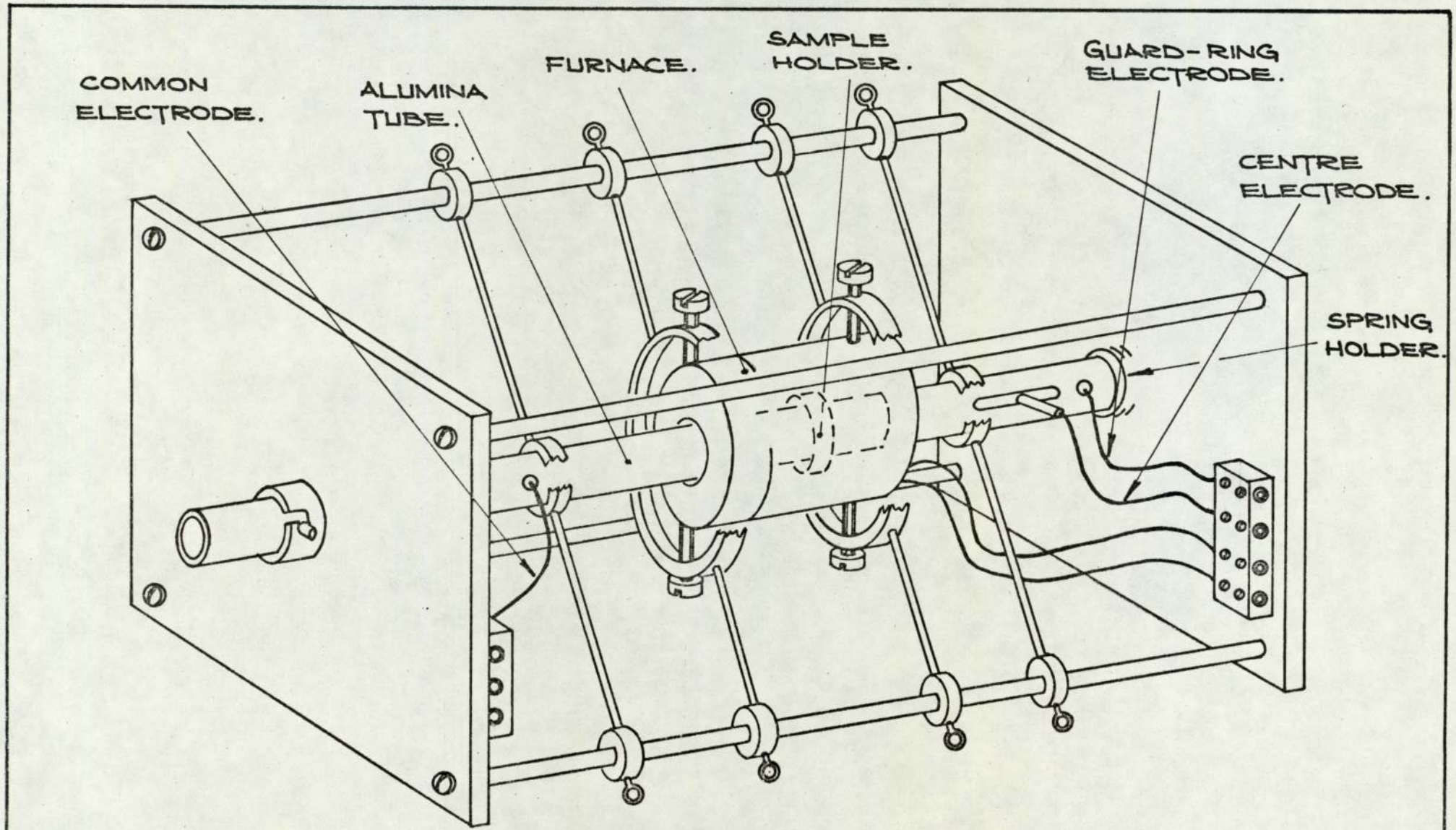

FIG.47. SCHEMATIC OF CONDUCTIVITY APPARATUS

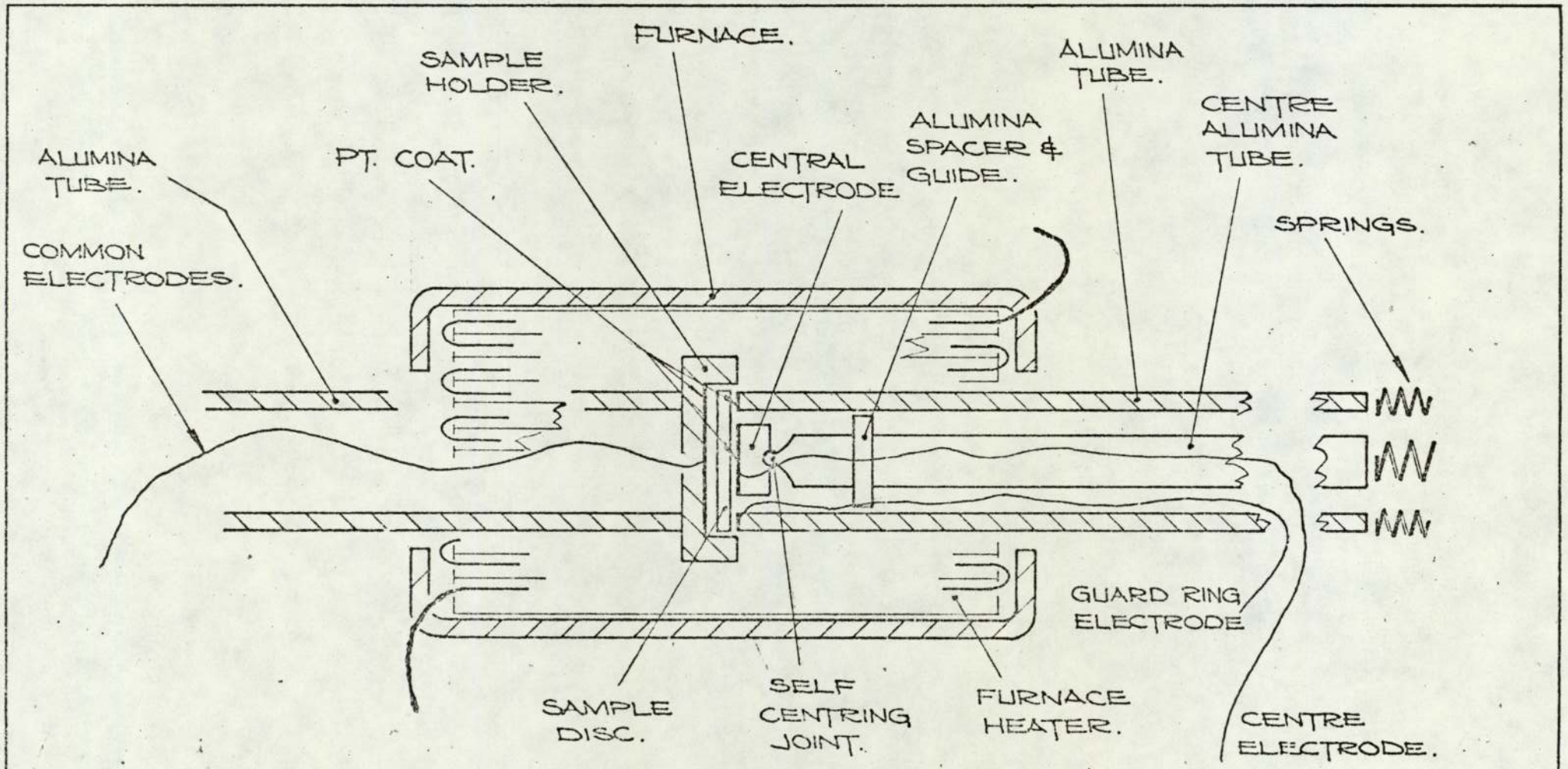

FIG.48. SCHEMATIC OF SAMPLE HOLDER AND ELECTRODES OF CONDUCTIVITY APPARATUS

For production use a simplified and smaller jig is envisaged, but using the same main features.

It is unfortunate that due to delays in the arrival and commissioning of the high temperature furnace which is still at present not functioning, and the need to submit this thesis within certain time limits, that this work was not pursued beyond the building of the apparatus and functionally testing it. As data on Yttria PSZ is scarce the work along these lines is to be continued and forms one of the main research topics for the company's R & D programme.

5.6. SENSOR ENDS DESIGN

Designing a high temperature gas-tight sensor end seal proved a very difficult problem. It consumed a lot of time and effort to solve satisfactorily. Initial work indicated that rigid sealing with ceramic based cements always led to eventual joint failure. Many cements some Zirconia based with matched characteristics were tried. The use of ceramic materials or a metal of similar characteristics as end caps proved also unsatisfactory. It was clear from this initial work that in order to take the length variations due to gross changes in temperature without breaking the Zirconia crucible nor the gas tight seal, a flexible form of support must be introduced. This would be the intermediate step between the ceramic and the eventual end cap material which due to the atmospheres anticipated would preferably be in a high temperature stainless steel. Thin stainless steel diaphragms were initially experimented with. The basic idea is shown in Fig. 49. The idea seemed to offer, if successful, a solution to the ceramic fracture problem caused by rigid mounting, a reduction of the possibility of gas tight seals breaking and makes the sensor able to stand a reasonable amount of shock and vibration which would be buffered by the flexible diaphragm. The successful solution required, however, a suitable diaphragm shape and material; the ability to produce a

diaphragm/zirconia gas tight seal and a diaphragm/stainless steel gas tight seal.

5.6.1. Zirconia - metal gas tight seals

When the sensor is operating at about 850°C its ends were found to rise no higher than about 500°C. This sets basically the anticipated working temperature of the zirconia-metal seal. The following avenues were investigated:

a) Ceramic adhesives - eventual breakage occured; considered unsatisfactory.

b) Mechanical seals - silicon rubber and PTFE gaskets tried and found unsatisfactory.

c) Electron beam welding (I.S. Ltd.) - this was tried with zirconia crucibles which had their ends platinized as shown in Fig. 50. Pt. paste fired at about 1450°C was used. Successful results were obtained - it was, however, deemed uneconomical due to the cost per sensor being about 1/12th of the desired sensor manufacturing cost.

d) Vacuum brazing - work on this was conducted at Edward High Vacuum (Crawley) Ltd. Platinized zirconia tube samples and diaphragms made out of EN58J S.S. (0.075mm thick) were used. A number of selected brazes (J & M Ltd.) in 0.015" wire were made into rings and placed between the platinized ceramic and the diaphragm as shown in Fig. 51. Pressures of 10^{-4} Torr were used and a brazing temperature of about 30°C above the braze temperature, so as to ensure sufficient fluidity to form the joint. A number of alloys were tried and successful seals were obtained with Pallabraze 840, 880, 1237 and 1090. Independent work was conducted by the M.O. Valve Co.Ltd. Their conclusions were that the ceramic should be coated at the end to be brazed by a molybdenum and a glaze mixture.

e) Glass sealing - this type of sealing has been used before (332) and the experience gained in sealing the zirconia disc at the centre of the tube using a special glass suggested that by the proper

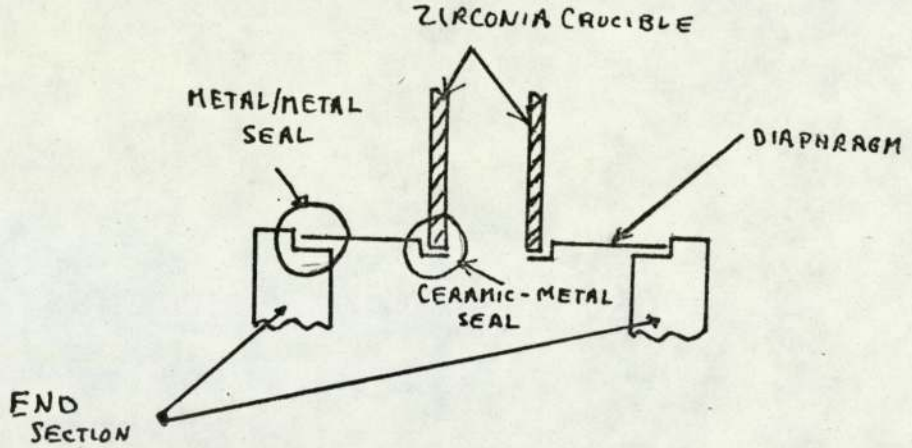

FIG.49. INITIAL DESIGN OF A FLEXIBLE DIAPHRAGM GAS TIGHT SEAL

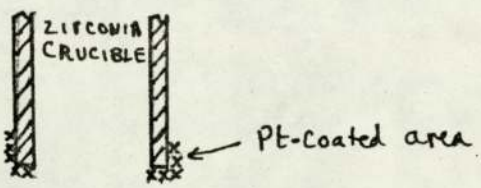

FIG.50. PLATINIZED AREAS AT ENDS OF ZIRCONIA CRUCIBLE

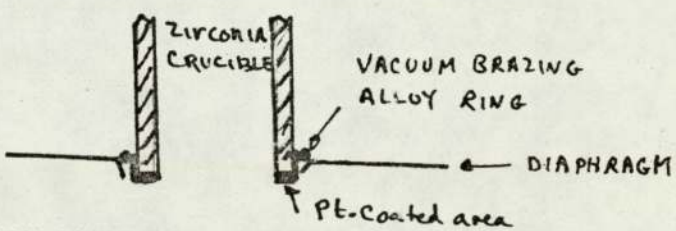

FIG.51. ZIRCONIA/METAL SEAL BY VACUUM BRAZING

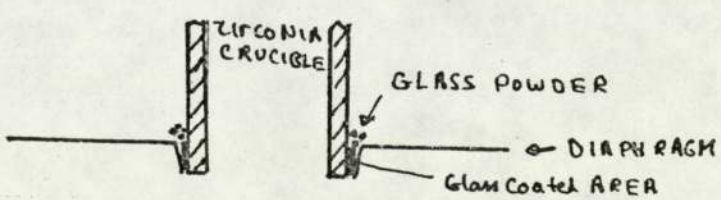

FIG.52. COMPRESSION ZIRCONIA/METAL GLASS SEAL

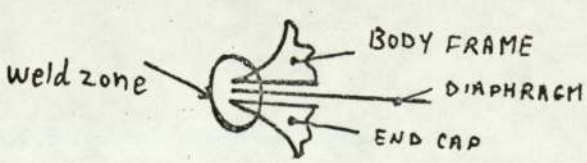

FIG.53. BODY FRAME AND END CAP TERMINATION AS REQUIRED BY ARGON-ARC PULSE WELDING

choice of glass a gas-tight seal may prove possible. Butt seals were tried using a number of Corning glasses - these were not very successful. Greater success was achieved with a compression seal where the metal is of a larger diameter than the ceramic at the glass melting temperature and allows it to run along the contact area, then as the sample cools the metal shrinks at a higher rate and ends by compressing the glass and the ceramic. A special corrosion resistant glass designed for coating S.S. vessels and manufactured by a sister company (Pfaudler) was found ideal for this application (Pfaudler 54 fired at 700-800°C). The platinum was not necessary here and it was replaced by applying with a brush a water based coat of the Pfaudler glass instead, as shown in Fig. 52. The simplicity, relative ease and low cost of this method prompted its adoption.

5.6.2. Metal-Metal gas tight seal

Tests showed that this point has to work at about 400°C, which allowed a wide choice of material and many vacuum brazing alloys were found to be satisfactory, but as a vacuum brazing furnace was a very expensive capital expenditure, alternative solutions were investigated. Trials with traditional argon arc welding did not prove very promising, but discussions with a miniature argon arc pulse welder manufacturer resulted in preparing some samples and building a suitable mechanical jig and the manufacturer brought his equipment and produced extremely good welds. The cost of the equipment and the cost per weld were considerably smaller than all other methods considered. Hence this method was chosen. The use of this method necessitates that the end cap of the sensor and its main frame be terminated to a thin section as shown in Fig. 53.

5.6.3. Choice of diaphragm shape and material

From the above it is clear that the diaphragm had to satisfy the following: it should be able to work without corroding or excessively

oxidising at 900°C; it must have suitable characteristics matched to the PSZ so as to produce a compression type seal; it should be able to weld easily to S.S. by the argon-arc; thin sections of it should remain porous free after at least a year in service.

Although as mentioned earlier initial trials were made with EN58J S.S. this material did not have suitable thermal characteristics for a compression joint and was found to scale and develop pinholes after a relatively short time. A search for a suitable material was started and ended with a nickel alloy that satisfied all the requirements. NILO Type of alloys (Henry Wiggin & Co.Ltd.) and Telcoseal Type of alloys (Telcon Metals Ltd.). These are nickel-iron base alloys developed for applications where controlled low and intermediate coefficients of thermal expansion are required. They are reasonably corrosion resistant and do not scale at high temperature. They are also amenable to vacuum brazing and welding operations. The characteristics of the alloy relative to that of the zirconia is shown in Fig. 54. The compression seal effect is clear from the examiniation of these graphs. The material used eventually was Telcoseal 6/4 which was 0.127mm thick.

5.7. HEATER DESIGN

Platinum or platinum/Iridium heater material wound tightly onto grooves cut in the ceramic body of the sensor and kept there, by ceramic cements, were used on the early models. Several problems were discovered. Most high temperature cements attacked the Pt. after a relatively short period and led to heater failure (free silica attack suspected). The change of the heater material led to the dissolution of some of the heater material into the solid electrolyte (mainly iron), but the most relevant problem was that of electrical interaction between the heater circuit and the sensor and thermocouple circuits. The use of S.S. insulated heaters and slug heaters were investigated and rejected on cost consideration (S.S. insulated heater cost was 85% of total required

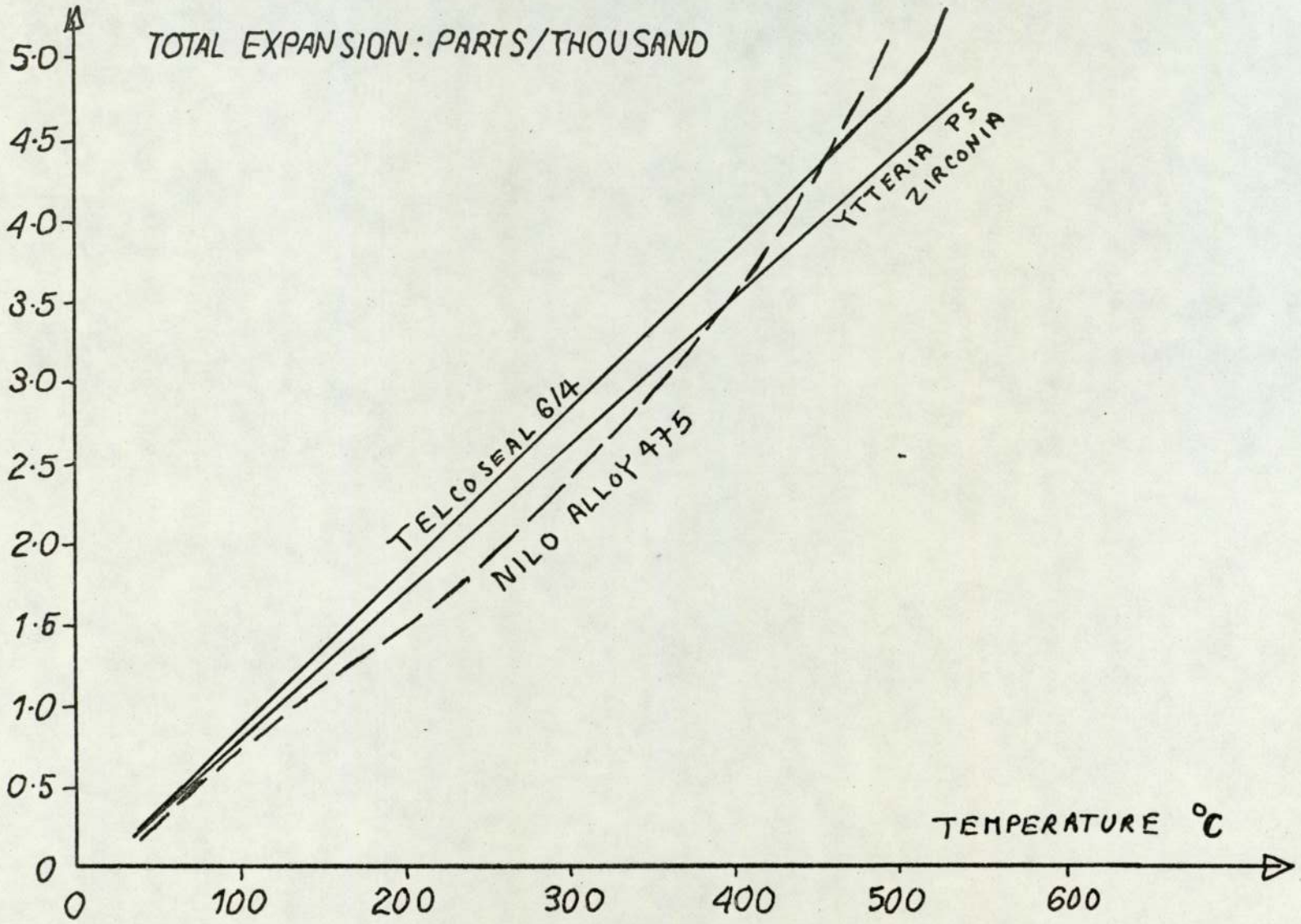

FIG.54. THERMAL EXPANSION CHARACTERISTICS OF SPECIAL NICKEL ALLOYS RELATIVE TO PSZ

sensor cost).

A certain degree of electrical insulation whilst maintaining at the same time the close thermal contact was required. Experiments with insulating the zirconia body with glass were not encouraging. Eventually a solution which met these requirements and resulted in a very simple, cheap and easy to manufacture design was evolved. This consisted basically of using a number (at least 21) very thin Alumina insulator tubes 1mm O/D cut to 20-16mm lengths threaded into the heater wire, then forming them as a skirt as shown in Fig. 55a. This is then bent into a cylindrical shape round the crucible as shown in Fig. 55b and c. The heater is secured by tightly wound wires at either end. The heater ends are brought out using larger diameter lengths of the same type of wire . Several types of wire material were tried; Fecr alloy 'A' (Resist Alloy Ltd.) 80/20 Vacrom (Nichrome) and Bright Ray Alloy (H.Wiggins & Co.Ltd.).

Bright Ray alloy 'C' bright annealed (0.28mm diameter) was selected because it had long life additions enabling it to cope with frequent switching and wide temperature fluctuations. It had an upper working temperature of 1150°C, a low temperature coefficient of resistivity (0.3 ohms in 8 ohms for 800°C rise)and high resistivity.

The temperature distribution along the central axis of the crucible for different types and lengths of heaters is shown in Fig. 56. A skirt heater 16mm long was considered the most suitable.

5.8. DESIGN OF GAS INLET AND OUTLET

The main requirements for this were: it should enable a fast exchange of gas; it should not introduce a cooling effect on the electrodes; it should not intrude too far into the ceramic tube (to avoid contact with wires) and it should introduce only little effects on the response time due to its positioning.

Some preliminary work on this was done on the pyrophyllite models,

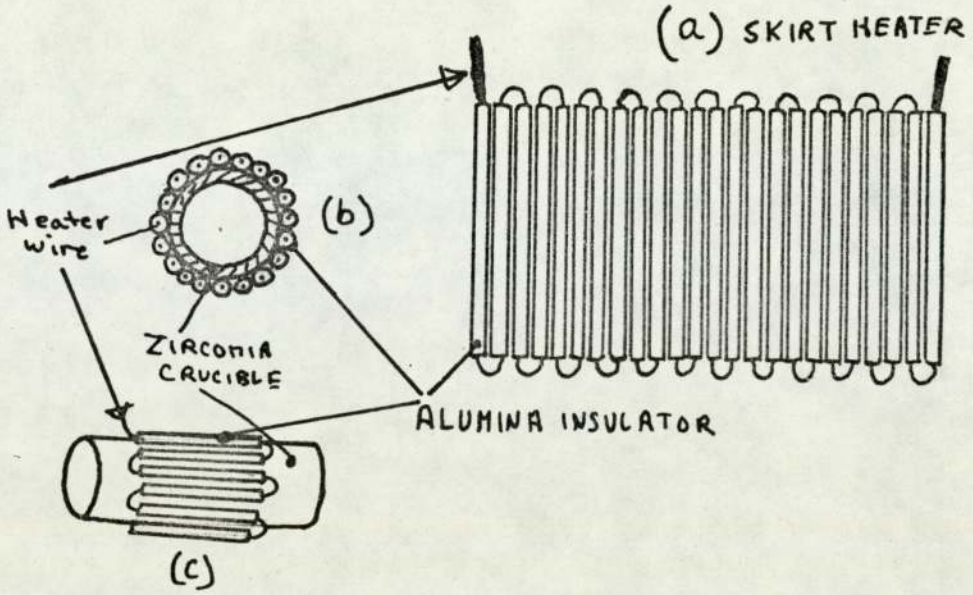

FIG.55. SKIRT HEATER

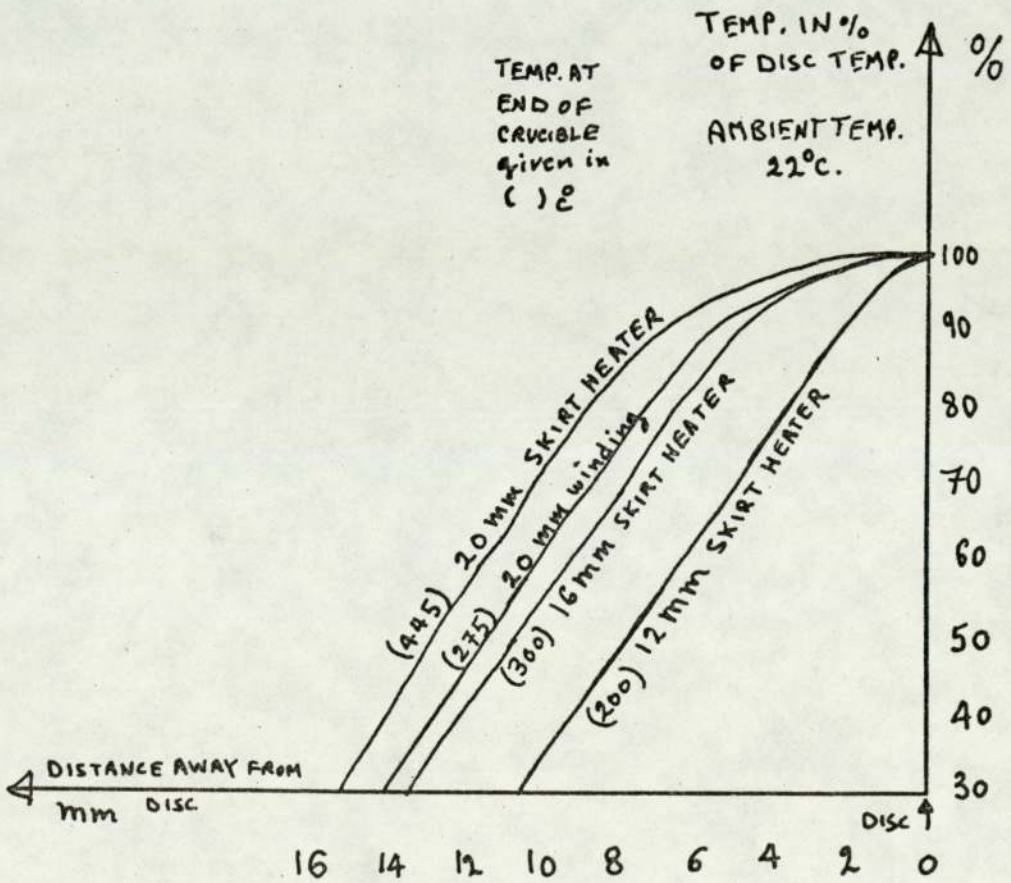

FIG.56. TEMP.DISTRIBUTION ALONG CENTRAL AXIS OF CRUCIBLE DUE TO DIFFERENT TYPES AND LENGTHS OF HEATERS

more work was done later on diffusion type gas connectors, on direct and on indirect impingement inlet pipes. None of these were satisfactory. This work led to the development of a design which satisfied all the requirements. This was basically concentric inlet and outlet pipes. The inlet pipe being central and goes a fraction into the ceramic tube (about 1mm) as shown in Fig. 57. The outlet pipe which is of a larger diameter rests on the end cap of the sensor. The outgoing hot gas heats the incoming cool gas, and as the inlet pipe is a long distance away from the electrode its cooling effect is reduced. The effect of positioning of the inlet pipe on the response time for a number of flow rates is shown in Fig. 58. The response plus delay for a flow rate of 200 ml/M and a positional tolerance of $\pm$ 2mm is about 1.5 seconds showing the suitability of the design.

5.9. SENSOR ELECTRODES

Numerous uses have been found for solid electrolytes [334], the choice of electrodes must be governed therefore by the intended application. For an oxygen concentration cell, the electrodes must satisfy four general types of operational criteria:[335]

(a) Chemical - chemical and phase stability in air and other expected gases for temperatures up to 1000^{o}C, and chemical stability with respect to the zirconia electrolyte and electrode leads.

(b) Electrochemical - a satisfactory oxygen electrode, that is the ability of the electrode to transport oxygen to the electrolyte.

(c) Mechanical - it must maintain physical integrity throughout all phases of its operation.

(d) Economical - the cost per unit must be only a fraction of the factory cost of the device.

Electrodes made of metals, oxides with current collectors, and conducting oxides have been used. However, due to the highly oxidizing environment

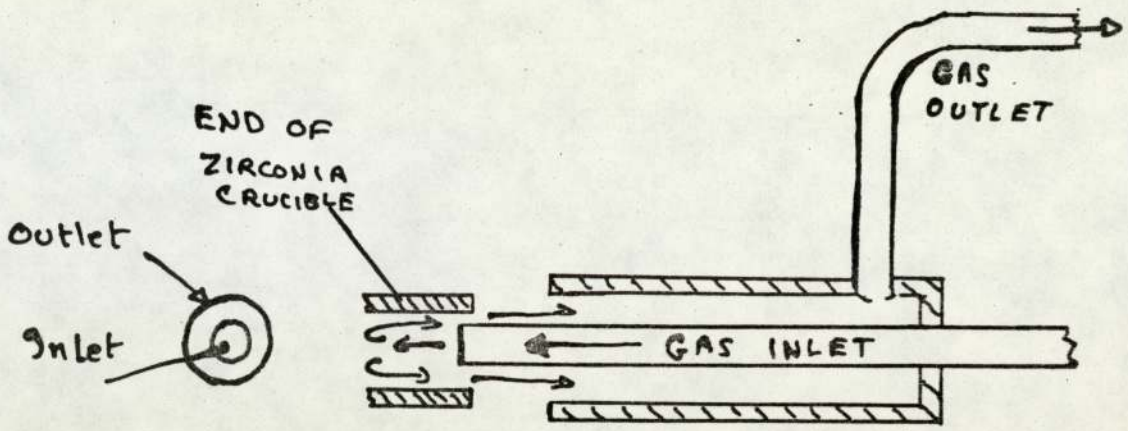

FIG.57. DESIGN OF GAS INLET AND OUTLET

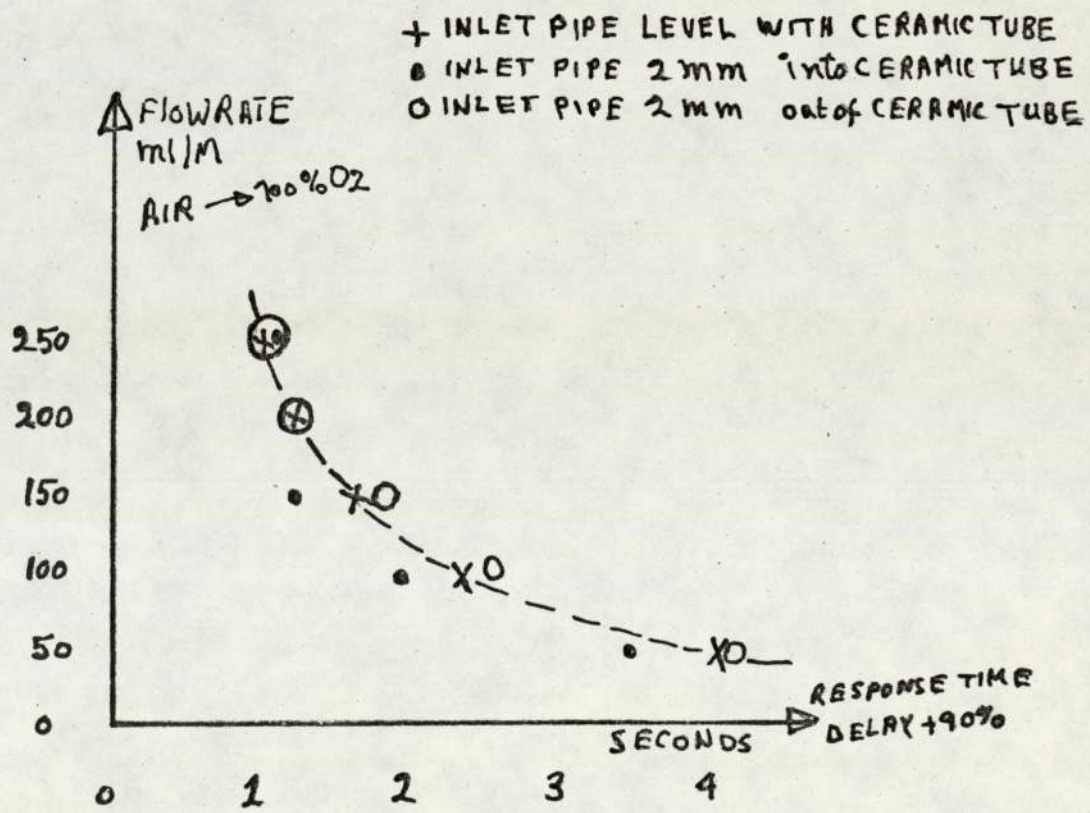

FIG.58. EFFECT OF INLET PIPE POSITION ON RESPONSE TIME

at the electrodes only the noble metals have been seriously considered. These metals have been applied to ceramics for many years. [336, 337] Organic solutions in which the metal atom is attached to a sulphur or oxygen atom which in turn is linked to a carbon atom are the most commonly used ones. Firing in a well ventilated furnace is essential so that all the organic matter is completely volatilized or burned away. Insufficient ventilation causes carbon to become occluded in the metallic film resulting in a scummed appearance and poor abrasion resistance. Though gold and silver have been used, platinum has been the most used and tested electrode material [338] and it has the added advantage of having nearly the same temperature coefficient of expansion as the Yttria - PSZ. Another advantage is that leads and thermocouples of the same material can be used.

5.9.1. Possible techniques of applying Pt. electrodes

Several possibilities exist:

(a) Vacuum deposition - the Pt. film is thin and the technique not suitable for the present design.

(b) Sputtering - excellent electrodes (adhesion and porosity) have been reported using this technique. Unfortunately the size and shape of the sensor makes the use of this technique extremely difficult.

(c) Pt-paste with silicates - this was found to be the easiest and most economical technique, and it was hence chosen.

(d) Other compounds of Pt - Chloroplatinic acid (applied mixed with water - no organic binder) or NP100 (J & M Ltd.) a paste with no silicates. These are under investigation.

(e) Molecular bonding [339, 340] - this is a ceramic metal reaction that leads to a sharp phase discontinuity at the metal-ceramic interface, this is maintained even after prolonged annealing in oxygen. This does not involve intermediate oxide phases, the maximum bond strength is reached after a few hours and does not deteriorate with time. This process is protected by patents

(e.g. CISRO UK 347,937) but it is worth pursuing. One instrument manufacturer already uses it (MITAKA).

5.9.2. Fabrication of sensor electrodes

Platinum Paste (J & M N758) fired with excess air at 850°C for at least 20 mins. (firing temperature range 700-1500°C). The work is introduced to a furnace at a temperature well below 100°C and having been dried under an infra red lamp at about 80°C. The ceramic is cleaned and heated to at least 600°C and cooled previous to the application of the paste. Films about 2 microns thick result. This paste has a solvent (Butyl Carbitol Acetate - F.P. 115°C) an organic binder and silicates for increased adhesion. The ease of its application and firing and its excellent adhesion were the main causes of its selection. Initially small areas on the disc face were coated, but tests showed an improvement in the response time for the larger electrode area models. Therefore full electrode area coverage was adopted.

Thin thermocouple wire 0.002" thick (low thermal loss, low cost) positioned on the centre of the disc's face, measure the disc's temperature and provide also an electrode output. Normal thermocouple material is not suitable in the sample gas zone. Pallador thermocouples were tested and were found to oxidize with time. Pt. Pt/10% Rh thermocouples were therefore selected. The thin electrodes are welded to a similar but larger diameter wire before they are taken through the ends of the zirconia crucible body. Insulation from the body is essential and is provided by a thin alumina tube which is sealed gas tight with high temperature glass to both the zirconia body and the wire. Electrical interaction arise if the wires touch the zirconia body. The wire is annealed in situ.

5.10. FINAL DESIGN OF SOLID ELECTROLYTE OXYGEN SENSOR

The final design of the sensor is shown in Fig. 59. The crucible is made in one piece (8 wt% Y_2O_3 stabilized zirconia). Its bore is divided into two chambers (reference and sample) by a thin disc. The

disc has electrodes on its opposed faces. The electrodes cover the whole disc area and hold a Pt/Pt 10% Rh thermocouple (0.002") on the centre of the disc. The wires are welded before they leave the tube to thicker (0.008") identical wires which go through the zirconia tube near the end through an alumina insulator which is sealed gas tight to the wire, and the zirconia by a high temperature glass.

A heater wire (0.28mm diameter) insulated by Alumina insulators (16mm, 1mm diameter) and arranged around the zirconia tube so as to provide equal temperature on either side of the disc. This skirt heater is secured by two wires on either end.

All the electrical wires pass through a ceramic insulator Fig. 60, and are then turned parallel to the main axis of the sensor and are fed into a multi-bore alumina insulator tube and then into a rulon tube; both of these are housed and securely held in a stainless steel tube which is screwed to the main body frame Fig. 61.

The zirconia tube is suspended from each end by a resilient diaphragm (0.005" thick) Fig. 62 which has a number of corrugations. The diaphragms are sealed gas tight to the ends of the tube using glass. The material of the diaphragm is selected to act as a compression seal (Telcoseal 6/4). The tube is housed in a steel body (410SS) Fig. 63 and is constrained on each end by end caps made of the same material Fig. 64. The points of contact between the body frame, the diaphragm, and the end cap are welded together using an argon arc. The end cap has a gas port and is threaded so as to accept the concentric inlet/outlet pipes which are secured to it by a nut. A stainless steel outer cover Fig. 65 protects the sensor body.

5.11. MANUFACTURING COST OF THE SENSOR

Detailed analysis of this indicated that a quarter of the cost is in materials, half the cost is in operator-manufacturing time and

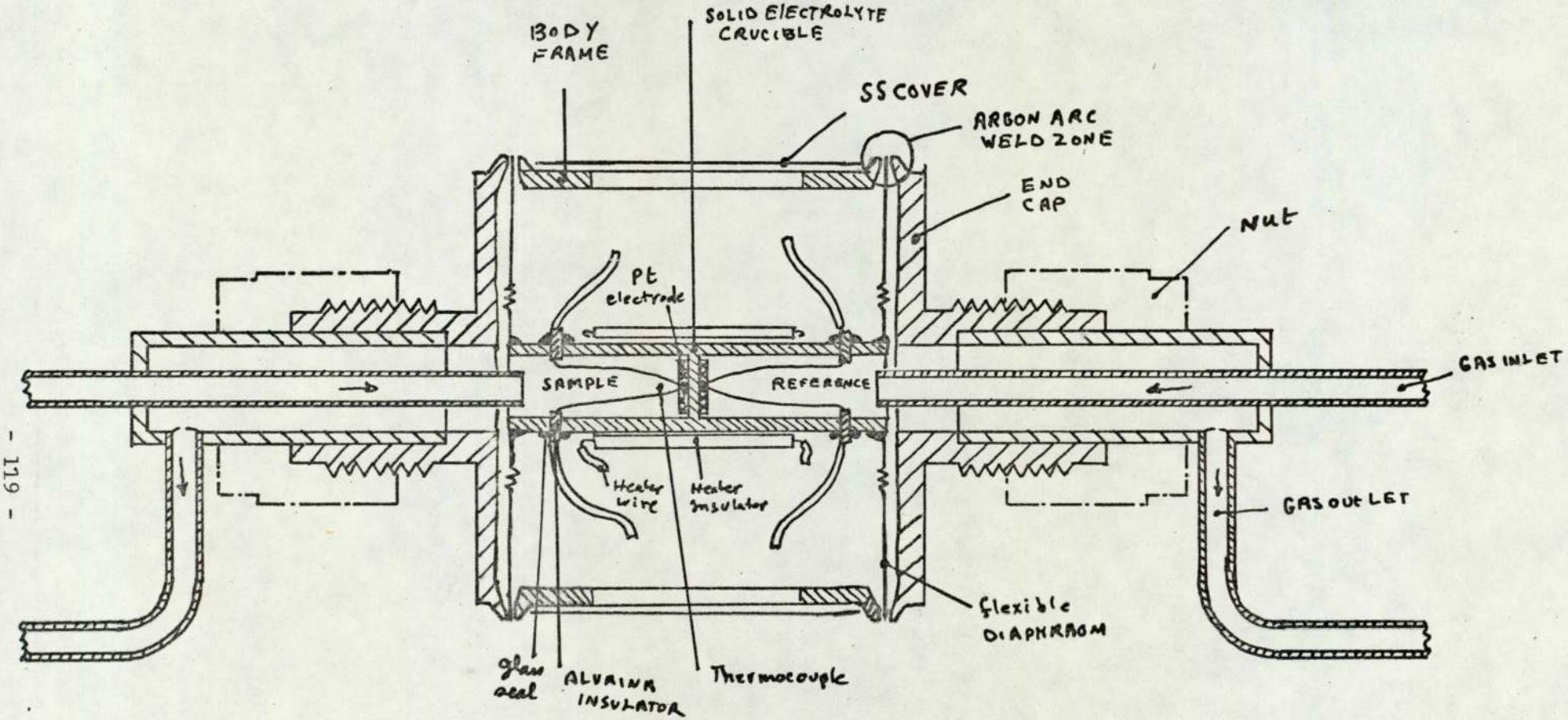

FIG.59. SCHEMATIC OF FINAL DESIGN OF SOLID ELECTROLYTE OXYGEN SENSOR

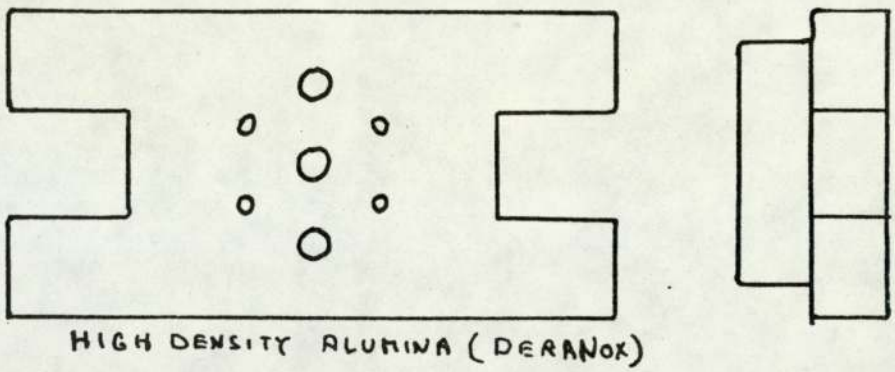

FIG.60. WIRE FEEDTHROUGH CERAMIC

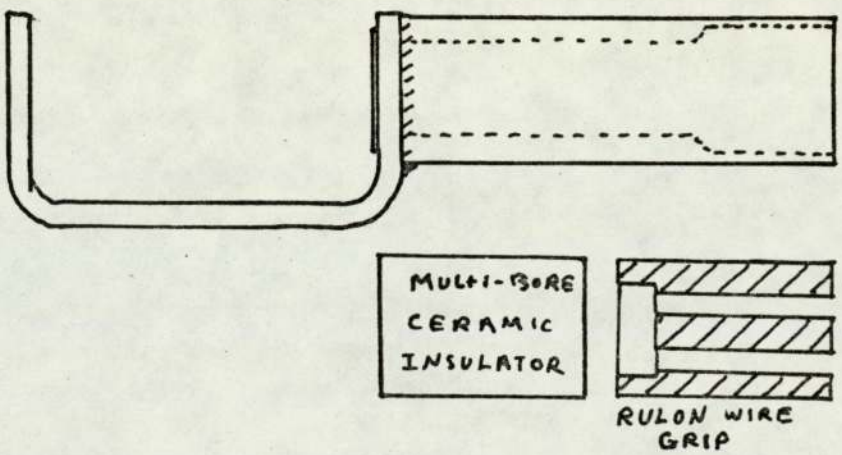

FIG.61. WIRE TERMINUS ASSEMBLY

FIG.62. DIAPHRAGM

FIG.63. SENSOR BODY FRAME

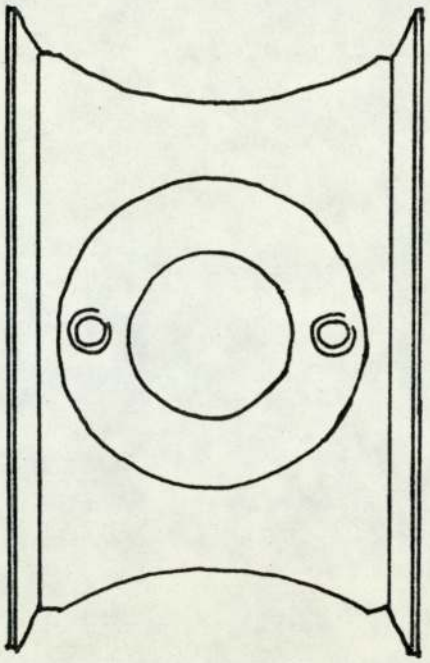

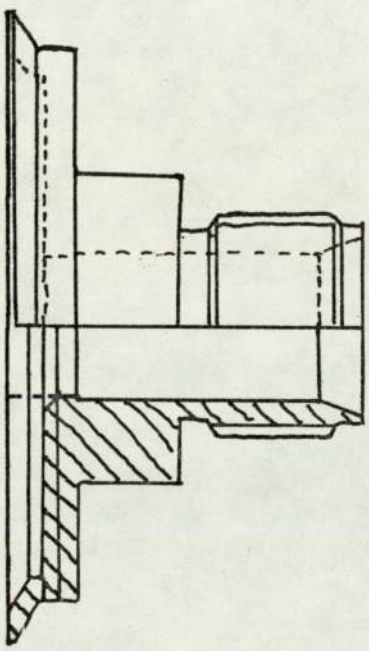

FIG.64. SENSOR END CAP

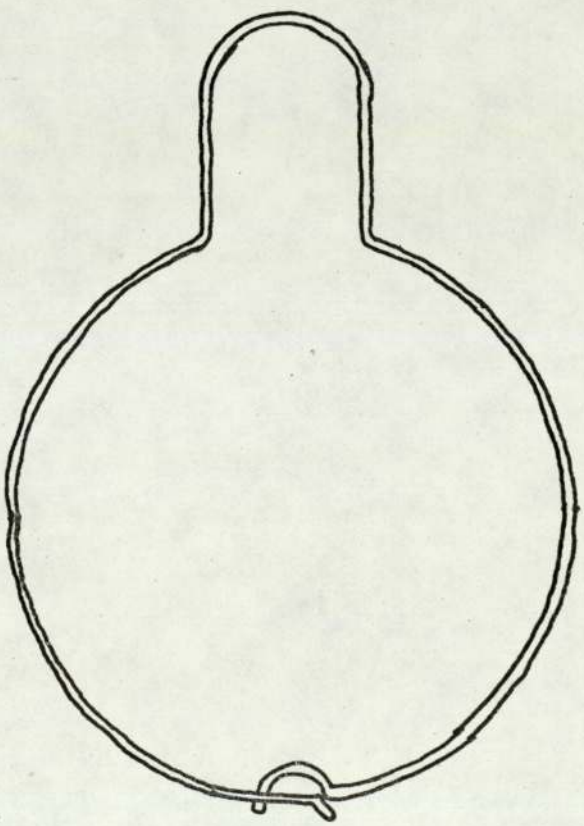

FIG.65.SENSOR OUTER COVER

a quarter of the cost is in testing time. The total estimated cost was 5/6th of the desired factory cost stipulated by the Marketing Department despite the passage of about 4 years since the initial request.

5.12. THE MANUFACTURING OF THE SENSOR

Prior to setting up a manufacturing facility, a batch of 50 prototype sensors were constructed to the final design in the science department. A manufacturing procedure was set up, based on this experience and manufacturing jigs and test equipment designed and made. A manufacturing area was set up and equipped with the necessary equipment. Two operators were trained in the manufacturing and testing of the sensor using a production batch of 50 sensors. Out of this 45 sensors were successful. No major problems have been encountered during this exercise.

5.13. ELECTRODE AGEING

Some sensors showed an increase in their response time, and it was thought at the time that the Pt. coat was not adequate and more paste was added which seemed to bring the response time back to normal levels. This behaviour was investigated further and the response time for a freshly made sensor was measured at different temperatures and at different times. Its response time seemed to settle down after about a month. The difference between the 90% response time of the sensor when freshly made and after a month is shown in Fig. 66. At a flow rate of 200 ml/M. the response time seems to double. A lowering of the conductivity was observed at the same time. To investigate this, six crucibles were made and fitted with electrodes, each two were fired at different temperatures (830-900 - 1000^{o}C). All these were kept at 800^{o}C and their conductivity was monitored daily (Wyne Kerr bridge B224). The changes in their conductivity are shown in Fig. 67. Some show signs of settling, others still show a considerable slope. The firing temperature does not seem to have an effect on the ageing though the

initial conductivity seems somehow to be influenced by it. A change in conductivity may however be associated with ageing of the solid electrolyte material itself, but the ability to restore sensors to lower conductivities by adding more paste suggests that this is an electrode problem. Work by Issacs and co-workers [341] indicated that the resistance of the electrolyte is negligible in comparison with the impedance of the electrode/electrolyte interface, and that it also varies more rapidly with temperature.

The electrode/electrolyte interface is a complex area within which many process take place simultaneously. It has received the attention of many workers [e.g. 187, 188, 300, 342-349, 354]. The adsorption mechanisms on the Pt. electrode are still not really well understood [350,351] and the formation of surface oxides [203, 352, 355] indicates that Pt. is not inert under all conditions. The need to have a porous electrode only increases the complexity of that area. [353] Electrodes for solid electrolytes have been discussed [299, 356, 357] and many forms proposed. What is important is the relation between the electrode process and the electrode structure. Pizzinni and co-workers [358] investigated the relationship between electrode preparation and electrode morphology. They reported that the structure may change with time as the small active crystallites of platinum agglomerate to produce large grains. This was also reported by Dorstine and co-workers. [321] This seems to be similar to what was observed on the six samples tested, but as the Pt. paste used had a silicate flux to promote adhesion [359] the pores could have been blocked by that, reducing the triple-phase contact area. Now Bauerle had reported [201] the use of heavy current treatment to artificially induce porosity. The differences between the electrode impedances is clearly seen on a complex admittance plot as shown in Fig. 68. To investigate whether the heavy current treatment helps, one of the sample of six was given a $\pm$ 150 mA for 2M - treatment at 1150^{o}C. Examination of its conductivity showed that it had returned

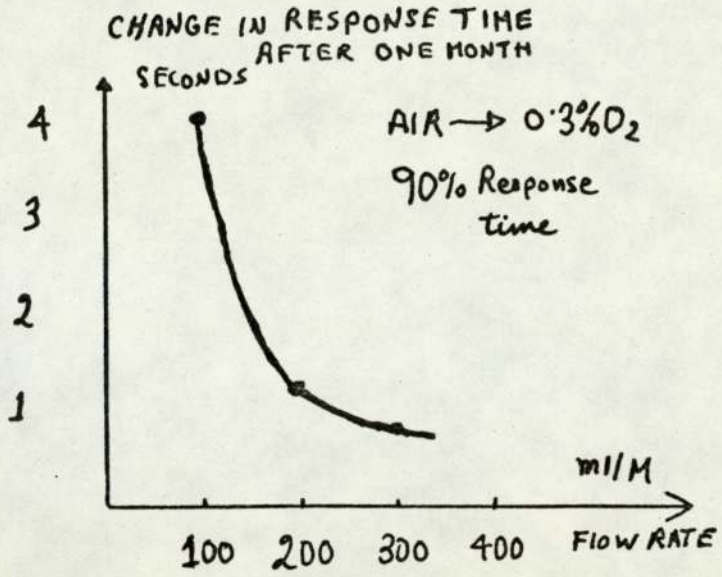

FIG.66.INCREASE IN RESPONSE TIME DUE TO AGEING

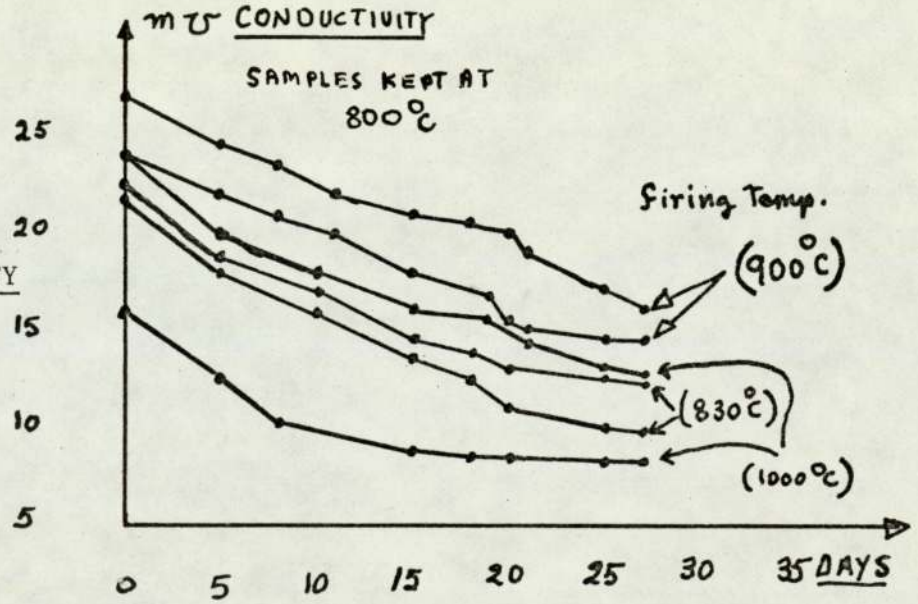

FIG.67.CHANGE IN CONDUCTIVITY WITH TIME

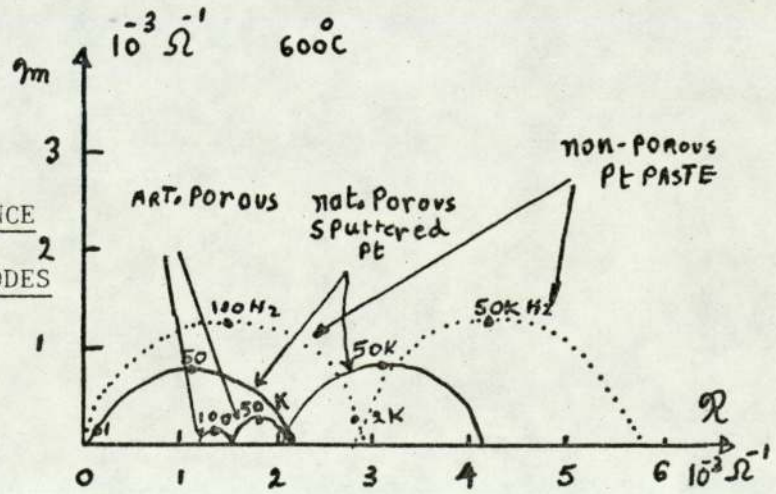

FIG.68.COMPLEX ADMITTANCE OF DIFFERENT Pt ELECTRODES

from 13.7 to about 20.5 m τ and its rate of change with time. has slowed to about a third of its previous rate. This is an interesting field of investigation which is being continued.

The stability and hence the constancy of the response time of the sensor is of great commercial importance, and methods, materials and treatments will be thoroughly investigated so as to find a production method that gives stable electrodes.

CHAPTER SIX

CHARACTERISTICS AND EVALUATION OF THE SENSOR

6.1. THERMAL CHARACTERISTICS

6.1.1. The heater

The variation of the sensor heater resistance with temperature is shown in Fig. 69. The nearly constant value of the resistance over the working temperature range is one of the attractive properties of the alloy of the heater wire. The wire constants are also listed on the graph.

The power level required to bring the electrodes to a given temperature range, whilst the sensor is at ambient temperature, is shown in Fig. 70 which gives also the required heater current.

The distribution of the heater resistance value is shown, for development sensors (sample of 15) and for production sensors (sample of 34) in Fig. 71. The results suggest a provisional heater resistance specification of 7.55 ± 0.35 ohms.

6.1.2. Heater - electrodes thermal time constant

The response of the sensor to a sudden application of 54 watts of power to the heater and then the switching off of that power is shown in Fig. 72 as the change in the temperature at the electrodes with time. The graph indicates a time constant of about one minute.

6.1.3. The thermal time constant of the sensor

The sudden insertion and later withdrawal of the sensor into an oven which is regulated at $200^{o}C$ is shown in Fig. 73, as the variation in the temperature of the electrodes with time. The graph indicates a time constant of the order of twenty five minutes.

6.1.4. Storing temperature

Sensors stored at $-20^{o}C$, operated normally after being left to reach ambient temperature. The storage of the sensor in conditions as low as $-40^{o}C$ should not affect its performance. The sensor can be used at an

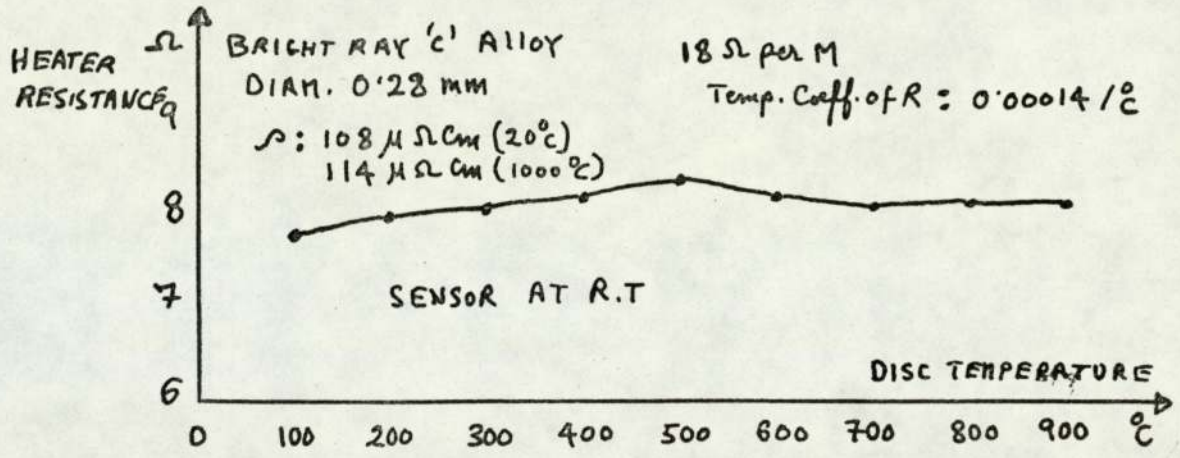

FIG.69. SENSOR HEATER RESISTANCE VARIATION WITH TEMPERATURE

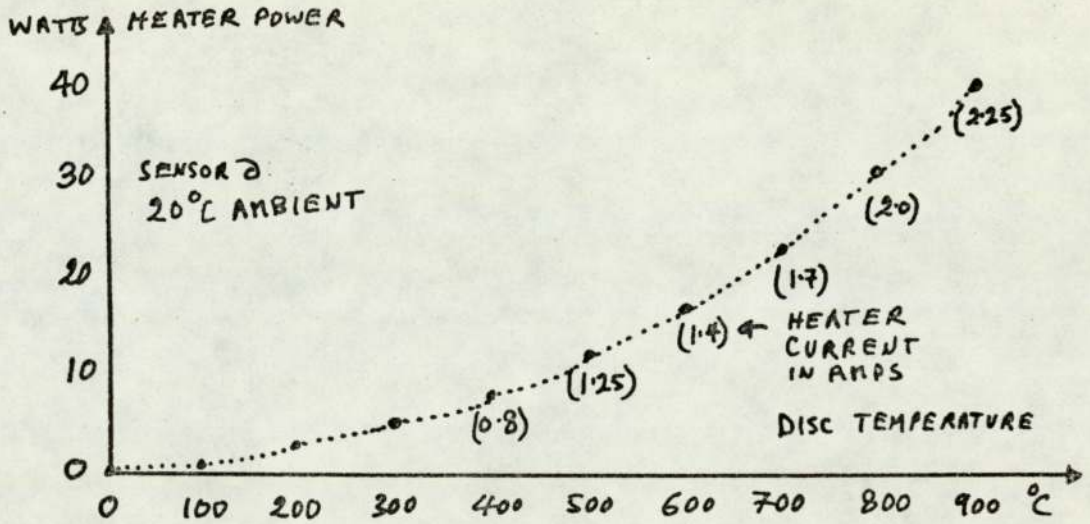

FIG.70.SENSOR POWER-TEMPERATURE CURVE

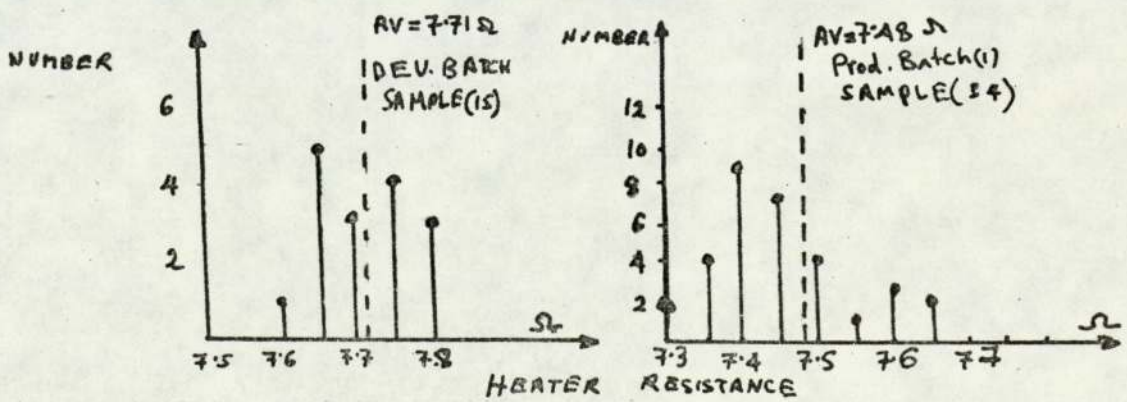

FIG.71.HEATER RESISTANCE SAMPLE DISTRIBUTION

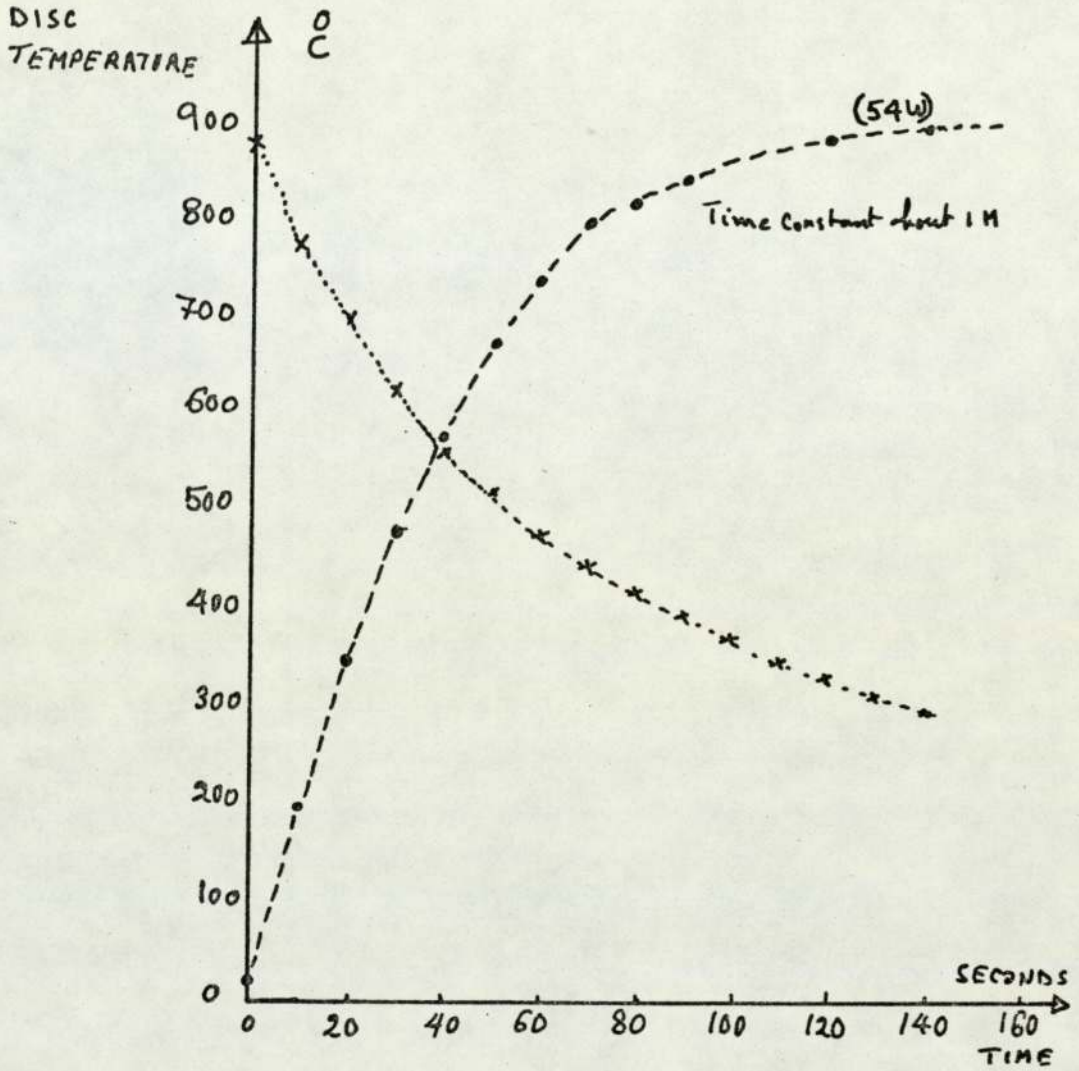

FIG.72.SENSOR HEATING AND COOLING CURVES

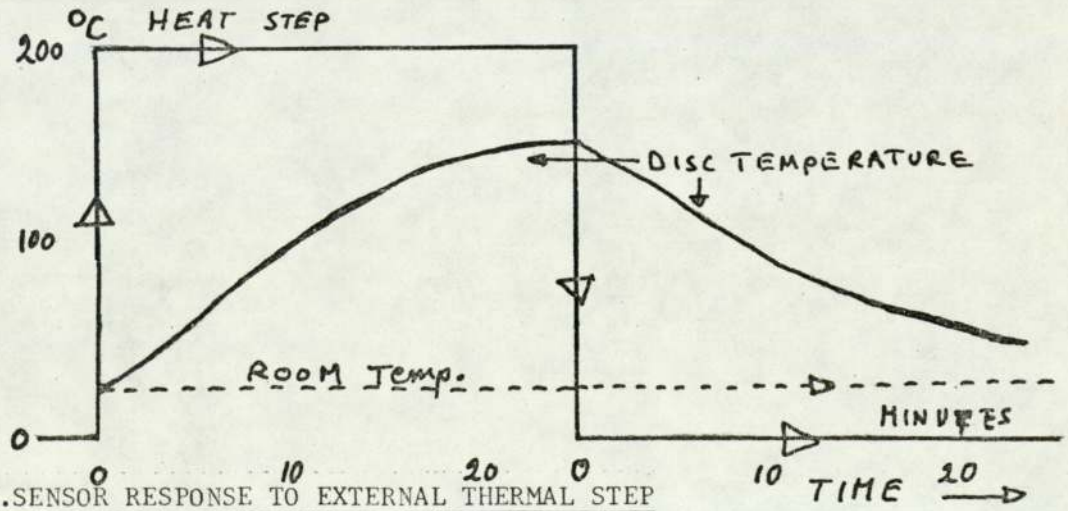

FIG.73.SENSOR RESPONSE TO EXTERNAL THERMAL STEP

ambient temperature of + 250°C. The flue gas analyser described in Chapter Eight houses the sensor in a nominal 200°C ambient environment.

6.2. INSULATION RESISTANCE

a) Heater to electrodes > 1.5M ohms.

b) Heater to body > 1.5M ohms.

c) Electrodes to body > 5K ohms

Operating tempeature of the electrodes was 800°C and an ambient temperature of 20°C.

6.3. OFFSET CHARACTERISTICS

Low offset emf between the electrodes, when both the sample and the reference chambers have the same oxygen partial pressure, is a feature of this sensor. It is also an indication of how close the temperatures of the electrodes are to each other. A temperature difference of one degree centigrade introduces a calculated offset of about 0.45 m Volts.

6.3.1. Offset emf variation with operating temperature.

The internal impedance of the sensor becomes quite high at temperatures below 600°C, and emf measurements across the electrodes becomes unreliable. The offset emf for a sensor with static air in both the reference and the sample chambers, and over the range 550 to 850°C is shown in Fig. 74. Down to 650°C the offset is well below one millivolt.

6.3.2. Offset emf variation with sample gas flow

The effect of the sample flow rate on the offset emf (static air in reference side) is shown as the difference between the temperatures of the electrodes in Fig. 75. The sensor being at ambient temperature (20°C) and operated at 850°C. The effect is nearly the same over an operating temperature range of 700-850°C. It is quite small below flow rates of 200 ml/M. Tests with air flow of 100 ml/M in the reference side and with air, 100% O_2, and 0.3% O_2 at the sample side show offsets of less than 0.45 mV for flow rates of less than 300 ml/M.

6.3.3. Offset emf long term stability

At constant sensor operating temperature and constant ambient

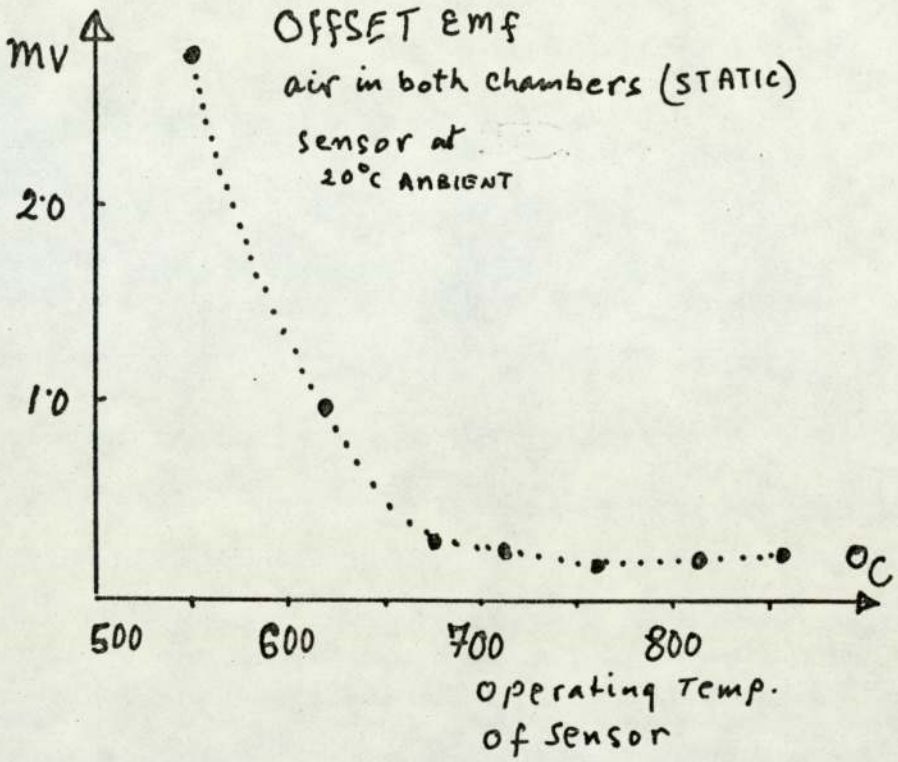

FIG.74. VARIATION OF OFFSET EMF WITH TEMPERATURE

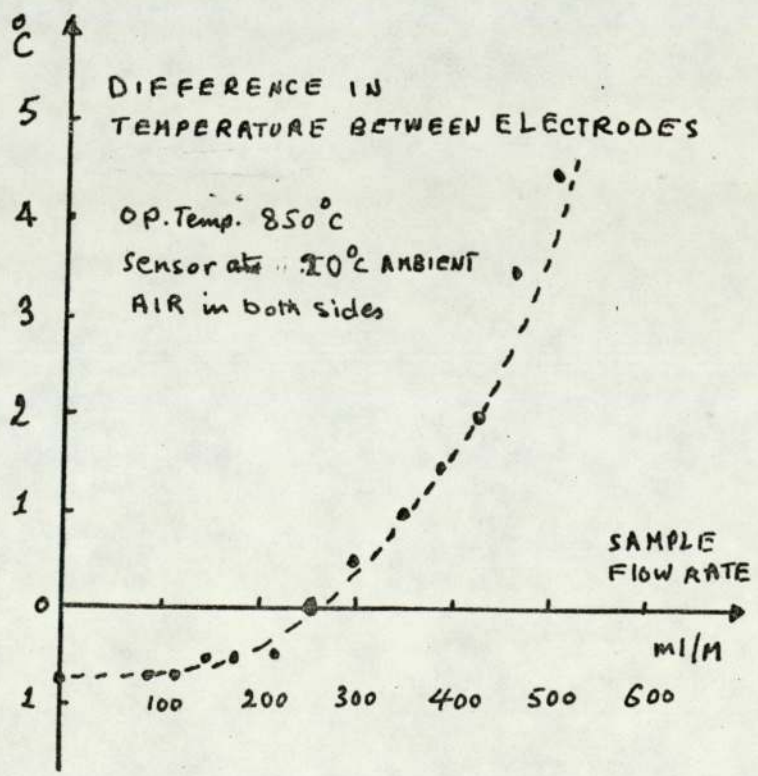

FIG.75. VARIATION OF OFFSET EMF WITH SAMPLE GAS FLOW

conditions (temperature, pressure and flow), offset variations of the order of less than $\pm$ 10 μ volt per week were observed.

6.3.4. The effect of orientation on the offset emf.

The offset emf of a sensor operating at 800°C and 20°C ambient temperature at different positions in space (rotated clockwise in 90° steps) is shown in Fig. 76. This effect is small.

The effect of forward and backward tilts of 45° and of 90° on the offset emf is shown in Fig. 77. This is a larger effect.

As the sensor is stationed normally in one fixed spatial position and considering also that with air in both chambers 0.1 mV corresponds to about 0.1% O_2, both effects are negligible.

6.3.5. Offset distribution

The offset emf's for sensors operating at 800°C and 200°C ambient with air in both chambers are shown for development sensors (sample of 33) and for production sensors (sample of 20) in Fig. 78. About 70% of the sensors were below 0.5mV - this corresponds to about one degree of temperature difference between the electrodes. None showed a difference greater than 2°C.

6.4. ELECTRICAL CHARACTERISTICS

The complexity of the electrical characteristics of the sensor was discussed in the previous chapter and can be demonstrated by an admittance plot. Fig. 79 shows admittance plots (conductance - susceptance) for a development and for a production sensor at 850, 800 and 750°C. The equipment used was as that described in Chapter Five. Using Bauerle's[201] interpretation of these diagrams an equivalent circuit can be derived. From the results of the development sensor at 850°C, an equivalent circuit as shown in the diagram can be proposed. This is mainly electrode effects, indicating a very small electrolyte (second phase) effect .

6.4.1. The effect of temperature on the conductivity and the capacity of the sensor.

An A.C. bridge was used (at ω = 10K Hz). to measure the conductance

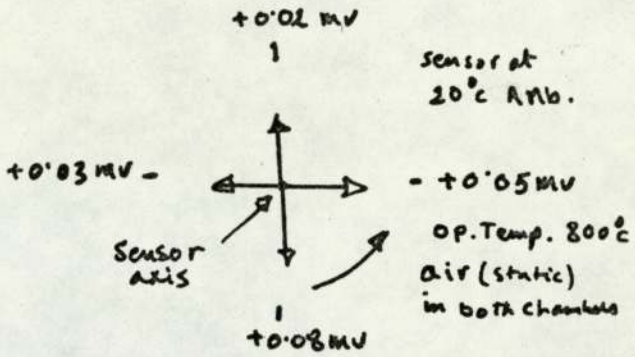

FIG.76. EFFECT OF ROTATION ON OFFSET EMF

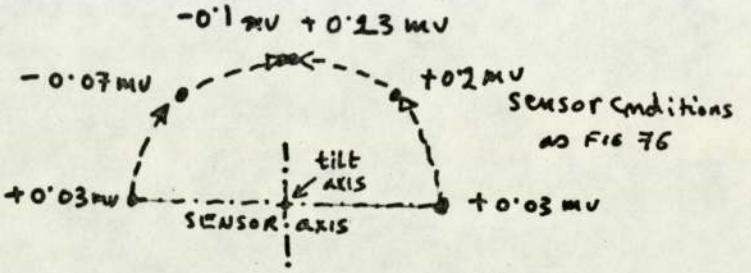

FIG.77. EFFECT OF TILT ON SENSOR OFFSET EMF

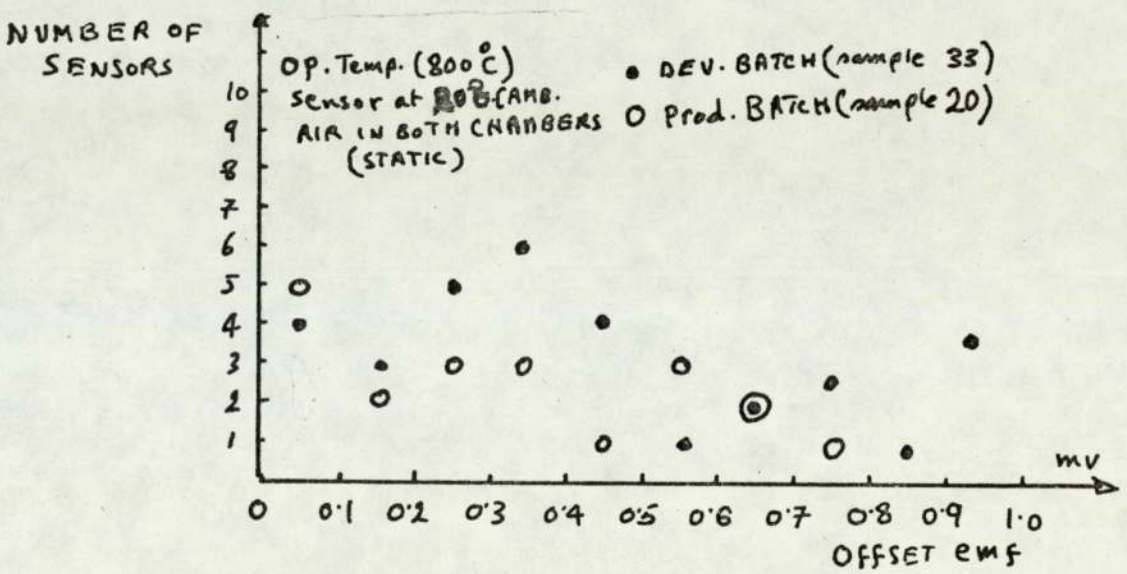

FIG.78. OFFSET DISTRIBUTION FOR DEVELOPMENT AND PRODUCTION SENSORS

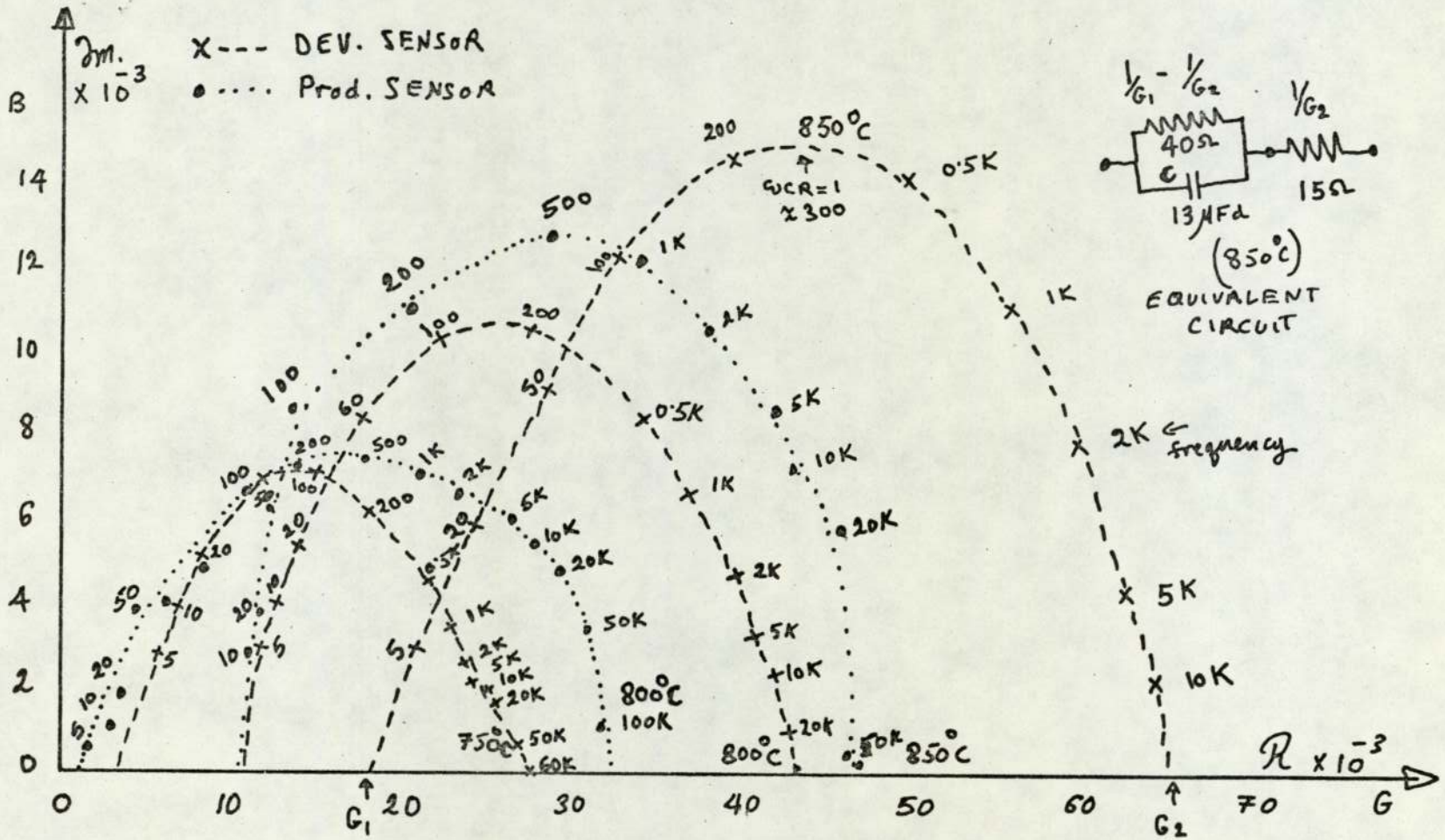

FIG.79.COMPLEX ADMITTANCE PLOTS FOR DEVELOPMENT AND PRODUCTION SENSORS AT DIFFERENT TEMPERATURES

and capacitance of a sensor at different temperatures - this is shown in Fig. 80. The spread in the conductivity values for production (sample of 20) and development (sample of 33) sensors at 800°C operating and 200°C ambient temperatures is shown in Fig. 81.

6.5. THE RESPONSE OF THE SENSOR TO OXYGEN CONCENTRATION CHANGES (299,329,360, 361,362,363, 364)

The sensor was tested by suddenly changing the sample gas from air to 0.3% O_2 in N_2 or the other way round. An electrically actuated change over valve having a small volume was used. Both gases continuously flowed through the valve ports and were adjusted to constant flows using flow regulators and a flow meter. The pipes were kept as short as possible and the output of the sensor was recorded on a fast response pen recorder through a unity gain isolating amplifier. The reference chamber had static air in it.

The processes involved in the sensor responding to a step change of oxygen concentration can be summarised as:

a) Flushing of sample pipes - This involves the clearing of the sample pipes and other volumes of the previous sample gas and replacing it with the new sample gas. This is referred to as a delay and is simply a function of the total volume involved and of the flow rate of the gas. The time delay the sample gas takes to reach the sensor volume for the test system is shown in Fig. 82, as a function of sample flow rate. The results suggest an equivalent volume (this includes the switching time of the valve, and the response time of the recorder) of about 3 ml.

b) Flushing of previous sample out of sensor volume - This is a dilution process which can be represented by an exponential single time constant equation:

either

$$\%O_2 = \%O_{2_s} \left(1 - \exp - \frac{t}{T_1} \right) \quad \ldots\ldots\ldots\ldots\ldots \quad (32)$$

or

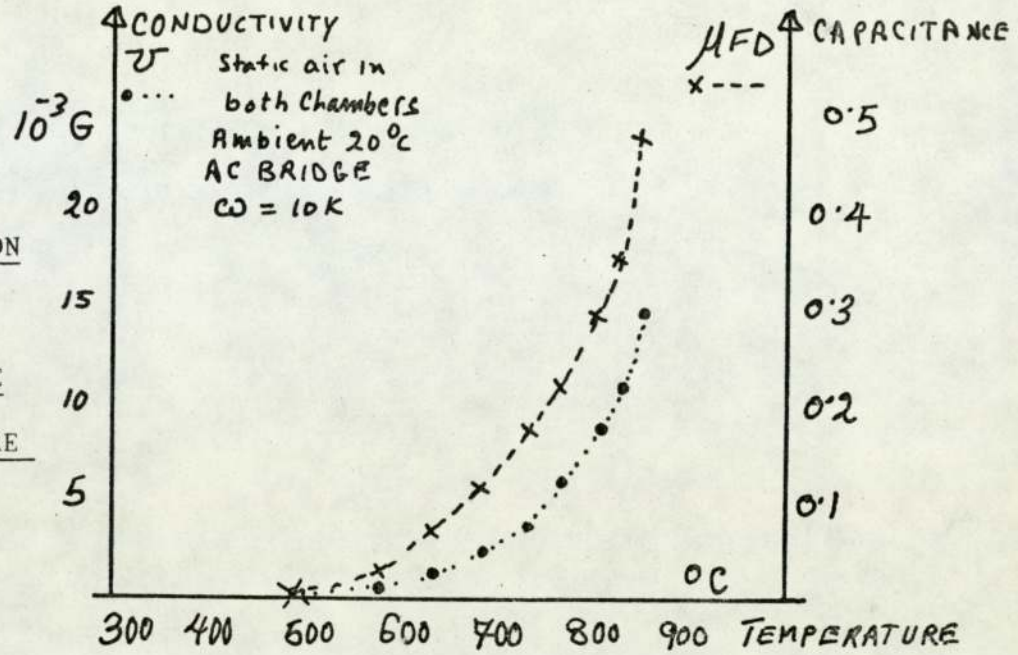

FIG.80.VARIATION OF CONDUCTANCE AND CAPACITANCE WITH TEMPERATURE

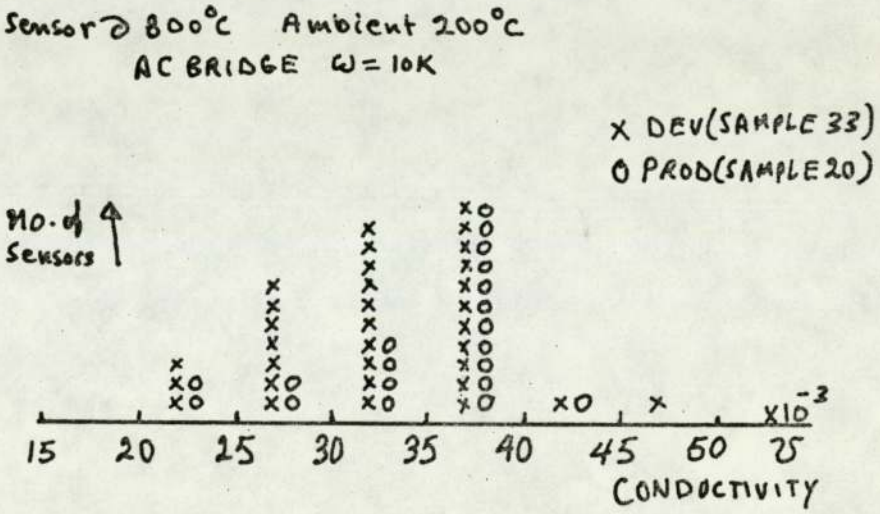

FIG.81.DISTRIBUTION OF DEVELOPMENT AND PRODUCTION SENSOR CONDUCTIVITY

$$\% O_2 = \%O_{2_s}(\exp - \frac{t}{T_2}) \quad \ldots\ldots\ldots\ldots\ldots\ldots (33)$$

depending on the direction of the oxygen concentration change taking place. Where $\% O_2$ is the percentage oxygen in the sample chamber, and T_1 and T_2 are time constants related to the sample flow rate and the volume of the chamber (nominally 0.25 ml).

These equations fit the practical results up to about 98% of the response. The remaining part of the response tends to be of a linear nature.

c) Gas phase diffusion - the diffusion of the oxygen gas into the porous or partially porous platinum electrode. This is influenced by gas concentration differentials and by ageing (blocking of pores).

d) Adsorption and chemisorption - Adsorption of molecular (or atomic oxygen on the pore walls of the electrode (a monolayer of tightly bound oxygen atoms has been proposed) and a weak chemisorption of oxygen molecules on this monolayer. (Oxygen can adsorp directly to the solid electrolyte which could also act as a catalyst).[363]

e) Surface diffusion of the oxygen molecules to the electrode/electrolyte interface. This is also hindered by loss of porosity and platinum particles coagulation, as the three phase areas are reduced then.

f) Dissociation of the oxygen molecule.

g) Electron transfer to the oxygen atoms.

h) Transfer of the oxygen atoms from the gas phase into the solid electrolyte (activation).

i) Ionic conduction by the $O^=$ ions in the solid electrolyte.

j) Electronic conduction in the solid electrolyte.

k) Diffusion of oxygen in the solid electrolyte.

The 90% response time of a sensor to a change from 0.3% O_2 to air is shown for different flow rates and at different temperatures in Fig. 83a. The sluggishness at 700°C is evident and it must be mentioned that some ageing of that electrode had taken place by then (reduction of

porosity). The 90% response time of a sensor to a change from air to 0.3% O_2 is shown for different flow rates and at different temperatures in Fig. 83b. The influence of the temperature here is not as great as in the previous case. The cause of this lies in steps (c) and (e) when the gas has to diffuse through the electrode, the diffusion speed is greater if there is a higher concentration difference between the two boundaries and if the temperature is higher. This is also impeded if due to ageing or other causes the pores are blocked and the platinum particles coagulate making it harder for the gas to diffuse through the platinum electrode. All the other processes involve much smaller times (assuming absence of polarization).

Complete sensor response curves are shown in Fig. 84, for a sensor operating at 800°C and 20°C ambient temperature, with still air in the reference chamber, and changes from air to 0.3% O_2 in N_2 and back at 200 ml/M sample flow rates. The curves show clearly their exponential nature and the longer response time when the gas is returning to a concentration near that of the reference gas. It shows also the effect of electrode ageing. If the ageing process could be controlled 90% response times of under one second at 200 ml/M would be feasible.

The distribution of development and production 90% response times for sensors tested at 800°C operating temperature and 200°C ambient with a flow rate of 100 ml/M is shown in Fig. 85a for a 0.3% O_2 to air change and in Fig. 85b for air to 0.3% O_2 change. The main cause of the spread is electrode ageing.

6.6. EFFECT OF FLOW RATE ON PRESSURE ACROSS THE SENSOR

The change in the pressure across the sensor due to changes in the sample gas flow rate from 0 to 300 ml/M is shown in Fig. 86. This is a linear relationship with a slope of about 0.055 mm H_2O per one ml/M gas flow.

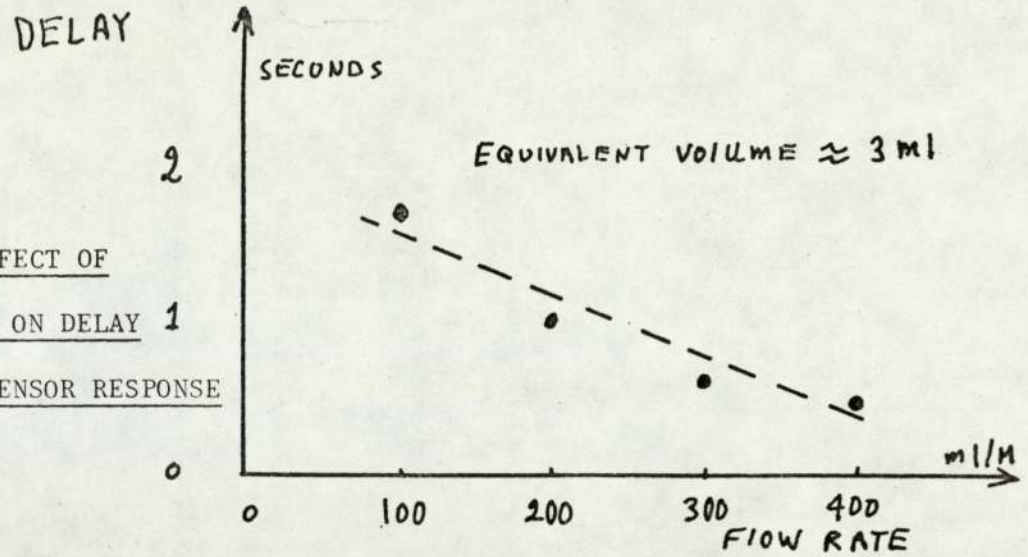

FIG.82.EFFECT OF FLOW RATE ON DELAY TIME OF SENSOR RESPONSE

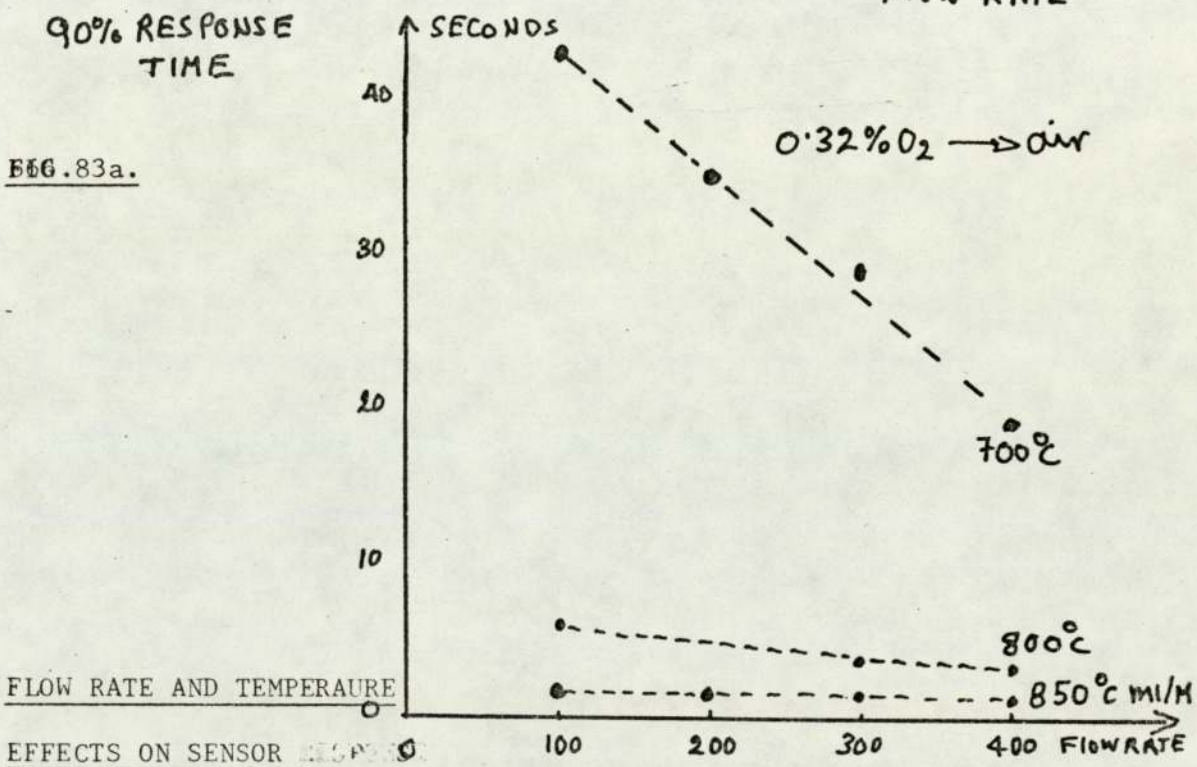

FIG.83a.

FLOW RATE AND TEMPERAURE EFFECTS ON SENSOR RESPONSE TIME

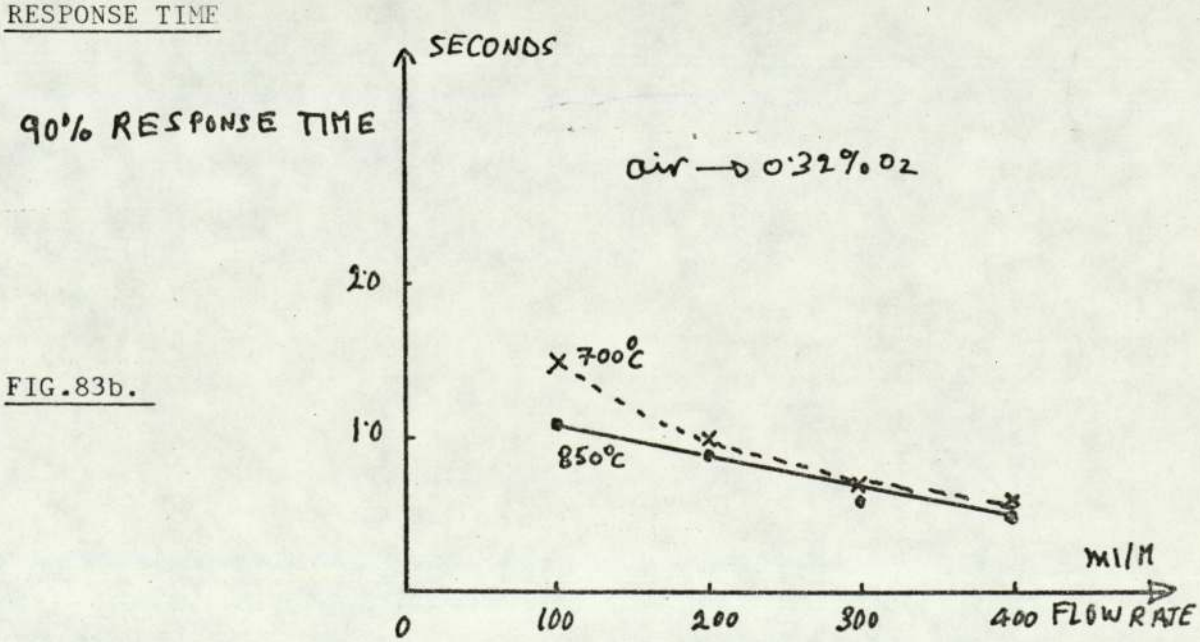

FIG.83b.

FIG.84.RESPONSE CURVES FOR NEW AND FOR AGED ELECTRODES

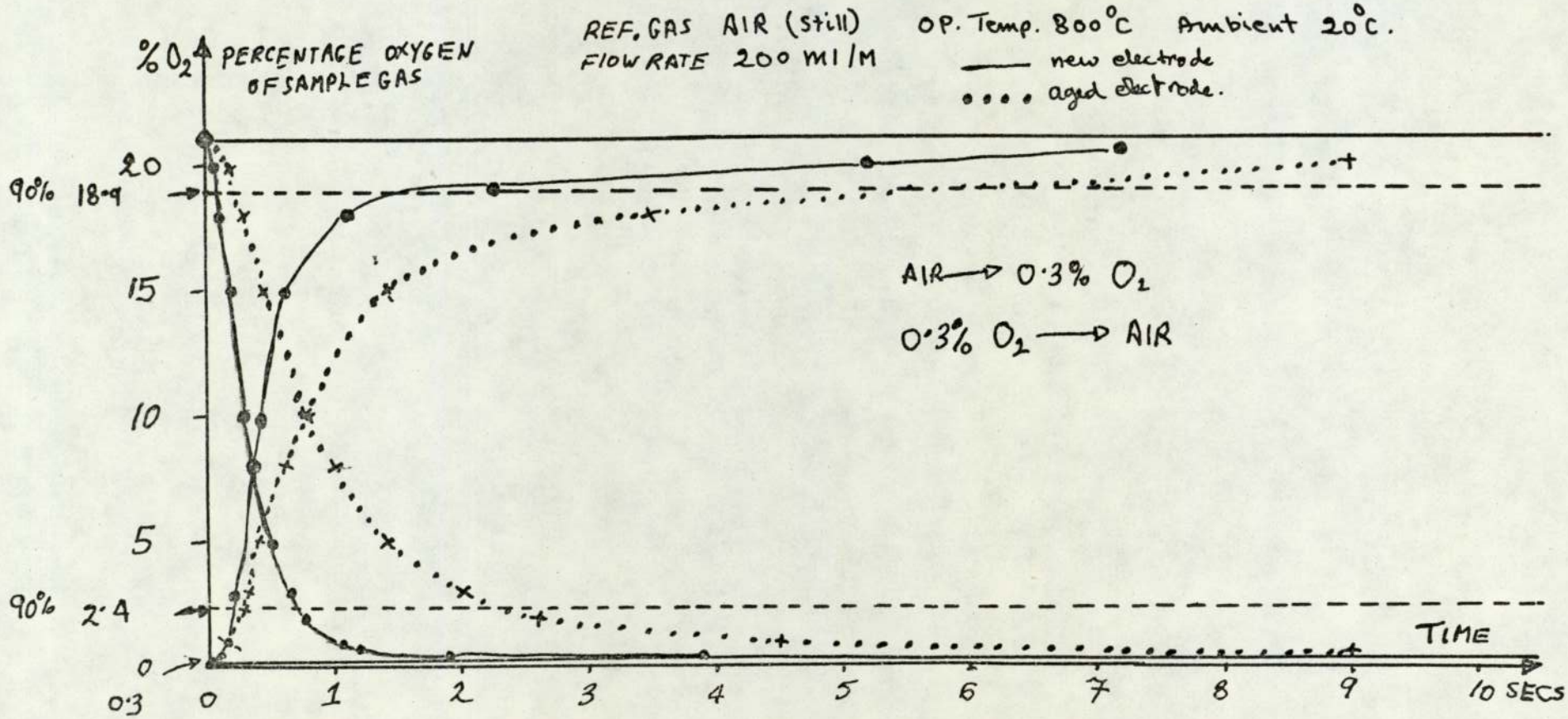

FIG.85a.

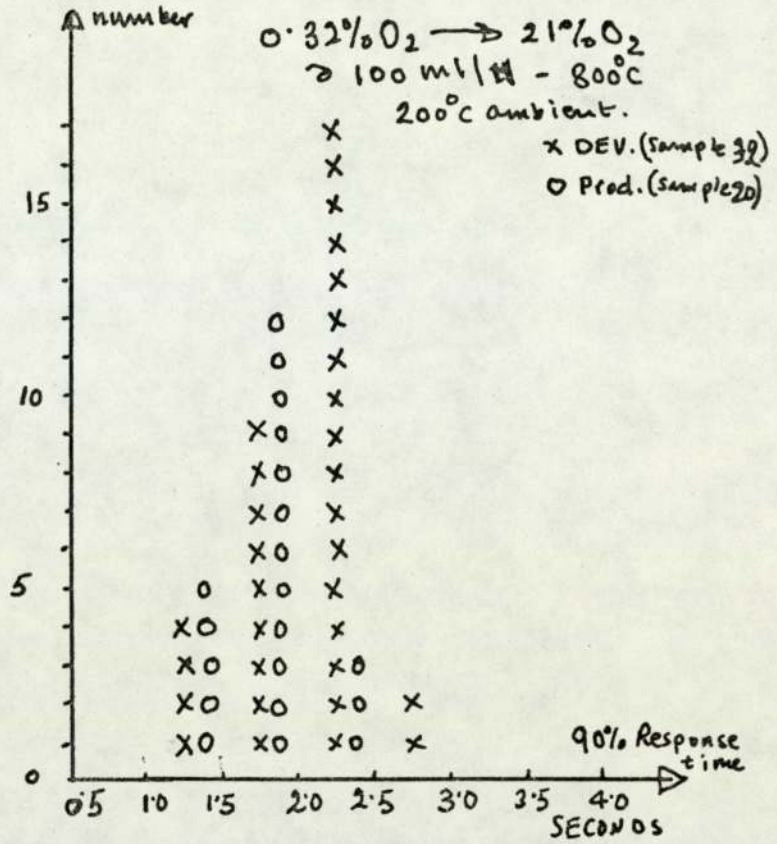

DISTRIBUTION OF DEVELOPMENT AND PRODUCTION SENSOR RESPONSE TIMES

FIG.85b.

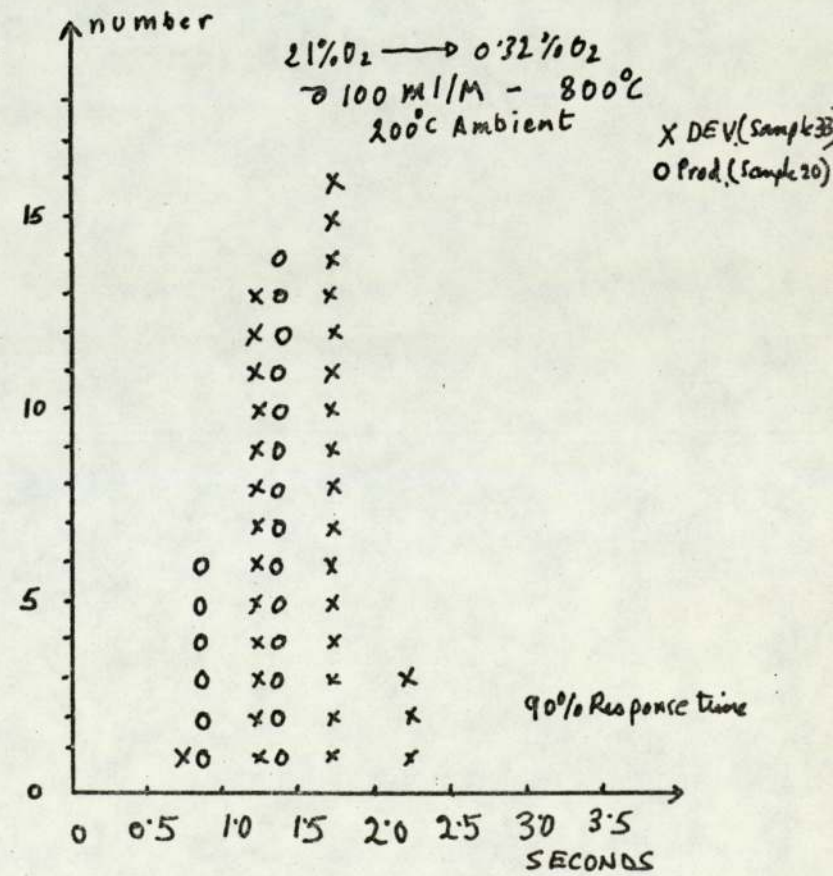

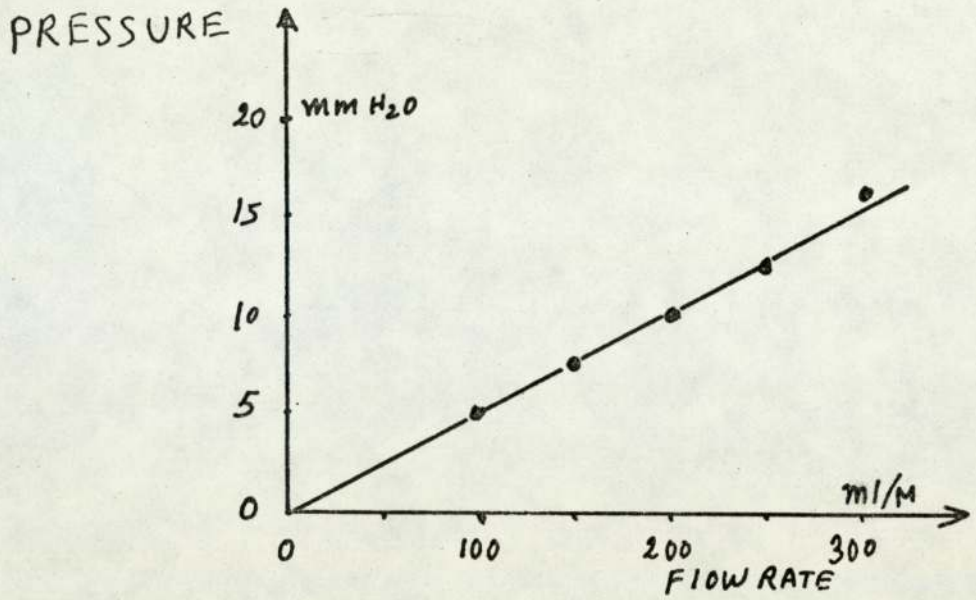

FIG.86.EFFECT OF FLOW RATE ON THE PRESSURE ACROSS THE SENSOR

CALIBRATION GASES % O_2	SENSOR OPERATING TEMPERATURE C^o				
	826	775	726	668	600
100 ± 0.1 %	0	0	0	0	0
10.6 ± 0.5%	0.1 %	0.2 %	———	0.5 %	2.0 %
2.15 ± 2%	0	0	1.0%	0	0.5 %
0.32 ± 2%	1.0%	0	———	0	2.5 %
260 ppm ±2%	0.8 %	1.1 %	1.0 %	4.0 %	5.4 %

TABLE 11.PERCENTAGE ERROR IN SENSOR READING RELATIVE TO NOMINAL CALIBRATION GAS VALUE

6.7. EFFECT OF SAMPLE GAS PRESSURE VARIATION ON SENSOR OUTPUT.

The flow of air into a sensor was kept constant at 100 ml/M by the use of a needle valve and flow meter whilst the pressure at the inlet of the sensor was monitored. The sensor was operated at 800°C and 200°C ambient with air at the reference side. The effect of a one percent variation in the pressure resulted in 0.25 mV change at the output, this corresponds to about 0.25% oxygen under this condition and hence to nearly one percent of reading. The effect of the pressure increase due to the flow rate can now be calculated (for 300 ml/M) giving about 0.05 mV, a negligible contribution.

The difference in temperature between the incoming gas and the operating temperature of the sensor produces a change in the pressure (thermo-molecular pressure) [365, 366] but this is quite small and appears as a contribution to the offset voltage.

6.8. SENSOR CALIBRATION

The sensor is expected to conform to the Nernst equation, and if it does,then, if the absolute electrode temperature is known and the pressures at the reference and sample chambers are equal we have a means of oxygen analysis which does not need any calibrating gases. Demonstrating that the sensor obeys the Nernst equation necessitates however some known gases. 100% oxygen and instrument air were chosen and these cylinders were calibrated using a high accuracy paramagnetic oxygen analyser,which was zeroed with dry, oxygen-free nitrogen (less than 20 ppm O_2) and spanned with dry and fresh atmospheric air (20.95% O_2). The pure oxygen was measured and found to be (100 - 0.1% O_2) and the instrument air was found to be (21% - 0.1% O_2). This was used as a reference gas and also for setting a reference point for the solid electrolyte sensor.

Two cylinders of oxygen in nitrogen were calibrated using the paramagnetic analyser and found to be 10.6 $\pm$ 0.5% of reading and

2.15 ± 2% of reading. Two further cylinders of O_2 in N_2 with analysis certificates of 0.32 ± 2% of reading and 260 ppm ± 2% of reading were obtained. The sensor was then set at different temperatures and the instrument air and pure oxygen cylinders were used to define two points on the Nernst equation, the expected emf for the gas mixtures at the operating temperature were calculated, and measured with a DVM. The percentage errors observed are given in Table 11. Increased response times were observed at temperatures below 750°C and as can be seen from the table the resulting errors begin to increase though still small. The results show that with careful calibration and operation (constant operating temperature, constant ambient temperature, constant flow and pressure) errors of the order of 1% can be expected for a range from ppm to 100% O_2. The operating temperature should be kept between 850 - 750°C. These results are shown in Fig. 87 as a plot of the logarithm of the ratio of reference to sample partial pressures against the output of the sensor in millivolts.

The distribution of the output of a sample of development and of production sensors is shown in Fig. 88a for 0.32% O_2 and in Fig. 88 b for pure oxygen. The nominal operating temperature is 800°C but it can vary by ± 10°C between sensors accounting thus for the spread in the results.

6.9. REPEATABILITY

At constant conditions (operating temperature, ambient temperature, flow rate and pressure) the repeatability is within ± 10 μ volts (air), and ± 20 μ V for (nom. 2% O_2 in N_2).

6.10. EFFECT OF COMBUSTIBLE GASES WITH EXCESS OXYGEN IN SAMPLE

Tests were conducted on sensors operated at a nominal 800°C and 200°C ambient, instrument air at 100 ml/M on the reference side and sample gas at 100 ml/M at the sample side. The sensor output was monitored with a DVM and a chart recorder.

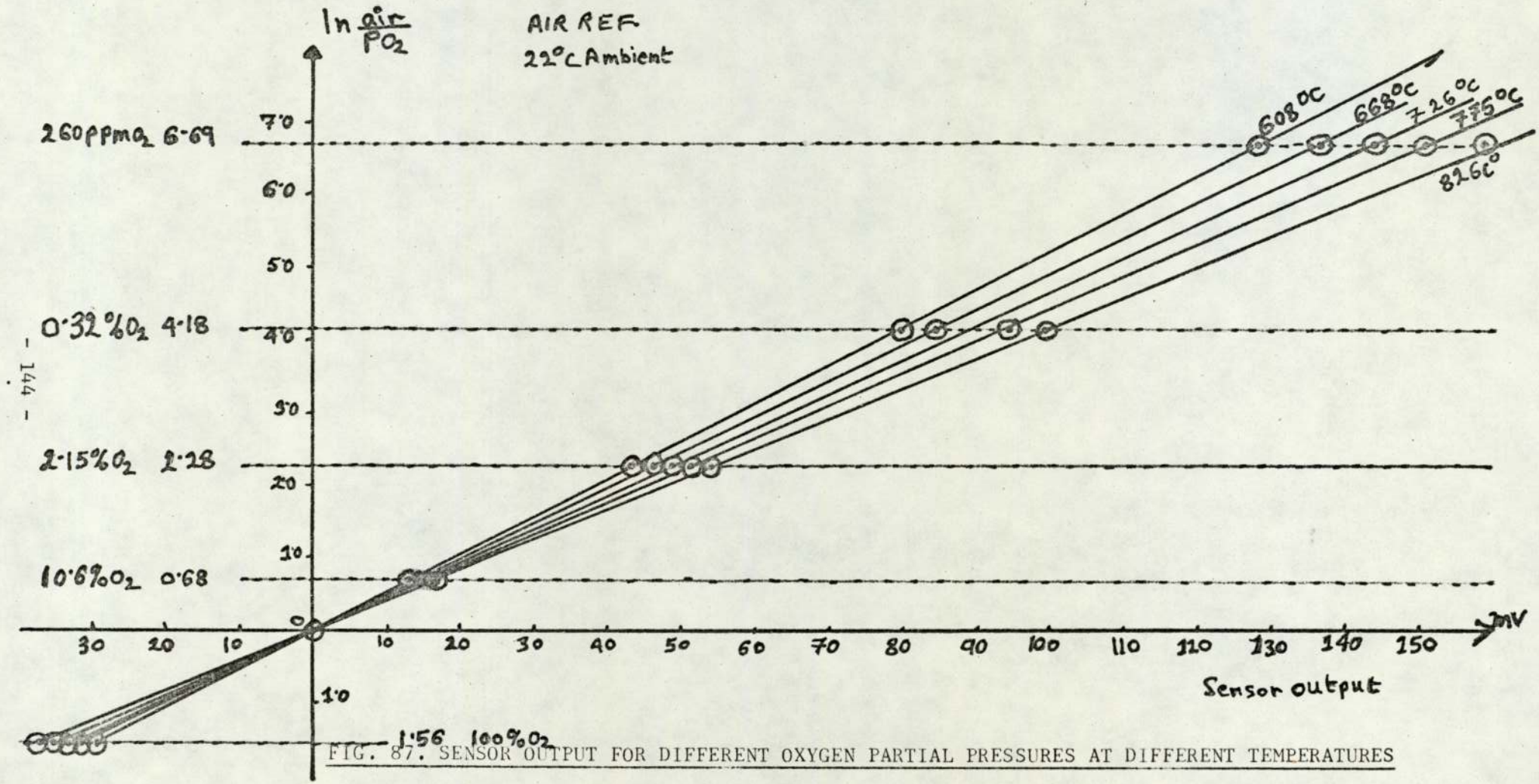

FIG. 87. SENSOR OUTPUT FOR DIFFERENT OXYGEN PARTIAL PRESSURES AT DIFFERENT TEMPERATURES

FIG.88a.

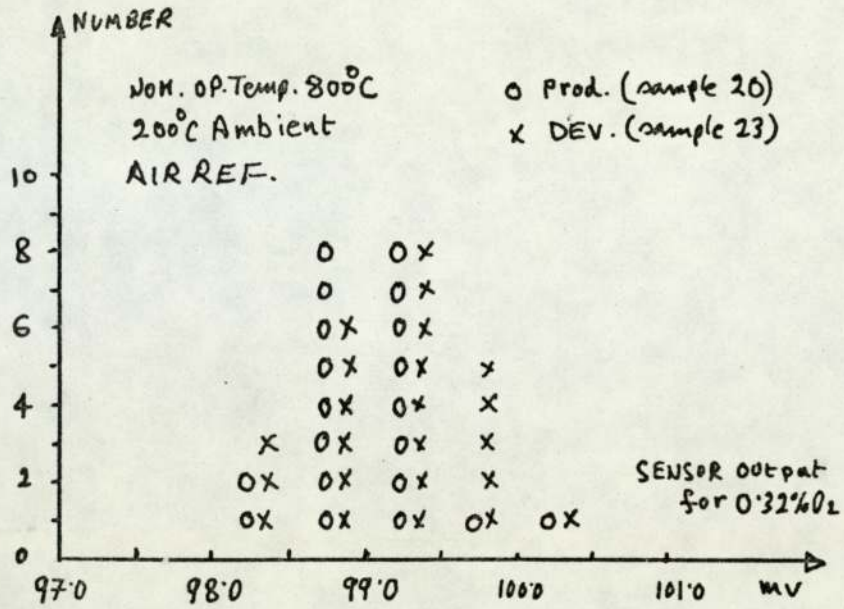

DISTRIBUTION OF DEVELOPMENT AND PRODUCTION SENSORS OUTPUT EMF

FIG.88b.

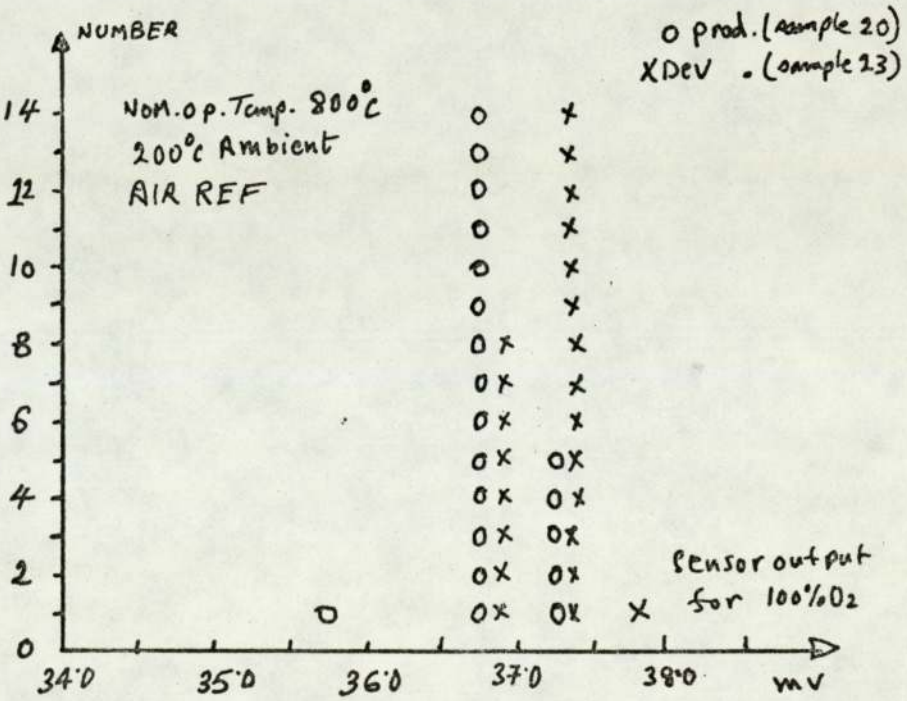

6.10.1. Carbon monoxide [367, 368]

A mixture of 1% CO, 2.7% O_2 and N_2 balance was admitted to the sample side of the sensor, the output corresponded to 2.25% O_2 the difference represents a complete combustion of the CO to CO_2. This complete combustion is possible due to the catalytic effect of the platinum electrodes. If non-catalytic electrodes [369] are used (gold, silver) the sensor reading will depend on the sample gas temperature and its flow rate.

There was no evidence of electrode deterioration after the test.

6.10.2. Water vapour [370]

N_2 with about 20 ppm O_2 was admitted to the sample side, first dry giving a reading of 14.5 ppm O_2, and then bubbled through water at 25°C (24mm Hg V.P.) which gave a reading of 14.0 ppm O_2. This is accounted for by the change in the percentages of the component gases due to the presence of water vapour. No reaction seems to take place.

There was no evidence of electrode deterioration after the test.

6.10.3. Nitrogen dioxide [371]

At 800°C this gas has a tendency to decompose to NO and oxygen, a certified mixture of 2.50% O_2 and 447 ppm NO_2 and N_2 balance was passed for one hour through the sample side, the mixture gave an output corresponding to 2.56% O_2.

There was no sign of electrode deterioration after the test.

6.10.4. Ethanol

Nitrogen (20 ppm O_2) was passed over ethanol at 20°C (5% concentration) and then admitted (half an hour) to the sample side of the sensor, an output corresponding to about 10^{-16} oxygen pressure was obtained indicating that the ethanol has taken up all the free oxygen present.

There was no evidence of electrode deterioration after the test. The sensor took about 15M to return back to its normal condition.

6.10.5 Diethyl-ether

Nitrogen (20 ppm O_2) was passed over diethyl-ether at 20°C (about 50%

concentration) and then admitted to the sample side of the sensor (half an hour). The output of the sensor indicated the equivalent of 10^{-19} O_2 pressure and later returned to 10^{-16} O_2 pressure for a nominal gas of 2% O_2 in N_2. Inspection of the sensor sample electrode revealed:

i) The pt lifted and peeled of the surface of the solid electrolyte.

ii) A thick deposit of a sooty material was found over the disc area.

6.10.6. Hydrocarbons (372)

With platinum electrodes the hydrocarbon-excess oxygen mixture will equilibriate and the effect will be similar to 6.10.1.

6.11. EFFECT OF SULPHUR COMPOUNDS

Pt electrodes deteriorate with the presence of elements such as active carbon, zinc, lead, arsnic and antimony. An element which is present in fuels is sulphur; its effect was investigated by passing 500 ppm H_2S in 2.5% O_2 in N_2 in the sample side (for half an hour), no change was observed, and by passing 3 ppm C S_2 in 2.5% O_2 in N_2 in the sample side (for half an hour), no change was observed. No damage to the electrode was detected in both cases. This is in agreement with the results reported by Haaland (369) at our working temperatures.

In flue gases under reducing atmosphere conditions, when fuel constituents are present ; H_2S, COS or S can form in the flue. This could react with the electrode material and form sulphides at high temperatures. When the excess oxygen condition is restored in the flue, pure Pt is reformed from the sulphides. Repeated cycling of these conditions will eventually damage the performance of the electrode by increasing its polarization resistance due to, the reduced contact of the electrode with the electrolyte, spalling of the electrode and corrosion around the edges of the electrode. Techniques for protecting sensing electrodes from sulfiding have been proposed, such as protective electronically conductive ceramics or mechanisms for ensuring an oxiding atmosphere in the vicinity of the electrode (Ruka, US Patent 4088,543).

CHAPTER SEVEN

THE CHARACTERISTICS OF THE SENSOR WITH A SEALED-IN REFERENCE AND IN THE PUMPING MODE; AND CONSIDERATION OF POSSIBLE FEEDBACK ARRANGEMENTS

7.1. THE CHARACTERISTICS OF THE SENSOR WITH A SEALED-IN REFERENCE

7.1.1. Situations where the use of a sealed-in reference is advantageous

For most normal applications (down to 10^{-7} atm. only, due to electrolyte porosity) [239,378] air is[a] suitable and convenient reference gas. There are however some applications and conditions when it is more convenient to use an alternative reference, such as:

i) The measurement of oxygen in molten metals.

ii) The measurement of very low oxygen equilibrium partial pressure (H_2/H_2O, CO/CO_2 etc.).

iii) Industrial atmospheres which contaminate the air with dirt or with combustible gases.

iv) Difficult positions where the reference air has to be piped a long way in a hostile environment.

An apprpriate sealed-in reference provides a simple solution to these difficult situations.

7.1.2. Types of sealed-in references

Oxygen/inert gas mixtures or gases in equilibrium with a stable oxygen partial pressure can be used or sealed in the reference side of the sensor. It is much more convenient however to use a metal/metal oxide. This must be stable enough so that at a given temperature a specific equilibrium (dissociation) oxygen partial pressure is present. A variety of solid references have been proposed and used: Cu - Cu_2O, Pb - PbO, Ni - NiO, Fe - FeO, Cr - Cr_2O_3, Pd - PdO..... [225, 238, 239, 264, 266, 374] Most of these are not stable enough [239] but the Ni -NiO and the Pd - PdO have been shown to have the required stability. The Ni-NiO provides a reference that is suitable for

measuring oxygen down to 10^{-27} atm. This is too low a range for the applications of interest to us. The calculated output of a sensor with such a reference and operating at 850°C for different oxygen sample concentrations is shown in Fig. 89.[238] The Pd - PdO on the other hand has an equilibrium oxygen partial pressure(around 830°C) which is nearly equal to air, as can be seen in Fig. 90.[364,375] A very successful miniature oxygen gauge uses this metal oxide as a reference - Fig. 4 (F.Patent 73,32671 Sept. 1973).

7.1.3. The output emf of the sensor with a Pd/PdO sealed-in reference

The output emf of an oxygen concentration cell with a metal/metal oxide sealed-in reference, operating at an absolute temperature T and with a sample gas with an oxygen partial pressure of PO_2 is given by,

$$E = E^{o}(T) + \frac{RT}{4F} \ln PO_2 \quad \ldots\ldots\ldots\ldots (34)$$

where $E^{o}(T)$ is the cell constant.

As the thermodynamic data for the system Pd/PdO is not accurate enough [375] a sensor with such a reference requires calibration. Fouletier et al give the following experimental equation for the cell constant, based on their work on the miniature gauge.[376]

$$E^{o}(T) = 444 - 0.51\ T(^{o}C) \quad \ldots\ldots\ldots\ldots (35)$$

E^{o} being in mV. The expression is the least square linear fit for experimental values with an average error of 0.4mV corresponding to about 1% uncertainty in the measured oxygen pressure. A plot of the equation is shown in Fig. 91.

7.1.4. The construction of a sensor with a Pd - PdO sealed-in reference

The design of the sensor makes the inclusion of a sealed in reference quite easy, as shown in Fig. 92. A Pt/Pt10%Rh thermocouple is placed at the sample electrode, and a Pt wire only on the reference electrode - this should make contact with the electrode area and the Pd/PdO powder which is tightly packed in (about 2mm corresponding to about 60 mg) on top of the electrode. The Pt conductor is brought out through the

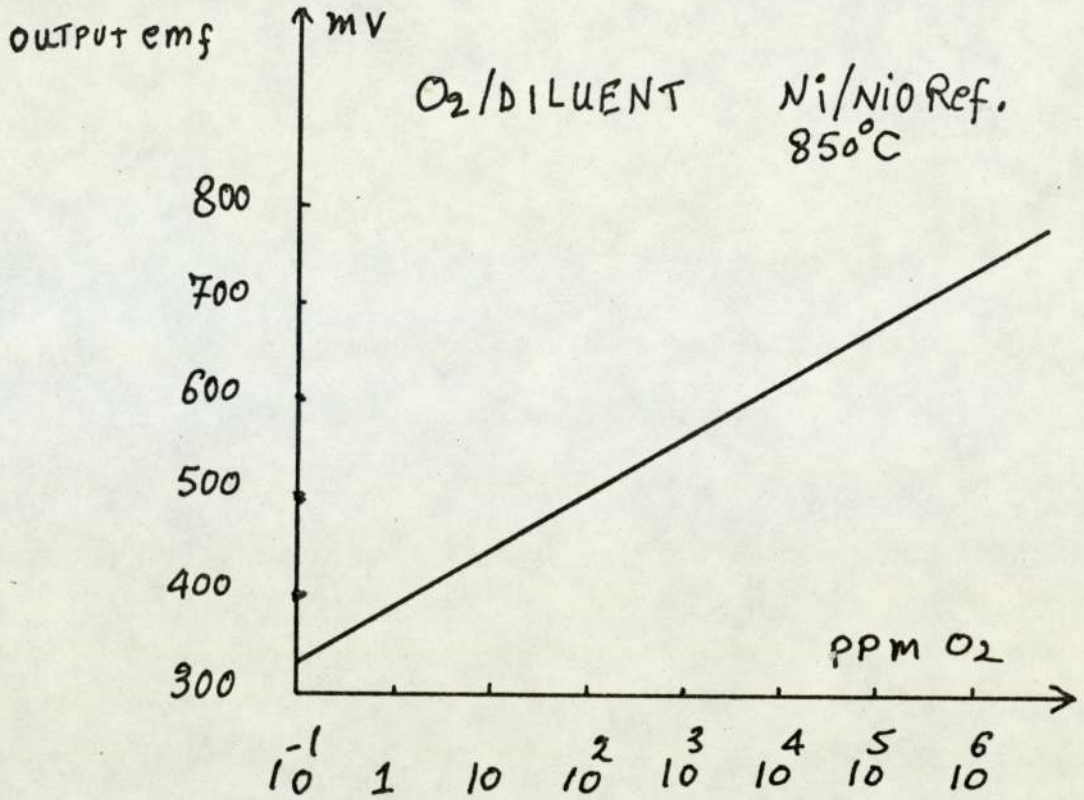

FIG.89. THE CALCULATED OUTPUT OF A SENSOR WITH Ni-Ni O SEALED-IN REFERENCE AT 850 °C FOR DIFFERENT OXYGEN CONCENTRATIONS

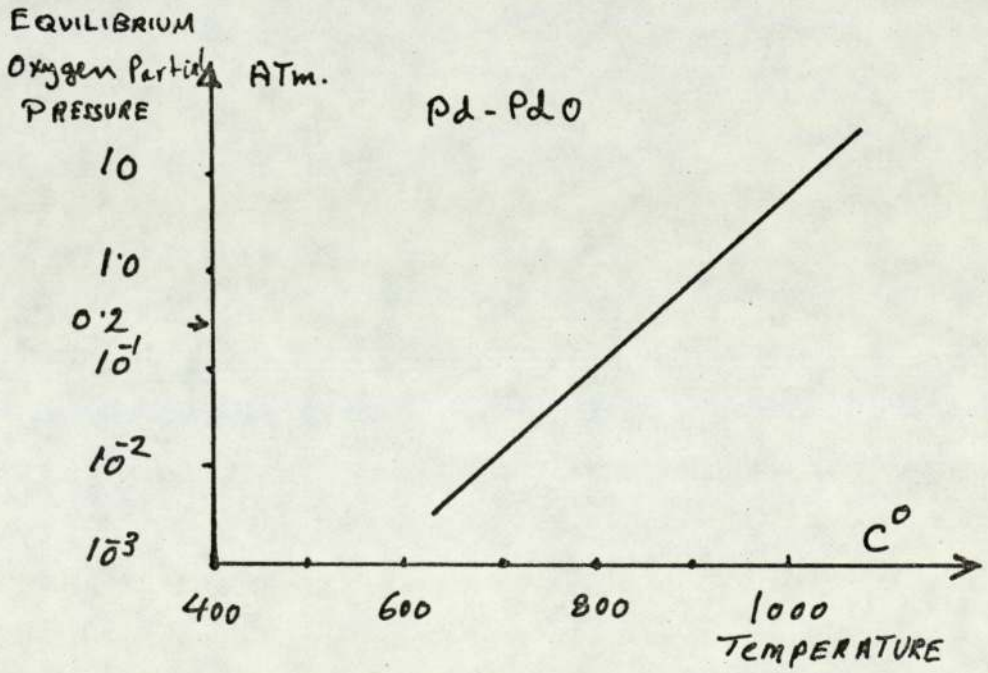

FIG.90. THE VARIATION OF THE EQUILIBRIUM OXYGEN PARTIAL PRESSURE OF THE Pd-PdO WITH TEMPERATURE

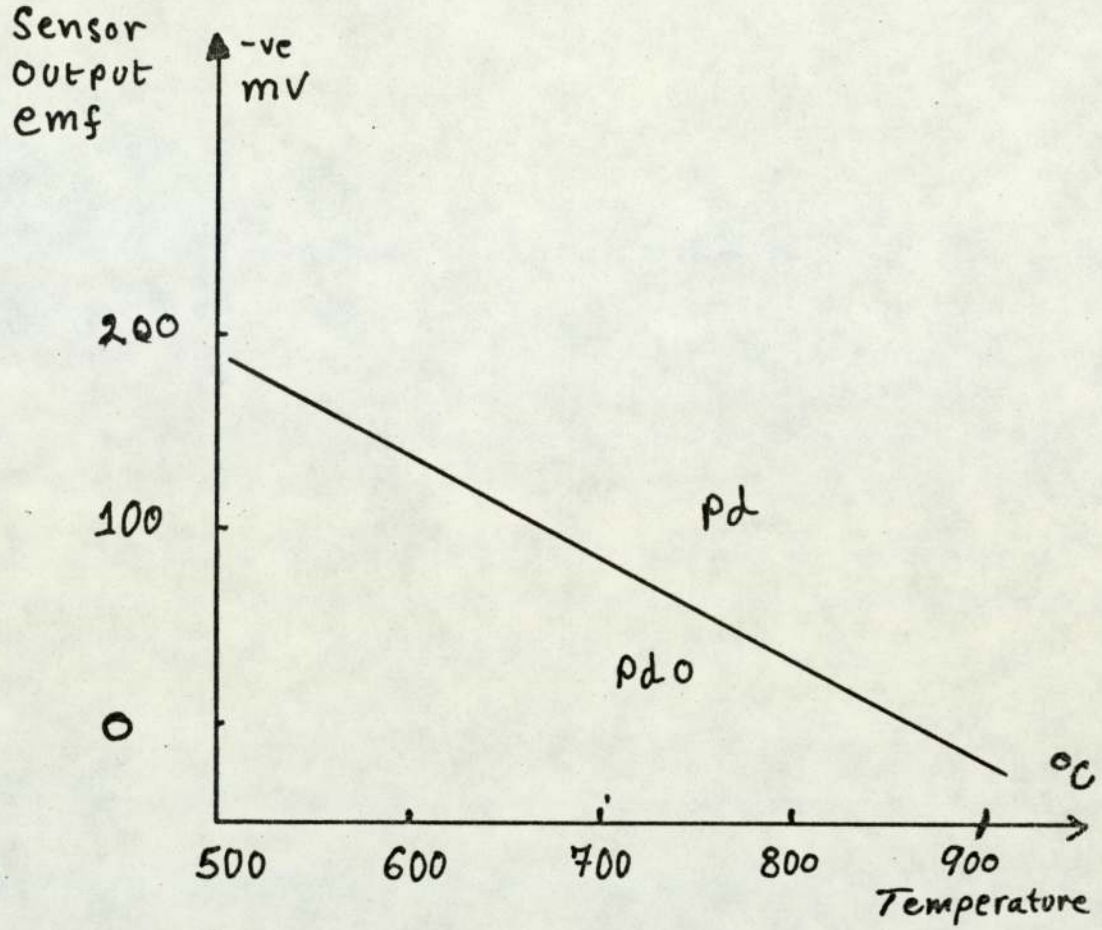

FIG.91.EQUILIBRIUM EMF OF A SENSOR WITH A Pd-PdO REFERENCE(MINIGAUGE)

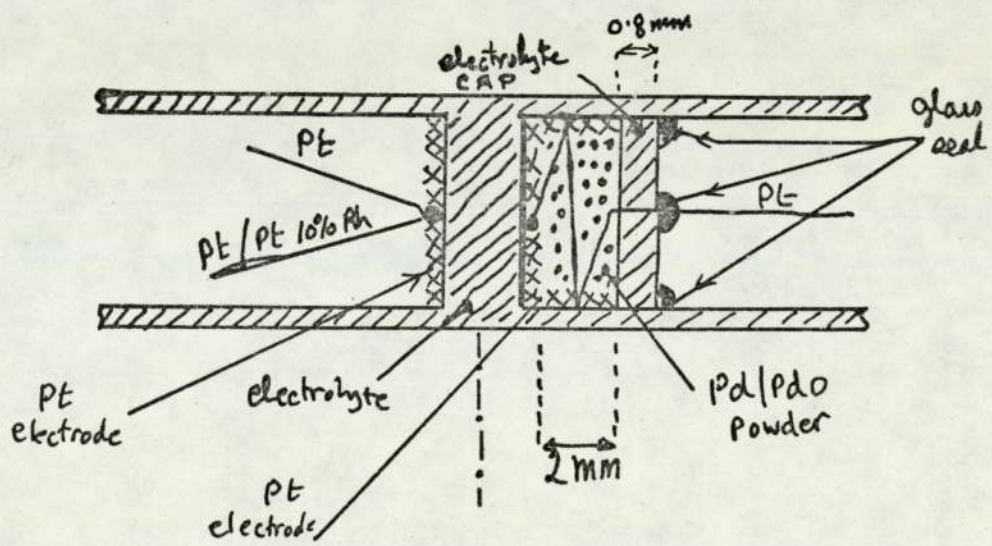

FIG.92. DIAGRAM OF THE SENSOR'S CONSTRUCTION WITH A SEALED-IN REFERENCE

centre of a zirconia circular disc (about 0.8mm thick, the same material as the electrolyte). The wire and the disc are sealed gas tight with a high temperature glass matched to the zirconia electrolyte. The rest of the sensor is identical to the one with air reference except that the gas connectors are not needed now for the reference end.

7.1.5. The activation and testing of the sensor

The sensor was tested first for possible air leaks into the sealed-in chamber by taking it up to about 750°C and monitoring the output emf which should be greater than that shown in Fig. 91 at that temperature on the palladium side (it depends on the amount of oxide powder used). Having ascertained that the sensor was gas tight, it was de-gased to get rid of the trapped free oxygen in the reference side. This was done by passing 5 MA for a few minutes at that temperature. The Pd/PdO was then activated by reversing the current and passing it for about 10M. This forms an oxide crust along the electrode/powder contact area. This crust was broken and evenly spread by cycling between 750°C (2 hours) and room temperature (about a dozen times, each cycle taking about 5 hours).

The output of the sensor was then measured with air at the sample side as the temperature was altered, this is shown in Fig. 93. The line obtained can be described by the equation:

$$E_o\ (mV) = 320 - 0.5T\ (^oC) \quad \text{.....(36)}$$

The constants of this equation differ from those given by Fouletier, the main cause of this is that a temperature gradient must exist along the powder mixture and the sample electrode. this can be minimized by: using a smaller amount of powder, by reducing the thickness of the cover cap, and by putting a thermocouple on the reference side, but as long as the thermal gradient is constant at a given nominal temperature the device can be used as an oxygen sensor, after it has been calibrated against some standard gases. The output emf of the sensor at a working temperature of 796°C and for a number of different oxygen mixtures (in N_2) which were passed through the sample chamber at 100 ml/M is shown in

Fig. 94.

The effect of variations in sample gas flow rate from 0 to 200 ml/M was about 0.2mV corresponding to about 0.5% uncertainty in the reading.

The 90% response time of the sensor was measured for a change from air to 0.32%O_2 (2S) and from 0.32% O_2 to air (4S) at a flow rate of 100 ml/M and a working temperature of 796°C.

7.1.6. The disadvantages of using a sealed-in reference

The results indicate the feasibility of easily adapting the sensor to having a sealed-in reference. They also show the Pd/PdO system to be very similar to having an air reference. There are however some main disadvantages connected with this mode of usage:

i) The large temperature gradient present necessitates a better temperature control or a form of temperature compensation.

ii) The sensor is no longer an absolute instrument, and requires to be calibrated with calibration gases.

iii) As the reference is sealed, the barometric pressure variations must be taken into account.

iv) A higher input impedance electronic circuitry is required ($>10^9$ ohms) so as not to introduce any cumalative variations in the sealed-in reference pressure due to pumping.

7.2. THE CHARACTERISTICS OF THE SENSOR IN THE PUMPING MODE [376]

When a d.c. current is passed through the sensor, oxygen is evolved at one electrode (positive side of the applied voltage) and removed at the other electrode. This is termed "pumping", and if pure oxygen ion conduction is assumed, it obeys the Faraday law. In a concentration cell pumping takes place due to the presence of the small electronic current, but this is normally very small. This effect has been used to generate gas mixtures with a specific oxygen partial pressures by injecting oxygen into an oxygen-free inert gas [255,256,381]; or to remove oxygen from a mixture with a known oxygen content [379] (Cathodic limiting

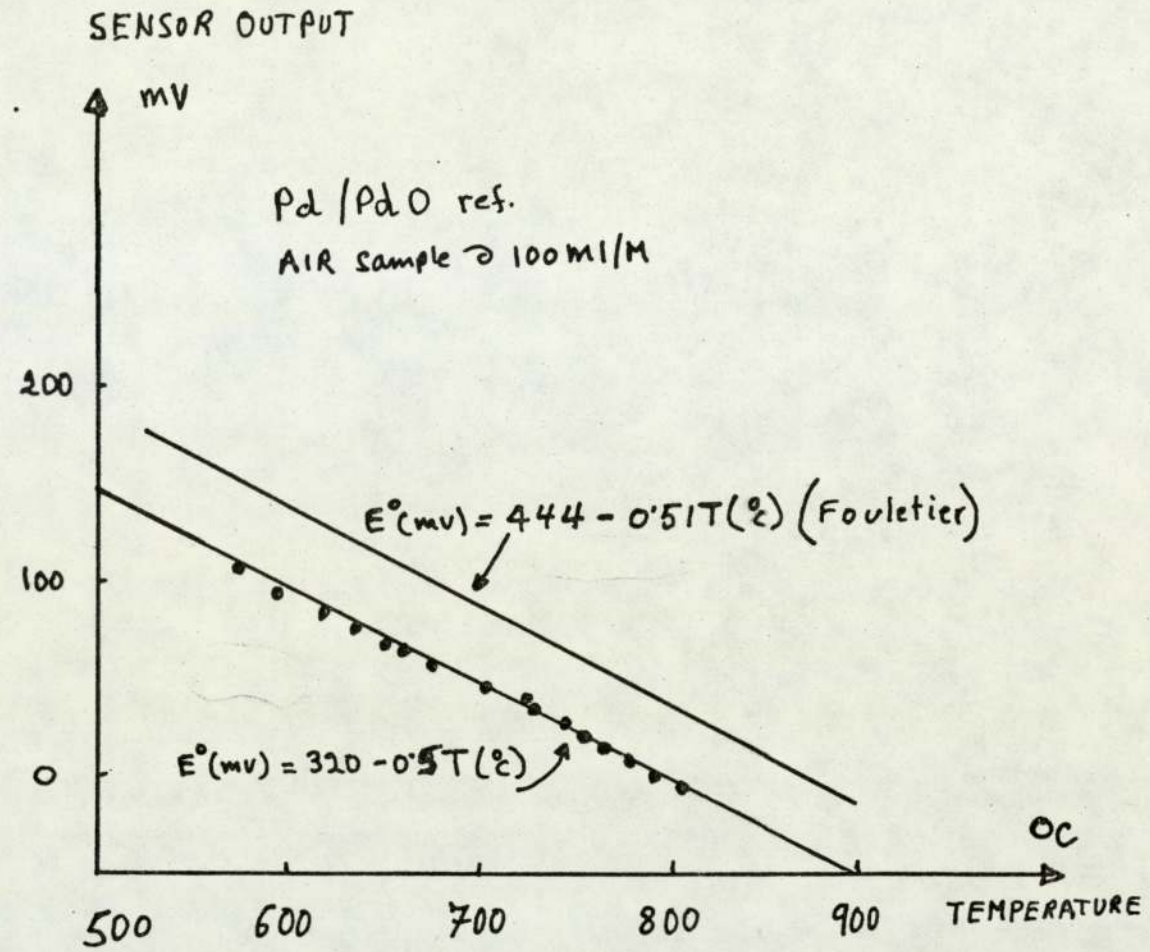

FIG.93. THE OUTPUT OF THE SENSOR WITH A SEALED-IN REFERENCE FOR AN AIR SAMPLE AT DIFFERENT TEMPERATURES

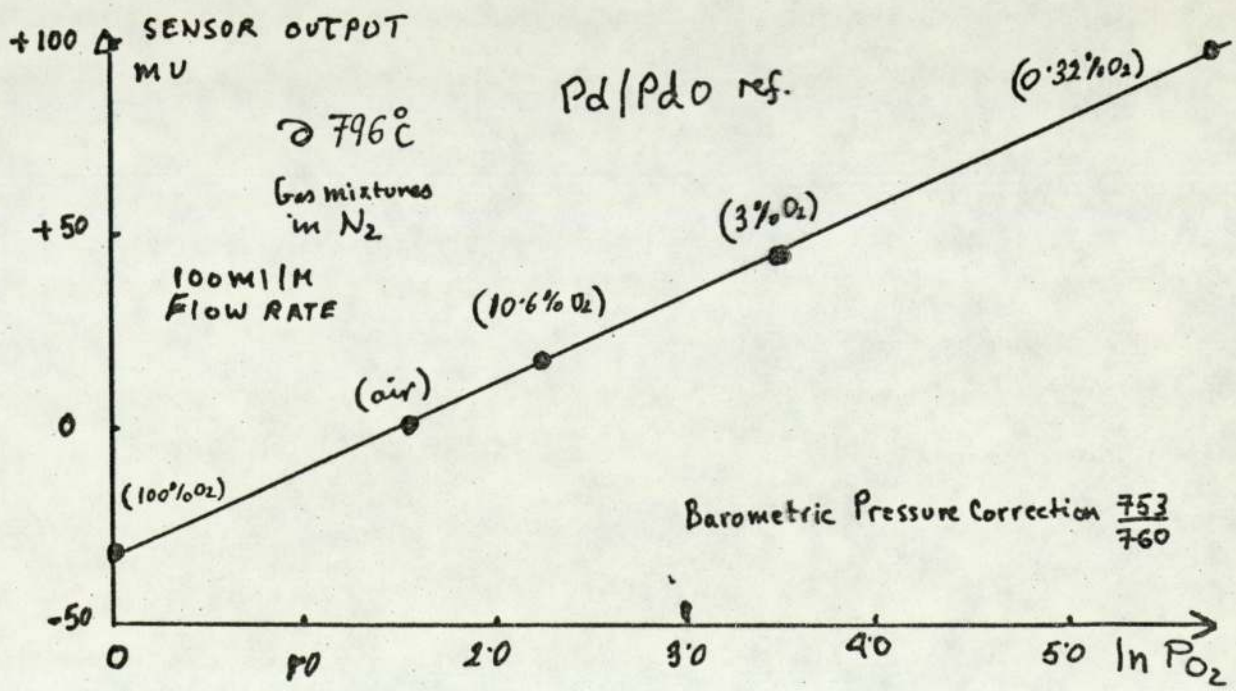

FIG.94. THE OUTPUT OF THE SENSOR WITH A SEALED-IN REFERENCE FOR DIFFERENT OXYGEN SAMPLES

currents appear when the oxygen content in the gas phase is very low, this leads to electron injection into the electrolyte if the applied voltage is high and hence the divergence from the Faraday law). It has been used also to produce an oxygen leak for testing high vacuum systems. (380)

This mode of use offers the possibility of feedback configurations using oxygen concentration cells, and oxygen pumps. (329, 382)

7.2.1. The voltage-current characteristics of the sensor

In order to determine the voltage-current characteristics of the sensor; a sensor was driven by applying current to it, the current and the emf across the sensor were monitored and the sensor was kept at 800°C. At the electrode connected to the positive side of the applied emf, a constant flow of nitrogen (about 13.5ppm O_2 content) was maintained at 100 ml/M and a similar flow of air was passed over the second electrode. The voltage-current characteristics are shown in Fig. 95 a & b. The non-linear (diode-like) (364) characteristics appear clearly in the graphs. Although no signs of damage were found on inspecting the electrodes, the emf values applied were excessive. The sensor internal resistance appears to change at the 1.7V - 0.5mA point and is reduced many times (from about 10K ohms to 170 ohms) in the 5 - 1.7 volt range. At high voltages currents of one amp. magnitude could be made to flow through the sensor. The passage of the current will induce local heating and the evolved oxygen must produce very high local gas pressures.

A detailed study of the characteristics to enable the identification and isolation of the many phenomena taking place, though of great interest, is beyond the scope of this present work.

7.2.2. The pumping characteristics of the sensor

If we assume that the sensor obeys the Faraday law in the pumping mode, and if a current I (mA) is passed through it, whilst a flow of L ml/M of an inert gas is maintained on the oxygen evolving side, the

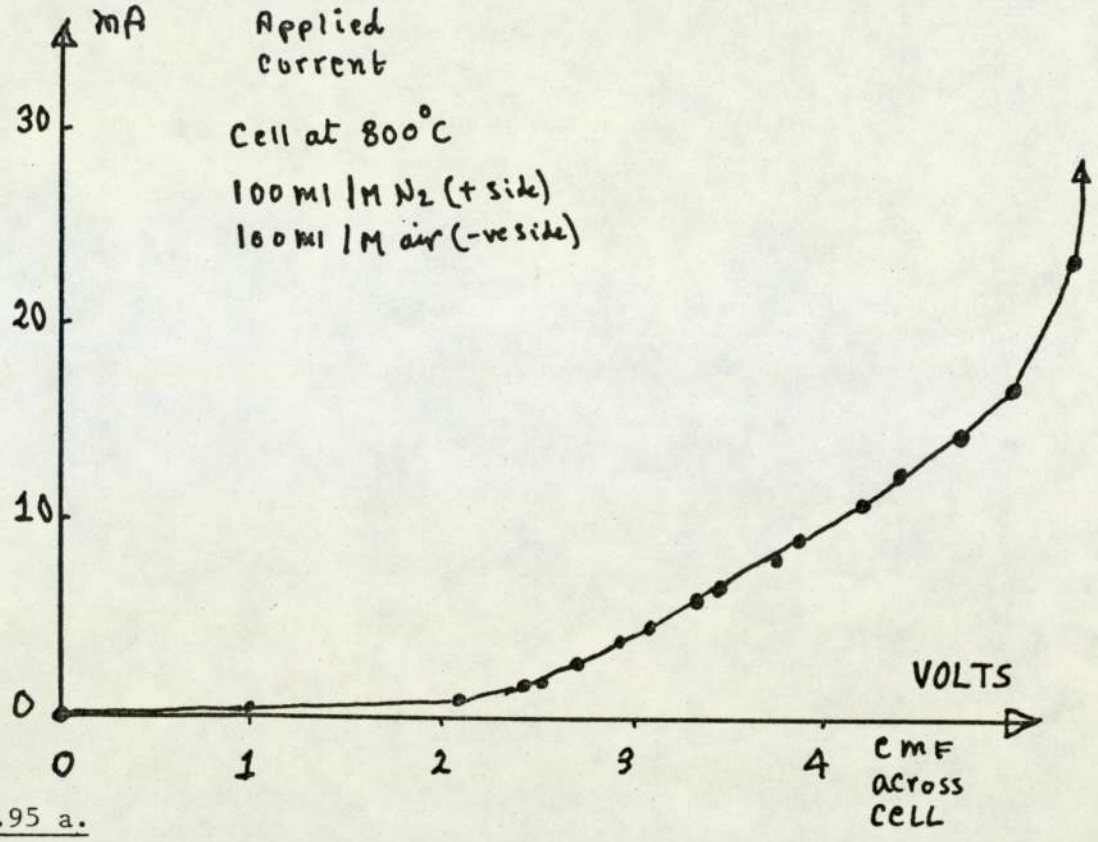

FIG.95 a.

FIG. 95 a&b. THE VOLTAGE-CURRENT CHARACTERISTICS OF THE SENSOR

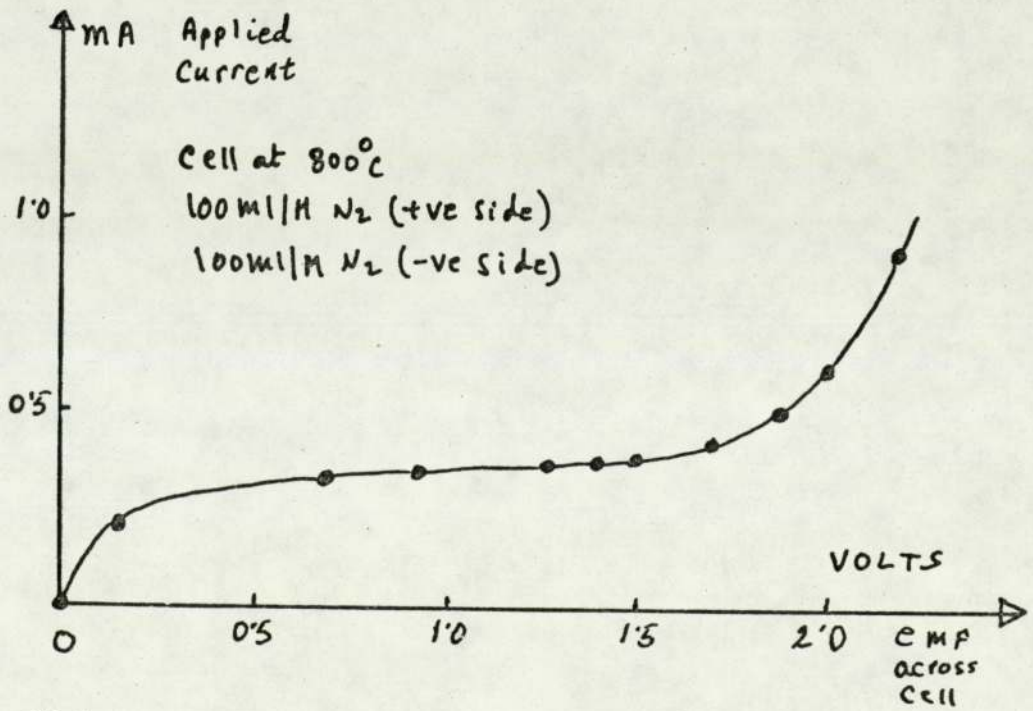

FIG. 95 b.

gas composition will be given (approximately) by:

$$\text{ppm } O_2 \text{ (in inert gas)} = \frac{3500 \times I}{L} \quad \text{.....(37)}$$

In order to test this, a solid electrolyte wide range oxygen analyser (described in the next chapter) was introduced at the output of the sensor under test (stainless steel pipes, and the system leak tested). The current-ppm O_2 characteristics of the sensor are shown in Fig. 96. The relationship obeys the Faraday law up to about 350 ppm corresponding to about 4 volts across the cell. The slope was 38 ppm/mA compared with the theoretical one of 35 ppm/mA, this is within the experimental errors of the test. As the voltage across the sensor increases the adherence to the Faraday law breaks down and diverges away from it rapidly. This is related to the sensor's electrode geometry and the previously discussed ageing problems. The results show however that the sensor could be used as a pump without any fear in the range 0-5mA. To get an idea of this pumping capacity, a volume of one millilitre which has 1% O_2 needs about 35 seconds so as to pump the oxygen away if a current of 5mA is used.

It is clear that if any sizable pumping action is intended a suitable design with a large surface area and low electrode resistance is necessary. If however a limited amount of pumping is required, the sensor can perform adequately.

7.3. CONSIDERATION OF POSSIBLE FEEDBACK ARRANGEMENTS

Feedback arrangements are attractive because they aim at a "null" condition whereby the measured and the measuring systems are brought nearly to the same state. Many advantages are claimed in general for feedback systems, but in most cases the conditions and improvements must be considered for that specific case. Some of the possible feedback arrangements that can be used in association with the solid electrolyte oxygen sensor will be discussed briefly.

7.3.2. Partial pressure equalisation

The Nernst equation (13) shows that when the reference oxygen partial pressure is made to be equal to the sample oxygen partial pressure, the output emf of the sensor is zero. Hence by monitoring the sensor's output and then by adjusting the oxygen partial pressure on the reference side so that the sensor's output is zero, and by relating this change to an easily measured parameter such as pressure or temperature, the output of the sensor can be calibrated in terms of this parameter.

A block diagram of a system whereby the oxygen reading is related to a pressure reading is shown in Fig. 97. The sample gas is passed through the sample chamber of the sensor and in the reference chamber a gas of known oxygen composition at atmospheric pressure (e.g. air) is used. The sensor emf is fed to a controllor which attempts to change the pressure in the reference chamber so that the oxygen partial pressure then equals that at the sample chamber. The controller achieves this by using a vacuum pump system or a compressor system depending on the sign of the emf received from the sensor. The final pressure in the chamber is read by a suitably calibrated pressure gauge. (Wilson, U.S. patent 3,442,773).

The fact that by varying the temperature of a gas in a sealed chamber its pressure is altered, is utilized as means of equalising the partial pressures between the sample and reference chambers. (Bazhenov et al USSR patent 371495). The temperature of the reference gas can be related to the oxygen concentration. This method requires severe temperature swings to cover a reasonable range of oxygen concentration. This situation can be improved if a sensor with a Pd/PdO reference is used. A block diagram of such a system is shown in Fig. 98. A reference emf which corresponds to a reference oxygen partial pressure is chosen (Fig. 93) and the controller set point is set to that. When a sample gas is passed through the sample chamber and if its composition is different from that in the reference chamber, the sensor produces an

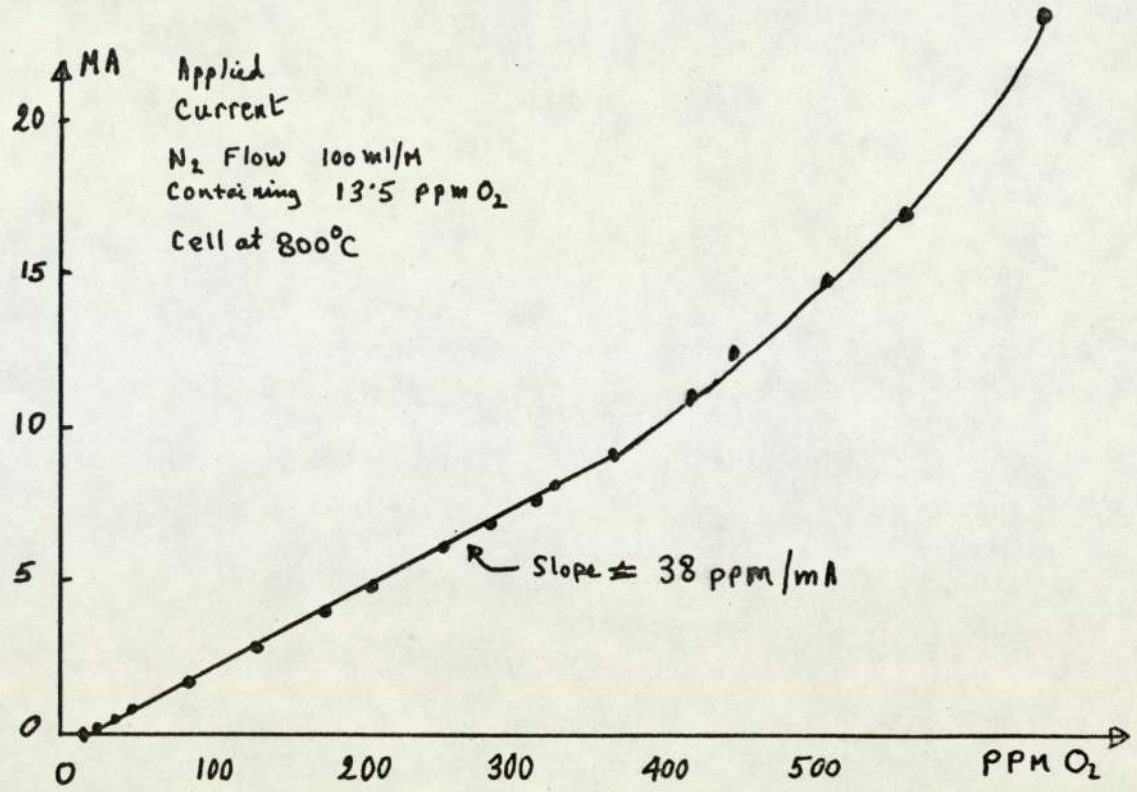

FIG.96. THE CURRENT-PPM O_2 CHARACTERISTICS OF THE SENSOR

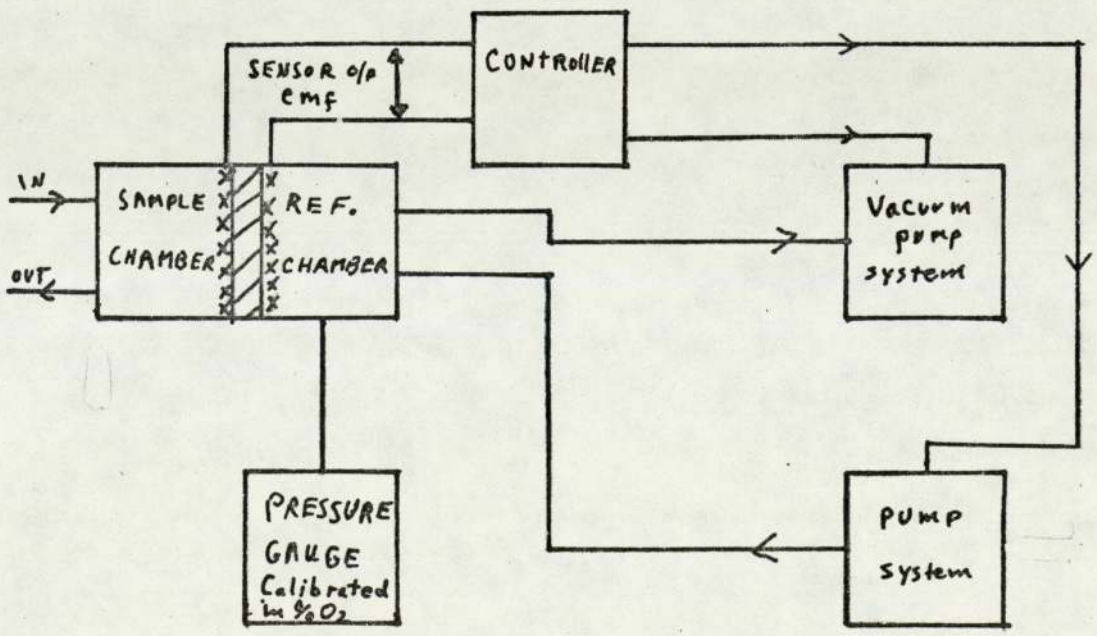

FIG.97. EQUALISATION OF PARTIAL PRESSURE FEEDBACK SYSTEM WITH PRESSURE READ-OUT

output emf which is different from the set point; the controller then drives the temperature controller so as to change the operating temperature of the sensor, this results in a change in the partial pressure of the oxygen in the reference chamber. A new sensor operating temperature is thus reached which produces in the reference chamber the desired oxygen partial pressure so as to null the emf's at the controller. The value of the operating temperature can be calibrated in terms of sample oxygen concentration.

7.3.2. Feedback by pumping (329, 382)

The pumping property of the solid electrolyte oxygen sensor can be utilized in a feedback system. A block diagram of such a system is shown in Fig. 99. The sample gas which is kept at a constant flow is passed first through a sensor used in the pumping mode and then through a sensor used in the sensing mode. Both having air as a reference. The output of the sensor is fed into a controller which compares it with the expected emf value for a low oxygen concentration (e.g. 0.01%O_2) if the signals are not equal a pumping current is increased slowly until the oxygen in the sample is pumped down to the pre-selected value. The pumping current is then an indication of the oxygen concentration. (US Patent 3,514,377).

A sensor can be designed to include the above system in one sensor as shown in Fig. 100. The sample side of the sensor is divided by a diaphragm with small diffusion holes in it, and it also has two separate electrodes. There is only a single electrode at the reference side. A suitable reference gas is chosen and the corresponding sensor emf output, set in the comparator. When a sample gas containing oxygen flows past the diffusion diaphragm, oxygen molecules will diffuse into the electrode area, the sensor part will sense this and a signal is fed to the comparator which feeds a signal to the controller, this induces a pumping current which flows in the pumping part of the sensor and results in pumping the

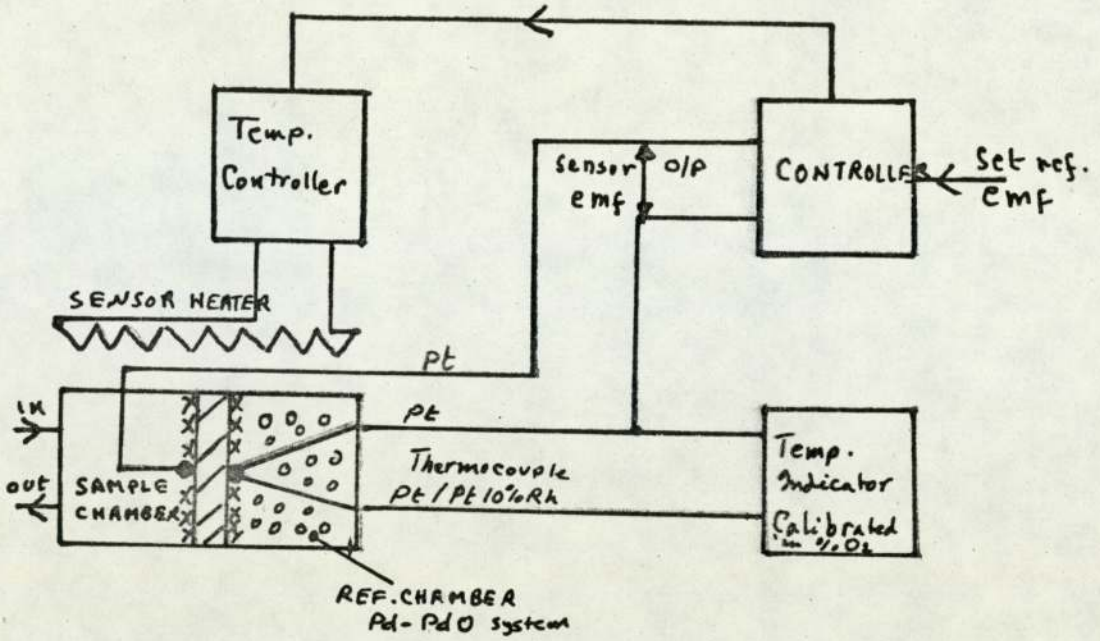

FIG.98. EQUALISATION OF PARTIAL PRESSURE FEEDBACK SYSTEM WITH TEMPERATURE READ-OUT

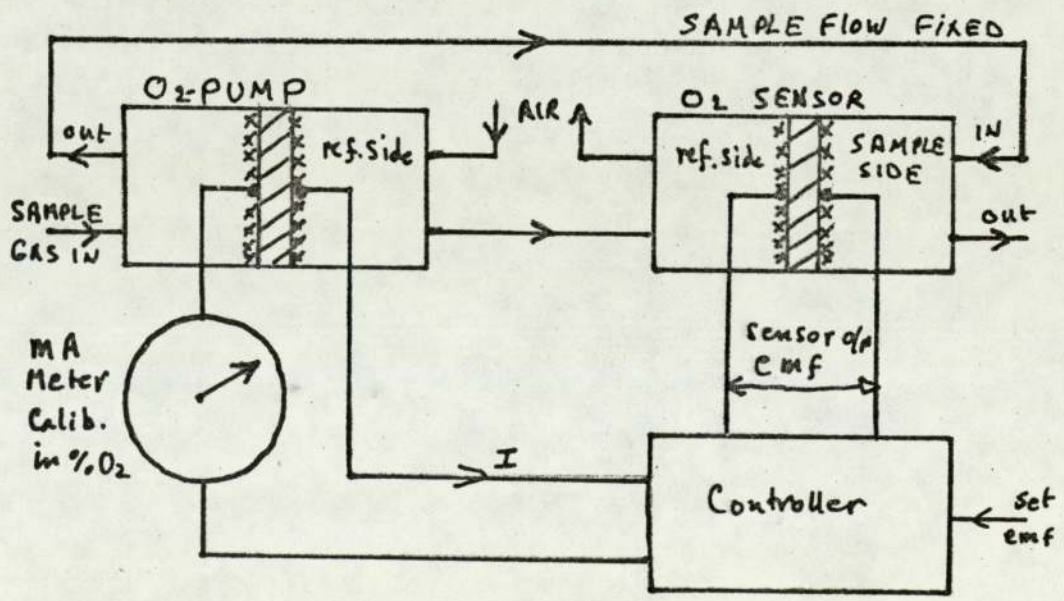

FIG.99. A SYSTEM UTILIZING PUMPING FOR FEEDBACK

oxygen from the electrode area to the reference area. The current will reach equilibrium when the arriving oxygen molecules are all pumped away and as they are proportional to the oxygen concentration in the sample, the pumping current can be calibrated in terms of oxygen concentration. (Ruka U.S. patent 4,088,543)

An alternative design is shown in Fig. 101.[369] This comprises basically two sensors sealed together to form a small cavity which contains an inert gas. The sample is admitted into the sample side and the oxygen concentration is sensed by the oxygen sensor and fed into a comparator. The controller is programmed to the following sequence:

i) Oxygen is pumped away from the inter-sensor cavity,by applying a constant current.

ii) The constant current is reversed and used to pump oxygen into the cavity until it reaches a concentration equal to that of the sample gas.

iii) A timer times the period between the initiation of the pumping and the time it stops . This time is related to the oxygen concentration of the sample gas.

Most of the systems described above are complex. The main advantage of using a feedback system is that in most cases a linear output is obtained , and the temperature regulation requirements become less stringent.

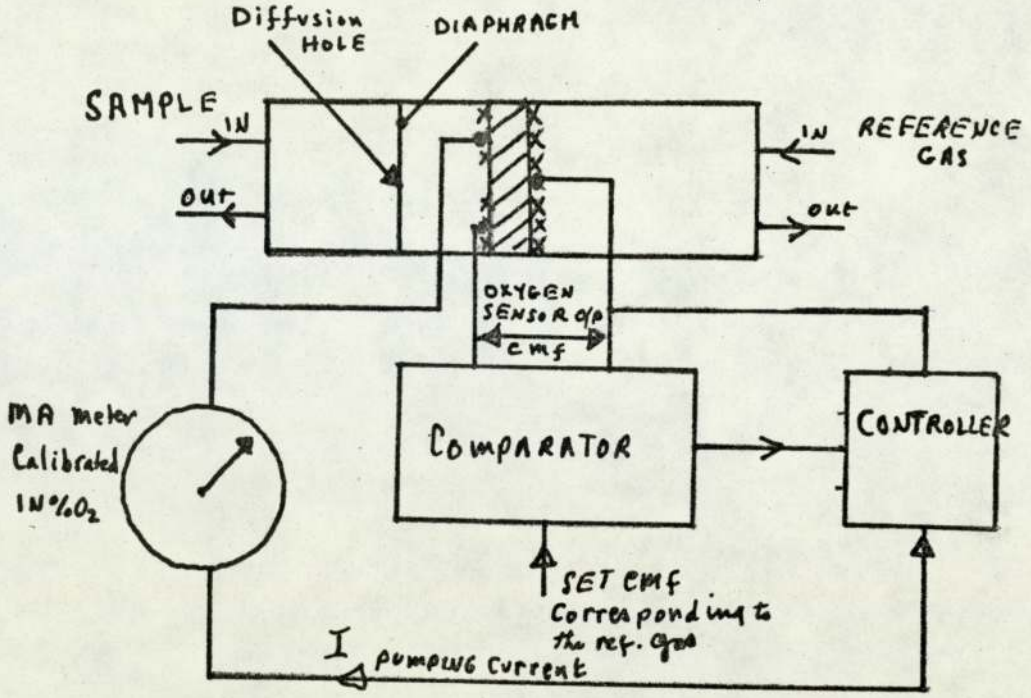

FIG.100. COMBINED SENSOR -PUMP SYSTEM

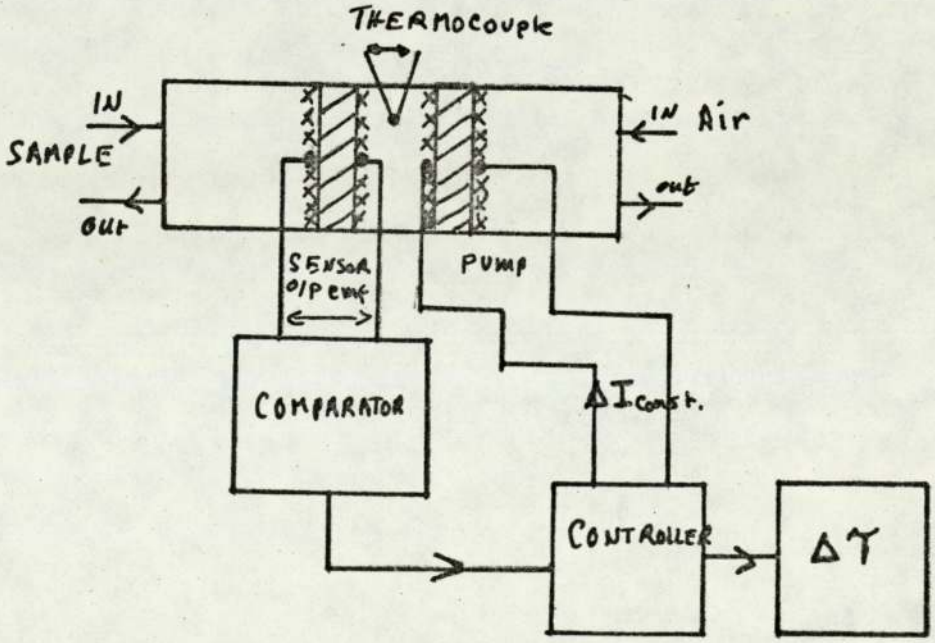

FIG.101. SEPERATE SENSOR-PUMP SYSTEM

CHAPTER EIGHT

THE USE OF THE SENSOR IN AN INDUSTRIAL FLUE GAS ANALYSER AND IN A WIDE RANGE INSTRUMENT

8.1. THE SERVOMEX (R) ZIRCONIA FLUE GAS OXYGEN ANALYSER

The need for and the advantages of oxygen trim control on combustion control applications have been described in Chapter 3. Two main types of industrial flue gas analysers were mentioned viz: in-stack probes, and out of stack instruments.

The Servomex (R) instrument is an out of stack type; a choice made mainly for the following reasons:

i) Actual gas flow (instead of diffusion)permits flow monitoring (awareness of filter blockage).

ii) Easy to replace components (sensor, filter etc.).

iii) Sensor cracks or leaks are easy to detect.

iv) The system allows the sample to be used for other analysis (CO, CO_2, combustibles etc.).

v) The system has better temperature control and lower temperature gradients.

vi) The sample gas presents small temperature variations to the sensor.

vii) The simple and direct wiring routes to the sensor do not require different materials in series which are in large temperature gradient areas.

viii) The system has a consistent response time (no diffusion, no convection).

The Servomex (R) instrument has two parts - an external to stack direct mounting flue gas sampling probe which houses the solid electrolyte oxygen sensor and the sample extracting unit, and a control and readout unit. The specifications of the analyser are given in Table 12.

8.1.1. The probe

The sampling system aims at extracting a representative sample from the

flue and delivering it to the sensor with the minimum of modifications, but suitably conditioned so that components such as particulates, flay ash etc. do not reach the sensor. The system aims also at avoiding the possibility of the sample condensing within the probe (dew point about 160^{o}C) so as to prevent any corrosion. Safety requirements necessitate the absence of a direct route between the hot surfaces in the probe and the flue area. A flame trap must buffer such routes.

The flue gas sample is extracted by an air aspirator. Two stainless steel pipes protrude into the flue and are welded into a flange which is secured tightly to the flue side. The aspirator draws a flue sample through the inlet pipe and discharges it together with the aspirating air and the reference air into the flue through the outlet pipe.

The basic components of the probe are shown in Fig. 102. They comprise the following:

i) A sample extraction aspirator - This is shown in Fig. 103 and is made up of:

a) An air ejector - High quality air (filtered and free from humidity and hydrocarbons) under high pressure is allowed to ascape through a narrow radial slit and by the phenomenom of wall attachment, the air flow follows the continuous divergent contour. This air flow induces a depression at the throat of the ejector that draws a sample through the inlet tube from the flue, it also ensures that no particulates from the sample settle on the walls of the system.

b) Venturi head section - The sample gas passes through a venturi section prior to being drawn through the ejector, this produces a pressure differential between the inlet and throat section that drives the sample through

TABLE 12

SPECIFICATIONS OF THE SERVOMEX (R) ZIRCONIA FLUE GAS OXYGEN ANALYSER

Accuracy

Logarithmic cell output ± 2.5% of reading or ± 0.02% O_2 whichever is greater.

Repeatability

± 0.5% of reading.

Range

Meter - 0.25 to 25% O_2 (logarithmic)

Output (logarithmic from module) 0 - 1 v corresponding to 0.25 to 25% O_2.

Response time

less than 10 seconds for the 90% point for a change from 4% O_2 to either 10%O_2 or 0.3%O_2.

Environment

Probe - -10°C to +50°C.

Control and readout - 10°C to +50°C.

Relative humidity - 0 - 95% RH

Sample Gas Temperature

200°C to 500°C

Probe to control and readout separation

50 metres maximum.

Electrical supply

117 - 240V 43 to 62 Hz, 1.5K watts.

Mains voltage effect

± 1% of reading for ± 10% voltage variation.

Aspirator and reference air supply

High quality air less than 1 ppm oil vapour 3 bar min. pressure.

Maximum consumption 30 lit/M.

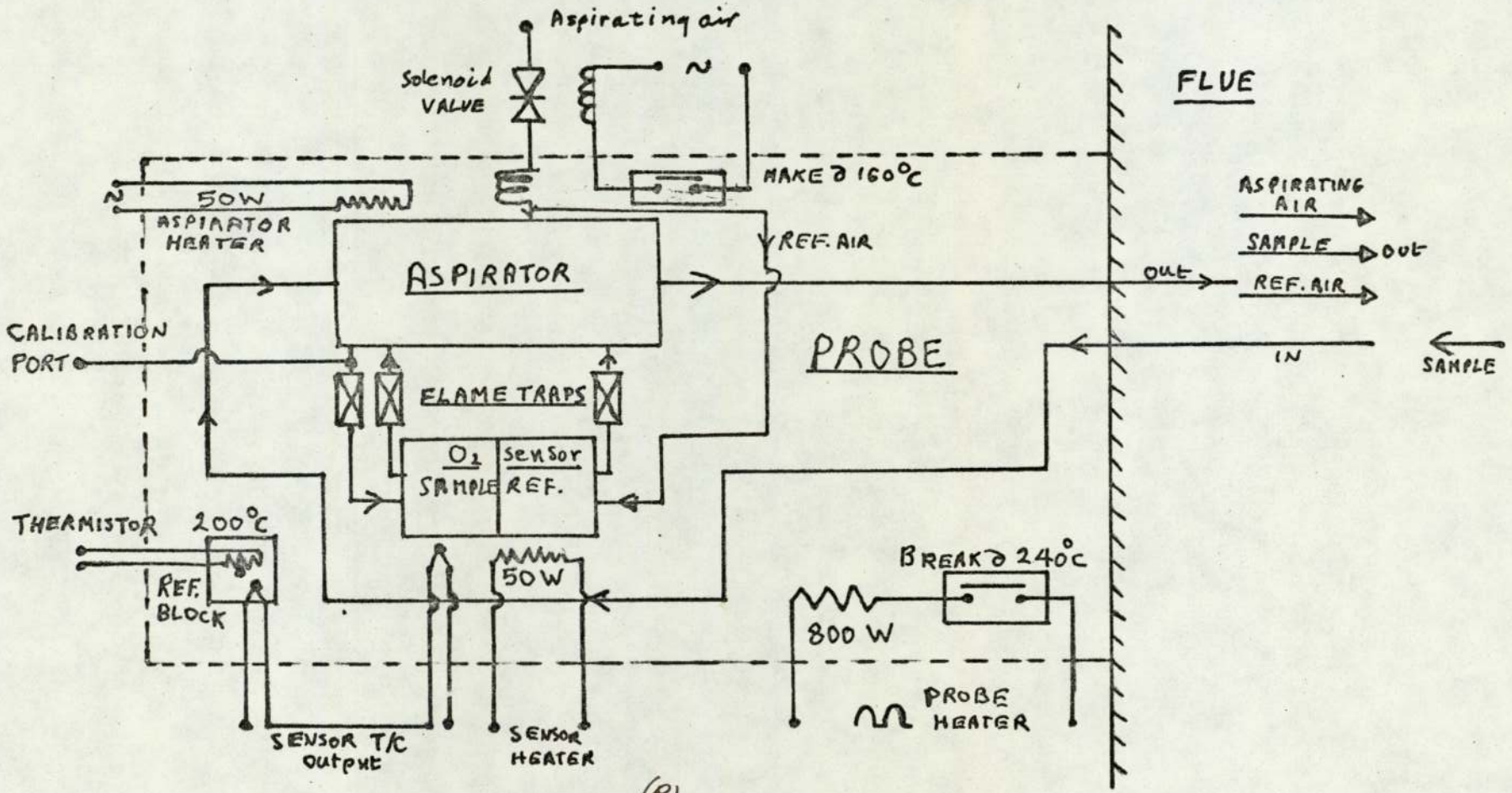

FIG.102.BLOCK DIAGRAM OF THE SERVOMEX (R) ZIRCONIA FLUE GAS ANALYSER PROBE

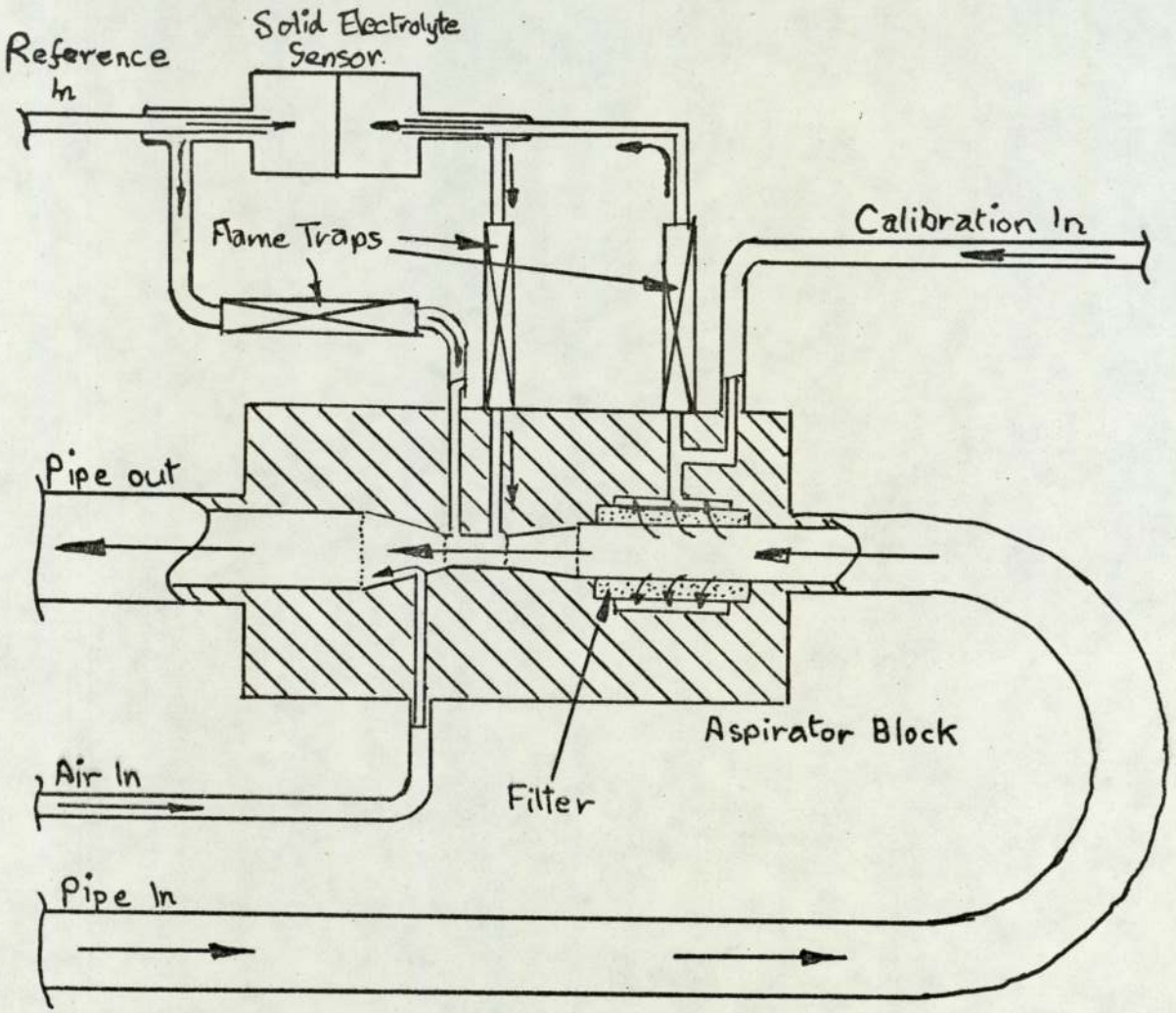

FIG.103 .DIAGRAM OF THE ASPIRATOR BLOCK

the flame traps and the sensor.

c) Slip stream filter - This method of filtering minimizes lag time and lengthens the life of the filter, as only the sensor flow is filtered.

The induced sample flow passes through the slip-stream filter where the sensor flow is drawn through the filter and the path is protected by two flame trpas. The sample is returned to the throat section of the venturi. The reference flow is tapped from the aspirating air through a restriction that controls the flow rate and is fed into the aspirator through a flame trap to the throat section of the venturi. Calibration gas can be introduced through an inlet which joins the sample side of the sensor prior to the flame trap.

ii) Aspirator heater block - The aspirating air is brought to the temperature of the probe by passing it through a long pipe and thus bringing its temperature to nearly that of the probe; it however expands within the aspirator block, this results in cooling the aspirator. This is counteracted by heating the aspirator block by a 50W heater up to about 300°C.

iii) Enclosure heater - The internal temperature of the probe is kept above 160°C (nom. 200°C) by controlling an 800W heater. The heater power line has a contact-break thermostat that breaks the circuit if the temperature exceeds 240°C.

iv) Cold junction and temperature sensor block - A thermistor which is housed in an aluminium block senses the internal temperature of the probe and that signal is used to control the heater power. The block houses also the reference junction thermocouple which in conjunction with the thermocouple in the sensor is used to control the operating temperature of the sensor.

v) Solid electrolyte sensor - This has been described elsewhere.

vi) Aspirating air solenoid valve - This valve is energised from the same power line as the probe, and will cut off the air supply if there is a power failure. A contact-make thermostat in its power line and housed in the probe ensures that aspiration does not take place until the inside temperature of the probe reaches about 160°C.

8.1.2. Control and read-out unit

The control and readout enclosure contains:

i) Sensor signal conditioning amplifiers:

a) Oxygen signal - The output of the oxygen sensor is amplified to give an output signal 0 - 1V for a 100mV - 3.8mV input corresponding to 0.25%O_2 to 25% O_2 logarithmic signal.

b) Temperature signal - The signal from the thermocouple in the sensor as referenced to the probe temperature, is amplified for use as an input to the temperature controller.

ii) Temperature controllers:

a) Sensor temperature controller - This is a d.c. variable on/off ratio controller which keeps the sensor temperature to within $\pm$ 1°C of a set temperature.

b) Probe enclosure temperature controller - This is an a.c. zero crossing controller that keeps the probe enclosure temperature to within a few degrees of the set point.

iii) Analogue meter - This is a direct indication analogue meter with a logarithmic calibration over the range 0.25 - 25%O_2.

iv) Modules - The following modules can be added:

a) Voltage output.

b) Current output non isolated.

c) 4-20 mA isolated.

d) Oxygen alarm.

e) High voltage outputs.

f) Linearizer.

g) Flow alarm.

8.1.3. Performance of the analyser

Laboratory tests on a number of these analysers showed them to meet their stated specifications.

Field trials on gas fired, heavy oil fired and mixed fired boilers have been conducted and have shown the analyser to be of a suitable design and being able to meet its stated specifications in the field also.

8.2. THE SERVOMEX (R) ZIRCONIA WIDE RANGE OXYGEN ANALYSER

This instrument which is still in the prototype stage aims to cover the range 10 ppm to 100% O_2. Although the 1 to 100% O_2 range is adequately covered with the paramagnetic range of instruments, the ability to use the same instrument over such a wide range is extremely attractive and practically very convenient. The instrument however is not suitable for use with any sample containing a combustible gas. The specifications of the instrument are given in Table 13.

A block diagram of the instrument is shown in Fig. 104. The instrument housing is temperature controlled ($50 \pm 0.3^{o}C$). An a.c. zero crossing controller drives a heater and senses the temperature of the box with a thermistor. The temperature gradients in the box are minimised by a mains driven fan. This is necessary because the housing must provide a constant temperature environment for the reference junction side of the sensor's thermocouple; this reduces also the temperature drift in the electronics. The sensor is housed in a separate heat insulated small box fixed to the side of the main

TABLE 13

SPECIFICATIONS OF THE SERVOMEX (R) ZIRCONIA WIDE RANGE OXYGEN ANALYSER

Accuracy

lorarithmic output ± 1% of reading or ± 15 ppm O_2 whichever is greater.

With linearizer add ± 0.5% of reading.

Repeatability

± 0.1% of reading.

Ranges

10 - 100% O_2 , 1 - 10% O_2, 0.1 - 1% O_2

100 - 1000 ppm, 10 - 100 ppm.

Environment

+ 10 to 40°C.

Mains voltage effect

± 1% of reading for 10% voltage variation.

Sample and reference flow rate

200 ml/M ± 25 ml/M.

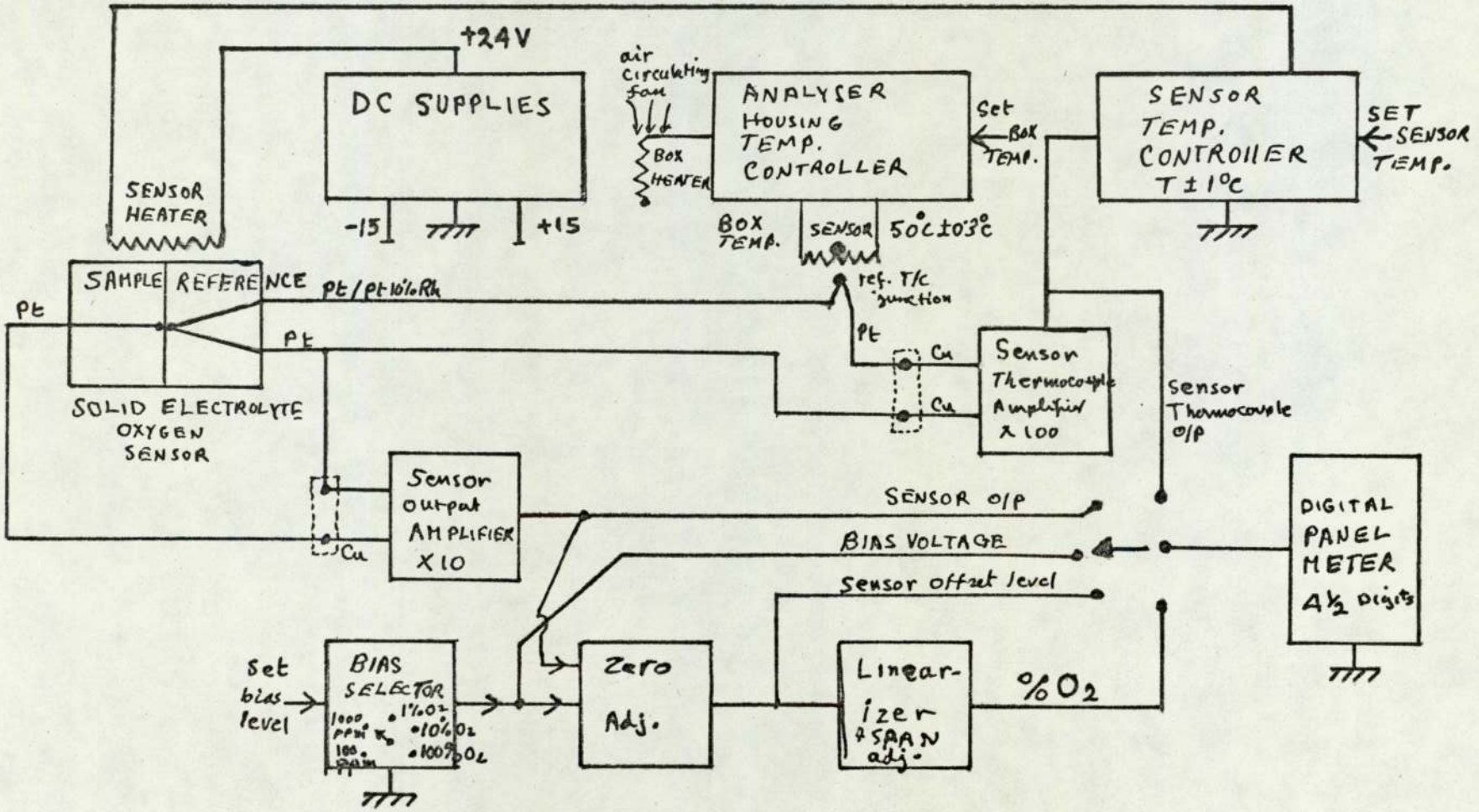

(R)

FIG. 104 BLOCK DIAGRAM OF THE SERVOMEX ZIRCONIA WIDE RANGE OXYGEN ANALYSER

instrument case. The sample and the reference gases are fed through flow regulators.

Two d.c. supply levels, both regulated, are provided. A - 15 - 0 - + 15 volt supply that feeds the amplifiers and linearizer; and a + 24 volt supply for the heater of the sensor.

The temperature of the sensor is controlled by a variable frequency on/off temperature control system. This keeps the sensor within $\pm$ 1°C of the set temperature of 800°C. The temperature of the electrode in the sample chamber of the sensor is measured with a Pt/Pt-10%Rh thermocouple which has its reference junction in the instrument housing. The emf of the thermocouple is amplified by a x 100 high stability amplifier before it is fed to the temperature controller. This output is available for display on the DPM.

The output of the sensor is also amplified by a high stability x 10 amplifier. This output is available for display on the DPM. A digital panel meter with 4½ digits corresponding to 1.9999 volts, and which has an error of less than 0.01% of reading $\pm$ 1 count is used. In order to make the reading of the meter correspond to a % O_2 reading, a bias and a linearizer system is utilized. Five ranges (100% O_2 down to 100 ppm O_2) are made available through a selector switch. The ranges were chosen so that their ratio corresponds to a decade. The expected emf from the sensor for a decade change is 53.23mV. The bias, which is available for display on the DPM, is set so that on the 100% O_2 range no bias is added and the signal from the sensor goes through a summing amplifier which has a zero adjustment that allows the cancellation of the sensor offset emf, this is available for display on the DPM; and a gain adjustment in the linearizer that allows the DPM to read 20.9500 % O_2 when air is present in both sample and reference chambers of the sensor. When the next range is selected (10% O_2) a bias of 532.3 mV is subtracted from the amplified (x 10) output of the sensor, before the signal is

further amplified. Each further range adds another 532.3 mV to the bias. The linearizer is an anti-log module (Analog Devices 755N) that accepts the amplified and biased logarithmic signal and anti-logs it and then allows it to be read by the DPM. The errors introduced by the linearizer are of the order of $\pm$ 0.5%. In this arrangement the input of the linearizer sees only about 1V whichever range is selected, improving thus its specified linearity by restricting its range to nearly one decade instead of the available six.

This prototype analyser has been found to be within its specifications when tested with calibration gases. It requires however further development and optimisation to make it suitable for marketing.

CHAPTER NINE

CONCLUSIONS

A comprehensive and systematic study of the major reported problems faced by the available marketed designs of solid electrolyte sensors (electrolyte cracking, gas leaks, electrode peeling, slowing of response time, errors, field maintenance difficulties etc.) has resulted in the identification of the roots of these problems. This was followed by the evaluation of several alternative solutions for a given problem and the selection of the one that was able to meet the specifications reliably and economically. The outcome of this approach was an evolutionary design that tended towards the simple, straightforward, and hence the elegant solution which seemed to satisfy a number of separate requirements simultaneously. The results discussed in the previous chapters show the sensor to be able to fully meet all the desired specifications set out for it.

The ruggedness and immunity to thermal shock of the sensor has been well demonstrated by its ability to stand successive cycles of heating and cooling, within a few minutes, without any sign of cracks or induced gas leaks. The minimising of thermal gradients between the electrodes has resulted in very small (sometimes only a few microvolts) sensor offset emfs. This was demonstrated practically in the field by the experience of changing sensors in flue gas analysers and finding that the instruments did not require re-calibration. The ability to measure the electrode temperature enables absolute oxygen analysers to be designed whose accuracy is limited by the stability of the temperature regulation and by the measurements of voltage and temperature. The longest continuously operating sensor in the field has been running for about four months to date on a heavy oil boiler installation. Sensor failure in the field has been found to be due to either thermal runnaway due to problems with the temperature control system, or the presence of particulates in

the gas chambers of the sensor.

The simplicity of the design and the ease in which it could be manufactured were demonstrated, when the sensor was put in production, by the speed and ease with which the operators learned to manufacture and test it, and by the 90% of the learning batch (50 sensors) passing the full test and inspection procedures.

The only part that is not yet satisfactory is the effect of electrode ageing on the response time of the sensor. For although the required analysers response times can be adequately met with aged electrodes, the knowledge that a much faster response time is possible; as demonstrated with fresh electrodes, sets the theme and direction for future research effort. Electrode forming techniques, composition and post treatment, are stuiable starting points. Current research work on alternative electrode materials such as cermets for example [370, 383] should be closely followed.

As one of the main causes of Pt electrode ageing is the high operating temperature of the sensor, a substantial lowering of this temperature resulting in the slowing of the ageing process, offers an alternative approach to the problem. Many promising electrolyte systems which are being investigated [310,314,320,321] have been mentioned and it seems that a very large number of possibilities still exist. [384]

The subject of solid electrolyte material is also of interest because the lowering of the operating temperature of the sensor offers a number of advantages related to several other factors. The possibility of using ions other than oxygen which have high conductivities below 500^{o}C and are reactive with oxygen (e.g. Na^{+}) deserves investigating.[316,320]

The versatility of the sensors' design has been demonstrated by the ease with which it was modified and adapted, to have a sealed-in reference, to function as a pump, and to be utilized in feedback systems. Although this versatility is a highly desirable feature, it should not be pushed beyond the limits of its usefulness. An all-

encompassing design is a very rare and improbable event. Careful examination of such products seems to reveal, in most cases an overenthusiastic sales drive. Success is more likely to be achieved by selecting a reasonably sized market and optimising the product so that the right product, at the right price and generating the right profit, emerges at the right time. The cliche: "a camel is a horse designed by a committee" is often quoted. One should reflect on the evidence that shows that for desert transportation, the camel, in its own class, is an optimaly designed product, whose suitability and efficiency have been demonstrated by real experience. Perhaps the committee was not, after all, a design committee, but a marketing one, which in its enthusiasm has tried to market the camel beyond the limits of its original specifications.

The techniques developed, the information collected and the experience gained in fulfilling the work presented in this thesis, can be utilized most effectively in the design of a number of sensors each optimised to suit a major specific requirement, be it cost, accuracy, or shape. The needs of modern industry are varied and many, and it is only by isolating these different requirements and optimising a product to cater for their needs that this market is best served.

APPENDIX I

LIST OF U.S. PATENTS REGISTERED FOR SOLID ELECTROLYTE SENSORS FOR THE MEASUREMENT OF OXYGEN IN MOLTEN METALS

3,297,551	3,309,233	3,359,188
3,378,478	3,403,090	3,464,008
3,468,780	3,481,855	3,578,578
3,616,407	3,619,381	3,630,874
3,642,599	3,645,720	3,657,094
3,661,749	3,711,394	3,718,546
3,723,279	3,713,995	3,723,279
3,752,753	3,755,126	3,758,397
3,764,269	3,772,177	3,776,831
3,784,459	3,785,947	3,791,954
3,809,639	3,817,707	3,864,231
3,864,232	3,869,369	3,904,486
3,935,079	3,980,543	4,007,106
4,035,277	4,046,661	4,067,792
4,105,507	4,139,421	4,141,812

APPENDIX II

LIST OF U.S. PATENTS REGISTERED FOR SOLID ELECTROLYTE

OXYGEN SENSORS

3,216,911	3,347,767	3,400,054
3,404,836	3,442,773	3,442,773
3,454,486	3,503,809	3,514,377
3,546,086	3,576,730	3,597,345
3,598,711	3,607,424	3,616,408
3,616,413	3,645,875	3,650,934
3,654,111	3,658,479	3,691,023
3,720,594	3,767,469	3,784,359
3,819,499	3,819,500	3,821,090
3,837,808	3,859,192	3,860,498
3,865,707	3,869,370	3,871,981
3,883,408	3,907,657	3,914,169
3,915,828	3,915,830	3,928,161
3,923,624	3,935,089	3,963,597
3,973,990	3,974,054	3,981,785
3,989,614	3,996,005	4,005,001
4,040,929	4,043,890	4,045,300
4,045,319	4,080,276	4,085,024
4,088,543	4,098,650	4,101,403
4,101,404	4,107,018	4,107,019
4,115,229	4,128,458	4,134,818
4,150,939	4,151,060	4,158,166
3,948,813	4,126,532	4,127,463
4,129,491	4,131,514	4,170,530

APPENDIX III

LIST OF U.S. PATENTS REGISTERED FOR SOLID ELECTROLYTE OXYGEN IN MOTOR CAR EXHAUST GAS SENSORS

3,616,274	3,738,341	3,745,768
3,768,259	3,786,462	3,835,012
3,841,987	3,844,920	3,891,529
3,909,385	3,915,135	3,940,327
3,941,673	3,948,081	3,960,692
3,960,693	3,962,866	4,019,974
4,021,326	4,033,170	4,038,034
4,040,930	4,049,524	4,055,792
4,057,477	4,063,897	4,065,372
4,076,608	4,094,186	4,096,048
4,096,050	4,097,353	4,098,653
4,105,524	4,111,778	4,116,795
4,116,797	4,119,512	4,119,513
4,159,234	4,127,464	4,128,469
4,123,344	4,132,615	4,136,000
4,141,813	4,145,272	4,152,232
4,152,234	4,155,827	4,140,611
4,155,828	4,157,282	4,157,948

APPENDIX 1V

PREPARATION OF SOLID SOLUTIONS BY THE MIXED POWDER METHOD

The purest material should be used: ZrO_2 ('S' grade from Magnesium Elektron Ltd.). Y_2O_3 (4N grade from Rhone-Poulene Ltd.)

1. Heat powders in Zirconia boats in air to 900°C for about 2 hours. Cool and store in dessicator.

2. Make a mixture to the ratio required by the solid solution (e.g. 8% wt. Y_2O_3 - 92% wt. ZrO_2).

3. Grind mixture dry to about 30 μ size.

4. Use propane - 2 - 01 and mill to about 1 μ size.

5. Dry mixture under I.R. lamp.

6. Heat mixture in air to 1450°C for about 48 hours. Cool down naturally.

7. Grind mixture in propane to 1 μ size.

8. Dry mixture under I.R. lamp and store in dessicator.

APPENDIX V

PREPARATION OF SOLID SOLUTIONS BY THE CO-PRECIPITATION METHOD

The purest material should be used e.g. spectroscopically pure.

An example: The preparation of a Y_2O_3 8 wt. % solution in ZrO_2.

The wt. ratio for this is 11.5 gm. zirconia for one grm. yttria.

This corresponds to a molefraction of about 4.6%.

The relevant chemical equations are:

$$ZrOCl_2 + 2NH_4OH + H_2O \longrightarrow Zr(OH)_4\downarrow + 2NH_4Cl$$

$$Zr(OH)_4 \xrightarrow{\text{heat}} ZrO_2 + 2H_2O\uparrow$$

$$2Y(NO_3)_3 + 6NH_4OH \longrightarrow 2Y(OH)_3\downarrow + 6NH_4NO_3$$

$$2Y(OH)_3 \xrightarrow{\text{heat}} Y_2O_3 + 6H_2O\uparrow$$

From the above:

1 gm. Y_2O_3 is produced from 3.39 gm. $Y(OH)_3$ hence $Y(NO3)_3$.11.5 gm.

$Zr O_2$ is produced from 30.06 gm. $ZrOCl_2$.

1. Weigh 3.39 gm. Yttrium Nitrate ($Y(NO3)_3 - 6H_2O$ 4N pure - Rare Earth Products Ltd.)

2. Weigh 30.06 gm. Zirconium oxychloride ($ZrOCl_2.8H_2O$ spec. pure grade J& M Chem. Ltd.)

3. Put the nitrate in about 100 ml. of distilled water and add the oxychloride adding a further 400 ml. of distilled water.

4. Stir vigorously for about 5M.

5. Add about 10 ml. (under a fume cupboard) ammonia (Analar BDH) whilst stirring vigorously, a white precipitate appears almost immediately.

6. Prepare Buchner funnel. Pour mixture and keep diluting with distilled water. Empty flask and keep adding water - rinse several times - add indicator during the third time to see if ammonia is present.

7. Stir the precipitate, and leave in air oven at about 120°C to dry for 48 hours.

8. Heat powder in air at 900°C for 4 hours. Cool and store in dessicator.

APPENDIX VI

PRESSING, MACHINING AND FIRING PROCEDURE

1. Clean the die using a traceless solvent and assemble it.

2. Wet all surfaces that will come into contact with the powder with release agent.

3. Fill die with the appropriate amount of powder and push top plug as far as it can go.

4. Place die under press, operate press to 8,000 psi and then repeat to 15,000 psi.

5. Carefully disassemble thedie and remove the ceramic bar.

6. Bring length of bar to desired size by passing over wet and dry paper.

7. Heat bars at 1000^{o}C for 1 hour. Leave to cool naturally.

8. Using flat drill, drill bar at one side and then directly opposite to required depth.

9. Place bar in covered zirconia boat and heat 1 hour at 1200^{o}C, allow to cool naturally.

10. Trim size if necessary.

11. Fire for 2 hours at 2000^{o}C taking it up at about 125^{o}C/hour. Allow to cool naturally.

BIBILOGRAPHY

1. Physics of Electrolytes (1) & (2)
   Haldik J Editor - Academic Press.

2. Measurement of Oxygen.
   Degn H el al Editors - Elsevier Sci. Pub. Co.

3. Solid State Reactions.
   Schmalzried H - Academic Press. Inc.

4. Introduction to Ceramics.
   Kingrey W D et al
   J. Wiley and Sons.

5. Solid State Chemistry of Energy Conversion and Storage.
   Goodenough J B and Whittingham M S
   Advances in Chemistry Series 163.

6. Treatise on Materials Science and Technology.
   Vol. 9 Ceramic Fabrication Processes.
   Edit. Wang F F Y
   Pub. Academic Press.

7. Ceramic Fabrication Processes.
   Edit. Kingery W D
   Pub. Tech. Press and J. Wiley and Sons.

8. Glass-to-Metal Seals
   by Partridge J H
   Pub. The Soc. of Glass Tech.

REFERENCES

1 . Kocache R and Tipping F
Oxygen Analyzers 6-118 & 6-129
Process Inst. and Control Handbook Considine, Editor McGraw Hill
Tipping F
paper presented at Process Anal. Inst.U. of Warwick (March 1974)

2 . Cunningham D J C et al
J.physiol. 169, 77 (1963)
Ellis F R and Nunn J F
Brit. J Anaesth. 40, 569 (1968)
Evans J M et al
Archives of Disease in Childhood 53, 330 (1978)
Lister G et al
Pediatrics 53 - 55, 656 (1974)

3 . Fixler D E et al
Circulation 50, 788 (1974)
Hamilton A G
Laboratory practice, 807 (Nov.1972)
Charsley E L and Schulz R A
J. of physics E 8, 147 (1975)

4 . Tipping F
Chem. & process Eng. (Oct.1968)
Tipping F
Tanker and Bulk Carrier (Aug.1968)
Snow D L
pollution control (March.1971)

5 . Shephard R J
Inst. Z.angew. Physiol. ein schl.Arbeit.physiol. 22, 279 (1966)

6 . D R P no. 104,872 (1897)

7 . Nernst W
Z. Elektrochem. 6, 41 (1900)
Nernst W & Wild W
Z. Elektrochem. 7, 373 (1900)

8 . Van't Hoff J H
Z.f Phys. Chem. 5, 322 (1890)

9 . Fritsch C
Wiedemanns Ann. 60, 300 (1897)

10 . Nernst W
Phys. Chem. 4, 117 (1889)

11 . Duane W
Ann. d.Phys.u.Chem. 65, 374 (1898)

12 . Reynolds H B
Dissertation, Gottingen (1902)

13 . Haber F und St Tolloczko
Z. anorg. Chem. 41, 407 (1904)

14 . Haber F und Moser A
Z. Elektrochem. 11, 593 (1905)

15 . Haber F und Fleischmann F
Z. anorg. Chem. 51, 245 (1906)

16 . Haber F
Z.f.Elektrochem. 12, 415 (1906)

17 . Haber F et al
Z. anorg. Chem. 51, 289 (1906)

18 . Haber F
Z. anorg. Chem. 51, 356 (1906)

19 . Katayama M
Z. Phys.Chem. 61, 566 (1908)

20 . de Boer J H
Zirconium, "Foote - Prints", 3(2), 3(1931)
21 . Ruff O und Lauschke G
Z.anorg. Chem. 87, 198 (1914)
22 . Ruff O und Lauschke G
Z.anorg. Chem. 97, 73 (1916)
23 . Ruff O and Moczalla J
Z. anorg. u. allg.Chem. 133, 193 (1924)
24 . Bohm J
Z. anorg. u. allg.Chem. 149, 217 (1925)
25 . Davey W P
Phys. Rev. 23, 763 (1924)
Phys. Rev. 27, 798 (1926)
26 . Goldschmidt V M
Geoch. Vert. Ges. 6-8. Oslo (1926-27)
27 . Ruff O und Ebert F
Z.anorg. u.allg. Chem. 180, 19 (1929)
28 . Ruff O et al
Z. anorg. u.allg. Chem. 180, 215 (1929)
29 . Ruff O et al
Z.anorg. u.allg.Chem. 180, 252 (1929)
30 . Ruff O et al
Z.anorg. u.allg.Chem. 185, 221 (1929)
31 . Ruff O et al
Z. anorg. u.allg.Chem. 196(3)335(1931)
32 . Ruff O et al
Z. anorg. u.allg.Chem. 207(3)308(1932)
33 . Ruff O et al
Z. anorg. u.allg.Chem. 213,333 (1933)
34 . Cohn W M und Tolksdorf S
Z.Phys.Chem. B8, 331 (1930)
35 . Ebbert F und Cohn E
Z. anorg.u. allg.Chem. 213,321 (1933)
36 . Clarck G L and Reynolds D H
Ind.Eng.Chem. 29(6)711(1937)
37 . Tingwaldt C
Phys. Z.36, 627(1935)
38 . Tingwaldt C und Ebert F
Phys. Z. 37, 471 (1936)
39 . Ketelaar J A A und Willems P J A
Rec.Trav.Chim. . Pays - Bas et Belg.(Amsterd.)
56, 29 (1937)
40 . Bussem W et al
Ber. Dtsch. Keram. Ges 18, 433 (1937)
41 . Ryschkewitsch E
Chem. App. 24, 137 (1937)
42 . Von Wartenberg H und Eckhardt K
Z. anorg. u.allg. Chem. 232, 179 (1937)
43 . Thiel - Joh
Phys. Z. 26, 321 (1925)
44 . Joffes A
Ann.d.Phys. 72, 461 (1923)
45 . Frenkel J
Z. Phys. 35, 652 (1926)
46 . Reinhold H -
Z. anorg.u.allg.Chem. 171, 181 (1928)
47 . Wagner C
Z. Phys.Chem. 11B, 139 (1930)
48 . Wagner C & Schottky W
Z.Phys.Chem.11B, 163(1930)

49 . Wagner C
Z.Phys.Chem (Leipzig) B21, 25 (1933)
50 . Schottky W
Wiss Veröff. Siemens werke 14 (H.2)1(1935)
51 . Wagner C
Z.Phys.Chem. B21, 42 (1933)
52 . Reinhold H
Z. Electrochem. 40, 361 (1934)
53 . Wagner C
Z. Electrochem. 40, 364 (1934)
54 . Jost W
Z.f. Phys.Chem. B16, 129 (1932)
55 . Jost W
J.Chem.Phys. 1, 466 (1933)
56 . Jost W.
Z.Phys. Chem. A169, 129 (1934)
57 . Schottky W
Z. Phys. Chem. B29, 335 (1935)
58 . Jost W & Nehlep G
Z.Phys.Chem. B32, 1(1936)
59 . Koch E and Wagner C
Z.Phys.Chem. B38, 295 (1937)
60 . Zintl E and Udgard A
Z. anorg.u. allg.Chem. 240, 150(1939)
61 . Zintl E and Croatto V
Z.anorg.u.allg. Chem. 242, 79(1939)
62 . Zintl E and Udgard A
Z.anorg.u.allg.Chem. 240, 150(1940)
63 . Sillen L G and Aurivillius B
Z. Kris. 101, 483 (1939)
64 . Sillen L G and Sillen B
Z.Phys.Chem. B49, 27(1941)
65 . Rogner H
Z. Elektrochem. ang.Phys.Chem. 46, (1) 25(1940)
66 . Wagner C
Naturwissenschaften 31,265(1943)
67 . Bauer F and Preis H
Z. Elektrochem. 43, 727(1937)
68 . Bauer E
Brennstoff. Chem. 20, 385 (1939)
69 . Geller R F and Yavorsky P J
J. Res.Nat.Bur.Standards 35(1) 87(1945)
70 . Curtis C E
J Am.Ceramic Soc. 30(6) 180 (1947)
71 . Croatto U and Bruno C
Ricerca Sci. 17, 1998 (1947)
72 . Croatto U and Bruno C
Gazz.Chim. Ital. 78, 881 (1948)
73 . Croatto U and Bruno C
Gazz. Chim. Ital. 79, 379 (1949)
74 . Hund F and Fricke R
Naturwiss. 37, 424 (1950)
75 . Hund F und Durrwachter W
Z.anorg.u.allg.Chem. 265, 67 (1951)
76 . Hund F
Z. Elektrochem. 55, 363 (1951)
77 . Hund F
Z. anorg.Chem. 265, 62 (1951)
78 . Hund F u. Mezger F
Z. Phys.Chem. 201, 268 (1952)

79 . Hund F
Z. Phys. Chem. 199, 142 (1952)
80 . Hund F
Z. Anorg. Chem. 274,105 (1953)
81 . Verwey E J W et al,
Philips Res. Rep. 5, 173 (1950)
82 . Jaffe G
Phys. Rev. 85, 354 (1952)
83 . Avgustinik A I and Antselevich N S
Zh. Fiz. Khim. 27, 973 (1953)
84 . Charlesby A
Acta Met. 1, 340 (1953)
85 . Trombe F and Foek M
Compt. rend. 236, 1783 (1953)
86 . Weininger J L and Zeimany P D
J.Chem. Phys. 22, 1469 (1954)
87 . Duwez P and Odell F
J. Am. Ceram. Soc. 33,(9) 274(1950)
88 . Duwez P et al
J. Electrochem. Soc. 98, 356 (1951)
89 . Duwez P et al
J. Am.Ceram.Soc. 35, 107 (1952)
90 . Trombe F et al
C.R.Acad.Sci. 233, 172 (1951)
91 . St Pierre P D S
Trans.Brit.Ceram.Soc. 51, 260 (1952)
92 . Lambertson W A and Mueller M H
J.Am. Ceram.Soc. 36, 365 (1953)
93 . Dietzel A and Tober H
Ber. Deut. Keram. Ges. 30, (3) 47(1953)
94 . Schusterius C and Padurow N
Ber. Deut. Keram. Ges.30, 235 (1953)
95 . Brown F H and Duwez P
J. Am.Ceram.Soc. 37, 129 (1954)
96 . Coughanour L W et al
J.Res.Nat.B.Stan. 52, 37 (1954)
97 . Roth R S and Coughanour L W
J. Res.Nat.Bur.Stand. 55, 209 (1955)
98 . Wallaeys R et Chaudron G
Colleq. Nat. sur la Chim. des Hautestemp. Paris, 155 (1954)
99 . Keler E K & Godina N A
Dokl. Akad. Nauk SSSR. 103,247 (1955)
100. Rabenau A
Z. Anorg. allg.Chem. 288, 221 (1956)
101. Wittels M and Sherril F
J. Appl. Phys. 27, 643 (1956)
102. Roth R S
J. Am. Ceram. Soc. 39, 196 (1956)
103. Weber et al
J. Am. Ceram. Soc. 39, 197 (1956)
104. Duwez P and LOH E
J. Am. Ceram. Soc. 40, 321 (1957)
105. Keler E K & Andreeva A B
Ogneapory 22, 65 (1957)
106. Fischer W A & Hoffmann A
Arch. Eisenhuttenwes. 28, 739 (1957)
107. Stocker J & Collongues R
C. R. Acad. Sci. 244, 83 (1957)
108. Stocker J & Collongues R
C. R. Acad. Sci. 245, 431 (1957)

109. Stocker J & Collongues R
C.R.Acad. Sci. 245, 695 (1957)
110. Stocker J et al
Coll.Nat. sur la Chim. des Haut.Temp. Paris, 39 (1957)
111. Collongues R Stocker J & Moser M
Coll. Nat. sur la Chim. des Haut. Temp. Paris 23 (1957)
112. Stocker J et al
Silicates Ind. 23, 67 (1958)
113. Stocker et al
C. R. Acad. Sci. 246, 1698 (1958)
114. Collongues R & Stocker J
C.R.Acad. Sci. 246, 3641 (1958)
115. Marglulis O M & Glul'Ko N V
Dokl. Akad. Navk. SSSR, 121, 523 (1958)
116. Sanbongi K & Ohtani M
Res. Inst. of Min. Dress. & Metal. 204 (1956)
117. Aronson S & Belle J
J. Chem. Phys. 29, 151 (1958)
118. Kiukkola K & Wagner C
J. Electrochem. Soc. 104, 379 (1957)
119. Peters H. & Mobius H H
Z. Phys. Chem. (Leipzig) 209, 298 (1958)
120. Peters H & Mobius H H
Naturwissenschaften 45, 309 (1958)
121. Peters H & Mann G
Z. Elecktrochem. 63, 244 (1959)
122. Mobius H H
Mitteilungsblatt d. Chem. Geselschaft D D R
6, 45 (1959)
123. Mobius H H
Mber, Dtsch. Akad. Wiss. Berlin 1, 34 (1959)
124. Mobius H H
DDR Patent 22030. Oct. (1961)
Peters H and Mobius H H
DDR Patent 21673 Aug. (1961)
Mobius H H
DDR Patent 48083 May (1966)
125. Cocco A
Chim. Ind. (Milan) 41, 882 (1959)
126. Keler E K & Nikitin E N
J. Appl. Chem (USSR) 32,(9), 2033 (1959)
127. Kingery et al
J. Amer. Ceram. Soc. 42, 393 (1959)
128. Noddack et al
Z. Phys. Chem. (Leipzig) 211, 180 (1959)
129. Stocker J
Ann. Chim. (Paris) 5, 1459 (1960)
130. Pal'Guef SF and Volchenkova Z S
Zhurnal fiz. Khimi. 34, 452 (1960)
131. Volchenkova Z S and Pal'guev S F
Trans. (Trudy) Inst. of Electrochem. (1) 97 (1961)
Translation by Consultants Bureau N.Y. 1961
132. Pal'guev S F and Neuimin A D
Trans. (Trudy) Inst. of Electrochem (1) 90(1961)
Translation by Consultants Bureau NY 1961
133. Collongues R et al
Bull. Soc. Chim. (France) 70(1961)
134. Lefevre J et al
C. R. Acad. Sci. (Paris) 253, 1334 (1961)

135. Stocker J
Bull. Soc. Chim. Fr. 78 (1961)
136. Weissbart J and Ruka R
Rev. Sci. Inst. 32, (5) 593 (1961)
137. Weissbart J and Ruka R
J. of Electrochem. Soc. 109, 723 (1962)
138. Weber B C
J. Am. Ceram. Soc. 45, 614 (1962)
139. Smith D K and Cline C F
J. Am. Ceram. Soc. 45, 249 (1962)
140. Perez Y Jorba M
Ann. Chim. 7, 479 (1962)
141. Buckley J D
NASA Tech. Note, D-1595 (1962)
142. Schmalzried H
Z. Elektrochem. 66, 572 (1962)
143. Aleshin E and Roy R
J. Am. Ceram. Soc. 45, 18 (1962)
144. Lefevre J
Ann. Chim. (Paris) 8, 177 (1963)
145. Buckley J D and Wilson HH
J. Am Ceram. Soc. 46, 510 (1963)
146. Smoot T W and King D F
IEEE Trans. Aerosp. AS-1, 1192 (1963)
147. Alcock C B and Steele B C H
Proc. 2nd Cmf. (BCS) and (NKV)
2 (26) 397 (13-17 May 1963)
Trans. AIME, 233, 1359 (1965)
148. Smoot T W and Whittemore D S
J. Am. Ceram. Soc. 48, 163 (1965)
149. Delamarre C and Perez Y Jorba M
Rev. Hautes Temp. Refract. 2, 313 (1965)
C.R. Acad. Sci. Paris 261, 5128 (1965)
150. Barbariol I
Ann. Chim (Rome) 55, 321 (1965)
151. Deportes C et al
Rev. Hautes Temp. Refract. 2, 159 (1965)
152. Mazdiyasni K S et al
J. Am. Ceram. Soc. 48, 372 (1965)
J. Am. Ceram. Soc. 5, 342 (1966)
153. Mazdiyasni K S et al
J. Am. Ceram. Soc. 50, 532 (1967)
154. Bartuska M
Silikattechnick, 17, 79 (1966)
155. Baker R and West J M
J.I. and S Inst. 204, 212 (1966)
156. Noguchi T et al
Solar Energy 11, 145 (1967)
157. Bessonov A F and Taksis G A
Russ J. Phys. Chem. 41, 974 (1967)
158. Demonis I M and Popil'skii R Y
Chem. Abst. 68, 116936 (1968)
159. Forestier M et al
Nat. Res. Bull 4, 727 (1969)
160. Duclot M et al
J. of solid state Chem. 2, 4883 (1970)
161. Michel D et al
C.R. Acad. Sci. Puis, 266, 1602 (1968)
162. Gravie R C
J. Am. Ceram. Soc. 51, 553 (1968)

163. Baukal W and Scheidegger R
Ber. Deut. Keram. Ges 45, 610 (1968)
164. Kohler E K and Gulshkova V B
Sc. of Ceram.4, 233 (1968)
165. Spitsbergen U and Houpt P M
Sc. of Ceram. 4, 247 (1968)
166. White D W
G E Report No. 68-G-254 (July 1968)
167. Jaffe G and Rider JA
J. Chem. Phys. 20, 1077 (1952)
Chang H and Jaffe G
J. Chem. Phys. 20, 1071 (1952)
168. MacDonald J R
Phys. Rev. 92, 4(1953)
169. Friauf R J
J. Chem. Phys. 22, 1329 (1954)
170. Danforth W E and Bodine J W
J. Frank Inst. 260, 467 (1955)
Danforth W E
J. Frank Inst. 266, 483 (1958)
171. Hoffmann A and Fischer W
Z. Phys. Chem. 35, 95 (1962)
172. Tien T Y & Subbarao E C
J. Chem. Phys. 39, 1041 (1963)
173. Cocco A and Barbariol I
NOTA I and II. Inst.Di.Chim.Appl. N14 and 15 (1963)
174. Vest R W
ARL report 63-116 (July 1963)
175. Dixon J et al
J. Electrochem. Soc. 110, 276 (1963)
176. Schmalzried H
Z. Physik. Chem. (Frankfurt) 38, 87 (1963)
177. Johansen H A and Cleary J G
J. Electrochem. Soc. 111, 100 (1964)
178. Tien T Y
J. Am. Ceram. Soc. 47, 430 (1964)
179. Tien T Y
J. Appl. Phys. 35, 122 (1964)
180. Strickler D W and Carlson W G
J. Am. Ceram. Soc. 47, 122 (1964)
181. Vest R W et al
J. Am. Ceram. Soc 47, 635 (1964)
182. Bray D T and Merten U
J. Electrochem. Soc. III 447 (1964)
183. Simpson L A and Carter R E
J. Am. Ceram. Soc. 49, (3) 139 (March 1966)
184. Rhodes W H and Carter R E
J. Am. Ceram.Soc. 49 (5) 244 (May 1966)
185. Takahashi T and Iwaharah H
Denki Kagahu 34, 254 (1966)
186. Lasker M F and Rapp R A
Z.fur Physik. Chem. N.F. 49, 198 (1966)
187. Hartung R and Moebius H H
Z. Chem. 7, 325 (1967)
188. Peters H and Radeke K H
Monatsbu. Deut. Akal. Wiss. Berlin 10, 819 (1968)
189. Patterson J W et al
J. Electrochem. Soc. S.S.S.114 (7) 752 (July 1967)
190. Steele B C H et al
Proc. B. Ceram. Soc. (10), 87 (March 1968)

191. Robert G et al
J. Chim.Phys. 64 (9), 1275 (1967)
192. Carter R E and Roth W L
Proc.Sym. N.R.G.I.C. London, 125 (13-14 April 1967)
193. Alcock C B
Proc.Sym. N.R.G. I.C. London, 109 (13-14 April 1967)
194. Duclot M and Deportes Ch
J. of Th. Anal. 1, 329 (1969)
195. Solov'eva L M et al
Akad. Nauk SSSR Trans.Inst. Electrochem. (13), 71(1969)
196. Etsell T H and Flengas S N
Chem. Rev. 70(3), 339 (1970)
197. Hammou A et al
Mat.Res.Bull 6, 823 (1971)
198. Iqbal M and Baker E H
Proc. B. Ceram.Soc. (19) 279 (March 1971)
199. Steele B C H and Floyd J M
Proc. B. Ceram.Soc. (19) 55 (March 1971)
200. Heyne L and Beekmans N M
Proc. B. Ceram.Soc. (19) 229 (March 1971)
201. Bauerle J E
J. Phys.Chem. Solids 30, 2657 (1969)
202. Etsell T H and Flengas S N
J. Electrochem. Soc. 119, 1 (1972)
203. Schouler E et al
J. Chim. Phys. 70, (6) 923 (1973)
204. Schouler E et al
J. Chim. Phys. 70 (9) 1309 (1973)
205. Schouler E and Kleitz M
J. Electroanal. Chem. 64, 135 (1975)
206. Schouler E et al
Mat.Res. Bull. 11, 1137 (1976)
207. Beekmans N M and Heyne L
Electrochim Acta 21, 303 (1976)
208. Foultier J and Kleitz M
J. Electrochem. Soc. 125, 751 (1973)
209. Mobius H H
Z. Chem. 2, 100 (1962)
210. Mobius H H
Z. Chem.3, 81 (1964)
211. Mobius H H and Rohland B
Z. Chem. 6, 158 (1966)
212. Rose B A et al
Disc. Farad. Soc. 4, 154 (1948)
213. Carter R E
J. Am. Ceram. Soc. 43, 448 (1960)
214. Schmalzried H
Z. Phys. Chem. 25, 178 (1960)
215. Benz R and Schmalzried H
Z. Phys. Chem.29, 77 (1961)
216. Horsley G W
UKAEA, AERA, R3427 (Jan. 1961)
217. Gerasimov T et al
Doklady Akad. Nank. SSR 136, 1372 (1961)
218. Rapp R A and Maak F
Acta. Met. 10, 63 (1962)
219. Kiukkola K
Acta Chem. Scand. 16, 327, (1962)
220. Hock M et al
J. Phys. Chem. Solids 23, 1463 (1962)

221. Rapp R A
Trans. AIME. 227, 371 (1963)
222. Blumenthal R N and Whitmore D H
J. Electrochem. Soc. 110, 92 (1963)
223. Tretjakow J D and Schmalzried H
Berichte der Bunsen Geselschaft 69 (5) 396 (1965)
224. Zador S
Proc. symp. NRG, I.C. (London) 145.(13-14 April 1967)
225. Kubik A and Alcock C B
Proc. Symp. NRG, I.C.(London) 43 (13-14 April 1967)
226. Rickett H and Steiner R
Z. Phys. Chem. 49, 127 (1966)
227. Alcock C B and Belford T N
Trans. Faraday Soc. 60, 822 (1964)
228. Pluschkell W and Engell H J
Z. Metal Kunde, 56 (7) 450 (1965)
229. Fischer W A and Ackermann W
Archiv Eisenhuttenmessen 36 (9) 643 (1965)
230. Osterwald J
Z. Phys. Chem. 49, 138 (1966)
231. Jeffes J H E and Sirdhar R
Proc. symp NRG, I.C.(London), 199 (13-14 April 1967)
232. Diaz C M and Richardson F D
Proc. symp. NRG, I.C.(London), 29 (13-14 April 1967)
233. Kolodney M et al
Electrochem. Tech. 3, (9) 244 (1965)
234. Pluschkell W and Engell H J
Z. Metallkde. 56 (7) 450 (1965)
235 Wilder T C
Trans. AIME 236, 1035 (1966)
236. Steele B C H
Proc. Symp. NRG, I.C.(London) 3 (13-14 April 1967)
237. Littlewood R
Steel Times 423 (Sept. 25.1964)
238. Spacil H S
G.E. IIS Report 67-C-449 (Dec.1967)
239. Ullmann H et al
Z. Phys. Chem. (Leipzig) 237, 337 (1968)
240. Lawrence S J et al
Automatica 5, 633 (1969)
241. Record R G H
Cont. and Inst. 31 (Feb. 1971)
242. Cooke M J et al
J. Inst. of fuel 153 (March 1972)
243. Brown J T et al
The Glass Indust. 12 (July 1976)
244. Fairbank L H
Heat Treatment of Metals 4, 95 (1977)
245. Zechnall R and Baumann G
Motor techn. 34 (1) 7 (1973)
246. Lindsay W T and Ruka R J
Electrochem. Acta. 13, 1867 (1968)
247. Rickert D H
Proc. Symp. NRG, I.C.(London), 59 (13-14 April 1967)
248. Roberts L E J
Science of Ceramics. 4, 329 (1968)
249. Casselton R E W and Watson M D S
Science of Ceramics 4, 349 (1968)
250. Butzelaar P F and Hoogeveen L P J
Philips. Tech. Res. 34, (5,6) 123 (1974)

251. Voorn G and Marlow J S
Effl. and Water Treatment J. 301 (June 1977)
252. Williams R J
NASA Tech. Briefs. 580 (Winter 1976)
253. Gauthier M et al
J. Electrochem Soc. Solid State Sci. and Tech.
124 (10) 1579-1584 (Oct. 1977)
254. LeBrusq H et al
Bull. Soc. Chim. France 5th series (12) 3913 (1966)
255. Mogab G J
Rev. Sci. Inst. 43 (11) 1605 (1972)
256. Agrawal Y K et al
J. Electrochem. Soc. 121, 354 (1974)
257. Foultier J and Kleitz M
Vacuum 25 (7) 195 (1975)
258. Hickam W M and Zamaria J F
Inst. and Cont. Sys. 40, 87 (Aug. 1967)
259. Wolber W G
Inst. Techn. 47 (Aug. 1978)
260. Ludvigsen K
Motor Week 42 (15th Jan. 1977)
261. Fitterer GR
Inst. in the Iron and Steel Ind. 20, 48 (1970)
262. Faurschou D K and Pope J C
Dept. EMR, Int. Report P M-1-69-11 (Dec.1969)
263. Fairbank L H and Palethorpe L G W
ISI Spec. Rep. 95 (1966)
264. Fairbank L H
Metallurgia 179 (May 1969)
265. Sayles D A and Gotter Jr JL
Inst.in the Iron and Steel Ind. (ISA) 20, 57 (1970)
266. Spacil H S and Schroeder D L
G E Report D F 68MI-61
267. Record R G H
ATM.MONIT with the O2 probe
Inst. Practice (March 1970)
268. Rudd D A
Solid Electrolyte O2 probe in Heat Treatment Furnaces
Iron and Steel (Oct. 1971)
269. Hoskins J W et al
Conf. on glass problems OSU (Nov.11 1976)
270. Pocock P C et al
Poll.Cont. Ass. Boston Mass. (15-19 June 1975)
271. Cooper H B H et al
Inst. Techn. 39 (March 1976)
272. McRanie R D
ISA, AC, 717, 1 (1973)
273. St. John D D
Control and Inst. (57) 24 (July 1973)
274. Anson D et al
J. Inst. of fuel 191, 191 (April 1971)
275. Davies R M and Oeppen B
J. Inst. of Fuel, 383 (July 1972)
276. Hurlbert A W
Inst. Techn. 57 (March 1978)
277. Monroe E S
Combustion, 30 (Sept. 1972)
278. May D L
Cutting Boiler full costs with Combusion Control
Chem. Eng. (22 Dec. 1975)

279. O'Mera Jr. J E
In. Techn. 47 (March 1979)
280. Hendler H E
70th Ann. Meeting of AICE (Houston Texas)
Sernon 3a (March 1975)
281. Taylor Inst. Ltd. Application notes
PIL 057 (Sept 1970)
ADS-8A101; ADS-8A110; ADS-8A151
Analytics 7986-0150
282. Farmer R
Kent Tech. Rev. (23) 7 (Nov.1978)
283. Bates R E and Littlewood R
BISRA Report SM/C/89/63
284. Wiacek B J
ISA ML 736552, 9 (1973)
285. Sayles D A and Caffman J
ISA IPP 746205, 25 (1974)
286. Maier H J
ISA AID 74422, 111 (1974)
287. Sayles D A et al
23rd Nat.Symp. Anal.Inst.Div. ISA.
Charleston W.Virginia (17 May 1977)
288. Pizzini S and Bianchi G
La Chimica e L'industria 54 (3) 224 (1972)
289. Moebius H H
Thesis Greifswald (1958)
290. Barker W W and Knop O
Proc. Brit. Ceram. Soc.no. 19, 15 (March 1971)
291. Wagner C
Adv. In Electrochem. and Electrochem. Eng. 4, 1 (1965)
292. Ure R W
J. Chem. Phys. 26, 1363 (1957)
293. Hartung R
Z. Phys. Chem. Leipzig 254, 5/6, 393 (1973)
294. Gotto K et al
Trans. Met. Soc. AIME, 245, 1662 (1969)
295. Gotto K and Puschkell W
Oxygen concentration cells 2, 539 (1972)
Physics of Electrolytes Edit. Hladik J pub. Academic Press.
296. Kleitz M et al
Electrode Processes in Solid State Ionics P. 1-17.
Proc. of Nato Adv. Study Inst. Corsica (1975)
Edit. Kleitz M and Dupuy J. Pub. Reidl.
297. Ruka R J et al
J. Electrochem. Soc. 115, 497 (1968)
298. Fouletier J et al
J. App. Electrochem. 4 (2), 305 (1974)
299. Brook R J et al
J. Electrochem. Soc. 118, 185 (1971)
300. Fouletier J et al
J. Electrochem. Soc. 123(2),204 (1976)
301. Vedel J
Electrode Proc. in Solid State Ionics pp(223-259)
Proc. of Nato Adv. Study Inst. Corsica (Aug. 1975)
Pub. Reidel, Edit. Kleitz M and Dupuy J.
302. Heyne L
Fastion Transport in Solids pp (123-139) Proc. Nato A.S. Inst. (Sept.72)
Pub. North Hollands Pub. Co. Edit. Van Gool W.
303. Pizzini S
ibid pp (461-476)

304. Fischer W A
ibid pp (503-512)
305. Kleitz M et al
C.R. des Journee s d'Etu de des Piles a Combustibles
354 (June 1967) Bruxelles.
306. Pizzini S et al
Z. Naturforsch. 25a, 559 (1970)
307. Fabray P et al
J. Solid State Chem. 5, 1 (1972)
J. Solid State Chem. 6, 230 (1973)
308. Takahashi T et al
J. Appl. Electrochem 2, 97 (1972)
309. Takahashi T and Iwahara H
J. Appl. Electrochem. 3, 65 (1973)
310. Takahashi T et al
J. Appl. Electrochem. 5, 197 (1975)
311. Takahashi T et al.
J.S.S. Chem. 16, 317 (1976)
312. Takahashi T et al
J. Appl. Electrochem. 7, 31 (1977)
313. Takahashi T et al
J. Appl. Electrochem. 7, 229 (1977) and 303-308.
314. Verkerk M J et al
J. Appl. Electrochem 10, 81 (1980)
315. Anderson H T and Wuensch B J
J. Am. Ceram. Soc. 56, (5) 285 (May 1973)
316. Yuan D and Kroger F A
J. Electrochem. Soc. 118, 841 (1971)
317. Park K and Logothetis E M
J. Electrochem. Soc. S.S. Sci and Tech.
124, (9) 1443 (1977)
318. Fishcer W A et al
Arch. Eisenhutten Wes. 47 (9) 525 (1976)
319. Wilhelm R V and Howarth D S
Gen. Motors R.Lab. Report GMR-2521 Sept. 19 (1977)
320. Lundsgaard J S and Brook R J
Measurement of Oxygen P. 159-167.
Elsevier Sc. Pub. Co.
321. Dirstine R T et al
Am. Ceram. Soc. Bull. 58, (8) 778 (1979)
322. Steele B C H
Elec. Process in Solid State Ionics pp 367-386.
Proc. of Nato Adv. Study Inst. Corsica (Aug. 1975)
Pub. Reidel, Edit. Kleitz M and Dupuy J.
323. Etsell T H et al
Electrochem. Oxygen Sensors - Analysis and modifications.
Electrochem. Soc. Meeting Toronto 19-16 May (1965).
324. Gravie R C and Nicholson P S
J. Am. Ceram. Soc. 55 (3) 152 (1972)
325. Green D J et al
J. Am. Ceram. Soc. 56, 619 (1973)
J. Am. Ceram. Soc. 57 (3) 136 (1974)
326. El-Shiekh A and Nicholson P S
J. Am. Ceram. Soc. 57 (1) 19 (1974)
327. Woodhead J L
Sc. of Ceram. 4, 105 (1968)
328. Thompson M A et al
J. Am. Ceram. Soc. 56 (12) 648 (1973)
329. Heyne L
Measurement of Oxygen p. 65.
Proc. symp. odense Univ. Denmark (26-27 Sept. 1974) Pub. Elsevier

330. Baukal W
Electrochem. Acta 14, 107 (1969)
331. Moulson A J and Popper P
Proc. Br. Ceram. Soc. no. (10) 41 (March 1968)
332. Freeman C H C and Moore P J
J. Phys. E. 11, 980 (1978)
333. Braunshtein D and Tannhauser D S
J. Phys. E 12, 921 (1979)
334. Vionov M
Electrode Proc. in S.S. ionics p(431-466)
Proc. Nato Adv. Study Inst. Corsica (Aug. 1975)
Edit. Kleitz M and Dupuy J. Pub. Reidel.
335. Tedmon C S et al
Abst. 355 Electrochem. Soc. Fall Meeting.
Montreal P Q Canada (6-11-1968)
336. Hopper R T
Ceram. Ind. 65 (June 1963)
337. Rapson W S
Gold Bull 12 (3) 108 (1979)
338. Wise E M and Eash J T
Trans. Am. Inst.of Min. & Metal Eng. 117, 313 (1935)
339. De Bruin H J et al
J. Mat. Sci. 7 (8) 909 (1972)
340. De Bruin H J
Nature 272, 712 (20.4.1978)
341. Issacs H S et al
Solid Electrolytes for fuel cells.
Symp. on Electrode Materials & Proces. 77-6, 584 (1977)
342. Raleigh D O
Electrode Proc. in S.S. ionics.
Proc. of Nato Adv. Study Inst. p(119-147) Corsica (Aug. 1975)
Pub. Reidel, Edit. Kleitz M and Dupuy J
343. Armstrong R D
ibid p(261-275)
344. Wagner Jr. J B
ibid p(489-502)
345. Kleitz M et al
ibid p(439-451)
346. Henisch H K
ibid p(309-329)
347. Wagner Jr. J B
ibid p(185-222)
348. Karpachev S V and Ouchimnkov Yu M
Sov. Electrochem. 5, 181 (1969)
349. Armstrong D
Electro anal Chem. & Interfacial Electrochem. 52, 413 (1974)
350. Sandler Y L & Durigon D P
J. Phys. Chem. 72, 1051 (1968)
351. Gland J
The Atomic Arrangement Tech. Rev. P20 (Feb. 1980)
352. Mayell J S & Langer S H
J. Electrochem. Soc. 111, (4) 438 (April 1964)
353. Weissman E Y
J. Electrochem. Soc. 114, (7) 658 (July 1967)
354. Fabry P & Kleitz M
Electro anal. Chem. & Interfacial Electrochem. 57, 165 (1974)
355. Darling A S et al
Plat. Met. Rev. 14 (2) 54 (1970)

356. Brook R J & Markin T L
Fast ion Trans. in Solids. Proc. Nato Adv. Study Inst. pp (533-541)
Sept. 1972 Pub. North Holland, Edit. Van Gool W
357. Grubb W T & Michalske C J
J. Electrochem. Soc. 477 (April 1964)
358. Pizzini S et al
J. Appl. Electrochem. 3, 153 (1973)
359. Turner N H
J. Electro anal. Chem. 87, 67 (1978)
360. Etsell T H & Flengas S N
J. Electrochem. Soc. 118, 1890 (1971)
361. Heyne L & den Englesen D
J.Electrochem. Soc. (S.S. Sci. & Tech.) 124, (5) 727 (May 1977)
362. Franklin A D
J. Am. Ceram. Soc. 58 (11-12) (1975)
363. Wen C J & Mason D M
J. App. Electrochem. 8, 81 (1978)
364. Kleitz M & Fouletier J
Measurement of oxygen. P. Pub. Elsevier
Proc. Symp. Odense U. Denmark (26-27 Sept. 1974)
365. Weber S & Schmidt G
Commun. Kamerlingh Onnes Lab.
U. Leiden Suppl. 22 no. (246C) (1936)
366. Los J M & Fergurson R R
Trans. Faraday Soc. 48, 730 (1952)
367. Fleming W G
J. Electrochem. Soc. 124 (1) 21 (1977)
368. Etsell T H & Flengas S N
Metallurgical Transactions 3, 27 (Jan 1972)
369. Haaland D M
J. Electrochem. Soc. 127 (4) 796 (April 1980)
370. Spacil H S et al
Ab. no: 356, 357, & 358
Fall meeting, Montreal, Electrochem. Soc. (6.11.68)
371. Gur T M & Huggins R A
J. Electro Chem. Soc. 126 (6) 1067 (1979)
372. Sandler Y L
J. Electrochem. Soc. 118 (8) 1378 (Aug. 1971)
373. Pizzini S & Bianchi G
La Chimica e 1' Industria 55, 966 (1973)
374. Worrell W L & Iskoe J L
Fast ion trans. in solids. Proc. Nato. Adv. Study Inst. pp (513-521)
Sept. 1972. Pub. North Holland, Edit. Van Gool W.
375. Kleykamp H
Z. Phys. Chem. 71, 142 (1970)
376. Fouletier J et al
J. Appl. Electrochem. 5, 111 (1975) and p. 177-185
377. Kleitz M Deportes C and Fabry P
The oxygen electrochemical pump - Applications to the
generation of controlled atmospheres. Report (1971)
378. Spacil H S
G.Elec. report no. 67-C-450 (Dec. 1967)
379. Alcock C B and Zador S
J. Appl. Electrochem. 2, 289 (1972)
380. Mogab C J
Rev. Sc. Inst. 43 (11) 1605 (1972)
381. Mari C M et al
J. App. Electrochem 7, 215 (1977)
382. Beekmans N M & Heyne L L
Philips Tech. Rev. 31, 112 (1970)

383. Accorsi R & Bergmann E
J. Electrochem. Soc. Electrochem. Sci. & Tech.
127 (4) 804 (April 1980)
384. Dristine R T et al
J. Electrochem. Soc. S-S Sci. & Tech.
126 (2) 264 (Feb. 1979)